The Significance of C-Met in Different Molecular Sub-Types of Invasive Breast Cancer

Submitted in partial fulfillment of the requirements of the Degree of Doctor of Philosophy

Colan Maxwell Ho-Yen, BSc (Hons), MB ChB, FRCPath

Queen Mary University of London

May, 2014

Statement of originality

I, Colan Maxwell Ho-Yen, confirm that the research included within this thesis is my own work or that where it has been carried out in collaboration with, or supported by others, that this is duly acknowledged below and my contribution indicated. Previously published material is also acknowledged below.

I attest that I have exercised reasonable care to ensure that the work is original, and does not to the best of my knowledge break any UK law, infringe any third party's copyright or other Intellectual Property Right, or contain any confidential material.

I accept that the College has the right to use plagiarism detection software to check the electronic version of the thesis.

I confirm that this thesis has not been previously submitted for the award of a degree by this or any other university.

Signature:

Date:

Details of collaboration and publications:

1) Collaboration with Nottingham University NHS Trust: tissue was supplied by Prof Ian O Ellis and Dr Andrew Green, accompanied by clinical and pathological data. I performed immunohistochemistry for c-Met on these samples, analysed the results (including statistical analysis), and prepared the manuscript. This collaboration resulted in the following publication:

   Ho-Yen CM, Green AR, Rakha EA, Brentnall AR, Ellis IO, Kermorgant S, Jones JL. C-Met in invasive breast cancer: is there a relationship with the basal-like subtype? *Cancer*. 2014 Jan 15;120(2):163-71. doi: 10.1002/cncr.28386. Epub 2013 Oct 21.

2) Collaboration with Experimental Cancer Medicine Centre, Barts Cancer Institute: I advised on the methodology for c-Met immunohistochemistry in renal cell carcinoma tissue samples, supervised the staining and semi-quantitatively scored the stained slides. This collaboration resulted in the following publication:

Sharpe K, Stewart GD, Mackay A, Van Neste C, Rofe C, Berney D, Kayani I, Bex A, Wan E, O'Mahony FC, O'Donnell M, Chowdhury S, Doshi R, Ho-Yen C, Gerlinger M, Baker D, Smith N, Davies B, Sahdev A, Boleti E, De Meyer T, Van Criekinge W, Beltran L, Lu YJ, Harrison DJ, Reynolds AR, Powles T. The effect of VEGF-targeted therapy on biomarker expression in sequential tissue from patients with metastatic clear cell renal cancer. *Clin Cancer Res.* 2013 Dec 15;19(24):6924-34. doi: 10.1158/1078-0432.CCR-13-1631. Epub 2013 Oct 15.

Other published material contained in this thesis:

1) Ho-Yen C, Bowen RL, Jones JL. Characterization of basal-like breast cancer: an update. *Diagnostic Histopathology*. March 2012.18(3):104-111.

2) Ho-Yen C, Bowen RL, Kermorgant S, Jones JL. Comment on 'High MET expression is an adverse prognostic factor in patients with triple-negative breast cancer'. *Br J Cancer*. 2013 May 28;108(10):2195-6. doi: 10.1038/bjc.2013.249. Epub 2013 May 14.

Abstract

Introduction: Basal-like (BL) breast cancer is an aggressive sub-type of breast cancer for which there is no targeted systemic therapy. C-Met is a receptor tyrosine kinase implicated in breast cancer. Clinical trials assessing the efficacy of anti-c-Met therapy are underway, yet few studies have analysed the clinical significance of c-Met expression and/or activation in breast cancer, in particular whether there is a correlation with molecular sub-type. The aims of this study are: 1) to establish the clinical significance of c-Met expression in invasive breast cancer, 2) evaluate the novel proximity ligation assay (PLA) as a method of measuring c-Met activation and 3) address the effect of hepatocyte growth factor (HGF)-mediated c-Met phosphorylation on migration and protein expression in cell lines representative of the BL sub-type.

Methods: Immunohistochemistry for c-Met was performed on 1455 cases of breast cancer using tissue microarray (TMA) technology. The PLA was performed on TMAs constructed from 181 breast cancers. C-Met expression and the PLA product were correlated with clinico-pathological parameters and survival. The effects of HGF on cell migration and protein expression were assessed using migration assays, western blots and immunofluorescent studies.

Results: C-Met expression was independently associated with BL breast cancer (odds ratio = 6.44, 95% confidence interval (CI) = 1.74-23.78, $p = 0.005$) and reduced overall survival (hazard ratio = 1.81, 95% CI = 1.07-3.06), $p = 0.026$). The PLA signal was not associated with molecular sub-type or survival. HGF stimulation was associated with a significant increase in BL cell migration ($p < 0.01$) but no evidence of epithelial-mesenchymal transition was observed.

Conclusion: My findings suggest BL breast cancer patients should be included in future trials of anti-c-Met therapy. Further work is necessary to establish the prognostic utility of the PLA as a measure of c-Met activation and the mechanisms driving HGF-mediated cell migration.

Index of Contents

Index of Figures

Index of Tables

List of Abbreviations

ABC	Avidin-biotin complex
ARD	Adjusted relative density
BCLs	Breast cancer cell lines
BCS	Breast conserving surgery
BCSS	Breast cancer specific survival
BL	Basal-like
BSA	Bovine serum albumin
CALLA	Common acute lymphoblastic leukaemia antigen
CI	Confidence interval
CK	Cytokeratin
DAB	Diaminobenzidine
DAPI	4',6-diamidino-2-phenylindole
DCIS	Ductal carcinoma *in-situ*
DMSO	Dimethyl sulphoxide
ECL	Electrogenerated chemiluminescence
EDTA	Ethylenediaminetetraacetic acid
EGFR	Epidermal growth factor receptor
EMA	Epithelial membrane antigen
EMT	Epithelial-mesenchymal transition
ER	Oestrogen receptor
FCS	Fetal calf serum
FFPE	Formalin-fixed paraffin-embedded
FISH	Fluorescent *in-situ* hybridisation
FRET	Förster resonance energy transfer
HCl	Hydrochloric acid

HGF	Hepatocyte growth factor
HIER	Heat-induced epitope retrieval
HR	Hazard ratio
HRP	Horseradish peroxidase
HRT	Hormone replacement therapy
IBC	Inflammatory breast cancer
IDC-NST	Invasive ductal carcinoma – no special type
IF	Immunofluorescence
IgG	Immunoglobulin
IHC	Immunohistochemistry
ILC	Invasive lobular carcinoma
IP	Immunoprecipitation
KD	Knock-down
LR	Likelihood ratio
MAPK	Mitogen-activated protein kinase
MC	Mucinous carcinoma
MEM	Minimal Essential Medium
NADH	Nicotinamide adenine dinucleotide
NADPH	Nicotinamide adenine dinucleotide phosphate
NPI	Nottingham Prognostic Index
OS	Overall survival
OR	Odds ratio
PAGE	Polyacrylamide gel electrophoresis
PBS	Phosphate buffered saline
PDGFR	Platelet-derived growth factor receptor
PFA	Paraformaldehyde
PI3K	Phosphoinositide 3-kinase

PKC	Protein kinase C
PLA	Proximity ligation assay
PR	Progesterone receptor
RCA	Rolling circle amplification
RCC	Renal cell carcinoma
RCP	Rolling circle products
RIPA	Radioimmunoprecipitation assay
RPMI	Roswell Park Memorial Institute
RTK	Receptor tyrosine kinase
SEER	Surveillance Epidemiology and End Results
SDS	Sodium dodecyl sulfate
SF	Scatter factor
STAT	Signal transducer and activator of transcription
TBS	Tris buffered saline
TBST	Tris buffered saline with Tween
TC	Tubular carcinoma
TDLU	Terminal duct lobular unit
TEMED	Tetramethylethylenediamine
TMA	Tissue microarray
TN	Triple negative
U	Unclassified
VEGF	Vascular endothelial growth factor
VEGFR	Vascular endothelial growth factor receptor
WB	Western blot

Acknowledgements

This work would not have been possible without my two supervisors – Professor Louise Jones and Dr Stephanie Kermorgant.

Professor Jones played a huge part in my decision to undertake a PhD. Since then, she has made every effort to make it as rewarding an experience as possible. Her advice, guidance, enthusiasm, and approach to research are inspirational and I feel privileged to have been part of her group.

I have been very fortunate to have had Dr Kermorgant as my second supervisor, given her extensive knowledge of c-Met. Her input into all aspects of this thesis has been considerably more than one could expect and I am very grateful for all her suggestions and insight.

I have received great support from the other members of the Breast and Spatial Signalling Groups. In particular, from the Breast Group I would like to thank: Dr Michael Allen for sharing his considerable scientific knowledge and providing help and advice on many of the technical aspects of my PhD, Dr Sally Dreger for the tuition on several techniques, word-processing tips and endless supply of cakes, Dr Sally Smith for selecting and retrieving my samples, George Elia for teaching me immunohistochemistry and cutting my sections and Dr Linda Haywood for helping me get the hang of the tissue microarray machine. From the Spatial Signalling Group I would like to thank Dr Ludo Menard for the supply of MDA-MB-468s, help with my tissue culture techniques and immunofluorescence, Dr Rachel Barrow for her advice on optimising my migration assays and for answering my numerous c-Met questions and Dr James Hulit for general advice and technical expertise.

From the Centre for Tumour Biology I would also like to thank Dr Sabarinath Vallath for the in-depth scientific discussions and daily dose of caffeine, Dr Linda Hammond for training me on the various microscopes and for always being available and happy to help whenever something strange happened and Dr Delphine Lees for troubleshooting the proximity ligation assay. I am also grateful to Dr Abasi Ene-Obong for introducing me to the X-Tile software package.

I would also like to express my gratitude to Dr Adam Brentnall (Wolfson Institute of Preventative Medicine) and Dr Paul Greaves (Centre for Haemato-Oncology) for their input into my statistical analysis.

I am grateful to my collaborators in Nottingham (Professor Ian Ellis, Dr Andrew Green and Dr Emad Rakha) for supplying me with TMAs from their extensive tissue bank. Being able to incorporate these samples into my analysis increased the power of this study enormously.

I am indebted to members of Rudbeck Laboratory in Uppsala, Sweden (Professor Ola Söderberg, Karin Grannas and Dr Bjorn Koos) for taking me through the proximity ligation assay, for responding to my many queries, for giving me so much of their time and for their unforgettable hospitality.

I would like to thank Cancer Research UK for funding my PhD.

Special thanks also go to Nilu for her support, tolerance and understanding.

1.0 Introduction

1.1 The normal breast

1.1.1 Anatomy and histology

The breast is bordered anteriorly by the skin (from where it originates) and posteriorly by pectoralis major, serratus anterior and by the superior rectus sheath (Going, 2006). The normal breast is composed of a variable number of major ducts that emerge from the nipple and branch to form the terminal duct lobular unit (TDLU, Figure 1.1) (Lester, 2005). The keratinising squamous epithelium of the nipple undergoes transition into the specialised breast epithelium that lines the ducts and TDLU. This bilayered epithelium is formed of an inner layer of milk-producing epithelial cells and an outer discontinuous layer of contractile myoepithelial cells that assist in structural maintenance and milk expression (Lester, 2005). The glandular component of breast tissue is surrounded by mixed connective tissue; the lobules are invested by specialised myxoid tissue that lacks elastic fibres (Rosai, 2004). This intralobular stroma merges with the interlobular stroma comprised of a variable proportion of dense fibrous and adipose tissue (Lester, 2005).

Both the epithelial and stromal components of the breast undergo pregnancy and age-related changes. Young women's breasts are characterised by mostly fibrous stroma and a relative lack of adipose tissue. During pregnancy, there is proliferation of the TDLUs and the epithelium undergoes lactational changes. With increasing age there is involution, characterised by lobular atrophy and a greater proportion of adipose tissue in the interlobular stroma (Lester, 2005).

Figure 1.1: The normal breast. The photograph shows a haematoxylin and eosin-stained section of normal breast tissue. The terminal duct feeds into the lobule. Together, the terminal duct and lobule form the terminal duct lobular unit (TDLU) (x10 objective, scale bar represents 40µm).

1.1.2 Cell lineage and stem cells

The two layers of epithelium that line the TDLU can be differentiated by immunohistochemistry. The inner layer of luminal epithelial cells generally expresses the cytokeratins CK7, CK8/18 and CK19 whereas the outer basal/myoepithelial cells show CK5, CK17 and CK14 reactivity (Haupt *et al*, 2010; Going, 2006). Other markers of the basal/myoepithelial cells include smooth muscle actin (SMA), p63, common acute lymphoblastic leukaemia antigen (CALLA, CD10) and S100 (Haupt *et al*, 2010; Going, 2006). The luminal cells also show steroid receptor (oestrogen (ER) and progesterone (PR)) positivity along with epithelial membrane antigen (EMA) expression (Haupt, 2010 *et al*; Going, 2006). Interestingly, the luminal epithelium does not show diffuse positivity for ER/PR; in particular, antibodies against these receptors rarely label proliferating cells (Going, 2006). This suggests that the steroid hormones stimulate proliferation in the normal breast via an indirect paracrine or juxtacrine pathway (Going, 2006).

While the cytokeratin profiles of the luminal and basal compartments appear distinct, certain cytokeratins do not appear particularly specific (Gusterson, 2009). Antibodies to CK5 and CK14 can label luminal cells in ducts and lobules (Figure 1.2); this is in contrast to murine mammary glands where CK14 is specific for basal cells (Gusterson, 2009). Moreover, intensity of CK5 and CK14 expression varies greatly, even within the same breast (Gusterson, 2009).

Work on murine models of mammary biology, including the discovery that an entire mammary gland can be generated from a single cell (Kordon and Smith, 1998) has stimulated considerable interest in the concept of progenitor or stem cells within adult breast epithelium (Boecker and Buerger, 2003). Using double-staining

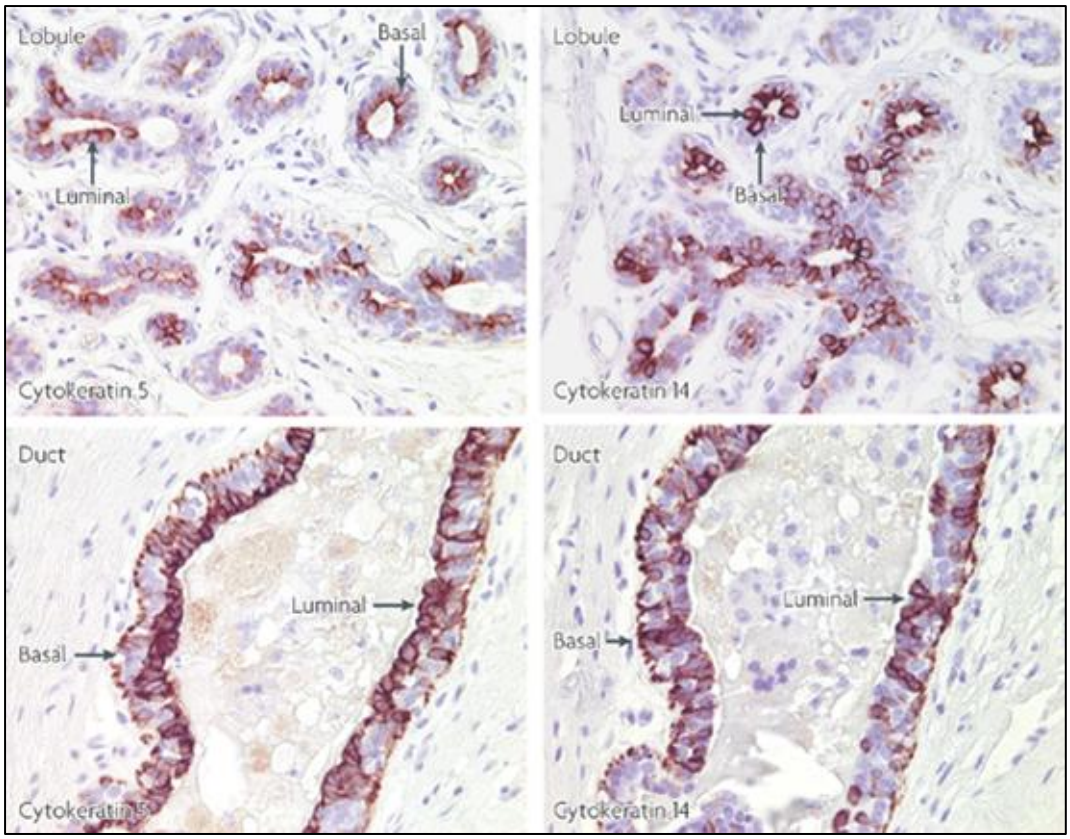

Figure 1.2: Cytokeratin immunohistochemical staining in the normal breast. The cytokeratins CK5 and CK14 are generally regarded as basal/myoepithelial markers however, both may also stain the luminal cells in normal ducts and lobules. Staining may also vary markedly within duct/lobules and in different parts of the same breast (Gusterson, 2009; reproduced with permission. Copyright (2009), Nature Publishing Group).

technology, Boecker and Buerger identified five sub-sets of normal breast epithelial cells: 1) only CK5 positive, 2) CK5 and CK8/18 positive, 3) only CK8/18 positive, 4) CK5/SMA positive and 5) only SMA positive (Boecker and Buerger, 2003). The authors suggested that the cells positive for CK5 only represented progenitor cells and that the additional presence of luminal (CK8/18) or myoepithelial (SMA) markers was indicative of intermediary luminal and myoepithelial cells respectively. Only the differentiated luminal (only CK8/18) and myoepithelial (only SMA expression) cells lacked CK5 reactivity (Boecker and Buerger, 2003). This progenitor cell concept would help explain the presence of CK5 positive cells in both the basal and luminal compartments.

1.2 Breast cancer

1.2.1 Incidence

According to the Surveillance Epidemiology and End Results (SEER) database, an estimated 232,670 American women will be diagnosed with breast cancer in 2014 and 39,620 will die from the disease (SEER, 2014). It is thought that 1 in 8 American women born today will be diagnosed with breast cancer over their lifetime (SEER, 2014). On a worldwide view, nearly 1.4 million women were diagnosed with breast cancer in 2008 and there were 459,000 deaths (Youlden *et al*, 2012). Here in the UK, there were 50,285 new diagnoses of breast cancer in 2011 and 11,762 breast cancer deaths in 2011 (Cancer Research UK, 2014).

1.2.2 Risk factors

Numerous parameters have been identified as being influential in a woman's likelihood of developing breast cancer.

1.2.2.1 Age and family history

Increasing age is a risk factor: the majority of tumours occur over the age of 50 (Lester, 2005). Women with a family history of breast cancer have approximately twice the risk compared to those without (Da Silva and Lakhani, 2010) and up to 5-10% of breast cancers may be due to germ-line mutations in one of several breast cancer susceptibility genes. These include the high risk *BRCA1, BRCA2, PTEN, TP53, LKB1/STK11, CDH1* genes and the low to moderate risk *CHEK2, TGFβ1, CASP8* and *ATM* (Mangia *et al*, 2011).

Breast cancers associated with *BRCA1/2* mutations have received considerable attention in both the media and scientific literature. Women harbouring germline mutations in either *BRCA1* or *BRCA2* are thought to have an 85% chance of developing breast cancer during their lifetime (Toft and Cryns, 2011). *BRCA1* has diverse cellular functions that include cell-cycle regulation, chromatin re-modelling and regulation of transcriptional processes (Da Silva and Lakhani, 2010). Perhaps the most interesting property of *BRCA1/2* is their role in DNA repair, more specifically, the repair of double-stranded breaks (DSBs) (Turner *et al*, 2004).

The process of homologous recombination (HR) utilises identical sister chromatids to repair damaged DNA in a conservative and error-free mechanism in which the BRCA1/2 proteins play a pivotal role (Da Silva and Lakhani, 2010). In the absence of functioning BRCA1/2, cells become dependent on alternative repair pathways

such as non-homologous end joining and single-strand annealing (Turner *et al*, 2004). Both of these processes are error-prone, resulting in DNA loss and chromosomal instability (Turner *et al*, 2004). Loss of BRCA1 may be particularly important in oestrogen-driven tumours because BRCA1 regulates oestrogen metabolism through enzymes such as CYP1A1 (Savage *et al*, 2014). In BRCA1-deficient cells, deregulated oestrogen metabolism generates increased numbers of toxic oestrogen metabolites resulting in DNA damage that cannot be effectively repaired, ultimately leading to genomic instability (Savage *et al*, 2014).

1.2.2.2 Reproductive and hormonal factors

A long duration of endogenous oestrogen exposure, due to late onset of the menopause is associated with an increased risk of breast cancer (Collaborative Group on Hormonal Factors in Breast Cancer, 1997). Oral contraceptives are thought not to increase a woman's chances of breast cancer - in a study involving over 9000 women, Marchbanks *et al* reported a relative risk of 1.0 for developing breast cancer in women currently using oral contraceptives (95% confidence interval (CI): 0.8-1.3) and 0.9 (95% CI: 0.8-1.0) in previous users (Marchbanks *et al*, 2002). Moreover, the risk did not increase with increasing dose, longer duration of treatment, younger age at initiation or in women with a family history of breast cancer (Marchbanks *et al*, 2002). In contrast, hormone replacement therapy (HRT) is a risk factor, particularly in current users (Collaborative Group on Hormonal Factors in Breast Cancer, 1997). Pregnancy is believed to convert breast epithelial cells into a more stable state and hence, a younger age at first pregnancy is linked with a reduction in breast cancer risk (Amir *et al*, 2010). Breast feeding also has a protective effect, possibly due to ovulatory delay, loss of oestrogens in breast milk, removal of carcinogenic agents,

changes in the pH of the mammary microenvironment and stimulation of terminal differentiation (Amir *et al*, 2010; Millikan *et al*, 2008; Lipworth *et al*, 2000).

1.2.2.3 Mammographic density

Mammographic density – the proportion of breast tissue that shows a dense appearance at mammography – is another recognised risk factor (Amir *et al*, 2010). In one study, women with mammographic density involving more than three-quarters of the breast tissue had five times the risk of those with dense areas occupying less than a tenth (Boyd *et al*, 2007). The increased risk of breast cancer persisted for at least eight years after study entry and was more pronounced in younger women (Boyd *et al*, 2007). Indeed, the authors calculated that in women below the median age of 56 years, 26% of all breast cancers and 50% of tumours detected within a year following a negative screening test, were due to density in 50% or more of the mammogram (Boyd *et al*, 2007).

1.2.2.4 Proliferative breast disease

Epithelial hyperplasia of usual type can be defined as the presence of three or more cell layers above the basement membrane (the normal number is two) and in the absence of atypical cytological features, increases the chances of future breast cancer by almost two-fold (Carter *et al*, 2006). However, when atypia is also present (referred to atypical ductal hyperplasia (ADH) where a proliferative lesion has some but not all the features of DCIS or is limited in extent) the risk increases to four to five-fold in the ensuing 10-15 years (Carter *et al*, 2006). *In-situ* lobular neoplasia is associated with 10 times increased risk of breast cancer (Dupont *et al*, 1993).

1.2.2.5 Obesity

Obesity has a conflicting influence on breast cancer risk: in younger women it results in a decrease in risk due in part to its association with anovulatory cycles whereas the production of oestrogen from adipose tissue renders obese women more prone to breast cancer in the post-menopausal group (Lester, 2005).

1.2.2.6 Ethnicity

Women from different ethnic groups have differing risks of breast cancer and breast cancer mortality: the SEER database shows that white women have the highest incidence at 127.9/100000 women versus just 79.3/100000 for American Indian/Alaskan native women (SEER, 2014). Black women also have a lower incidence of breast cancer than white women (122.8/100000) but, strikingly have a much higher incidence of breast cancer-related death than all the other ethnic groups at 30.8/100000 women. The next highest mortality rate is 22.1/100000 and this applies to white women (SEER, 2014). Similarly, British black women have been found to have a higher rate of mortality for tumours measuring 2cm or less, as well as presenting some 21 years earlier than their white counterparts (Bowen *et al*, 2008).

Although breast cancer incidence in Western Africa is lower compared to western countries at around 20/100000 (Fregene and Newman, 2005), studies observing indigenous African women show many parallels with western domiciled black women, including high mortality rates, early-onset disease and tumours presenting at a higher stage (Fregene and Newman, 2005; Huo *et al*, 2009; Adesunkanmi *et al*, 2006).

The aetiology of this racial disparity appears multifactorial, with features such as tumour biology, socioeconomic status and treatment factors all thought to influence the poorer outlook for black women (Ademuyiwa *et al*, 2011).

1.2.3 Ductal carcinoma *in-situ* (DCIS)

In contrast to the above risk factors, ductal carcinoma *in-situ* (DCIS) is regarded as a precursor to invasive breast cancer and is defined as a proliferation of neoplastic cells within the breast ducts and lobules, that has not yet invaded through the myoepithelium/basement membrane (Jones, 2006). As most patients with DCIS undergo surgery following diagnosis, there is little data on the natural history of DCIS. Nevertheless, small retrospective and follow-up studies have shown that 40-46% of patients with untreated DCIS go on to develop invasive breast cancer (Sanders *et al*, 2005; Collins *et al*, 2005).

1.2.4 Prognostic factors in breast cancer

Several factors exert an influence on the outlook for breast cancer patients.

1.2.4.1 Metastasis

Probably the most important prognostic factor is the presence or absence of metastasis, since a full recovery in unlikely when there is distant spread. The most common sites of breast cancer metastasis are: the lungs, bones, liver, adrenal glands, brain and meninges (Lester, 2005).

1.2.4.2 Lymph node status, tumour size and pathological grade

Both axillary lymph node involvement by tumour and increasing primary tumour size are independent but additive poor prognostic factors (Carter *et al*, 1989).

Pathological grading of tumours has in the past been problematic, mostly due to poor reproducibility (Elston and Ellis, 1991). Over the years, modification and refinement of the grading system has resulted in an objective technique that takes into account tubule formation, mitotic activity and nuclear pleomorphism to give an overall grade between 1 and 3 (Elston and Ellis, 1991). This grading system has been shown to be both robust and prognostic, with grade 1 tumours showing a markedly better prognosis compared to grade 2/3 cancers (Elston and Ellis, 1991; Pereira *et al*, 1995).

These three prognostic factors: lymph node status, grade and tumour size together form the Nottingham Prognostic Index (NPI) for primary breast cancer (Galea *et al*, 1992). The index divides patients into good, moderate and poor prognostic groups based on the chances of survival over a 15 year period (Galea *et al*, 1992) and it is widely used to stratify patients and guide therapy.

1.2.4.3 Histological sub-type

Histological tumour classification is fundamental to the assessment of breast tumours since many have a characteristic morphology that also has prognostic significance. A key limitation however, is that most breast cancers (approximately 70%) fall into a single category: invasive ductal carcinoma, not otherwise specified (IDC-NOS) or no special type (IDC-NST)(Harris *et al*, 2006; Berg and Hutter, 1995). Patients with these tumours have a very variable prognosis and it is these women who stand to gain most from new methods of tumour classification (Harris *et al*, 2006). Of the so-called 'special types' of breast cancer, the bulk are associated with a more favourable outlook compared to IDC-NST and include the well-differentiated tubular carcinoma, the related cribriform carcinoma, mucinous (or

colloid) carcinoma, medullary carcinoma, papillary carcinoma and adenoid cystic carcinoma (Harris *et al*, 2006; Berg and Hutter, 1995). It should be noted that even within special types, behaviour is variable, so sub-typing should be combined with grading to more accurately gauge prognosis (Pereira *et al*, 1995).

1.2.4.4 Other factors

The presence of tumour cells within vascular spaces (lymphovascular invasion) correlates with reduced survival and an increased chance of recurrence (Pinder *et al*, 1994; Mohammed *et al*, 2013). Tumours that express oestrogen receptor (ER) and/or progesterone receptor (PR) have a better prognosis than those that do not (Cheang *et al*, 2008). In contrast, cancers that over-express the receptor tyrosine kinase Her2 have a worse outcome (Cheang *et al*, 2008). Perhaps more importantly though, patients whose tumours express/over-express any of these three receptors can be treated with targeted endocrine therapy or trastuzumab (Payne *et al*, 2008).

1.2.5 Treatment and outcome

The key elements of breast cancer treatment are surgery, radiotherapy, chemotherapy, endocrine therapy and anti-Her2 treatment (reviewed in Wolters *et al*, 2012). Surgical options include breast conserving surgery (BCS) or mastectomy. BCS is recommended if the primary tumour can be resected without involvement of the margins and when the tumour size to breast volume ratio is not excessive (Wolters *et al*, 2012). Mastectomy is the procedure of choice when there is tumour multifocality, widespread malignant calcifications, inflammatory carcinoma or if radiotherapy (normally advised after BCS by most guidelines) is contra-indicated. Patient preference may also influence the surgical decision (Wolters *et al*, 2012).

Axillary surgery should be performed to stage invasive breast cancers when no morphological abnormalities are identified at axillary ultrasound scanning (NICE, 2009). The National Institute for Health and Clinical Excellence (NICE) guidelines recommend biopsy of the sentinel node (the first node to receive lymphatic drainage from a defined anatomical site) in preference to lymph node clearance, which is associated with significant morbidity (NICE, 2009).

In addition to the post-BCS scenario, radiotherapy is recommended in situations when the risk of relapse is high, these include: positive resection margins, large tumour size (greater than five cm) and the presence of more than three involved lymph nodes (Wolters *et al*, 2012).

Chemotherapy, like radiotherapy, is indicated for the treatment of tumours at high risk of recurrence, including lymph node positive tumours (Wolters *et al*, 2012). The taxane-containing chemotherapeutic agents (such as docetaxel) are recommended in the adjuvant treatment of cancers with nodal metastasis (Wolters *et al*, 2012; NICE, 2009).

According to the consensus of opinion from the St Gallen conference, any positive expression of ER is sufficient justification for the use of endocrine therapy (tamoxifen in pre-menopausal patients and aromatase inhibitors in post-menopausal women) in most cases (Goldhirsch *et al*, 2009). Elsewhere, the American Society of Clinical Oncology/College of American Pathologists advise treating patients with anti-oestrogen therapy if the tumour exhibits at least 1% reactivity (Hammond *et al*, 2010). Regarding the use of the anti-Her2 agent trastuzumab, protein over-expression or gene amplification is considered adequate for initiating treatment, except in those cases where the risk of progression is very low, for example in Her2

positive tumours less than 1cm in size with negative lymph nodes (Goldhirsch *et al*, 2009).

The outlook for breast cancer patients is highly variable and is dependent on many of the factors outlined above. Overall, 55-80% of breast cancer patients should survive to 10 years (Cheang *et al*, 2008).

1.3 Molecular sub-typing in breast cancer

The variation in natural history of breast cancer prompted a novel approach to breast cancer classification using gene expression microarrays (Perou *et al*, 2000; Sørlie *et al*, 2001; Sotiriou *et al*, 2003; Sørlie *et al*, 2003). By capturing the gene expression patterns of different breast cancers and relating this to patient outcome, these workers hoped to improve the taxonomy of breast cancer (Perou *et al*, 2000; Sørlie *et al*, 2003). These cDNA-based studies identified five main molecular sub-types: luminal A, luminal B, Erbb2 (Her2)-positive, normal-like and basal-like (BL)(Perou *et al*, 2000; Sørlie *et al*, 2003; Figure 1.3).

Other less well characterised sub-groups include the molecular apocrine tumours (characterised by *AR, FAS, ERBB2, XBP1* gene expression), claudin-low tumours (identified by low claudin protein expression and high *CD44, SNA13* gene expression) and the interferon group (with over-expression of interferon-related genes such as *STAT1*)(Weigelt *et al*, 2010; Hu *et al*, 2006). A more recent study identified 10 different sub-types by gene expression/copy number analysis (Curtis *et al*, 2012).

The potential of this new classification has stimulated a drive to generate immunohistochemical profiles of the main molecular sub-types that are more

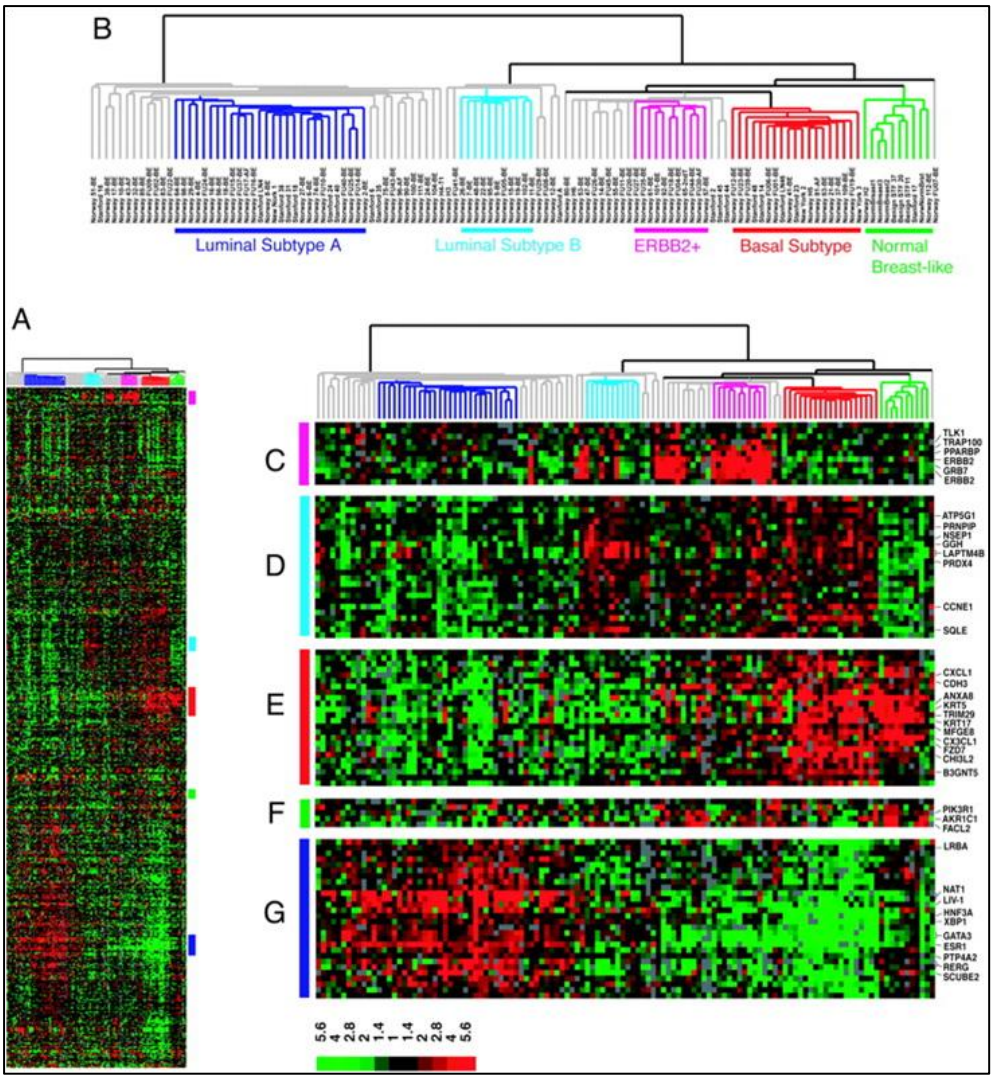

Figure 1.3: Gene expression profiles and molecular sub-types of breast cancer. **A** shows a scaled-down image of the 534 genes and 122 tissue samples used to group tumours based on their gene expression profile. **B** is a dendrogram showing the arrangement of the tumour samples into one of five main sub-types; the grey branches identify those samples that do not show strong correlation with any sub-type. **C** shows the *ERBB2* (Her2 positive) sub-type and associated genes, **D** contains the luminal B cluster, **E** shows the BL cluster, **F** shows the genes associated with the normal-like sub-type and **G** contains the luminal A cluster, including the ER (*ESR1*) gene. The scale bar represents the fold change of a gene compared to the median level of expression for all samples, red is over-expression, green is under-expression (Sørlie *et al*, 2003; reproduced with permission. Copyright (2003) National Academy of Sciences, U.S.A).

applicable to the diagnostic setting. This process has not been straight-forward: the lack of commercially available antibodies to certain gene products, variations in the gene expression profiles used by different groups and different cut-points used to determine biomarker over-expression are some of the likely reasons. This is particularly true of the BL sub-type.

1.3.1 Luminal A tumours

The luminal A tumours account for approximately 71% of breast cancers (Blows *et al*, 2010) and have the best outcome of all the sub-types, with a 79-84% 10-year survival (Carey *et al*, 2006; Cheang *et al*, 2008). These tumours show high expression of *ER, GATA binding protein 3, X-box binding protein 1, KRT8* and *KRT18* (Sørlie *et al*, 2001; Weigelt *et al*, 2010). Luminal A tumours can be identified at immunohistochemistry (IHC) by positivity for ER and/or PR and negativity for Her2 (Carey *et al*, 2006; Cheang *et al*, 2008; Blows *et al*, 2010).

1.3.2 Luminal B tumours

Luminal B tumours make up about six percent of breast cancers (Blows *et al*, 2010) and have an intermediate prognosis – 10-year survival is between 60 and 87% (Carey *et al*, 2006; Cheang *et al*, 2008). The gene expression profile is one of low-to-moderate expression of luminal-related genes, but a higher amount of proliferation-associated genes compared with luminal A tumours (Sørlie *et al*, 2001; Weigelt *et al*, 2010). There is over-expression of Her2, hence the immunoprofile is: positivity for ER and/or PR together with Her2 reactivity (Carey *et al*, 2006; Cheang *et al*, 2008; Blows *et al*, 2010).

1.3.3 Her2 positive tumours

Some six percent of breast cancers (Blows *et al*, 2010) show high expression of *ERBB2* and *GRB7* (Sørlie *et al*, 2001; Weigelt *et al*, 2010). At IHC, these tumours show Her2 positivity and are ER and PR negative (Carey *et al*, 2006; Cheang *et al*, 2008; Blows *et al*, 2010). Patients with Her2 positive tumours have a poor prognosis, with a 10-year survival rate of 52-55% (Carey *et al*, 2006; Cheang *et al*, 2008). However, it is important to remember that this survival data pre-dates the widespread use of trastuzumab for the treatment of early breast cancer in the UK, which was recommended by NICE in 2006 (NICE, 2006). Hence one would expect these survival rates to be more favourable under current treatment regimes.

1.3.4 Normal breast-like tumours

Cancers that cluster in the normal breast-like category show high expression of genes associated with adipose tissue and cell types other than those of epithelial origin, such as *CD36*, *PTN*, *FABP4* and *ITGA7* (Sørlie *et al*, 2001; Weigelt *et al*, 2010). While this sub-type remains poorly understood, some feel that this category is an artefact due to tumour samples being contaminated with too much normal breast tissue (Hu *et al*, 2006).

1.3.5 BL tumours

Basal-like (BL) breast cancers make up 10-25% of breast cancers, depending on the characteristics of the underlying study population (Perou, 2011). BL cancer has been recognised for more than 20 years when a proportion of invasive carcinomas were found to express basal cytokeratins (Nagle *et al*, 1986). The BL sub-group is of particular interest because they have a poor outcome (10-year survival is 62-75%

with a particularly steep survival curve in the first five years) and, since they generally lack expression of ER and Her2, they have limited treatment options. Chemotherapy remains the only form of systemic therapy available (Ray *et al*, 2010).

Triple negative (TN) cancers account for 12-17% of breast cancers and lack expression of ER, PR and Her2 (Foulkes *et al*, 2010). The BL and TN tumours are defined differently: BL like tumours are normally identified at gene expression profiling (although surrogate IHC markers are now available) whereas TN tumours are identified using IHC for ER, PR and Her2 (FISH is also used for cases with borderline Her2 IHC positivity) (Foulkes *et al*, 2010). TN tumours have much in common with BL tumours but are not synonymous – 29% of TN tumours have been shown to have a non-basal expression signature following cDNA microarray analysis (Bertucci *et al*, 2008). A recent genomic study of TN breast cancers found considerable variation in the number of mutations in this sub-group, with some tumours showing only a few mutations in selected pathways and others showing more extensive clonal evolution (Shah *et al*, 2012). Interestingly, the BL TN cancers were found to have higher clonality than the non-BL TN cancers (Shah *et al*, 2012). Other molecular sub-types postulated to make up the non-BL TN tumours are the claudin-low and interferon-rich groups (Hu *et al*, 2006; Perou *et al*, 2011).

1.3.5.1 Clinical and epidemiological features of BL tumours

Compared with other sub-types BL tumours are associated with younger patient age, with a higher proportion of patients presenting under 40 years of age (Cheang *et al*, 2008) and are more likely to present as interval cancers i.e present between regular mammograms (Collett *et al*, 2005). BL cancer is more common in women in the

African-American (AA) ethnic group (Millikan *et al*, 2008). Risk factors for this sub-type include earlier menarche, increased waist-to-hip ratio and a lack of breast-feeding combined with high parity; unlike the more common luminal A subtype, in which having multiple children and a younger age at first full-term pregnancy are protective, these factors increase the risk of BL cancer (Millikan *et al*, 2008). The vast majority (80-90%) of breast cancers arising in *BRCA1* germ-line mutation carriers are BL tumours (Foulkes *et al*, 2003). BL tumours are an aggressive form of breast cancer, linked with a lower disease-specific survival (Nielsen *et al*, 2004; Cheang et al, 2008) and a higher risk of local and regional relapse (Voduc *et al*, 2010).

1.3.5.2 Pathological features

At presentation BL tumours tend to be larger than other breast cancers (Foulkes *et al*, 2004), with a median size of 2 cm in one series (Rakha *et al*, 2006). Microscopically, the majority of BL cancers fall into the histological category of invasive ductal carcinoma, NOS/NST (Fulford *et al*, 2006; Rakha *et al*, 2006; Carey *et al*, 2006) however, mixed tumours, lobular, tubular, medullary, mucinous, papillary, adenoid cystic and metaplastic tumours can show a basal phenotype (Rakha *et al*, 2006). In particular, most metaplastic carcinomas have been shown to have a basal phenotype (Reis-Filho *et al*, 2006) and one study demonstrated that 17% of BL cancers showed medullary-like features, based on a simplified definition of prominent inflammation coupled with anastomosing sheets in at least 30% of the tumour (Marginean *et al*, 2010). Other architectural features of BL tumours include: a pushing border, a ribbon-like appearance and areas of geographic necrosis (Livasy *et al*, 2006) (Figure 1.4). Central scarring within the tumour is also more common than in non-BL lesions

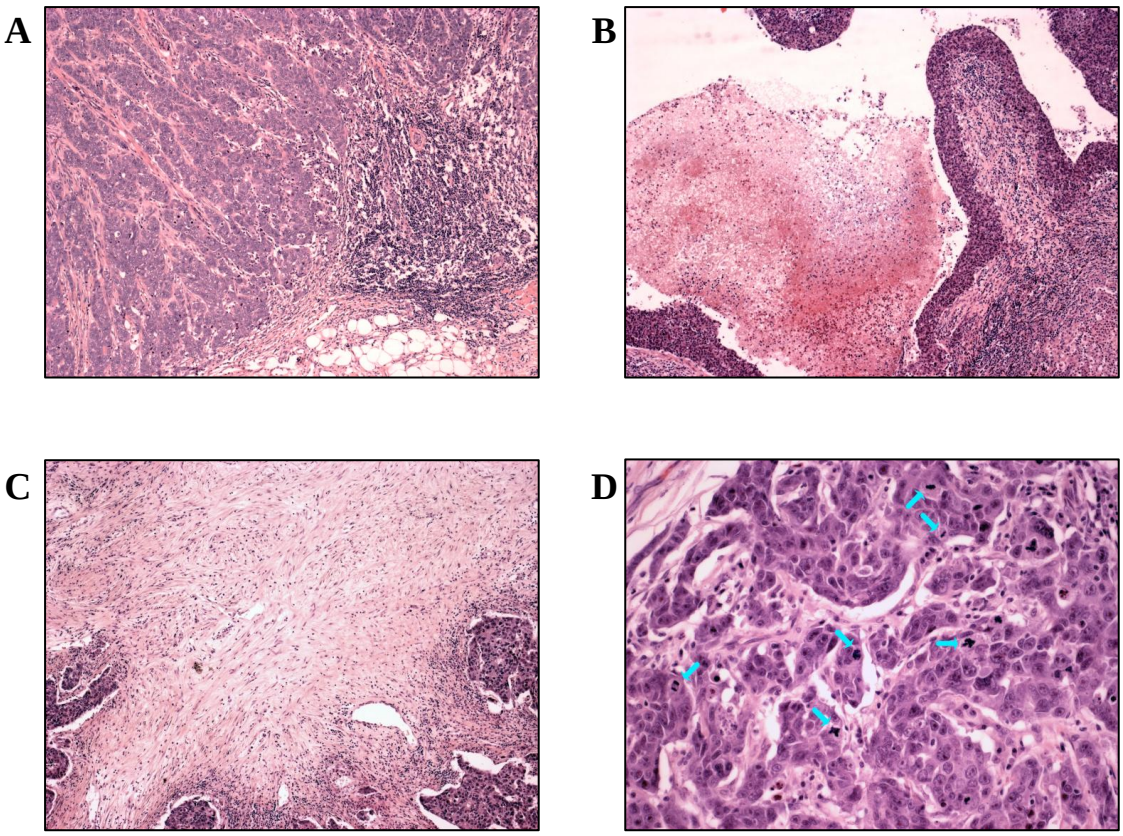

Figure 1.4: Histological features of BL breast cancer. The photographs are of haematoxylin and eosin-stained breast cancers showing some of the distinctive features more often seen in BL cancer. **A** shows a 'pushing', circumscribed invasive tumour front on the left side, with an associated chronic inflammatory cell infiltrate. **B** shows a band of tumour cells creating a 'ribbon-like' appearance along with some adjacent tumour necrosis. In **C** there is a prominent area of tumour-associated fibrosis and **D** shows poor tumour differentiation with a lack of tubule formation and frequent mitosis (see arrows; Ho-Yen *et al*, 2012; reproduced with permission. Copyright (2012), Elsevier).

(Fulford *et al*, 2006). Cytologically, the tumour cells tend to have minimal cytoplasm, with a high nuclear/cytoplasmic ratio and round/oval nuclei containing variable vesicular to coarse chromatin; nucleoli are a common finding (Livasy *et al*, 2006). Another useful feature is the presence of spindle-cell, clear cell or squamous differentiation (Fulford *et al*, 2006). Apoptotic cells may be numerous (particularly when associated with geographic necrosis) and the mitotic count is high – average or median counts of 45-48 per 10 high power fields (Livasy *et al*, 2006; Fulford *et al*, 2006) have been recorded.

A basal sub-type of *in-situ* carcinoma has been described (Dabbs *et al*, 2006; Clark *et al*, 2011). Foci of DCIS are usually small, in one series the *in-situ* component accounted for no more than 10% of the total tumour volume (Dabbs *et al*, 2006). In fact, in many cases of BL carcinoma no *in-situ* component is seen, perhaps as a result of rapid progression to invasive carcinoma or obliteration of the precursor lesion (Badve *et al*, 2011).

1.3.5.3 Molecular profile

The BL tumours show a gene expression profile characteristic of the basal epithelial layer at cDNA microarray analysis, these highly expressed genes include *KRT5*, *KRT17*, integrin β4 (*ITGB4*) and laminin (*LAM*)(Perou *et al*, 2000; Sørlie *et al*, 2001). The epidermal growth factor receptor (*EGFR*)(Sørlie *et al*, 2003; Nielsen *et al*, 2004) together with c-Kit (*KIT*), *FOXC1* and P-cadherin (*CDH3*)(Hu *et al*, 2006) also forms part of the gene expression cluster. Conversely, these tumours show absent or reduced expression of *ER* and transcription factors that characterise the luminal sub-type or *ER* positive cluster (Sørlie *et al*, 2001). Similar studies have found an increase in cell growth and cell cycle associated genes such as

topoisomerase IIa (*TOP2A*), mitotic feedback control protein Madp2 homolog (*MAD2L1*), cell division control protein 2 homolog (*CDC2*) and proliferating cell nuclear antigen (*PCNA*)(Sotiriou *et al*, 2003). The epithelial to mesenchymal transition (EMT) related gene *SLUG* has also been linked to BL tumours (Storci *et al*, 2008).

Following the identification of tumourigenic stem cell-like cells with high expression of the cell surface protein CD44 and low expression of CD24 (Al-Hajj *et al*, 2003), Honeth *et al* found a positive association between $CD44^{+}/CD24^{-}$ cells and the BL sub-type (Honeth *et al*, 2008). The authors concluded that BL cancers were enriched with tumour-initiating cells (Honeth *et al*, 2008) suggesting that the presence of these cells contributes to the natural history of BL cancer.

The high proportion of *BRCA1* mutated tumours that have a BL gene expression profile (Foulkes *et al*, 2003) has prompted some to examine the role of *BRCA1* dysfunction in sporadic BL cancer. Aside from *BRCA1* mutation, other mechanisms may contribute to *BRCA1* dysfunction, such as promoter methylation and negative regulation of the gene (Turner *et al*, 2007). In a study of sporadic breast cancers, Matros *et al* found promoter methylation in 21% of tumours, and this was associated with lower expression of the BRCA1 protein (Matros *et al*, 2005). These workers found that most BL cancers in fact had no *BRCA1* methylation and high BRCA1 protein expression, most likely due to the higher rate of proliferation in these tumours (indicative of normal BRCA1 cell regulation)(Matros *et al*, 2005). A later study by Turner *et al* confirmed the absence of increased *BRCA1* methylation in BL cancers but, found significantly lower *BRCA1* mRNA expression compared to controls (Turner *et al*, 2007). Furthermore, *ID4*, a negative regulator of *BRCA1* was

found at levels over nine times higher than controls, implicating *ID4* in *BRCA1* dysregulation in BL cancer (Turner *et al*, 2007).

The connection between BRCA1 and BL cancer is supported by a more recent study showing that *BRCA1* and c-Myc (*MYC*) form a transcriptional repressor complex on the promoters of three genes associated with the BL phenotype: *KRT5* (cytokeratin 5), *KRT17* (cytokeratin 17) and *CDH3* (P-Cadherin). This may explain the increased expression of these genes and proteins in *BRCA1* mutated tumours (Gorski *et al*, 2010).

Mutations in the *TP53* tumour suppressor gene are common in the BL phenotype with frequencies of 82-92% (Sørlie *et al*, 2001; Manié *et al*, 2009) and this compares with a mutation rate of just 13% in luminal A tumours (Sørlie *et al*, 2001). Other molecular features described in this sub-type are: chromosome 3q gains and 5q losses (Holstege *et al*, 2010) and abnormalities of the X chromosome resulting in an increase in the expression of a subset of X chromosome genes (Richardson *et al*, 2006).

1.3.5.4 Immunohistochemical profile

Currently, there is no consensus on the ideal IHC signature for BL tumours and different definitions have been utilised or proposed in the literature (Nielsen *et al*, 2004; Livasy *et al*, 2006; Carey *et al*, 2006; Fulford *et al*, 2006; Rakha *et al*, 2007; Ihemelandu *et al*, 2007; Cheang *et al*, 2008; Rakha *et al*, 2009; Table 1.1). Nevertheless, most of the larger clinical studies find the profile of ER/PR/Her2 negative, CK5/6 (Figure 1.5) and/or EGFR positive to be robust and specific in identifying BL tumours (Cheang *et al*, 2008; Blows *et al*, 2010). Importantly, negativity for ER, PR and Her2 alone is not regarded as a good proxy for the BL

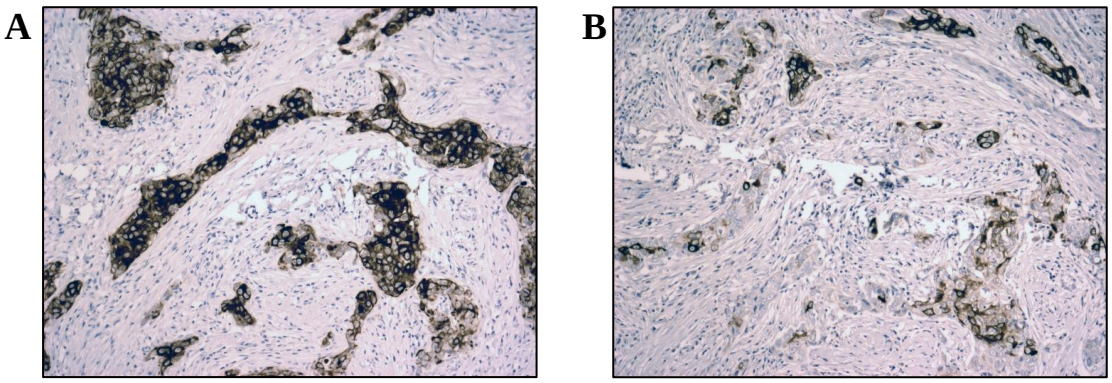

Figure 1.5: Immunohistochemical staining for cytokeratins in BL breast cancer. **A** shows strong and diffuse staining of the tumour cells by CK5, whereas staining for CK14 (**B**) is more often patchy in nature (Ho-Yen *et al*, 2012; reproduced with permission. Copyright (2012), Elsevier).

sub-type since BL tumours have a worse outcome and appear distinct from TN tumours that lack basal cytokeratin/EGFR expression (Cheang *et al*, 2008; Blows *et al*, 2010). Other immunohistochemical markers may also be relevant to the BL category; these include p53, Ki67 and E-Cadherin.

Journal article	ER	PR	Her2	CK5/6	CK14	CK17	CK8/18	EGFR	Vimentin
Ihemelandu *et al*, 2007	Neg	Neg	Neg	-	-	-	-	-	-
Livasy *et al*, 2006	Neg	-	Neg	Pos	-	-	Pos	Pos	Pos
Carey *et al*, 2006; Cheang *et al*, 2008	Neg	Neg	Neg	Pos/Neg*	-	-	-	Pos/Neg*	-
Nielsen *et al*, 2004	Neg	-	Neg	Pos/Neg*	-	-	-	Pos/Neg*	-
Rakha *et al*, 2007	-	-	-	Pos/Neg*	Pos/Neg*	-	-	-	-
Rakha et al, 2009	Neg	Neg	Neg	Pos/Neg*	Pos/Neg*	Pos/Neg*	-	Pos/Neg*	-
Fulford et al, 2006	-	-	-	-	Pos	-	-	-	-

Table 1.1: Range of immunohistochemical profiles used by different studies to identify BL cancer. The lack of a broad consensus has resulted in considerable variation in what researchers regard as a BL tumour. The table shows a selection of studies and the markers used, ranging from a single cytokeratin to a cocktail of seven markers (* = positive for at least one of these markers; modified from Ho-Yen et al, 2012).

1.3.5.4.1 p53

The tumour suppressor protein p53 (encoded by the *TP53* gene), also known as the 'guardian of the genome', has several roles in cell biology, such as apoptosis, cell-cycle arrest and senescence (Inoue *et al*, 2012; Turner *et al*, 2013). A key function of p53 is the induction of cell-cycle arrest via the G_1S checkpoint mechanism to allow DNA repair or apoptosis in response to cellular stress (Inoue *et al*, 2012). *TP53* mutations are common in human cancer, most of which lead to the accumulation of non-functioning protein in the nucleus (Allred *et al*, 1993), possibly because these mutations disrupt the process of ubiquitin-mediated degradation (Inoue *et al*, 2012).

Unlike wild-type p53, mutant p53 can be detected by IHC (Allred *et al*, 1993; Biganzoli *et al*, 2011) where expression has been associated with high tumour proliferation, early recurrence and early death in lymph node negative breast cancer (Allred *et al*, 1993). In keeping with the high frequency of *TP53* mutations detected in BL cancer (Sørlie *et al*, 2001), p53 immunopositivity has been found in 81% of sporadic BL cancers (Manié *et al*, 2009).

1.3.5.4.2 Ki67

The nuclear antigen Ki67 is expressed at all stages of the cell cycle except the resting phase (G_0) and is considered by some to be a better prognostic marker than mitotic count in breast cancer (Yerushalmi *et al*, 2010). The prognostic significance of Ki67 expression has been confirmed in two large meta-analyses, where a high Ki67 index correlated with worse disease-free and overall survival (de Azambuja *et al*, 2007; Stuart-Harris *et al*, 2008).

Some groups use Ki67 positivity (in more than 14% of tumour cells) to define luminal B tumours as an alternative to Her2 positivity in ER and/or PR positive cancers, based on the importance of the 'proliferation cluster' in identifying luminal B tumours at gene expression analysis (Cheang *et al*, 2009; Hu *et al*, 2006). Similarly, consistent with the high expression of cell-cycle associated genes in BL tumours (Sotiriou *et al*, 2003), 79.6% of BL tumours were found to express high levels of Ki67 by IHC compared to just 29.1% of non-BL tumours (Kuroda *et al*, 2008).

1.3.5.4.3 E-Cadherin

The transmembrane glycoprotein E-Cadherin (endoded by the *CDH1* gene) is regarded by some as an inhibitor of tumour progression (Mahler-Araujo *et al*, 2008). IHC for E-Cadherin is widely used in diagnostic pathology as a marker of *in-situ* and invasive lobular carcinoma, where there is loss of membranous expression of the protein (Mahler-Araujo *et al*, 2008).

In non-lobular invasive breast carcinoma, loss of membranous E-Cadherin has been associated with poor prognostic factors and reduced survival (Rakha *et al*, 2005). While many BL tumours show normal IHC expression of E-Cadherin, studies have shown that down-regulation of the protein is more common in BL tumours (Mahler-Araujo *et al*, 2008; Sarrió *et al*, 2008), consistent with the EMT-like characteristics of BL cancer and suggesting that loss of E-Cadherin may have a role in promoting metastasis.

1.3.5.5 Treatment in BL cancer

Due to the absence of ER and Her2 expression in BL cancer, chemotherapy remains the only established form of systemic therapy (Ray *et al*, 2010). While anthracycline-based adjuvant chemotherapy appears to be less effective (Banerjee *et al*, 2006), most data suggests that the taxane class of chemotherapeutic agents (such as paclitaxel) is the current treatment of choice in BL cancer patients (De Laurentiis *et al*, 2010; Rouzier *et al*, 2005).

In recent years, there has been considerable interest in the development of novel therapies that specifically target BL cancer. Amongst these, inhibitors of EGFR, poly

(ADP-ribose) polymerase (PARP) inhibitors and anti-angiogenic agents have shown some promise (De Laurentiis *et al*, 2010).

1.3.5.5.1 PARP inhibitors

The possible involvement of *BRCA1* dysfunction in BL breast cancer, and particularly *BRCA1* mutated (hereditary) BL breast cancer has drawn attention to a novel class of drugs known as poly (ADP-ribose) polymerase (PARP) inhibitors. The enzyme PARP is a key component of base excision repair (Rehman *et al*, 2010). Inhibition of the enzyme normally results in single-strand breaks that are repaired by homologous recombination (HR) in the presence of functioning *BRCA1/2* (Farmer *et al*, 2005). In *BRCA1/2* deficient cells however, HR is severely impaired, resulting in permanent cell arrest or apoptosis (Farmer *et al*, 2005). This concept of 'synthetic lethality', whereby loss of either of two related genes is compensated by the other gene in normal cells, but loss of both results in cell death in tumour cells, has been demonstrated in *in-vitro* and *in-vivo* models using *BRCA1/2* deficient cells (Farmer *et al*, 2005; Rehman *et al*, 2010; Figure 1.6).

PARP inhibitors are now being evaluated in the clinical setting; it is not yet clear if patients with sporadic (non-*BRCA1* mutated) BL cancer will also derive benefit from these drugs.

1.3.5.5.2 Anti-angiogenics

The angiogenic protein – vascular endothelial growth factor (VEGF) is associated with a poor outcome in breast cancer (Linderholm *et al*, 2001). Furthermore, high expression of a 13-gene signature that contains several angiogenic factors (VEGF included) distinguishes distant metastatic breast cancer deposits from primary

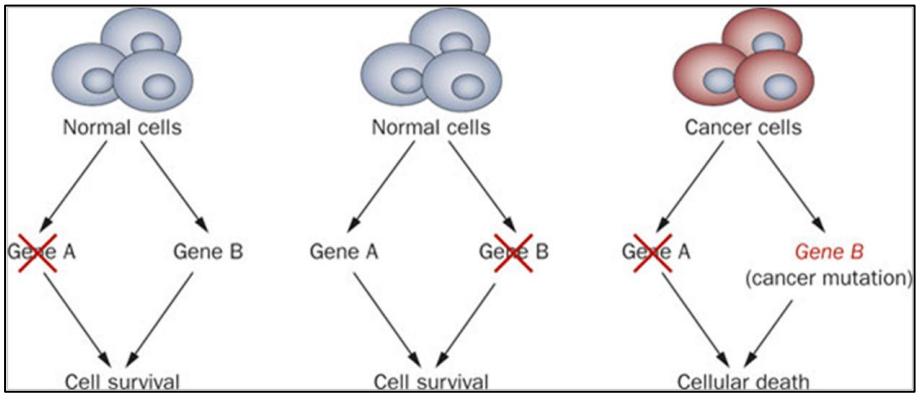

Figure 1.6: The principle of synthetic lethality. Targeting one of two related genes does not affect cell survival in normal cells, since each gene compensates for the loss of the other. However, cancer cells harbouring a mutation in one gene are susceptible to pharmacological intervention targeting the related gene, resulting in cell death with sparing of the adjacent normal tissue (Rehman *et al*, 2010; figure reproduced with permission. Copyright (2010), Nature Publishing Group).

tumours and regional metastasis (Hu *et al*, 2009). This 'VEGF-profile' was also linked to poor prognosis and the authors hypothesised that metastatic tumour cells had the ability to form new blood vessels, thus favouring survival in hypoxic conditions (Hu *et al*, 2009).

While these data implicate VEGF in breast cancer progression, the anti-angiogenic compound, sunitinib, which targets the VEGF receptor, has shown limited benefit in unselected breast cancer patients (De Laurentiis *et al*, 2010). Appropriate patient selection may in fact be crucial in the assessment of anti-angiogenics, as studies have shown a positive correlation between VEGF expression and ER negative status and BL breast cancer (Linderholm *et al*, 2001; Perou, 2011). Sunitinib and another agent with inhibitory effects on VEGF (bevacizumab) now form part of separate clinical trials focusing on TN breast cancer (Linderholm *et al*, 2001; Perou, 2011).

1.3.5.5.3 Anti-EGFR agents

The role of EGFR as an oncogenic factor has been established in several human cancers including glioblastoma, lung cancer and head and neck cancers where it is regarded as an attractive therapeutic target (Burness *et al*, 2010). Although less well studied in breast cancer, numerous studies have found an association between EGFR and the BL phenotype (Cheang *et al*, 2008; Blows *et al*, 2010). Dysregulation of EGFR signalling promotes tumour proliferation, reduced apoptosis, increased survival, angiogenesis and metastasis (Burness *et al*, 2010).

In BL breast cancer, the importance of EGFR is endorsed by evidence that signalling pathways downstream of EGFR – the Ras/Raf/mitogen-activated protein kinase kinase (MEK) and phosphatidylinositol 3-kinase (PI3K)/Akt pathways – are activated in BL cancer (López-Knowles *et al*, 2010; Hoeflich *et al*, 2009). BL breast

cancer cell lines are highly sensitive to MEK inhibition compared to breast cancer cell lines from the other molecular sub-types and the combination of a MEK inhibitor and PI3K inhibitor is synergistic, impairing the growth of BL cells/tumours in *in-vitro* and *in-vivo* models (Hoeflich *et al*, 2009). Furthermore, inositol polyphosphate 4-phosphatase type II (INPP4B), a regulator of PI3K/Akt signalling has been noted to be absent in over 80% of BL cancers (Fedele *et al*, 2010).

Despite the rationale for targeting EGFR in breast cancer, the results of clinical trials have so far proven disappointing (Burness *et al*, 2010). Various factors may contribute to this discrepancy. Clearly, EGFR dysregulation is a complex process, and it may be necessary to tailor strategies towards specific abnormalities, such as protein over-expression or activating mutations (Burness *et al*, 2010). However, this approach is itself not without complications, since abnormal EGFR activation for example can occur in the absence of protein over-expression (Burness *et al*, 2010). It is also apparent that there is a wide variation in the definitions used to quantify IHC EGFR staining, and there is at present no international criterion for evaluating EGFR in breast cancer (Arnes *et al*, 2009). Of course, the down-stream signalling pathways activated by EGFR (the MEK pathway for instance) are not exclusive to the receptor (Burness *et al*, 2010) and it very possible that other RTKs make a significant contribution to BL cancer cell activation.

One possible candidate is c-Met, an RTK associated with a poor outlook in breast cancer (Camp *et al*, 1999; Tolgay Ocal *et al*, 2003; Ghoussoub *et al*, 1998) and implicated in the BL phenotype (Charafe-Jauffret *et al*, 2006; Garcia *et al*, 2007a; Graveel *et al*, 2009).

1.5 C-Met

1.5.1 Structure and function

C-Met was originally identified as the product of a transforming gene generated from a chemically transformed osteosarcoma cell line (Cooper *et al*, 1984). In 1991, c-Met was discovered to be the receptor for hepatocyte growth factor (HGF), a protein that had previously been shown to promote hepatocyte growth in culture (Nakamura *et al*, 1984; Bottaro *et al*, 1991). C-Met is a transmembrane RTK, produced first as a 170kDa precursor that is subsequently cleaved to generate a 50kDa α subunit and a 145kDa β subunit (Giordano *et al*, 1989; Hanna *et al*, 2009). The α subunit is extracellular and bound by a disulphide bond to the transmembrane β subunit (reviewed in Trusolino *et al*, 2010). The extracellular portion of the receptor is comprised of a Sema domain, PSI domain (so-called because it is found in plexins, semaphorins and integrins) and four immunoglobulin-like fold shared by plexins and transcription factors (IPT) domains (Trusolino *et al*, 2010).

The intracellular portion contains three domains: the juxtamembrane region, which is important in the downregulation of signalling following Ser975 phosphorylation, the catalytic region that includes the Tyr1234 and 1235 residues and the multifunctional carboxy-terminal docking site (Trusolino *et al*, 2010; Figure 1.7).

HGF, also known as scatter factor, is the only known mammalian agonistic ligand for c-Met (Goldoni *et al*, 2009). Like c-Met, HGF is first secreted as a single-chain precursor that undergoes proteolytic cleavage to form an α and β-chain heterodimer (Trusolino *et al*, 2010). Upon HGF binding, there is dimerisation of c-Met followed by autophosphorylation of the Tyr 1234 and 1235 residues in the kinase domain

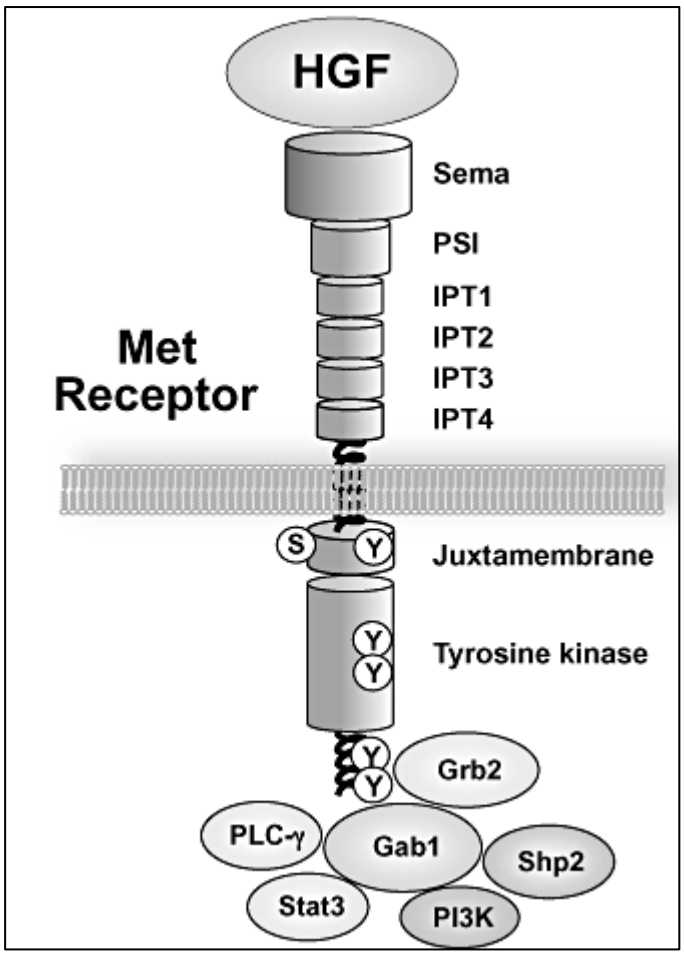

Figure 1.7: Diagrammatic representation of the c-Met receptor. The key structural and functional components are illustrated and include the extracellular region containing the Sema domain (found in semaphorin receptors), the PSI domain (which is present in plexins, semaphorins and integrins) and four IPT domains (present in immunoglobulins, plexins and transcription factors). The intracellular region contains the juxtamembrane domain which is important in signalling down-regulation, together with the catalytic tyrosine kinase domain and the multifunctional docking site at the C-terminus; transduction molecules such as Grb2 and Gab1 bind to the receptor in this region (Nakamura *et al*, 2011; reproduced with permission. Copyright (2011), John Wiley and Sons).

(Hanna *et al*, 2009). Subsequent to this, phosphorylation of the docking site tyrosines 1349 and 1356 facilitates the binding of the downstream signal transduction molecules Growth-factor-receptor-bound protein 2 (Grb2), Grb2-associated binder 1 (Gab1), Shc, Src and p85 (Hanna *et al*, 2009). These molecules promote downstream signalling through several c-Met regulated pathways, including : mitogen-activated protein kinase (MAPK)/extra-cellular signal regulated kinase (Erk) cascades, phosphoinositide 3-kinase (PI3K)/Akt cascades, signal transducer and activator of transcription 3 (STAT3) and the PI3K/nuclear factor-κB pathway (Trusolino *et al*, 2010; Figure 1.8). Together, these pathways regulate cellular proliferation, differentiation, apoptosis, survival and tubulogenesis (Trusolino *et al*, 2010). In addition, signalling via the RAC1-CDC42 pathway can influence migration through the E-cadherin/β-catenin complex (Gherardi *et al*, 2012).

After c-Met activation the receptor undergoes ubiquitinisation and downregulation, as is the case with several RTKs (Peschard and Park, 2007). The ubiquitin ligase Cbl binds to and ubiquitinates the receptor which is then internalised in a clathrin-coated vesicle and sorted into a multivesicular body, whereupon lysosome fusion results in degradation of the receptor (Peschard and Park, 2007). Although c-Met internalisation is part of the process of signal attenuation, trafficking of the receptor within endosomes under the control of protein kinase C (PKC) results in sustained phosphorylation and is necessary for HGF-mediated migration (Kermorgant *et al*, 2004; Kermorgant and Parker, 2008). Moreover, in NIH3T3 cells harbouring the *MET* mutation originally indentified in human papillary renal cell carcinomas, blocking endocytosis inhibited *in-vivo* tumour growth and metastasis (Joffre *et al*, 2011).

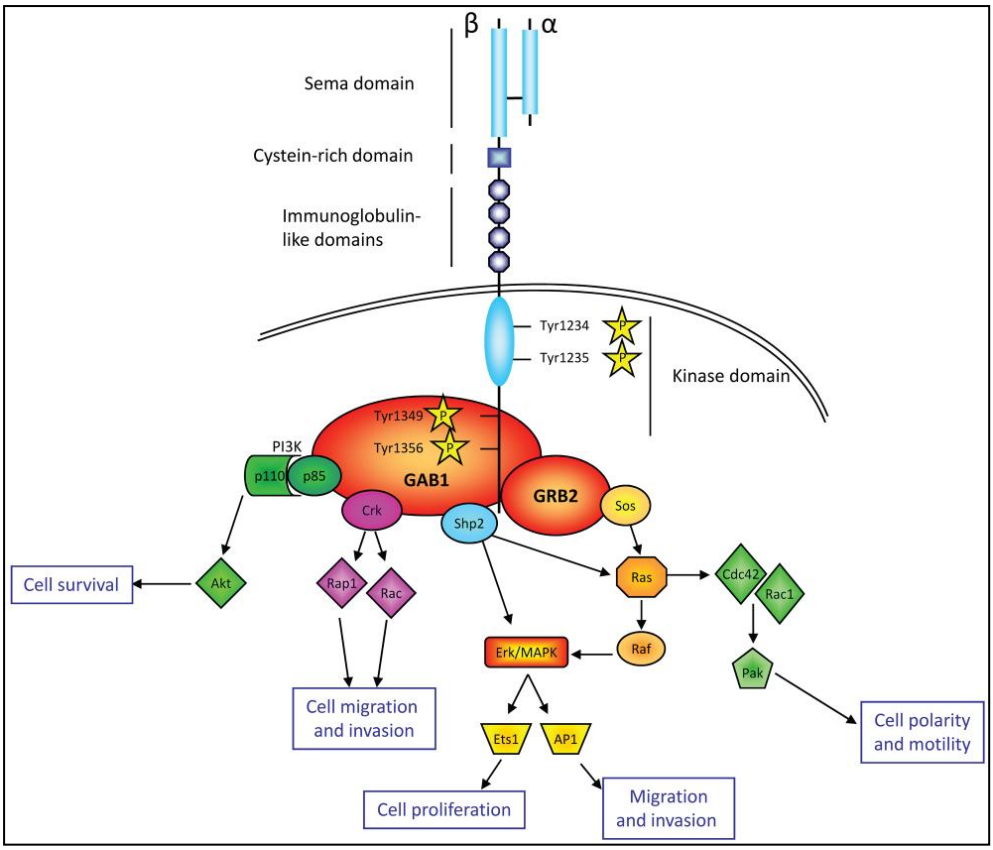

Figure 1.8: Diagram of c-Met with its associated downstream signalling pathways. HGF binding results in receptor homodimerisation and autophosphorylation of the tyrosine residues in the kinase domain (Tyr 1234/1235). Subsequent phosphorylation of the docking tyrosines (Tyr 1349/1356) recruits scaffolding and transducer proteins that activate downstream signalling via different pathways, including the Erk/MAPK and Akt/PI3K cascades, involved in the invasive process (Gastaldi *et al*, 2010; Figure reproduced in accordance with BioMed Central's open access charter).

1.5.2 Cross-talk between c-Met and other membrane receptors

C-Met has been shown to interact with other cell surface proteins including CD44, β4 integrin, Plexin β1, EGFR and RET (Trusolino *et al*, 2010; Lai *et al*, 2009; Figure 1.9). The transmembrane protein CD44v6 is necessary for HGF-mediated signalling through the MAPK/Erk pathway (Orian-Rousseau *et al*, 2007). The MAPK/Erk pathway is also stimulated via interactions between c-Met and the integrin β4, during which c-Met promotes β4 phosphorylation and the recruitment of Gab1 and Grb2 (Bertotti *et al*, 2006). The involvement of β4 in this pathway can sustain HGF-mediated anchorage-independent growth (Bertotti *et al*, 2006). The Plexin β1 ligand Sema 4D can phosphorylate Plexin β1, Gab1 and c-Met and activation of the c-Met related RTK RET can phosphorylate Met by a Src-dependent process (Lai *et al*, 2009).

The RTK EGFR can transphosphorylate c-Met (and vice versa) and activation of EGFR has been shown to induce cleavage and ectodomain shedding of c-Met through the MAPK/Erk signalling cascade (Nath *et al*, 2001; Lai *et al*, 2009). Moreover, lung cancer cell lines that have EGFR mutations become resistant to EGFR inhibitors as a result of *MET* amplification (Engelman *et al*, 2007). Growth inhibition can then be restored with concurrent anti-c-Met and anti-EGFR treatment (Engelman *et al*, 2007; Bean *et al*, 2007), suggesting a close relationship between these two related receptors.

Another cell surface protein thought to be linked to c-Met signalling is the adhesion molecule E-cadherin (Reshetnikova, 2007). It has been proposed that E-cadherin adhesion sites permit the accumulation of signalling proteins including RTKs (Reshetnikova, 2007). Work on pharyngeal carcinoma cell lines has shown that HGF

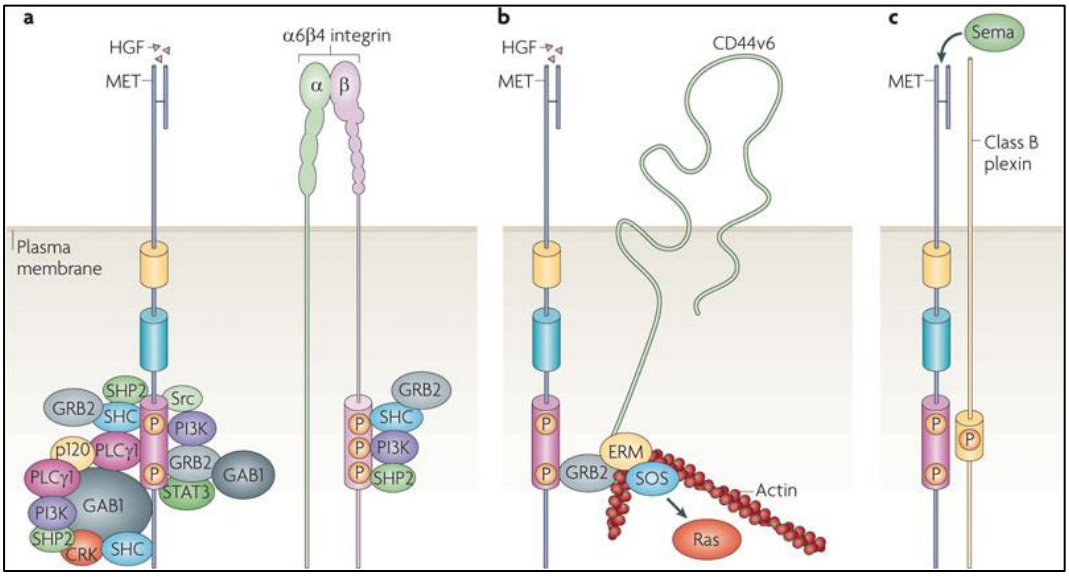

Figure 1.9: Cross-talk between c-Met and other proteins. **A** depicts c-Met and the α6β4 integrin which can associate with c-Met, increasing the number of docking sites for signal transducers such as Grb2. The hyaluronan receptor CD44 (**B**) can bind to c-Met, linking the receptor to actin microfilaments and facilitating Ras activation. Close association between c-Met and class B plexins (**C**) can result in c-Met phosphorylation in the absence of HGF via Sema binding (Trusolino *et al*, 2010; figure reproduced with permission. Copyright (2010), Nature Publishing Group).

stimulates internalisation of E-cadherin along with enhanced invasion (Kim *et al*, 2007; Xie *et al*, 2010). Cell treatment with anti-E-cadherin antibody was noted to result in a similar scattering effect to that seen following HGF administration (Kim *et al*, 2007). These authors postulated that HGF stimulation results in E-cadherin separating from β-catenin, with subsequent endocytosis and degradation of E-cadherin (Kim *et al*, 2007). Elsewhere, a study comparing different breast cancer cell lines found that c-Met expression increased as E-cadherin expression diminished in more aggressive cell lines (Götte *et al*, 2007), raising the possibility that the relationship between these two proteins may vary between different tumour types.

1.5.3 Role in development and repair

C-Met is mainly expressed in epithelial and endothelial cells (Peschard and Park, 2007; Hanna *et al*, 2009) whereas HGF is expressed in mesenchymal cells (Peschard and Park, 2007). HGF is necessary for normal embryological development and mice lacking the gene die *in utero* with impaired survival of liver hepatocytes and placental trophoblast (Schmidt *et al*, 1995; Uehara *et al*, 1995). The HGF-c-Met signalling axis is also important in tissue repair in a variety of different tissue types including liver, lung, spleen, kidney, nervous tissues, cutaneous and cardiovascular tissues (Nakamura *et al*, 2011). HGF may contribute to tissue regeneration by suppressing inflammation and promoting proliferation, 3-D morphogenesis and degradation of components of the extracellular matrix (Nakamura *et al*, 2011).

1.5.4 Role in cancer

The biological effects of the HGF-c-Met axis that are key in development and repair have also been implicated in cancer, where aberrant c-Met signalling may promote cancer progression and have a detrimental effect on prognosis (Lai *et al*, 2009).

Perturbations in the c-Met pathway may be due to a variety of mechanisms, these include: gene rearrangement, gene mutation, amplification, protein over-expression, increased paracrine stimulation, acquisition of autocrine signalling and cross-talk with other receptors (Cooper *et al*, 1984; Peschard and Park, 2007; Sierra and Tsao, 2011).

These mechanisms have been described in renal, breast, lung, gastric, bone and pharyngeal cancers (Cooper *et al*, 1984; Schmidt *et al*, 1997; Lengyel *et al*, 2005; Kim *et al*, 2007; Engelman *et al*, 2007; Li *et al*, 2012). *MET* mutations were first described in germline and sporadic papillary renal cell carcinomas (Schmidt *et al*, 1997). Although *MET* mutations are in fact rare, one study identified mutations in 30% of cancers of unknown primary origin (Stella *et al*, 2011). *MET* amplification appears to be particularly common in lung carcinomas treated with anti-EGFR therapy, where 21-22% of tumours show amplification of chromosome 7q, in which *MET* resides (Engelman *et al*, 2007; Bean *et al*, 2007).

1.5.5 Role in breast cancer

In the normal breast, c-Met is expressed in the mammary epithelium and stromal cells but not in the stroma itself (Jin *et al*, 1997; Lindemann *et al*, 2007). HGF, being a secreted protein has been identified by IHC in mammary epithelial cells, fibroblasts, blood vessel walls and in the acellular stroma (Jin *et al*, 1997; Lindemann *et al*, 2007). C-Met expression shows a spectrum of intensity in healthy and diseased breast tissue: low levels are seen in normal/hyperplastic breast tissue, moderate levels in DCIS and the highest expression is seen in invasive breast cancer (Jin *et al*, 1997).

Several studies have found increased c-Met expression in a sub-set of invasive breast cancers and associated this with a poor outcome. Camp *et al* and Tolgay Ocal *et al*, looked at samples from 113 and 324 patients respectively with lymph node negative breast cancer (Camp *et al*, 1999; Tolgay Ocal *et al*, 2003) and Ghoussoub *et al* studied 91 patients, composed of a mixture of lymph node positive and negative cases (Ghoussoub *et al*, 1998). The cause of c-Met over-expression is most likely transcriptional/post-translational regulation and hypoxia-induced, since amplification of the *MET* gene is not a common event (Carracedo *et al*, 2009). The transcription factor, hypoxia-inducible factor 1α (HIF1α) has been correlated with c-Met and a poor outcome in a series of 104 node-negative breast cancers and it has been put forward that tumour hypoxia increases c-Met expression via HIF1α (Chen *et al*, 2007).

In contrast to its role as a poor prognostic factor in breast cancer, evidence linking c-Met to BL cancer is more limited. In 2009, two studies utilising different mouse models of activated c-Met found that *MET* gene expression in the resultant mammary tumours clustered with the BL sub-type (Graveel *et al*, 2009; Ponzo *et al*, 2009). In human cancers, a gene expression signature that includes *MET* over-expression has been shown to separate BL from luminal cancers (Charafe-Jauffret *et al*, 2006) and high protein expression of c-Met on IHC has been significantly associated with the BL sub-type (Graveel *et al*, 2009).

1.5.6 Anti-c-Met therapy

There are several different ways of targeting the c-Met signalling pathway: 1) kinase inhibitors (KIs), 2) antibodies directed against c-Met and 3) HGF inhibitors, such as anti-HGF antibodies (Gentile *et al*, 2008; Nakamura *et al*, 2011; Figure 1.10).

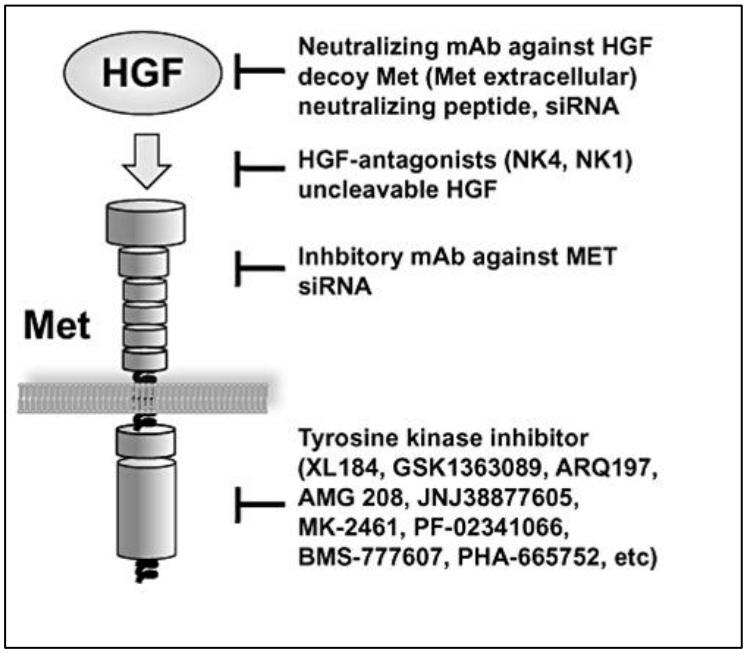

Figure 1.10: Strategies for targeting HGF/c-Met in anti-cancer treatment. There are several different methods of antagonising c-Met signalling. Amongst those under investigation are anti-HGF therapies (neutralising antibodies against HGF and antagonists of the ligand) as well as antibodies directed against the receptor itself. Many investigators have focused on the tyrosine kinase inhibitors such as Cabozantinib (XL184) and ARQ197, which are currently being investigated as possible breast cancer treatments (ClinicalTrials.gov, 2014) (figure reproduced with permission, Nakamura *et al*, 2011; Copyright (2011), John Wiley and Sons).

One of the first targeted small molecule inhibitors of c-Met to be developed was SU11274, an adenosine triphosphate (ATP)-competitive inhibitor of Met kinase (Sattler *et al*, 2003). SU11274 selectively inhibits c-Met without inhibition of PDGFβ and with only 2% inhibition of FGFR-1 at the IC_{50} for c-Met (Sattler *et al*, 2003). Compared to c-Met, the inhibitory effect of SU11274 against Ron (the tyrosine kinase which c-Met is most closely related to) is 10 times less potent (Wang *et al*, 2003). *In-vitro* studies have demonstrated that the inhibitory effect of SU11274 extends to several cellular processes regulated by the HGF/c-Met signalling axis, including HGF-dependant cell proliferation and motility (Sattler *et al*, 2003; Wang *et al*, 2003). Moreover, SU11274 reduces phosphorylation of key components of the PI3K signalling pathway, resulting in increased apoptosis and induction of G_1 cell cycle arrest (Sattler *et al*, 2003). In addition, tubulogenesis assays have shown that HGF-mediated formation of invasive tubular structures by rat intestinal epithelial-1 (RIE-1) cells is inhibited by SU11274 (Wang *et al*, 2003). Although SU11274 is not considered to be a candidate for *in-vivo* development (Wang *et al*, 2003), these *in-vitro* studies demonstrated the potential for small molecule inhibitors of c-Met as a novel form of cancer treatment.

Currently, numerous compounds are being evaluated in clinical trials (ClinicalTrials.gov, 2014), although many are still in their early phase. However, four agents that show particular promise are ARQ197 (also known as tivantinib), AMG 102 (rilotumumab), MetMab (onartuzumab) and PF-2341066 (crizotinib) (Yap and de Bono, 2010; Gordon *et al*, 2010; Yap *et al*, 2011; Sequist *et al*, 2011; Yano and Nakagawa, 2014).

Tivantinib belongs to the c-Met KIs class of anti-c-Met therapies (Cecchi *et al*, 2010). Unlike most KIs which compete for the ATP binding site, thus preventing phosphorylation, tivantinib is a non-ATP competitive c-Met inhibitor (Cecchi *et al*, 2010; Yap *et al*, 2011). A phase I trial of tivantinib in 51 patients with solid tumours found the inhibitor to be well tolerated, with fatigue, nausea and vomiting being the most common adverse effects (Yap *et al*, 2011). Furthermore, when pre-treatment and 'on-treatment' tumour biopsies were compared, there was a reduction in total and phosphorylated c-Met expression in the 'on-treatment' samples suggesting tivantinib inhibited intra-tumoural c-Met signalling (Yap *et al*, 2011).

Studies describing frequent *MET* amplification in non-small cell lung carcinomas (NSCLC) resistant to anti-EGFR therapy (Engelman *et al*, 2007; Bean *et al*, 2007) stimulated interest in combined anti-c-Met/anti-EGFR strategies (Sequist *et al*, 2011). A phase II randomised trial in NSCLC patients, consisting of a combined tivantinib/anti-EGFR (erlotinib) arm and an erlotinib plus placebo arm found prolonged progression-free survival in the tivantinib/erlotinib (ET) arm (Sequist *et al*, 2011). Notably, the ET combination was particularly efficacious in patients with *KRAS* mutations (Sequist *et al*, 2011). Since *KRAS* mutations confer resistance to erlotinib (Massarelli *et al*, 2007), the authors proposed that tivantinib may increase the number of NSCLC patients who may benefit from erlotinib-based treatment (Sequist *et al*, 2011).

AMG 102 is a fully humanised HGF/SF neutralising monoclonal antibody (Yap and de Bono, 2010; Gordon *et al*, 2010). In a phase I study looking at the safety, pharmacokinetics and pharmacodynamics of AMG 102 in 40 patients with advanced solid cancers (including four breast cancer patients), AMG 102 was found to be safe and well tolerated (Gordon *et al*, 2010). In this study, the maximum tolerated dose

was not reached and although anti-tumour activity was not a key study objective, at least half of the ovarian cancer patients showed a reduction in tumour size or in the serum marker CA-125 (Gordon *et al*, 2010). Phase II studies are now underway, assessing AMG 102 alone and in combination with other therapies (Yap and de Bono, 2010). One criticism of anti-HGF therapies is that they only antagonise HGF-mediated c-Met activation (Gentile *et al*, 2008) so their efficacy would be limited in tumours where c-Met is activated by HGF-independent processes such as *MET* amplification or mutation.

MetMab is an anti-c-Met monoclonal antibody (Yano and Nakagawa, 2014). Unlike many other anti-c-Met antibodies, MetMab is monovalent so it does not promote dimerisation when it binds to c-Met, thus avoiding agonistic effects associated with similar therapies. MetMab is currently being trialled in lung, colon and breast cancer (Yano and Nakagawa, 2014). Crizotinib is an anaplastic lymphoma kinase inhibitor which is also possesses anti-c-Met activity (Yano and Nakagawa, 2014). Crizotinib has been approved for the treatment of NSCLCs harbouring the *EML4-ALK* fusion gene but it has also been shown to be effective in a NSCLC patient with no *ALK* rearrangement but with de novo *MET* amplification (Yano and Nakagawa, 2014; Ou *et al*, 2011).

Turning to breast cancer, tivantinib (ClinicalTrials.gov Identifier: NCT 01542996), another c-Met KI – cabozantinib (also known as XL184; ClinicalTrials.gov Identifier: NCT 01738438) and MetMab (ClinicalTrials.gov Identifier: NCT 01186991) are currently being investigated for the treatment of metastatic TN breast cancer (ClinicalTrials.gov, 2014).

While the sheer number of anti-c-Met/HGF therapies currently being evaluated and the results of early clinical trials offer considerable promise, a key consideration is how to identify which patients are likely to gain from these specific treatments (Cecchi *et al*, 2010).

Many of the challenges that have hindered the introduction of anti-EGFR therapy into breast cancer treatment regimens (Burness *et al*, 2010) may also apply to anti-c-Met therapy, particularly the lack of studies validating methods of assessing expression and/or activity of c-Met (Gherardi *et al*, 2012). C-Met expression/activation is often ignored in clinical trial study design, but appropriate patient stratification is a necessary part of improving cancer therapy (Gherardi *et al*, 2012).

2.0 Study Introduction

The main objective of this study is to investigate the significance of c-Met expression and activation in invasive breast cancer, with particular reference to BL breast cancer in view of the poor prognosis and limited treatment modalities for patients with these tumours.

Although several studies have linked c-Met over-expression with a poor outcome in breast cancer, the majority of these were based on a relatively small cohort of patients and few have looked at more than 200 subjects (Ghoussoub *et al*, 1998; Camp *et al*, 1999; Tolgay Ocal *et al*, 2003; Chen *et al*, 2007). Similarly, studies describing higher levels of c-Met in the BL sub-type have looked at limited numbers of patients and/or not fully taken into account the impact that relevant confounding factors may have had on their analyses (Ponzo *et al*, 2009; Graveel *et al*, 2009).

Increasingly, tissue microarrays (TMAs) are being used by researchers for immunohistochemical analysis because of their many advantages in the evaluation of biomarkers. These include: the ability to analyse large numbers of samples in a rapid, efficient process that is cost-effective and results in less experimental bias because all samples are stained at the same time (Pinder *et al*, 2013). When accompanied by clinical, pathological and other biomarker data together with long-term follow-up, TMAs represent a powerful resource in the assessment of prognostic and predictive markers in cancer research.

A valid criticism of biomarker studies in general is that surprisingly few tumour markers progress through the clinical trial process, given the number of published studies describing promising new targets (McShane *et al*, 2005; Brennan *et al*, 2007). In an effort to correct this anomaly, guidelines have been compiled with

specific reference to key elements of study design. These include recommendations on study methodology (describing the characteristics of the study population), statistical analysis (such as the handling of missing data and cut-point determination) and data analysis (relationship of the given marker to prognostic variables and multivariate analysis) (McShane *et al*, 2005). The aim of these guidelines is to promote transparency in the field of biomarker analysis, allowing the wider community to evaluate effectively the impact of such studies (McShane *et al*, 2005). Adherence to such guidelines is now a requirement of some journals (Hayes *et al*, 2006).

Taking these points on board, the current study will seek to clarify and confirm the significance of c-Met expression using TMAs constructed from two separate, well-characterised breast cancer cohorts, comprising samples from over 2000 patients.

The autophosphorylation of RTKs that follows ligand binding is pivotal in the subsequent activation of downstream signalling pathways that become hijacked in oncogenesis (Hunter, 2009). However, to date studies looking at RTK phosphorylation have struggled to demonstrate the prognostic and predictive utility of measuring protein phosphorylation and whether this is superior to measuring expression of the receptor (Blokzijl *et al*, 2010). This may be because the phospho-antibodies used in conventional assays were limited by poor specificity (Blokzijl *et al*, 2010).

The recent development of a novel proximity ligation assay (PLA) offers the opportunity to quantify protein phosphorylation with a high degree of sensitivity and specificity (Söderberg *et al*, 2008). Using this new technology, I will quantify c-Met

phosphorylation in our ‘in-house’ cohort of invasive breast cancers and discuss the relationship with prognostic and molecular parameters.

With over 50 different breast cancer cell lines (BCLs) now available (Neve *et al*, 2006), researchers are in a position to select specific BCLs that have similar molecular features to the primary tumours they are studying. Using models of BL breast cancer, the current study will appraise the functional and phenotypic influence of the HGF/c-Met pathway in this sub-type.

To make interpretation easier, this thesis will be divided into 2 parts. In the first part I will outline the steps I have taken to validate the antibodies and techniques that will subsequently be applied to the study cohort of breast cancers. I will also explain my choice of BCLs, which will then be used to model HGF-mediated effects *in-vitro*.

In the second part I will address the following study aims:

1) Establish definitively whether c-Met expression is associated with the BL sub-type in a large series of breast cancers.

2) Confirm whether c-Met expression is an independent poor prognostic factor in breast cancer and describe its relationship to established prognostic factors.

3) Measure c-Met activity using the PLA in a cohort of breast cancers and determine the prognostic value of this assay in FFPE samples.

4) Study the functional and phenotypic effects of HGF-mediated c-Met phosphorylation using *in-vitro* models of BL breast cancer.

It is hoped that the data produced from this study will be useful in the development of anti-c-Met therapy and in the design of future clinical trials.

3.0 Validation of the Methods: Immunohistochemistry

3.1 Introduction

The technique of immunohistochemistry (IHC), which amalgamates the two fields of immunochemistry and tissue morphology has developed greatly over the last decades and is now a key part of diagnostic pathology and research (Buchwalow and Böcker, 2010). New approaches to antigen retrieval, signal amplification and reducing background staining, together with the proliferation in antibodies available have increased the complexity and applicability of IHC, resulting in many possibilities for each step in the technique.

The choice of primary antibody is of course a crucial decision, not only in terms of the specific epitope recognised by the antibody, but also the clonality and species they are raised in: monoclonal antibodies are usually produced in mice and result in high specificity whereas the polyclonal rabbit antibodies generally demonstrate better antigen recognition (Buchwalow and Böcker, 2010).

The widespread availability of formalin-fixed paraffin-embedded (FFPE) tissue from pathology laboratories and tissue banks makes FFPE sections a valuable resource for researchers. However, the process of formalin fixation may alter protein structure, rendering epitopes inaccessible to certain antibodies and resulting in a negative result on IHC (Montero, 2003; Buchwalow and Böcker, 2010). The ideal method of antigen retrieval depends on several factors including method of fixation, type of tissue and the epitope itself (Buchwalow and Böcker, 2010).

Numerous antibodies directed against c-Met are now commercially available (see Table 3.1 for the antibodies used in this study). Evidence from the literature suggests that different c-Met antibodies show a low level of reproducibility due to the features of the antibodies themselves or the effects of tissue fixation and paraffin embedding (Pozner-Moulis *et al*, 2007; Cecchi *et al*, 2010). Given this lack of reproducibility, every effort should be made to adequately validate c-Met antibodies (Pozner-Moulis *et al*, 2007; Gherardi *et al*, 2012) and this would seem particularly important in large clinical studies utilising archived material.

The aim of this initial study was to select an anti-c-Met antibody that showed reproducible staining, confirm its specificity for the receptor and validate it for subsequent use on the main study cohort of invasive breast cancers.

3.2 Materials and Methods

3.2.1 Tissue samples

3.2.1.1 Formalin-fixed, paraffin-embedded sections (FFPE)

3.2.1.1.1 Whole breast cancer sections

Whole sections from 11 invasive breast cancers from the Barts Cancer Institute Breast Tissue Bank were used to validate c-Met antibodies. These FFPE sections were paired with snap-frozen sections (section 3.2.1.2).

3.2.1.1.2 Tissue microarrays: invasive breast cancers

In addition to whole breast cancer sections, sections of previously constructed tissue microarrays (TMAs) were also available. These TMAs represent part of the 'in-house' Homerton cohort (section 6.0) and included cores from 181 patients.

3.2.1.1.3 Tissue microarrays: renal cell carcinoma (RCC)

FFPE tissue from patients (n=56) enrolled into 3 separate prospective phase II clinical trials investigating the effects of anti-VEGFR therapy in metastatic clear cell renal cell carcinoma (RCC) were included in this analysis. Patients in these trials received either sunitinib (50mg, 4 times in 2 weeks) or pazopanib (800mg once daily) (Boleti *et al*, 2012; Powles *et al*, 2011; Bex *et al*, 2011) before planned nephrectomy (institutional review board approval: EudraCT 2006-004511-21, 2006-006491-38 and 2009-016675-29).

Paired tissue samples were available in the form of excess tissue from renal biopsies (pre-treatment samples) and post-treatment nephrectomies (post-treatment samples), arranged into TMAs.

3.2.1.2 Frozen sections

Tumour tissue snap-frozen in liquid nitrogen was available from a cohort of 11 invasive breast carcinomas sampled in the fresh state. These samples also formed part of the Barts Cancer Institute Breast Tissue Bank and were paired with the FFPE tissue in section 3.2.1.1.1.

3.2.2 Antibodies

See Table 3.1 for details of the primary antibodies used in this study. The anti-c-Met antibodies targeted different parts of the receptor, including the intracellular and extracellular regions (Figure 3.1).

Antibody	Target	Supplier	Species	Dilution (IF, IHC)	Dilution (WB)
CVD13	c-Met	Invitrogen	Rabbit	1:100	1:500
8F11	c-Met	Novocastra	Mouse	1:150	n/a
3D4	c-Met	Invitrogen	Mouse	1:100	n/a
AF276	c-Met	R&D Systems	Goat	1:50	n/a
B-6	HSC70	Santa Cruz	Mouse	n/a	1:10000
CD31	CD31	AstraZeneca	Mouse	1:600	n/a

Table 3.1: Primary antibodies utilised in this IHC validation study. Abbreviations: IF = immunofluoresence, IHC = immunohistochemistry, WB = western blot, n/a = not applicable.

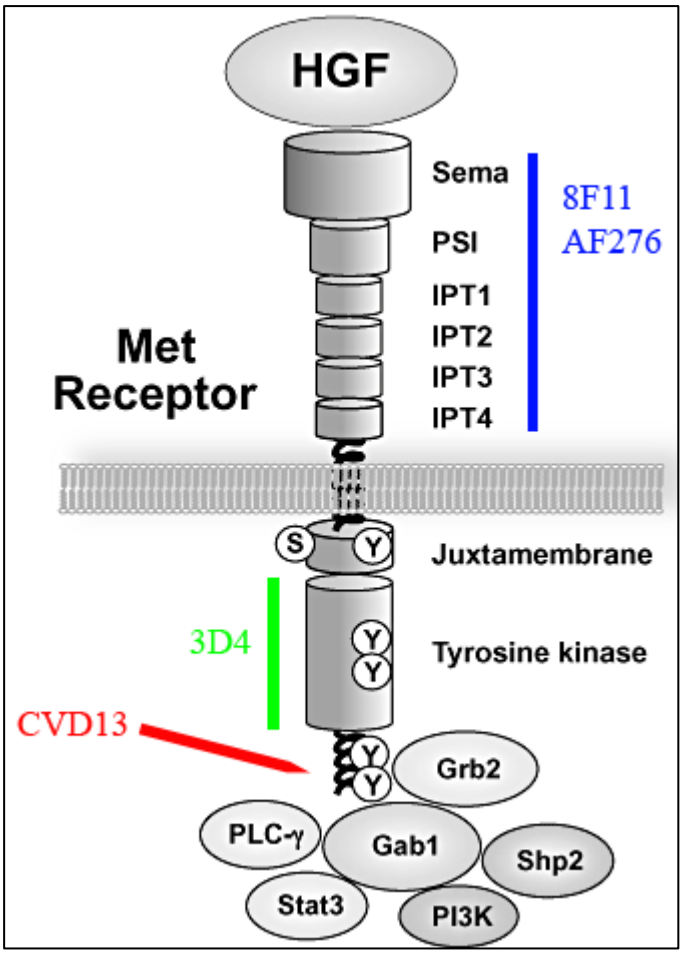

Figure 3.1: Binding sites of commercially available anti-c-Met antibodies. The four anti-c-Met antibodies tested in this study targeted different parts of c-Met. The 8F11 (Novocastra Laboratories, 2010) and AF276 (Dietz *et al*, 2013) bind somewhere in the extracellular domain. The 3D4 antibody binds to the region between amino acid (AA) 1200 and AA 1270 (personal communication with manufacturer) and CVD13 binds to the C-terminus of the receptor, in the region of AA 1340 (personal communication with manufacturer). Figure modified from Nakamura *et al*, 2011.

3.2.3 Immunohistochemistry (IHC)

3.2.3.1 Paraffin sections

The chemicals used were from Fisher Scientific, Loughborough, UK unless otherwise stated. Unstained paraffin sections were de-waxed by first warming the slides to 60^{o}C in an incubator for 10 minutes and placing them in xylene for 10 minutes. The sections were re-hydrated through graded alcohol solutions and placed in 3% hydrogen peroxide solution for 10 minutes to block endogenous peroxidise activity. Antigen retrieval was performed by microwave treating the sections in 0.1M citrate buffer (CVD13, 8F11, 3D4, AF276, CD31) at pH 6 for 10 minutes. The slides were rinsed in water.

3.2.3.2 Frozen sections

Frozen sections were retrieved from the -80^{o}C freezer and allowed to warm to room temperature. The sections were fixed in 4% paraformaldehyde (PFA; Cell Path, Newton Powys, UK) for 5 minutes in a fume hood. Endogenous peroxidise activity was blocked by placing the sections in 3% hydrogen peroxide solution for 10 minutes. Slides were rinsed in water and then treated as in section 3.2.3.3.

3.2.3.3 Blocking, antibody incubation and developing

After washing in phosphate buffered saline (PBS), normal serum (horse for mouse primary antibodies and goat for rabbit primary antibodies) was deposited on the sections for 15 minutes at a dilution of 1:75 in 1% bovine serum albumin (BSA; Sigma-Aldrich, Dorset, UK)/PBS to block non-specific antibody binding. After draining the sections, the primary antibody was incubated for 1 hour at room temperature (see Table 3.1 for dilutions). Following PBS washes, the secondary

biotinylated antibody (Vector Laboratories, Peterborough, UK) was applied to the sections at a dilution of 1:200 for 40 minutes. The sections were washed in PBS then incubated with avidin-biotinylated peroxidase complex (Vectastain ABC kit, Vector Laboratories) for 30 minutes. The reaction was developed using a DAB kit (Vectastain, Vector Laboratories), after which sections were counterstained with haematoxylin (Sigma-Aldrich), rinsed and dehydrated through alcohol to xylene and mounted with coverslips. Negative controls consisted of a TMA containing 10 invasive breast cancer samples in triplicate, with omission of the primary antibody.

IHC on the renal tissue was performed by Mr Kevin Sharpe (KS).

3.2.3.4 Scoring system

C-Met IHC on breast tissue was scored using a semi-quantitative approach, combining numerical scores for intensity and area of reactivity in the cytoplasmic and membranous compartments. Intensity was scored on a scale of 0-3 (0 = negative, 1 = weak, 2 = moderate, 3 = strong) and area on a scale of 0-4 (0 = <1%, 1 = 1-25%, 2 = 26-50%, 3 = 51-75%, 4 = >75%), giving a total score between 0 and 14. All cores were scored twice by me, on two separate occasions to ensure reproducibility.

C-Met IHC on renal carcinoma cells was scored using a similar approach: staining on the tumour cells was graded in intensity (0 = negative, 1 = weak, 2 = moderate, 3 = strong) and this was multiplied the percentage area of tumour reactivity (0-100%) to give a combined score between 0 and 300.

For quantification of c-Met on tumour-associated blood vessels, sequential sections were first stained for the endothelial marker CD31. The total number (identified by CD31 positivity in tubular structures) was then counted. Any blood vessel reactive

for c-Met (on the adjacent section) was regarded as positive and c-Met positive vessels were then expressed as a percentage of total vessels. IHC on renal tissue was scored by KS and me.

3.2.4 Tissue culture

3.2.4.1 Cell lines and media requirements

The basal-like (BL) breast cancer cell line (MDA-MB-468) utilised in this study was previously established in the laboratory. Cells were cultured in Dulbecco's Modified Eagle's Medium (DMEM; Sigma-Aldrich), supplemented with 10% fetal calf serum (FCS; PAA, Sommerset, UK).

3.2.4.2 Propagation and sub-culture

Cells were grown in T75 flasks (Fisher Scientific) and incubated at 37^{o}C in 8% CO^{2}. The cells were monitored using an inverted phase contrast microscope. Growth media was changed every 3-4 days unless the cells were confluent. At approximately 80% confluence, cells were passaged by removing and discarding the media and adding 3 mls of 0.25% (w/v) Trypsin – 0.53 mM EDTA solution (PAA). The flask was placed at 37^{o}C for 5-10 minutes until the cells had detached. The cells were then washed in 3 mls of media and spun down in a centrifuge for 3 minutes at 1200 rpm into a pellet form. The supernatant was discarded and the pellet re-suspended in 10 mls of media prior to being transferred into a new T75 flask at a sub-cultivation ratio of 1:3.

3.2.4.3 Preservation and de-frosting

Cells were preserved in either a -80^{o}C freezer (if going to be used within weeks of freezing) or in liquid nitrogen for longer-term storage. Freezing media was

formulated from 50% growth media, 40% FCS and 10% dimethyl sulphoxide (DMSO) and the pellet was re-suspended in 1ml of freezing media per cryovial. The cryovial was cooled slowly in a foil-wrapped polystyrene container. For re-constitution, frozen cells were thawed rapidly by placing the cryovial in a water bath set at 37^{o}C. The DMSO was washed off by gently mixing the vial contents with 1ml of media before adding the suspension to 9mls of media in a 15ml tube. The cells were centrifuged at 1200 rpm for 3 minutes, re-suspended in 10mls of media and added to a new T75 flask.

3.2.4.4 Knock-down of c-Met

MDA-MB-468 cells were trypsinised at approximately 80% confluence and re-suspended in an equal volume of DMEM. Cells were counted using a haemocytometer; 10µl of cell suspension was pipetted into a well in the haemocytometer and the number of cells per 4x4 grid were counted under inverted phase contrast microscopy. An average cell count of 2 4x4 grids was taken and then multiplied by 10000 to give the number of cells per ml. Approximately 1.5 million cells were transferred into a 1.5ml eppindorf and centrifuged at 1200 rpm for 3 minutes. The supernatant was discarded and the cell pellet was mixed with 100µl Nucleofector Solution V (Lonza, Berkshire, UK) and 2µg of Met siRNA (Dharmacon, Leicestershire, UK). Scrambled siRNA (Dharmacon) was used as a control. After homogenisaton, the solution was transferred to a cuvette and placed in the Nucleofector device (Lonza) and Nucleofector Programme X-005 was selected. Upon completion, 500µl of growth media was added to the cuvette and the solution was homogenised. The cell suspension was placed in a 6-well or 24-well plate at a

concentration of 200000 cells per well or 20-30000 cells per well respectively. The plates were then incubated at 37^{o}C, 8% CO^{2} for 2-4 days.

3.2.5 Western blot

3.2.5.1 Cell lysis

Once cells were confluent, medium was removed and culture plates washed in cold PBS, before adding cold radioimmunoprecipitation assay (RIPA) buffer (50mM Tris-HCl pH 8.0, 150 mM NaCl, 1mM ethylenediaminetetraacetic acid (EDTA), 1% Igepal CA-630 (NP-40; Calbiochem, Millipore, Nottingham, UK), 0.1% sodium dodecyl sulphate (SDS)) mixed with a cocktail of protease inhibitors (Calbiochem) at 1:100. The plate was scrapped and the suspension was placed in a fresh eppendorf and incubated on ice for 20 minutes. The eppendorf was centrifuged at 10000 rpm, 4^{o}C for 5 minutes. The pellet was discarded and the supernatant was placed in a fresh eppendorf. The protein concentration was assessed with a Bio-Rad DC Protein Assay (Bio-Rad Laboratories, Hertfordshire, UK). Cell lysates and BSA standards (diluted in distilled water) were added at 5µl volumes to a 96-well plate in triplicate, before adding 25µl of solution A/S (1000µl reagent A and 20µl reagent S) per well followed by 200µl of reagent B per well. The reagents were left to incubate for 10 minutes at room temperature before reading on a microplate reader (Labtech) at 620 nm. An absorbance versus concentration curve was plotted using the BSA standards and this was used to estimate the sample protein concentration. The samples were stored at -20^{o}C until needed.

3.2.5.2 SDS Gel Electrophoresis

An SDS-Polyacrylamide gel electrophoresis (SDS-PAGE) gel was prepared, with component volumes adjusted depending on the molecular weight of the protein of

interest, for c-Met (~145kDa) a 6% gel was cast. The resolving gel solution (5.3 mls distilled water (dH_2O), 2 mls 30% acrylamide mix (National Diagnostics, Hessle, UK), 2.5 mls 1.5M tris (pH 8.8), 100µl 10% SDS, 100µl 10% ammonium persulphate (APS; National Diagnostics) and 8 µl TEMED (National Diagnostics)) was dispensed into a 1mm thick gel cassette (Invitrogen) and 1ml of dH_2O was overlain to allow sample diffusion. After the gel was set (approximately 10 minutes later), the dH_2O was poured off. A 5% SDS-PAGE stacking gel solution (2.1 mls dH_2O, 500 µl 30% acrylamide mix, 380 µl 1M tris (pH 6.8), 30 µl SDS, 30 µl 10% APS and 3µl TEMED) was added to the cassette, a 1mm 10-15 well comb was inserted and the gel was left to set for about 10 minutes. The comb was removed and the cassette placed in a gel tank containing 500mls of running buffer (50 mls tris-glycine SDS in 450 mls dH_2O).

After thawing, 10µg of each protein sample was added to 4X sample buffer (5% SDS, 20% buffer (0.5M tris, 0.2M NaH_2PO_4 pH 7.8), 5% β-mercaptoethanol (Promega, Hampshire, UK), 50% glycerol, 0.01% bromophenol blue (Sigma-Aldrich) and 20% dH_2O) to give an end concentration of 1X. The samples were then boiled for 6 minutes at 98^{o}C. The samples were loaded into the gel, along with 7.5µl of PageRuler pre-stained protein ladder (Fermentas, Loughborough, UK) and run for 90 minutes at 125V, room temperature. Transfer buffer (50 mls tris-glycine buffer in 450 mls 80% dH_2O/20 % MeOH) was prepared, transfer sponges and a nitrocellulose membrane (Amersham Biosciences, Buckinghamshire, UK) were soaked in transfer buffer while the cassette was removed from the gel tank and the stacking gel separated. A sandwich was created within the transfer apparatus, containing wet sponges, filter paper, the gel and pre-soaked nitrocellulose membrane, with the membrane immediately adjacent to the gel. Any bubbles were

removed by gently rolling a glass tube along the sandwich before sealing the lid and placing the apparatus into the inner chamber of the gel tank. Transfer buffer was added to the top of the inner chamber and dH_2O added to the outer chamber before running at 30V for 90 minutes.

After transfer, the membrane was removed and blocked in 3% BSA/TBST (0.1% Tween 20 (Applichem, Leicestershire, UK) in TBS) for 1 hour with gentle rocking. The membrane was inserted into a 50ml centrifuge tube containing 7mls of primary antibody (diluted in 3% BSA/TBST) and incubated overnight at 4^oC on a roller mixer. The membrane was then washed in TBST three times for 15 minutes each time, after which the membrane was placed in a fresh 50ml centrifuge tube containing 7mls of secondary antibody (anti-rabbit/mouse IgG HRP, 1:1000; Dako, Cambridgeshire, UK) and incubated for 1 hour at room temperature on a roller mixer. The membrane was washed 3 times (15 minutes each) in TBST and the protein was visualised by developing in ECL detection (GE Healthcare, Hertfordshire, UK) reagent.

3.2.6 Immunofluorescence (IF)

Glass coverslips measuring 13mm in diameter were placed in a 24-well plate and MDA-MB-468 cells were seeded at a density of 30000 cells per well and incubated for 36 hours at $37^oC/8\%$ CO_2. Cells were rinsed in warm PBS before fixing in ice-cold methanol for 5 minutes. After rinsing in PBS, the cells were blocked and permeabilised in 0.1% Triton 100X (Alfa Aesar, Lancashire, UK)/2% BSA/ PBS for 15 minutes. The primary antibody (CVD13) was diluted 1:100 in 2% BSA/PBS and a 23µl droplet per cover-slip was placed onto parafilm. The cover-slips were retrieved from the 24-well plate and placed ‘cell side down’ on the droplet for 20

minutes at room temperature. The coverslips were washed 3 times in PBS and incubated with the secondary antibody diluted in 2% BSA/PBS at 1:200 (donkey anti-rabbit Alexa 488 (Invitrogen, Paisley, UK)) on parafilm for 20 minutes at room temperature. The coverslips were rinsed 3 times in PBS and once in distilled water before mounting on glass slides in DAPI Prolong Gold anti-fade reagent (Invitrogen). The mounting media was then allowed to polymerise overnight at 37^{o}C before visualising under fluorescence microscopy.

3.2.7 Statistical analysis

For the breast tissue samples, correlative statistics were performed using Spearman's correlation coefficient (IBM SPSS Statistics 19).

The Student's t-test was used to compare c-Met expression in renal tumour cells and tumour-associated blood vessels in the pre and post-treatment RCC groups. Statistical analysis on the renal tissue samples was performed by KS using Prism 5.

A p-value <0.05 was regarded as significant in all statistical analyses.

3.3 Results

Of the four commercially available c-Met antibodies tested (Table 3.1), only the CVD13 and 8F11 antibodies showed clean and reproducible tumour staining, with minimal background reactivity. The staining pattern was predominantly cytoplasmic but also membranous.

3.3.1 Correlation between CVD13 and 8F11 – breast tissue samples

There was a positive correlation between CVD13 and 8F11 IHC scores on pre-constructed 'in-house' TMA sections, comprising 181 samples (Spearman's coefficient = 0.294, p = 0.002). However, in several tumours reactivity for the antibodies was notably different (Figure 3.2).

An inverse correlation was seen when 8F11 FFPE scores on whole sections were compared with frozen sections from the same tumour (Figure 3.3), stained with either 8F11 or CVD13, although this wasn't statistically significant (Table 3.2, $p > 0.05$). In contrast, CVD13 FFPE scores showed a positive relationship with CVD13 or 8F11 frozen section scores (Table 3.2, $p > 0.05$), suggesting sub-optimal antigen retrieval for the 8F11 antibody.

Antibody	Processing method	Correl. with CVD13 (FFPE)	Correl. with 8F11 (FFPE)
CVD13	FFPE	n/a	-0.194
CVD13	Frozen	0.146	-0.346
8F11	FFPE	-0.194	n/a
8F11	Frozen	0.463	-0.418

Table 3.2: Correlation between anti-c-Met antibodies on FFPE and frozen sections. Spearman's correlation coefficients between FFPE and frozen sections using CVD13 anti-c-Met and 8F11 anti-c-Met antibodies (all p-values > 0.05). Abbreviations: FFPE = formalin-fixed, paraffin-embedded, n/a = not applicable.

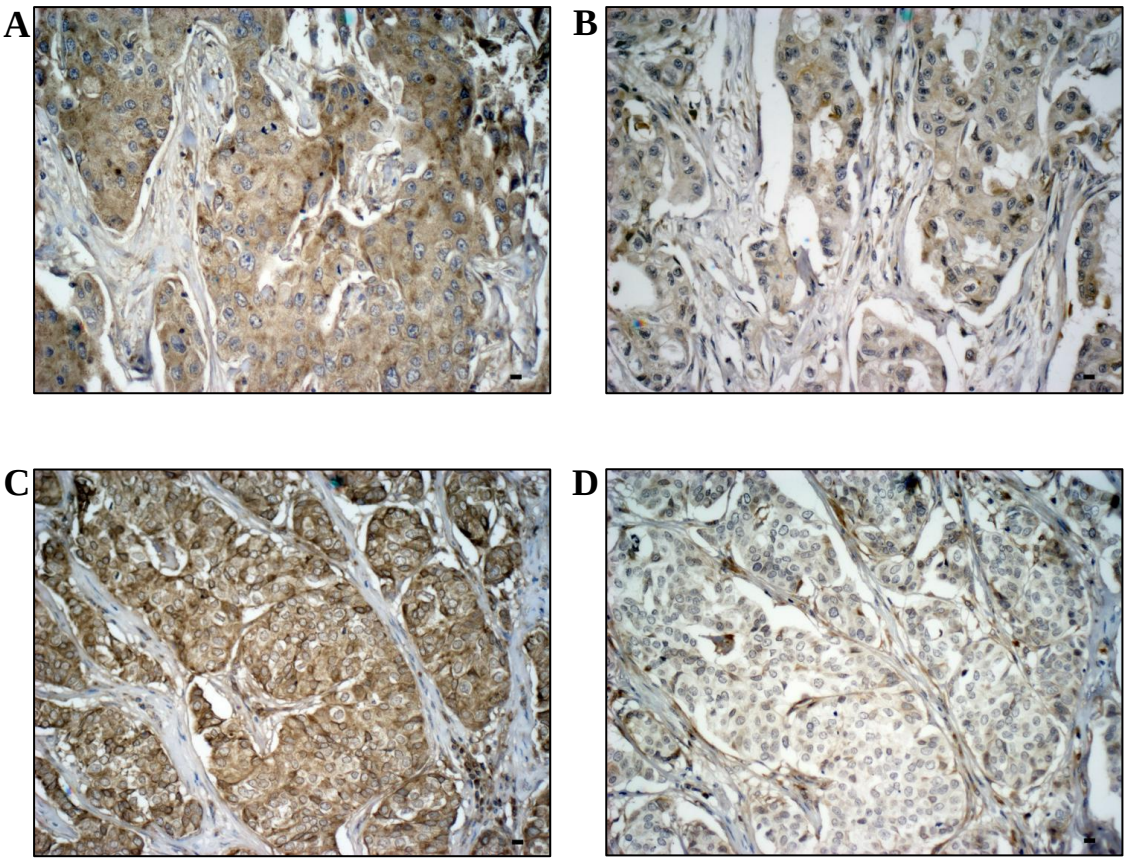

Figure 3.2: Variation in staining intensity of anti-c-Met antibodies. Photographs **A** and **B** are from the same tumour, stained with the mouse monoclonal antibody 8F11 and rabbit polyclonal antibody CVD13 respectively. Photographs **C** and **D** are of a different tumour, stained with 8F11 and CVD13 respectively. All photographs were taken with a x40 objective lens (scale bar = 10µm).

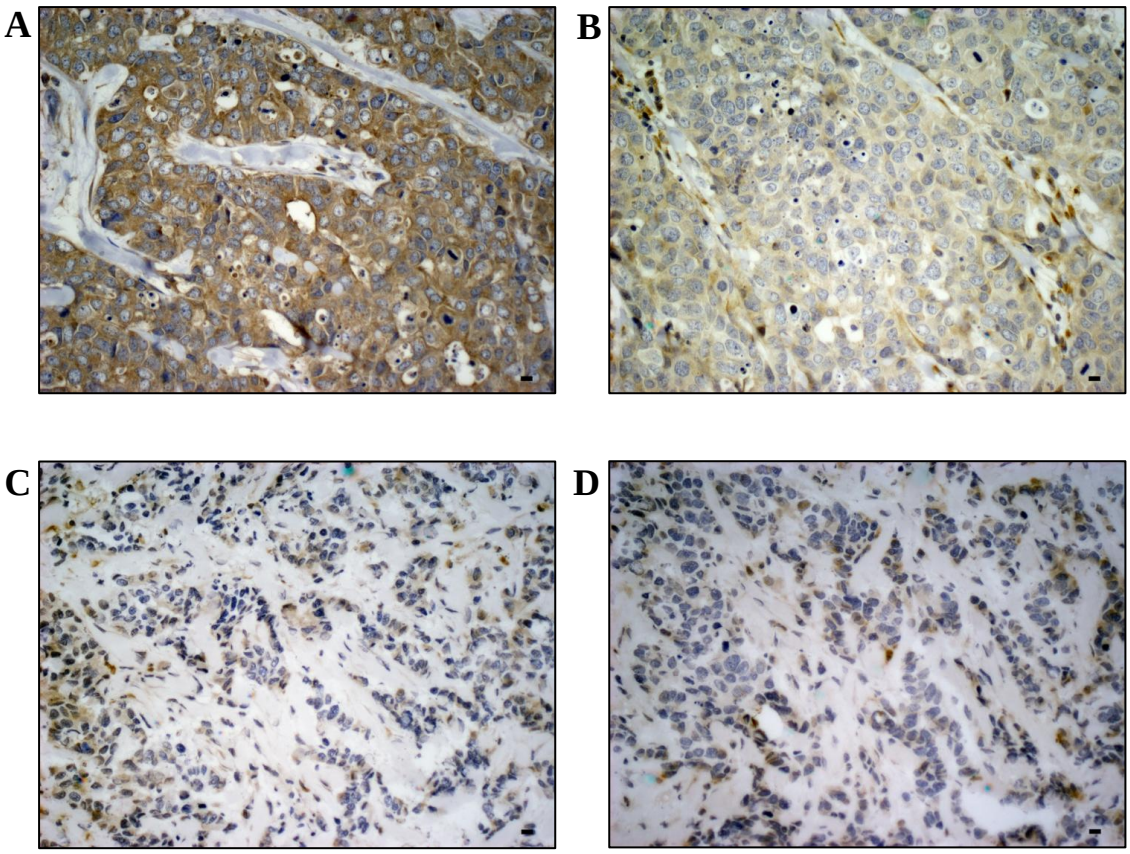

Figure 3.3: Anti-c-Met antibodies on FFPE and frozen sections. All photographs are of the same tumour. **A** and **B** are FFPE sections stained with 8F11 and CVD13 respectively, **C** and **D** are of frozen sections stained with 8F11 and CVD13 respectively. C-Met staining is considerably more intense in the 8F11 stained FFPE section compared with the other sections. All photographs were taken with a x40 objective lens (scale bar = 10µm).

3.3.2 Specificity of CVD13 – breast cancer cell line

Knock-down of c-Met resulted in a reduction in intensity of the band detected by CVD13 at western blot (Figure 3.4A) and a loss of membranous staining at immunofluorescence (Figure 3.4B and C), suggesting this antibody was specific for c-Met.

3.3.3 CVD13 in RCC – renal tissue samples

C-Met was expressed in tumour cells and endothelial cells (Figure 3.5). C-Met scores in pre-treatment renal tumour cells (mean score = 80.5, 95% CI = 0-210.5) were not statistically different from those in the post-treatment group (mean score = 77.5, 95% CI = 0-3.1, $p > 0.05$, Figure 3.6A). There were significantly more c-Met positive tumour-associated blood vessels in the post-treatment group (percentage of positive vessels = 1.9, 95% CI = 0-9.0) compared to the pre-treatment group (percentage of positive vessels = 0.4, 95% CI = 0-3.1, $p = 0.04$, Figure 3.6B).

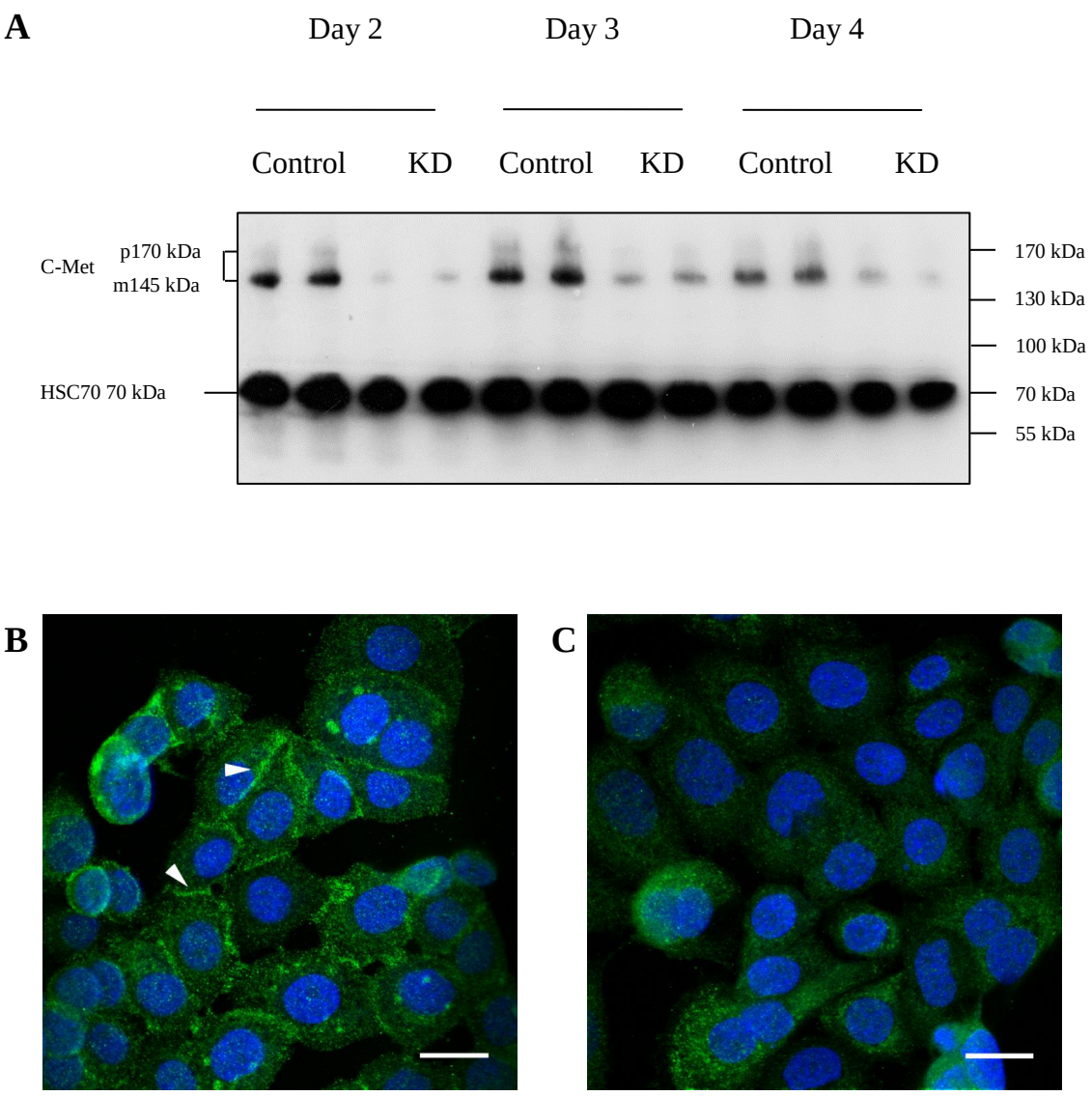

Figure 3.4: C-Met knock-down in MDA-MB-468 cells. **A** shows a western blot with partial loss of c-Met when the membrane is probed with CVD13 at 2,3 and 4 days following siRNA knock-down (lanes are in duplicate). C-Met is seen here in both the precursor (p170 kDa) and mature forms (m145 kDa). HSC70 is the loading control. Abbreviations: KD = knock-down. **B** shows MDA-MB-468 cells stained with CVD13 (in green), showing a predominantly membranous pattern (see arrows). **C** shows CVD13 staining in the same cells following siRNA knock-down, with absent membrane staining (immunofluorescence; confocal microscope, x63 objective under oil immersion; scale bars represent 20µm).

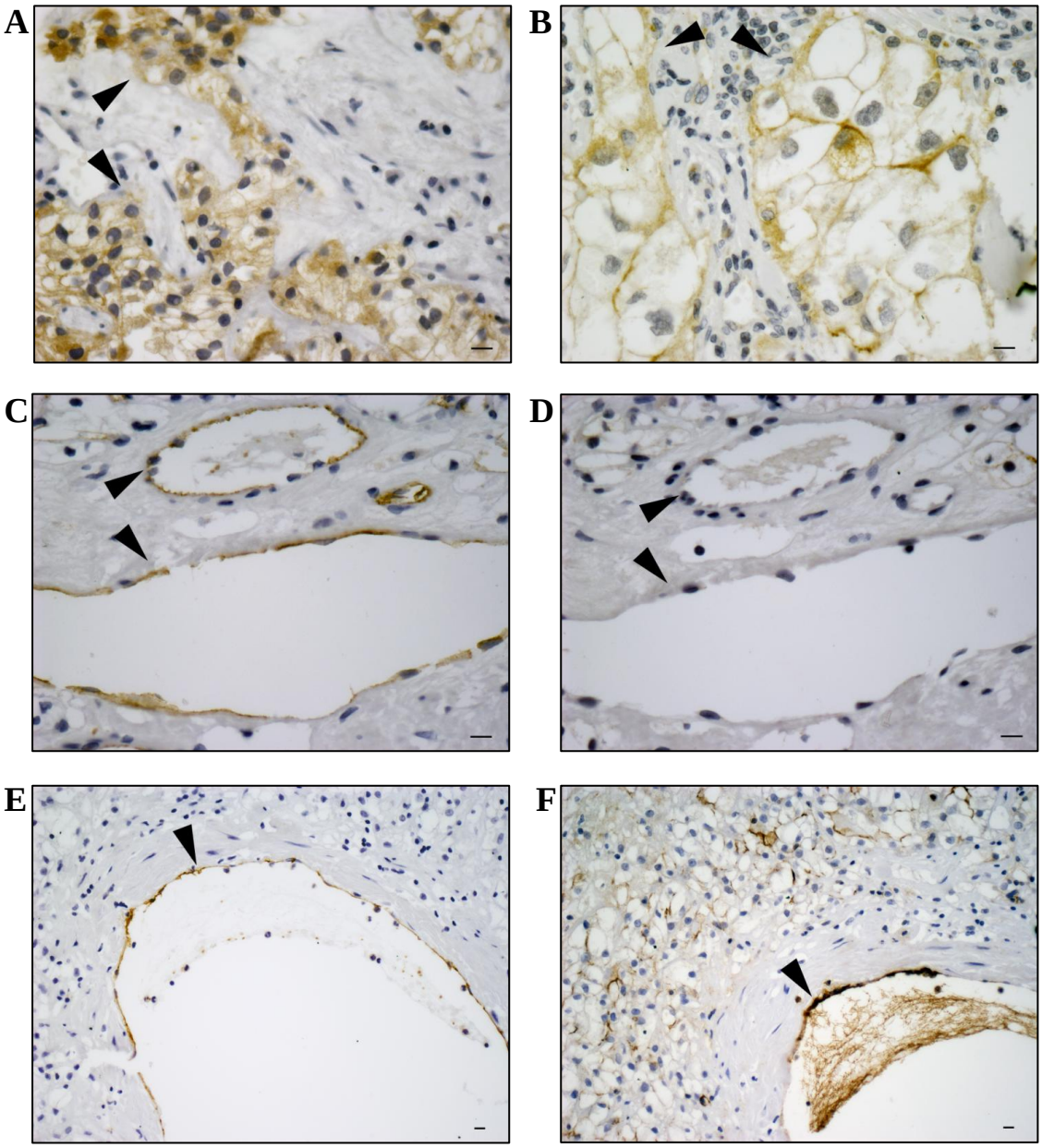

Figure 3.5: C-Met staining in renal tissue samples. IHC showing positivity for c-Met (CVD13) in pre and post-sunitinib tumour cells (**A** and **B** respectively, see arrows). IHC for CD31 in **C** and c-Met (CVD13) in **D**, showing c-Met negative vessels (see arrows) in a pre-sunitinib sample. IHC for CD31 in **E** and c-Met (CVD13) in **F**, showing a c-Met positive vessel in a post-sunitinib sample. **A-D** taken using a x40 objective, **E and F** taken with a x20 objective. All scale bars = 10µm.

A

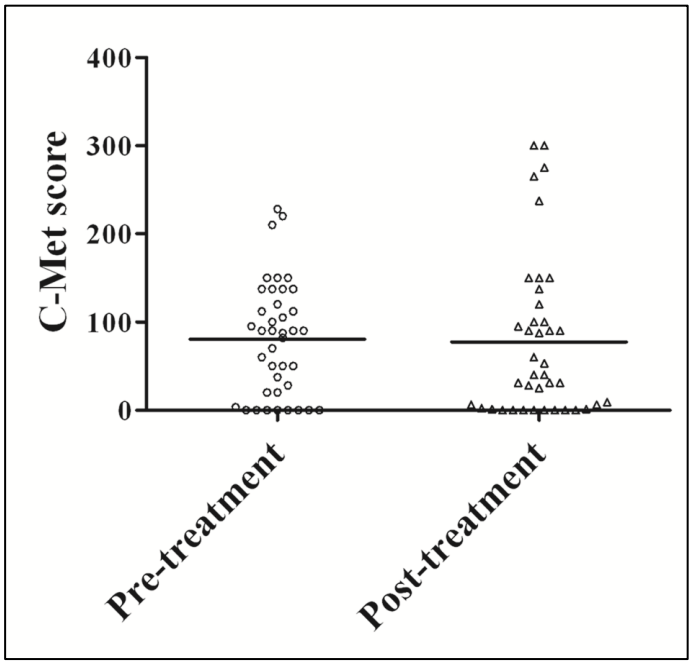

B

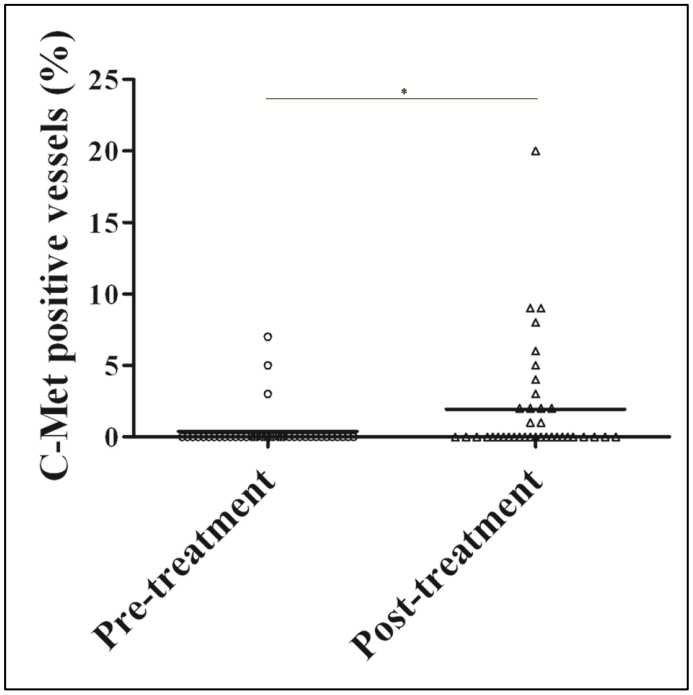

Figure 3.6: Quantification of c-Met expression in renal tissue. The scatter-plots show tumour cell c-Met scores (**A**) and percentage of vessels expressing c-Met (CVD13) (**B**) before and after treatment with a VEGFR inhibitor. Horizontal bars represent mean values. *: p=0.04.

3.4 Discussion

3.4.1 Selection of the primary anti-c-Met antibody: CVD13

The results of this validation study suggest the rabbit polyclonal antibody CVD13 is a reproducible and specific anti-c-Met antibody. Firstly, the staining pattern of CVD13 on FFPE (and frozen) sections of breast cancers – cytoplasmic and membranous decoration of tumour cells – is consistent with published studies that have evaluated c-Met expression using IHC on similar samples (Ghoussoub *et al*, 1998; Kang *et al*, 2003; Lengyel *et al*, 2005, Lindemann *et al*, 2007). Secondly, the positive correlation between CVD13 scores on FFPE and frozen sections indicates that the epitope recognised by CVD13 can be effectively retrieved in processed tissue using heat-induced antigen retrieval. Lastly, using si-RNA technology, knock-down of c-Met resulted in the loss of membrane staining and a less intense band when incubated with CVD13 at immunofluorescence and western blotting respectively.

The lack of a strong correlation between CVD13 and the 8F11 antibody on TMA sections was not entirely surprising as others have commented on the poor agreement between different c-Met antibodies (Pozner-Moulis *et al*, 2007). In a study looking at five antibodies directed against the intracellular domain of c-Met (including CVD13), Pozner-Moulis *et al* found that only two showed a good correlation (MAB3729 from Chemicon and C28 from Santa Cruz)(Pozner-Moulis *et al*, 2007). Whilst tumour heterogeneity for c-Met may in part explain this finding (Pozner-Moulis *et al*, 2007), other technical reasons may be responsible (Kang *et al*, 2003; Tolgay Ocal *et al*, 2003; Pozner-Moulis *et al*, 2007). Lot-to-lot variation has been

recognised by many workers, particularly with some polyclonal antibodies (Tolgay Ocal *et al*, 2003), but also with monoclonal ones, where staining the same spot of a tumour with different lots of the mouse monoclonal antibody 3D4 resulted in markedly different staining patterns (Pozner-Moulis *et al*, 2007). The binding characteristics of the antibody also seem to be a key consideration. In a study utilising antibodies raised against both the intracellular and extracellular regions of the c-Met receptor, Kang and co-workers found overall correlation but noted expression was dissimilar in many cases (Kang *et al*, 2003). Furthermore, they found that expression of the cytoplasmic tail and not the N-terminus had prognostic power at statistical analysis (Kang *et al*, 2003). This observation may in part explain the positive but not strong, correlation between 8F11 (which binds to the extracellular portion) and CVD13 (which recognises the cytoplasmic tail) in the TMA based component of this validation study and supports the decision to select CVD13 for further analysis.

3.4.2 CVD13 expression in renal cell carcinoma

Using renal tissue samples before and after patient treatment with the anti-VEGFR therapies sunitinib and pazopanib, it was possible to validate further the use of CVD13 in FFPE tissue. In this analysis, no difference was found between tumour cell c-Met expression before and after treatment, but there was a significant increase in c-Met positive tumour-associated blood vessels in post-treatment samples (Sharpe *et al*, 2013).

Others have looked at the effect of anti-VEGFR therapy on c-Met expression in tumour models (Sennino *et al*, 2012; Sennino *et al*, 2013; Cooke *et al*, 2012). In mouse models of pancreatic neuroendocrine tumours, treatment with sunitinib results

in increased tumour invasiveness and number of metastatic deposits (Sennino *et al*, 2012; Sennino *et al*, 2013). While these workers did identify vascular expression of c-Met after sunitinib treatment, it was only in the tumour cell compartment that higher levels of c-Met were identified (Sennino *et al*, 2012; Sennino *et al*, 2013). While the findings of this and the previous studies do differ, both would be consistent with the theory that targeting the endothelial/pericyte compartment with sunitinib results in vascular permeability leading to increased stromal pressure, reduced blood flow and hypoxia, and ultimately, induction of c-Met expression (Cooke *et al*, 2012).

3.4.3 Conclusion

In conclusion, CVD13 is a reproducible and specific anti-c-Met antibody. The staining characteristics of CVD13 on FFPE tissue from different organs are consistent with the published literature and taken together, these results validate this clone for use on the study cohort of breast cancer samples.

4.0 Validation of the Methods: Proximity Ligation Assay

4.1 Introduction

While phospho-specific antibodies may be used to assess receptor phosphorylation in fresh frozen samples using techniques such as western blotting, attempts to use these antibodies on FFPE samples have generally proven unreliable (Blokzijl *et al*, 2010; Koos *et al*, 2009; Dua *et al*, 2011). The use of phospho-specific antibodies in IF and IHC is limited by poor sensitivity and specificity, often resulting in difficulty identifying the protein (Jarvius *et al*, 2007; Blokzijl *et al*, 2010; Dua *et al*, 2011). Hence, there is a need to develop alternative, more reliable methods for quantifying receptor phosphorylation.

The proximity ligation assay (PLA) is a relatively novel assay that allows specific and sensitive detection of proteins, protein-protein interactions and post-translational modifications (including phosphorylation) in cells and tissues, with single molecule resolution (reviewed in Weibrecht *et al*, 2010). The PLA relies on the detection of a dual recognition event when both target molecules are in close proximity. Briefly, two primary antibodies raised in different species bind to their targets. Secondary antibodies with attached oligonucleotides (known as proximity probes) then bind to the primary antibodies. More oligonucleotides are then added, which are ligated into a circular DNA strand, creating a template for subsequent rolling circle amplification (RCA), forming 1000s of rolling circle products (RCPs) that can be visualised under fluorescence microscopy following the addition of fluorescently-labelled oligonucleotides (Figure 4.1).

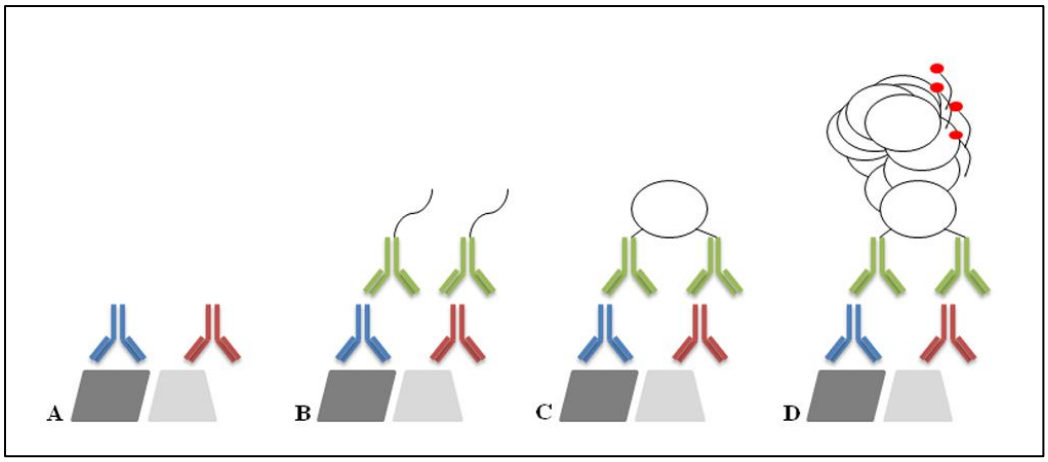

Figure 4.1: Diagram of the proximity ligation assay (PLA). In the first step (**A**) the primary antibodies (in red and blue), raised in different species, bind to their respective epitopes. In the second step (**B**), the species-specific secondary antibodies (proximity probes; in green) bind to the primary antibodies. These proximity probes are conjugated to an oligonucleotide chain that forms a closed circle of DNA when ligase is added, if the proximity probes are close together (**C**). In the final, rolling circle amplification (RCA) step, polymerase catalyses the amplification of the DNA template 1000s of times (**D**). This rolling circle product (RCP) can then be visualised under fluorescence microscopy after the addition of fluorescently-labelled oligonucleotides (seen as a red circle) that are complementary to part of the amplified DNA (reviewed in Weibrecht *et al*, 2010).

The PLA resembles another technique used to analyse protein interactions and post-translational modifications - Förster resonance energy transfer (FRET). FRET harnesses the energy transfer between two adjacent fluorophores acting as split reporter molecules: the donor (which has an emission spectrum with a longer wavelength than its excitation spectrum) and the acceptor (which has an excitation spectrum that overlaps with the emission spectrum of the donor (Weibrecht *et al*, 2010). Detection of the acceptor emission spectrum (following donor excitation) at fluorescence microscopy indicates that the target proteins are in close proximity (usually 5-10nm) (Weibrecht *et al*, 2010). Unlike the PLA, FRET is hampered by photobleaching, high background autofluorescence (particularly in FFPE samples) and inadvertent simultaneous excitation of both the acceptor and donor fluorophores (Weibrecht *et al*, 2010).

The PLA also has key advantages over conventional IHC and IF: 1) the requirement of dual binding makes the technique more specific, 2) the presence of an RCA step enhances sensitivity and 3) the fluorescent RCP allows for automated quantification and is easily distinguished from autofluorescence (Blokzijl *et al*, 2010).

Before applying the PLA to the study cohort of patient samples, it is essential to first carry out a series of control experiments to validate the method and its key components. In particular, the antibodies used in the assay (both the primary antibodies and secondary proximity probes) should bind properly to the intended target (Leuchowius *et al*, 2011) and the method should be compatible with FFPE samples.

Since my intention was to use the CVD13 antibody to detect phosphorylated c-Met (in combination with the pan-phosphotyrosine antibody 4G10), the first aim of this validation study was to confirm that c-Met phosphorylation does not hinder the ability of CVD13 to bind the receptor. The other aims of this study were: to demonstrate the PLA signal using the CVD13/4G10 combination in fixed cells of known phosphorylation status and to evaluate the specificity of the proximity probes and PLA signal in FFPE samples. The effect of sample fixation and embedding on the PLA product will also be assessed.

4.2 Materials and Methods

4.2.1 Tissue culture

MDA-MB-468 cells were propagated, sub-cultured and preserved as in section 3.2.4.

4.2.2 Tissue samples

4.2.2.1 FFPE samples

FFPE invasive breast carcinomas were retrieved from the Barts Cancer Institute Breast Tissue Bank for validation of the PLA. Whole tumour blocks from 25 patients with triple negative (TN) breast cancer were selected and placed onto a tissue microarray.

4.2.2.2 Frozen samples

Frozen samples, paired with selected cases in section 4.2.2.1 were retrieved from the Barts Cancer Institute Breast Tissue Bank. The criteria for selecting the cases are outlined in section 4.2.8.

4.2.3 Tissue microarray (TMA) construction

Sections were cut at 4µm thickness on each tumour block, placed onto a glass slide and stained with haematoxylin and eosin by George Elia (senior research technician). I then examined the slides and at least 2 regions of invasive carcinoma were highlighted. The highlighted slides were then placed over the paraffin block and the corresponding area was marked on the block. 'Doner' cores, 1mm in diameter were removed from the tumour block and placed into a new 'recipient' paraffin block, using Alphelys TMA machine and Minicore software package (Alphelys, Plaisir, France). Cores were placed in duplicate or triplicate depending on the volume of

tumour present within the block. Control cores (human spleen) were placed in triplicate at the start of the 'recipient' TMA block for orientation. Upon completion, 4µm sections were cut from the TMA and placed onto glass slides (performed by George Elia).

4.2.4 Antibodies

See Table 4.1 for details of the primary antibodies used in this study.

Antibody	Target	Supplier	Species	Dil. (IF/IHC)	Dil. (PLA)	Dil. (WB)
CVD13	c-Met	Invitrogen	Rabbit	1:100	1:500	1:500
D24	Phospho-c-Met	Cell Signalling	Rabbit	N/A	N/A	1:1000
4G10	Phospho-tyrosine	Millipore	Mouse	1:100	1:500	N/A
24E10	E-Cadherin	Cell Signalling	Rabbit	1:100	1:100	N/A
NCH38	E-Cadherin	Dako	Mouse	1:100	1:100	N/A
MIB-1	Ki67	Dako	Mouse	1:100	1:100	N/A
B-6	HSC70	Santa Cruz	Mouse	N/A	N/A	1:10000

Table 4.1: Primary antibodies used in the validation of the PLA. Abbreviations: Dil. = dilution, IF = immunofluorescence, IHC = immunohistochemistry, PLA = proximity ligation assay, WB = western blot, N/A = not applicable.

4.2.5 Immunoprecipitation

MDA-MB-468 cells were seeded in 10cm culture plates at a density of 1.8 million cells per plate. The cells were left for 36 hours to adhere and treated with SU11274 (2µM; Calbiochem, Millipore, Nottingham, UK) for 10 minutes at 37^{o}C followed by HGF (100ng/ml; R&D systems, Abingdon, UK) for 20 minutes at 37^{o}C where appropriate. The plates were aspirated, washed in cold PBS and then cold RIPA buffer was added, containing protease and phosphate inhibitors (Calbiochem) at a dilution of 1:100. The plates were scraped and aspirated after which the aspirates were transferred into fresh eppendorfs and incubated on ice for 15 minutes. The eppendorfs were then placed on a rotating wheel (30rpm) for a further 15 minutes at

4°C. The lysates were centrifuged at 10000rpm for 5 minutes and the supernatant transferred into a fresh eppendorf.

Protein A sepharose beads (Invitrogen) and, for the positive control Agarose anti-mouse IgG beads (Sigma-Aldrich) were prepared by centrifuging 400µl and 200µl respectively at 5000rpm for 1 minute at 4°C and then washing 3 times in 500µl of cold PBS. The lysate was pre-cleared by mixing 60µl of beads with 600µl of each lysate and incubating for 1 hour on a rotating wheel at 4°C. The lysate/bead mixture was centrifuged at 5000rpm for 2 minutes at 4°C; the supernatant was retrieved and a Bio-Rad DC Protein Assay was performed to estimate the post-clearing protein concentration.

The beads were blocked by mixing 20µl per sample of beads with 500µl 3% BSA/PBS in a fresh eppendorf and then rotating for 1 hour at 4°C. At the same time, 150µg of protein from each sample was incubated with 3µg of c-Met antibody on a rotating wheel for 1 hour at 4°C. The beads were centrifuged at 5000rpm for 2 minutes, washed in cold RIPA buffer 3 times, mixed with the lysate/antibody solution and rotated for 1 hour at 4°C. After incubation, the eppendorfs were centrifuged and washed in cold RIPA buffer 3 times before re-suspending the beads in 4X sample buffer and heating to 98°C for 5 minutes. The entire sample (except the beads) was loaded into a 6% gel and a western blot was performed. The membrane was probed for phospho-c-Met (D26) and c-Met (CVD13). A lane containing beads, lysate and IgG served as a negative control.

4.2.6 Western blot

Western blotting was performed as outlined in section 3.2.5.

4.2.7 Immunofluorescence

Immunofluorescence (IF) on glass cover-slips was performed as outlined in section 3.2.6. Where appropriate, cells were treated with SU11274 (2µM for 10 minutes at 37^{o}C) and HGF (100ng/ml for 20 minutes at 37^{o}C) 36 hours after seeding.

4.2.8 Immunohistochemistry

Immunohistochemistry (IHC) for E-Cadherin (24E10, NCH-38) and Ki67 (MIB-1) was performed on the TN TMAs as outlined in section 3.2.3. Stained sections were evaluated for expression of E-Cadherin and Ki67 and cases that showed strong expression of all three antibodies were selected for the PLA and paired with the corresponding frozen sections.

4.2.9 Proximity ligation assay (PLA)

4.2.9.1 Chamber slide preparation

Chamber slides (Fisher Scientific) were prepared by seeding 20000 MDA-MB-468 cells per well and allowing them to adhere for 36 hours. The chambers were treated with SU11274 (2µM for 10 minutes at 37^{o}C) and HGF (100ng/ml for 20 minutes at 37^{o}C) as appropriate before rinsing in PBS and then fixing in ice-cold methanol for 5 minutes. The wells rinsed again in PBS before removing the polystyrene walls. The slides were then used in the PLA or dried and stored at -20^{o}C for later use.

4.2.9.2 PLA

The following method applies to the chamber slides, FFPE TMAs and frozen sections. TMAs were first de-waxed, hydrated through graded alcohols and subjected to heat-induced epitope retrieval as in section 3.2.3 (Immunohistochemistry). The

frozen sections were prepared as in section 3.2.3 with the exclusion of the endogenous peroxidase block. All incubation steps were conducted in a moisture chamber to prevent drying of the cells/tissue sections. The reagent quantities are based on a 30ul reaction volume (equivalent of about $1cm^2$). The slides were blocked with blocking solution (Olink Biosciences, Uppsala, Sweden) for 30 minutes at room temperature. Primary antibodies (CVD13, 4G10) were diluted at 1:500 or 1:100 (24E10, NCH-38, MIB-1) in antibody diluents (Olink Biosciences) and incubated for 1 hour at room temperature. The proximity probes (anti-mouse and anti-rabbit; Olink Biosciences) were prepared about 20 minutes before the end of the primary antibody incubation step: proximity probes were diluted in antibody diluents at a ratio of 1:5, vortexed and left to stand at room temperature. The slides were tapped on tissue paper to remove the reagents and washed in buffer A (0.01M tris, 0.15M NaCl, 0.05% Tween 20) twice for 5 minutes each, with gentle agitation. The proximity probes were incubated for 1 hour at 37^oC.

The slides were tapped on tissue paper and washed for 5 minutes, twice, in buffer A with agitation. The ligation mixture was prepared by diluting the ligation stock 1:5 in distilled water. Immediately prior to adding the ligation mixture (Olink Biosciences) to the samples, ligase (Olink Biosciences) was added at a dilution of 1:40. The ligation mixture was incubated for 30 minutes at 37^oC.

The slides were washed twice in buffer A for 5 minutes each. During this time, the amplification and detection mixture was prepared by diluting the amplification stock (1:5; Olink Biosciences) in distilled water and adding polymerase (1:80; Olink Biosciences) just before adding to the samples. The amplification/detection mixture was incubated for 100 minutes at 37^oC. The slides were then washed twice in buffer B (0.2M tris, 0.1M NaCl) for 10 minutes each and once in 0.01X buffer B for 1

minute. The slides were then left to dry in darkness before mounting in the PLA mounting media (Olink Biosciences) and stored at 4^{o}C until visualisation under fluorescent microscopy. Negative controls consisted of MDA-MB-468 cells/breast cancers with omission of the primary antibodies.

4.2.9.3 Quantification of the PLA product

For each sample, at least 4 images were captured on an Axioplan epifluorescent microscope using a 63x objective under oil immersion. As PLA signals are identified at different planes of focus in the samples, consistency was obtained by selecting the plane that contained the most abundant signal. For each image, the nuclei were counted by eye, using the ImageJ software package and cell counter plug-in. The PLA product was quantified using the Duolink ImageTool (Olink Biosciences). The mean number of PLA signals per cell was then calculated by dividing the PLA product by the number of nuclei.

4.2.10 Statistical analysis

All statistical analyses were performed using SPSS 19.0. For comparisons of variance across multiple groups, the Kruskal Wallis test was performed. Subsequent post-hoc analyses were performed using the Mann-Whitney test. For paired cases, the Wilcoxon test was used. A two-sided p-value of less than 0.05 was considered significant; where multiple groups were present the p-value cut-off was lowered by dividing 0.05 by the number of comparisons (e.g for 4 groups there are 6 comparisons so a p-value of 0.008 (0.05/6) was considered significant).

4.3 Results

4.3.1 CVD13 binds to active (phosphorylated) c-Met

To confirm that CVD13 binds to active c-Met, immunofluorescence (IF) was performed on MDA-MB-468 cells subjected to different treatment conditions: un-stimulated cells, cell stimulated with HGF for 20 minutes, cells treated with SU11274 and cells treated with both HGF and SU11274. Trafficking of the receptor from a membranous location to the perinuclear compartment (Figure 4.2) was noted in the HGF stimulated cells only, suggesting that CVD13 recognises active c-Met.

The IF findings were confirmed at immunoprecipitation (Figure 4.3). After MDA-MB-468 cell lysates were immunoprecipitated with CVD13, subsequent western blotting with a phospho-c-Met antibody, resulted in a band in the immunoprecipitate from HGF stimulated cells but not the un-stimulated cells.

4.3.2 PLA signals in breast cancer cells

To establish if the PLA could be used as a measure of c-Met activity, the assay was performed (using the CVD13/4G10 primary antibody combination) on MDA-MB-468 cells subjected to different treatment conditions. Under fluorescence microscopy, higher levels of the PLA product (sub-micrometer sized red fluorescent dots) were seen in the HGF stimulated cells (Figure 4.4).

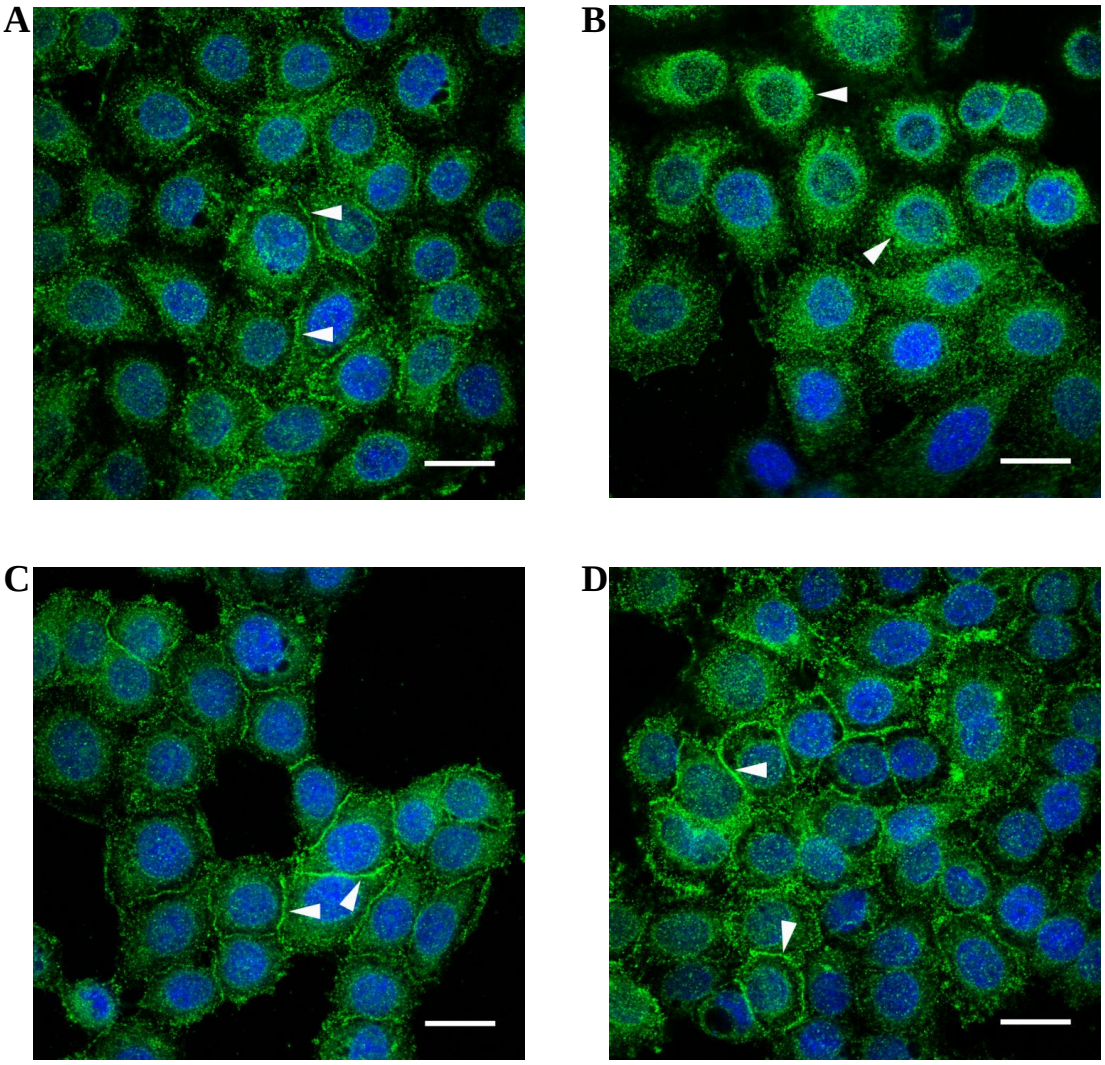

Figure 4.2: C-Met trafficking in MDA-MB-468 cells following HGF-stimulation. **A** shows un-stimulated cells with a membranous (see arrows) and cytoplasmic staining pattern, **B** shows perinuclear accumulation (see arrows) of c-Met following stimulation with HGF. In **C** and **D** the membrane (see arrows) expression is present in SU and SU/HGF treated cells respectively (CVD13 is in green, nuclei are stained blue; immunofluorescence, confocal microscope with x63 objective under oil immersion; scale bars represent 20µm).

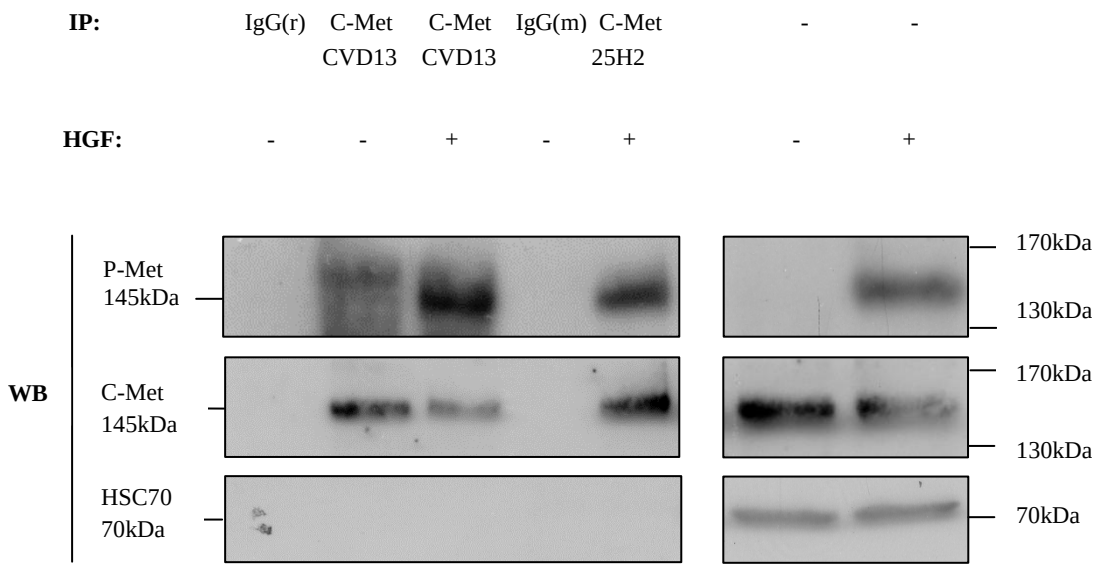

Figure 4.3: Immunoprecipitation (IP) of c-Met. The upper left panel shows a strong band in the HGF-stimulated sample for phospho-Met (D24), suggesting CVD13 binds to active c-Met. The middle left panel confirms the successful immunoprecipitation of c-Met with the CVD13 antibody. The lower left panel shows the loading control (HSC70). Rabbit IgG (IgG(r)) served as a negative control. Another anti-c-Met antibody known to bind phosphorylated c-Met (25H2) was included as a positive control and since this is a mouse antibody, a mouse IgG control was also included. The right panels represent the lysate.

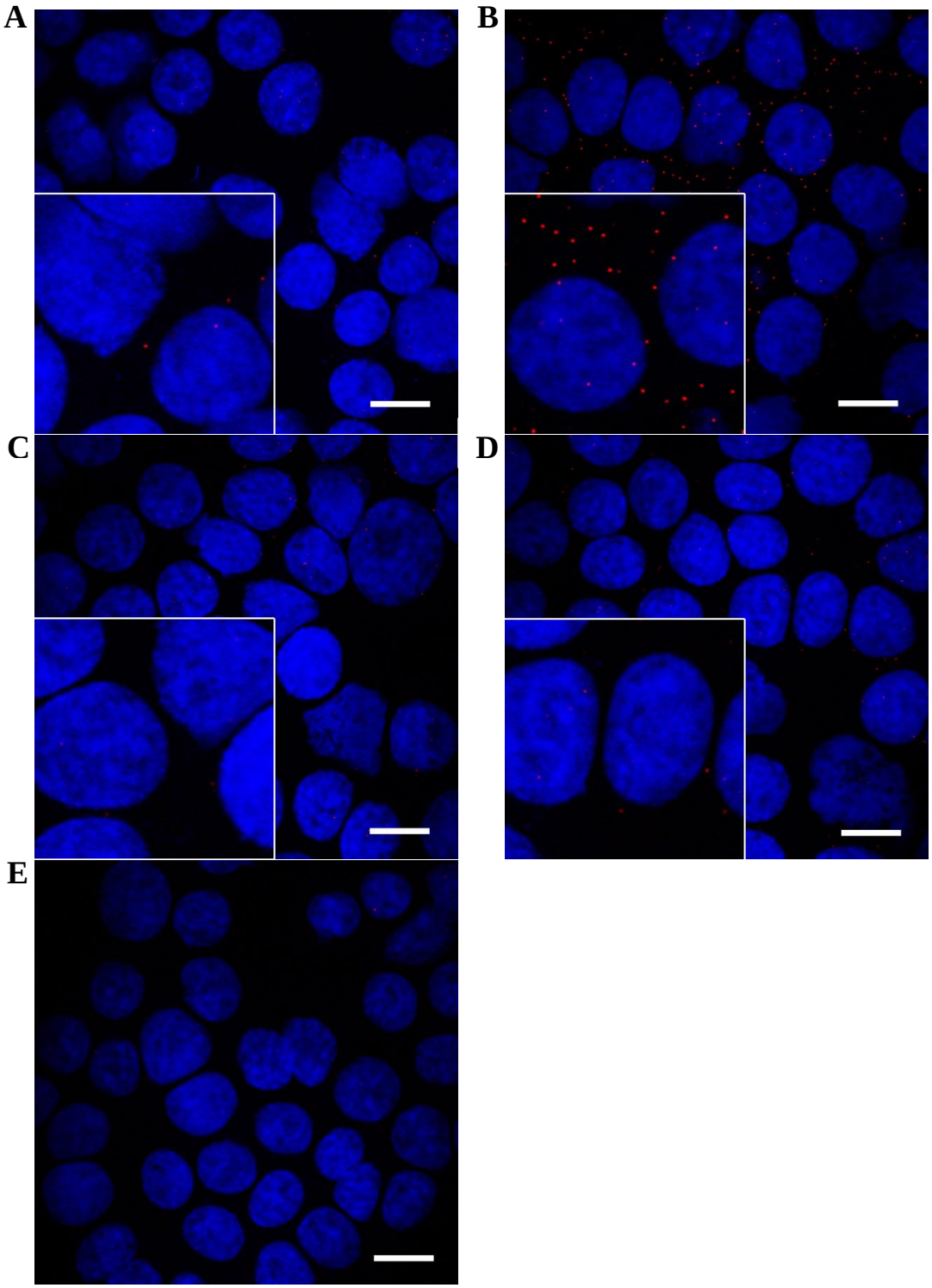

Figure 4.4: The PLA signals in breast cancer cells. Confocal microscope images of MDA-MB-468 cells that are **A** untreated, **B** treated with HGF, **C** treated with SU and **D** treated with HGF and SU. **E** is the negative control. The PLA product is markedly increased image **B** only (PLA, nuclei are stained with DAPI (blue) and the PLA product is in red; all images captured with a x63 objective; inset images are at 200% magnification, scale bars represent 20µm).

The mean number of PLA signals per nucleus showed significant variation across all treatment groups (Figure 4.5, $p < 0.001$). Mean signals were significantly higher in HGF stimulated cells (17.8, 95% confidence interval (CI): 16.0-19.6) compared to un-stimulated cells (8.8, 95% CI: 7.6-10.1; $p < 0.001$), SU treated cells (7.2, 95% CI: 5.3-9.1; $p < 0.001$) and SU/HGF treated cells (7.8, 95% CI: 6.2-9.4; $p < 0.001$). There were no significant differences between the other groups.

4.3.3 PLA signals in FFPE samples

Since FFPE samples of known c-Met phosphorylation status were not available, the PLA was validated on FFPE samples, by performing the assay on serial sections using 2 different combinations of primary antibodies. The purpose of this experiment was to show a difference in PLA signal when antibodies against close epitopes (2 different E-Cadherin antibodies) were used, compared with antibodies directed against distant epitopes (E-Cadherin and Ki67). The presence of more signals in the former would suggest that the proximity probes were specific for the primary antibodies and that the signal depended on the proximity of the epitopes (Figure 4.6).

The mean number of PLA signals per nucleus was higher in the E-Cadherin/E-Cadherin (24E10/NCH38) combination compared to the E-Cadherin/Ki67 (24E10/MIB1) combination in all of the 4 cases tested, although this was of borderline significance (Figure 4.7; $p = 0.068$; $n = 4$).

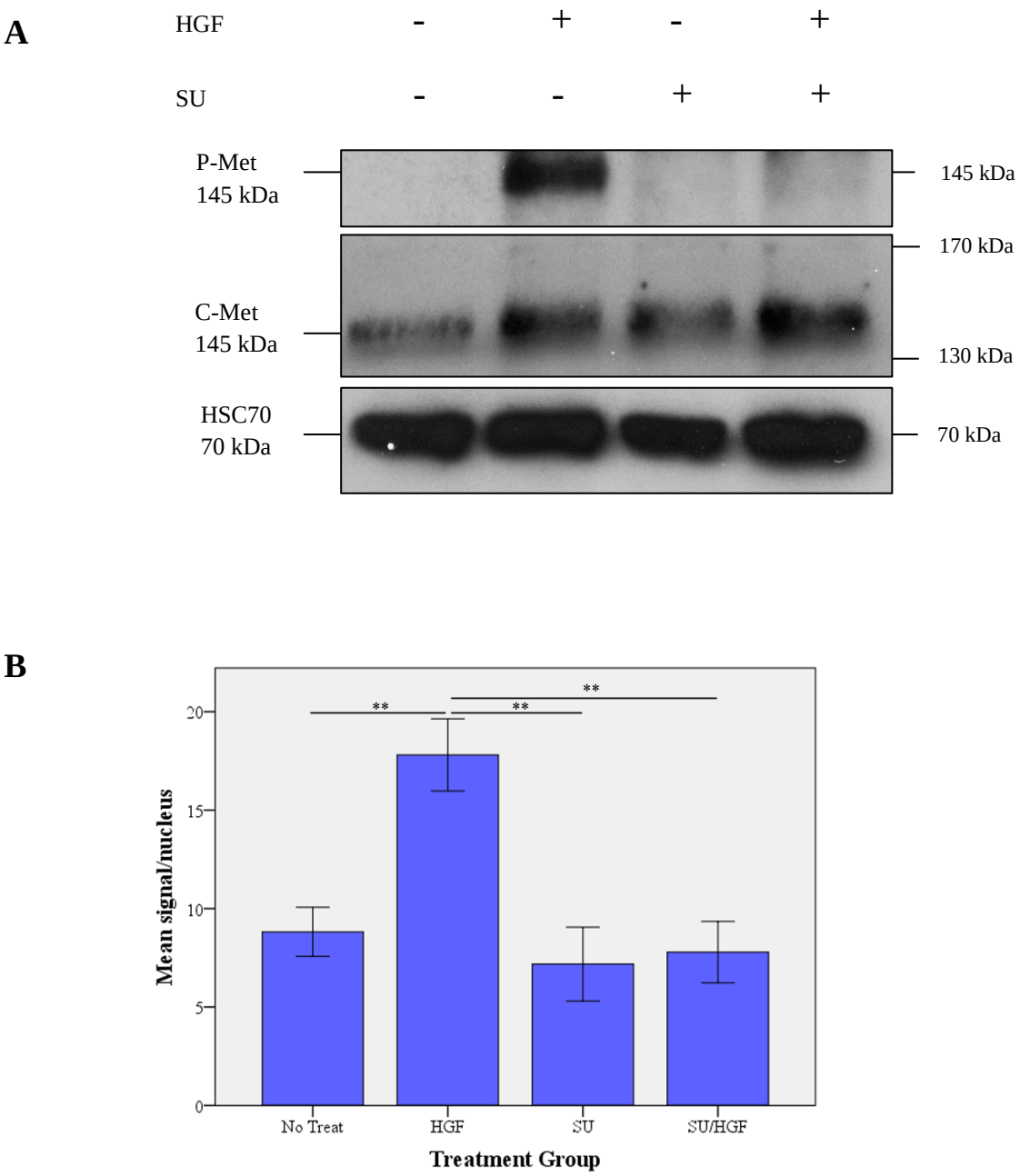

Figure 4.5: C-Met phosphorylation status in breast cancer cells and quantification of the PLA signals. **A** is a Western blot showing phospho-c-Met (P-Met) and c-Met expression in MDA-MB-468 cells. Phospho-c-Met is only seen in HGF stimulated cells, in the absence of SU. Loading control: HSC70. **B** is a bar chart showing the mean PLA signals per nucleus in the 4 treatment groups. There is a significant increase in the HGF-treated cells compared to the other groups (** = p-value <0.001, Mann-Whitney test; error bars represent the 95% confidence interval; n=8).

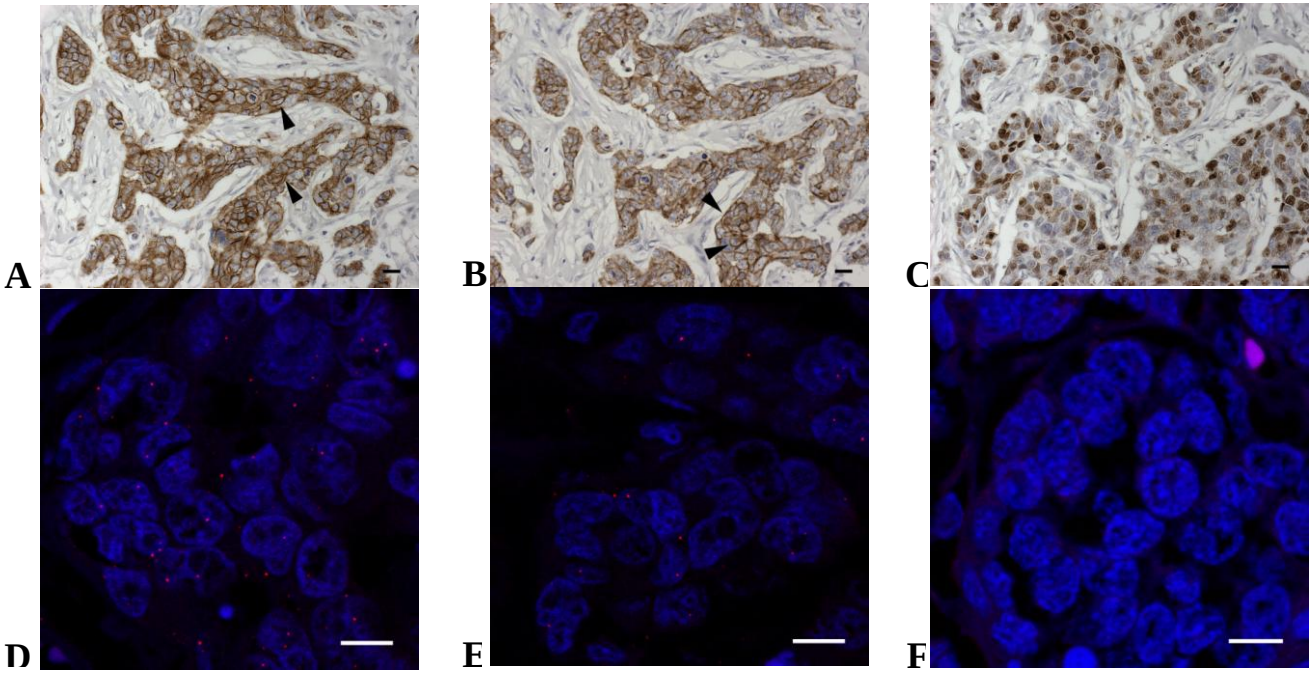

Figure 4.6: The PLA in FFPE samples. All images are from the same tumour. **A-C** are brightfield images of **A** E-Cadherin (24E10) showing membrane staining (see arrows), **B** E-Cadherin (NCH38) also with membrane staining (see arrows) and **C** Ki67 (MIB1) with nuclear positivity (IHC, images acquired with a x20 objective; scale bars represent 10µm). **D-E** are confocal fluorescent images of **D** the 24E10/NCH38 combination showing more PLA signal compared to the 24E10/Ki67 combination in **E**; **F** is the negative control (PLA, nuclei are stained with DAPI (blue) and the PLA product is in red; images acquired with a x63 objective; scale bars represent 10µm).

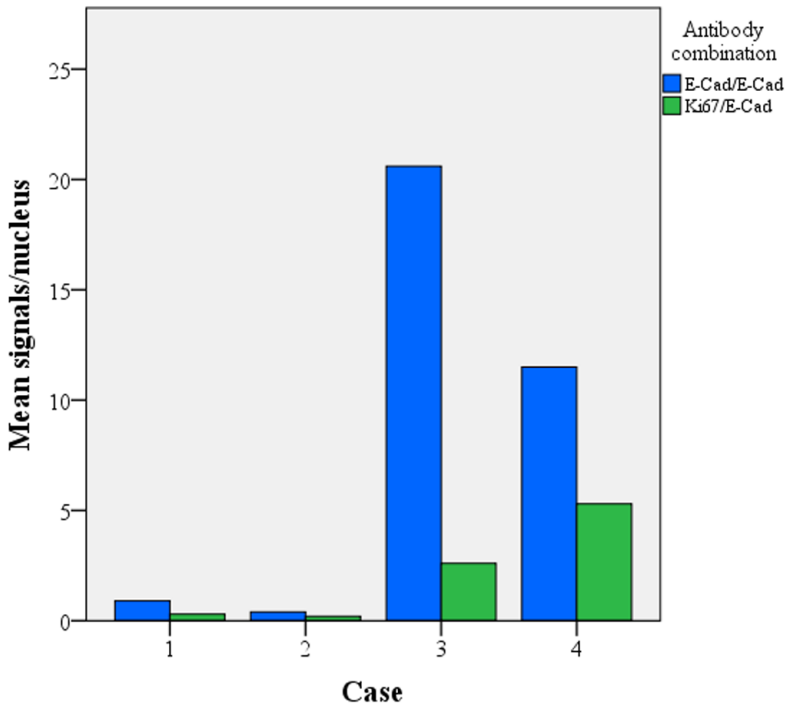

Figure 4.7: Mean PLA signals per nucleus in FFPE sections using E-Cadherin/Ki67 antibodies. In each of the 4 cases, incubation with 2 primary E-Cadherin antibodies (24E10 and NCH38) produced more signals than incubation with primary antibodies against Ki67 (MIB1) and E-Cadherin (24E10), although this was of borderline significance (p=0.068, Wilcoxon test; n=4).

4.3.4 PLA signal in frozen versus FFPE samples

To establish if the processes of fixation and embedding of breast tumour samples affects detectable c-Met phosphorylation using the PLA, the assay was performed on paired frozen and FFPE samples with the CVD13/4G10 combination of primary antibodies.

The mean number of PLA signals per nucleus was higher in each of the frozen samples compared to FFPE samples, although this was of borderline significance (Figure 4.8; $p = 0.068$; $n = 4$).

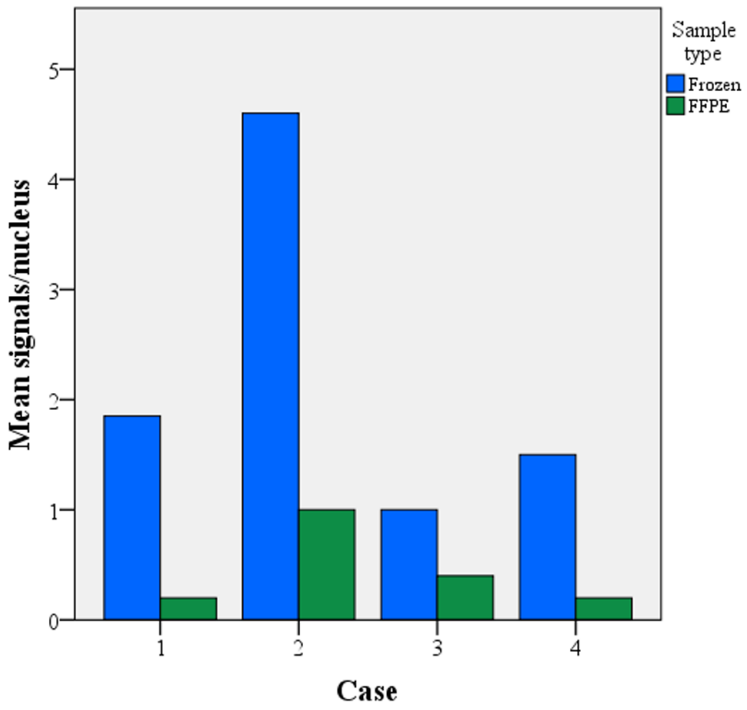

Figure 4.8: Mean PLA signals per nucleus in matched frozen and FFPE samples. In each of the four cases, more signals are seen in the frozen sections, although this was of borderline significance (p=0.068, Wilcoxon test; n=4).

4.4 Discussion

4.4.1 CVD13 recognises active c-Met

In section 3.0, CVD13 was shown to be specific for the c-Met receptor. The current results show that the antibody still recognises the receptor after it has been activated: phospho-c-Met is detected following IP of c-Met in cells stimulated with HGF and immunofluorescent studies demonstrate trafficking of c-Met to the perinuclear compartment in HGF stimulated cells only. This finding demonstrated that the phosphorylation of c-Met did not impede CVD13 from binding to the receptor, thus the antibody was suitable for use in the PLA.

The trans-cytosolic movement of c-Met following HGF-mediated activation has previously been demonstrated in HeLa cells (Kermorgant *et al*, 2003 and 2004). In resting (unstimulated) HeLa cells, c-Met is mostly expressed at the plasma membrane, with only scattered perinuclear positivity (Kermorgant *et al*, 2003). Upon incubation with HGF, the receptor is internalised and enclosed within cytosolic endosomes and traffics to the perinuclear compartment in a process that is regulated by protein kinase C (PKC) and facilitated by the microtubular network (Kermorgant *et al*, 2003). The resultant pattern of predominantly perinuclear vesicular positivity for c-Met, with minimal membranous expression contrasts with the pattern seen in the resting state (Kermorgant *et al*, 2003). This trafficking of c-Met within endosomes has subsequently been shown to be important in c-Met-induced migration, tumourigenesis and metastatsis (Kermorgant *et al*, 2004 and 2008; Joffre *et al*, 2011).

4.4.2 The PLA signal is increased in HGF-stimulated breast cancer cells

Stimulation of MDA-MB-468 cells with HGF resulted in a significantly higher PLA signal compared to unstimulated cells or cells treated with the c-Met kinase-specific inhibitor SU11274 or combined HGF/SU11274 treatment. This result is corroborated by the findings at IF (showing receptor trafficking) and western blot (showing a band when probed with a phospho-c-Met antibody) in ligand-stimulated cells only.

Importantly, this result supports the use of the CVD13/4G10 combination of primary antibodies in the PLA and demonstrates for the first time that this assay can be used for the relative quantification of c-Met activity. Others have conducted similar experiments to evaluate the PLA – most notably in assessing platelet-derived growth factor receptor (PDGFR) signalling (Jarvius *et al*, 2007; Koos *et al*, 2009). Using both human embryonic kidney 293 (HEK293) and choroid plexus epithelial cell lines, these workers visualised the RCPs of the PLA as sub-micrometer sized fluorescent objects (Jarvius *et al*, 2007; Koos *et al*, 2009), similar to those seen in the current study. As in the current study, cellular stimulation with the appropriate ligand (platelet-derived growth factor) generated increased PLA signals (Jarvius *et al*, 2007; Koos *et al*, 2009).

4.4.3 The PLA in FFPE samples

In common with IHC, tissue fixation and embedding can have a profound effect on the PLA result (Söderberg *et al*, 2008; Leuchowius *et al*, 2011). Although others have successfully applied the PLA to FFPE samples (Jarvius *et al*, 2007; Koos *et al*, 2009), it remains necessary to validate the technique (especially the antibodies) on samples similar to the study cohort. In section 3.0, the suitability of CVD13 for use on FFPE samples following HIER was demonstrated. The secondary antibodies

(proximity probes) also require attention: poorly conjugated proximity probes and non-specific binding by the probes may cause reduced PLA signals and high background signal respectively. Furthermore, the process of antibody conjugation (to produce the proximity probes) can also adversely affect the antibody by interfering with the binding site, thus hindering their ability to recognise the target epitopes (Leuchowius *et al*, 2011).

Since FFPE samples of known c-Met phosphorylation status were not available, I took an alternative approach to validate the proximity probes. Instead of using pan-c-Met and pan-phosphotyrosine antibodies, I used primary antibodies directed against different cellular compartments: the membranous compartment (E-Cadherin) and the nuclear compartment (Ki67) (Cheuk and Chan, 2004). By incubating FFPE breast cancer samples with an E-Cadherin/E-Cadherin and E-Cadherin/Ki67 primary antibody combination, I was able to demonstrate a higher PLA signal with the former. Although the differences were of borderline significance, the analysis was performed on only four pairs of cases and, importantly in all pairs, the PLA product was higher in the E-Cadherin/E-Cadherin combination. The findings suggest that in FFPE samples the proximity probes show specificity for the primary antibodies, and that it is the proximity of the target proteins that dictates that quantity of the PLA signals.

4.4.4 The PLA in frozen versus FFPE samples

Comparison of frozen and FFPE samples from the same cases showed that the majority of the PLA signal is lost due to fixation/embedding. As above, the small sample size perhaps explains the borderline significance, but again, in all pairs it was the frozen sections that showed the more numerous PLA products. This finding is

not entirely surprising. Söderberg *et al* estimate that the requirement of a dual recognition event in the PLA may reduce the epitopes available for detection to just 9% in FFPE tissue, assuming that fixation reduces the available fraction of any given epitope to 30% (30% x 30% = 9%) (Söderberg *et al*, 2008). Therefore, the efficiency of the PLA in detecting c-Met phosphorylation in FFPE samples would seem to be no worse than expected.

4.4.5 Conclusion

In conclusion, the results of this validation study confirm that CVD13 can bind to c-Met after it has been phosphorylated, a pre-requisite for its use in the PLA. In cells of known c-Met phosphorylation status, more signals were seen in cells stimulated with HGF compared with un-stimulated cells and in FFPE samples, the PLA output was dependent on the proximity of the target epitopes/primary antibodies. Finally, although the PLA would seem better suited to frozen sections there is no reason to suggest that relevant data cannot be obtained from FFPE samples. Together, these findings validate the PLA and the selected antibodies for the analysis of c-Met phosphorylation in the study cohort of breast cancer samples.

5.0 Breast cancer cell line characterisation

5.1 Introduction

Breast cancer cell lines (BCLs) have contributed significantly to our current knowledge of breast cancer through *in-vitro* and *in-vivo* studies (Charafe-Jauffret *et al*, 2006). BCLs have several attributes that make them ideal for modelling the pathogenesis of breast cancer: they represent a pure population of cancer cells without stromal cell contamination, they are easy to handle, self-replicate and can be manipulated both genetically and pharmacologically, the effects of which can be studied in an array of functional assays (Charafe-Jauffret *et al*, 2006; Kao *et al*, 2009).

With over 50 different BCLs now available, including those originating from primary breast cancers as well as metastatic effusions (Neve *et al*, 2006) they clearly represent a diverse resource. The landmark paper that demonstrated the molecular heterogeneity of human breast cancer samples at gene expression profiling included an analysis of selected BCLs, illustrating that these cells lines could be clustered into the luminal or BL molecular sub-types (Perou *et al*, 2000). Since then, several studies have extended the characterisation of these cell lines to include proteomic, transcriptomic, genomic and epigenomic profiling (Neve *et al*, 2006; Charafe-Jauffret *et al*, 2006; Grigoriadis *et al*, 2012). Investigators are now in the position of being able to select those specific BCLs that most closely resemble the tumour type they are studying.

The aim of this validation study was to characterise the protein expression of a panel of BCLs that are considered representative of the BL phenotype. The protein

expression profile of these BCLs will be compared with the literature to select the most appropriate models of HGF/c-Met signalling in BL breast cancer.

5.2 Materials and Methods

5.2.1 Tissue culture

The 3 cell lines already established in the laboratory were: MDA-MB-468s, MDA-MB-231s and SUM159s. The other cell lines (HCC1937s, BT-20s, HCC38s and Hs578ts) were purchased from ATCC/LGC Standards (Middlesex, UK). The MDA-MB-468s were cultured as described in section 3.2.4. MDA-MB-231s were cultured in DMEM, supplemented with 10% FCS. Hs578ts were cultured in DMEM supplemented with 10% FCS and 0.01 mg/ml bovine insulin. The HCC38s and HCC1937s were cultured in Roswell Park Memorial Institute (RPMI) media (PAA), supplemented with 10% FCS. The BT-20s were cultured in Eagle's Minimal Essential Medium (MEM; PAA), supplemented with 10% FCS and the SUM159s were cultured in Ham's F12 (PAA), supplemented with 10% FCS.

The cell lines were propagated, sub-cultured and preserved as set out in section 3.2.4.

5.2.2 Antibodies

See Table 5.1 for details of the primary antibodies used in this study.

Antibody	Target	Supplier	Species	Dilution
CVD13	C-Met	Invitrogen	Rabbit	1:500
1005	EGFR	Santa Cruz	Goat	1:1000
G20	ER	Santa Cruz	Mouse	1:200
M45	Her2	Cell Signalling	Rabbit	1:1000
D5/16 B4	CK 5/6	Dako	Mouse	1:500
36/E-Cadherin	E-Cadherin	BD Transduction Labs	Mouse	1:1000
B6	HSC70	Santa Cruz	Mouse	1:10000

Table 5.1: Primary antibodies utilised in this cell characterisation study.

5.2.3 Western blot

Western blots were performed as set out in section 3.2.5.

5.3 Results

All of BL cell lines were negative for ER and Her2, but showed EGFR expression. C-Met was also present in all cell lines. CK5/6 and E-Cadherin were present in the HCC1937s, MDA-MB-468s, HCC38s and BT-20s only (Figure 5.1 and Table 5.2).

Cell line	ER	Her2	EGFR	C-Met	E-Cadherin	CK 5/6
HCC1937	-	-	+	+	+	+
Hs578t	-	-	+	+	-	-
468	-	-	+	+	+	+
231	-	-	+	+	-	-
SUM159	-	-	+	+	-	-
HCC38	-	-	+	+	+	+
BT-20	-	-	+	+	+	+

Table 5.2: Protein expression of BL cell lines, as determined by western blot.

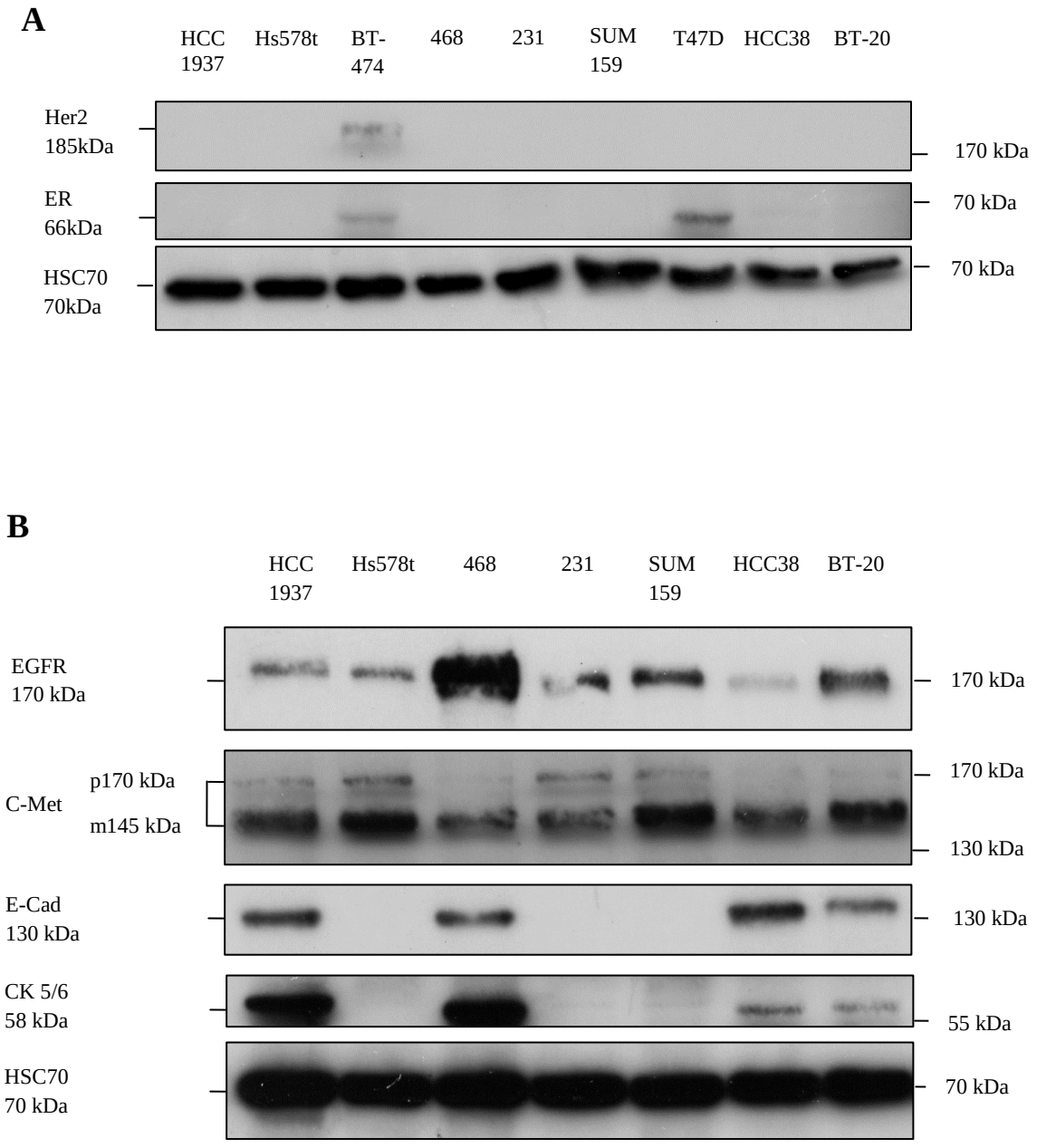

Figure 5.1: Protein expression by different BL BCLs. Representative western blots from 3 experiments, showing no bands for ER and Her2 in each of the BL cell lines (positive controls: T47D (ER) and BT-474 (Her2) in **A**. **B** shows BL cell line expression of the basal markers EGFR and CK5/6, together with c-Met (seen here in both the precursor (p170 kDa) and mature (m145 kDa) forms) and E-Cadherin. Loading control: HSC70.

5.4 Discussion

5.4.1 BL marker expression in breast cancer cell lines (BCLs)

All seven BCLs were found to be negative for ER and Her2 and (variably) positive for EGFR. CK 5/6 expression was limited to the HCC1937s, HCC38s, MDA-MB-468s and the BT-20s. The findings with regard to ER, Her2 and EGFR expression were largely in line with those of other studies that have assessed these markers in protein based and/or gene expression assays (Neve *et al*, 2006; Charafe-Jauffret *et al*, 2006; Kao *et al*, 2009; Lehmann *et al*, 2011; Grigoriadis *et al*, 2012). Admittedly, Charafe-Jauffret *et al* found no expression of CK5/6 in BT-20s and HCC1937s (Charafe-Jauffret *et al*, 2006), a finding that contrasts with the western blot bands in the current study. This discrepancy may be due to the different detection methods used in the two studies, with the previous study utilising IHC on cell pellet paraffin blocks (Charafe-Jauffret *et al*, 2006).

Although all seven BCLs profiled here could be considered BL based on the IHC profile proposed by Nielsen *et al* (ER and Her2 negative, CK5/6 and/or EGFR positive) (Nielsen *et al*, 2004), several groups have attempted to further divide the BL/TN BCLs into at least two distinct groups (Neve *et al*, 2006; Kao *et al*, 2009; Lehmann *et al*, 2011; Grigoriadis *et al*, 2012). The first group, referred to here as BL (also known as 'Basal A' elsewhere) are characterised by over-expression of the keratin (*KRT*) *5*, *14* and *17* genes (Neve *et al*, 2006; Grigoriadis *et al*, 2012). The second group, the so-called mesenchymal-like cells (known as 'Basal B' elsewhere) lack *KRT 5* and *17* expression; instead there is vimentin (*VIM*), caveolin (*CAV1*) and *VEGFR* over-expression (Neve *et al*, 2006; Lehmann *et al*, 2011; Grigoriadis *et al*, 2012). The broad consensus from these studies was that the MDA-MB-468s and

HCC1937s clustered into the BL group and the Hs578ts, SUM159s and MDA-MB-231s fell into the mesenchymal-like category (there was some disagreement as to whether the HCC38s and BT-20s could be classified as BL)(Neve *et al*, 2006; Lehmann *et al*, 2011; Grigoriadis *et al*, 2012). The CK5/6 western blot findings of the current study would correlate well with the BL designation given to the MDA-MB-468s and HCC1937s and also with the mesenchymal-like BCLs by virtue of their lack of CK5/6 expression.

According to Kao *et al*, the BL BCL gene expression cluster more closely resembled the profile of BL tumour samples than the mesenchymal-like cluster (Kao *et al*, 2009), suggesting that the MDA-MB-468s and HCC1937s are the most appropriate choices for modelling BL cancer.

5.4.2 C-Met expression in BCLs

C-Met was expressed in all of the BCLs profiled. This finding is partly supported by the work of Charafe-Jauffret *et al*, who found positivity for c-Met in the BT-20s, HCC38s and MDA-MB-231s. However, they found no c-Met reactivity in the HCC1937s or Hs578ts (Charafe-Jauffret *et al*, 2006). Again, as with CK5/6 expression, this difference may be explained by the different techniques used by this study and the previous one.

Gene expression studies have identified *MET* over-expression in BCLs with a BL profile (Lehmann *et al*, 2011) and BL or mesenchymal-like profile (Grigoriadis *et al*, 2012). Thus, c-Met/*MET* over-expression appears to be a consistent finding in BL/mesenchymal-like BCLs.

5.4.3 E-Cadherin expression in BCLs

The results for E-Cadherin expression mirrored those for CK5/6, with a band present in the HCC1937s, MDA-MB-468s, HCC38s and BT-20s. This result is in keeping with the western blot analysis performed by Neve *et al*, who demonstrated E-Cadherin in the BT-20 and HCC38 cell lines but not in the Hs578ts or MDA-MB-231s (western blots were not presented for the other cell lines profiled in the current study)(Neve *et al*, 2006). Elsewhere, in an IHC analysis of different BCLs, Chekhun and co-workers found high E-Cadherin expression in the MDA-MB-468s and low expression of the protein in MDA-MB-231s (Chekhun *et al*, 2013).

The fact that the Hs578t, MDA-MB-231 and SUM159 lysates show no band following E-Cadherin probing, lends credence to their designation as mesenchymal-like cell lines. In the study by Lehmann and colleagues, the mesenchymal-like BCLs were partly defined by the expression of epithelial-mesenchymal transition (EMT) associated genes, with increased *TWIST1* and *SNAI2* and reduced expression of the E-Cadherin gene *CDH1* (Lehmann *et al*, 2011).

The question of whether the mesenchymal-like cluster corresponds to a specific sub-type of breast cancer is one that several workers have pondered (Kao *et al*, 2009; Prat *et al*, 2010; Lehmann *et al*, 2011). Previously, it had been suggested that mesenchymal-like cells relate to a rare tumour sub-type not yet characterised or a sub-population of progenitor/stem cells preferentially selected in tissue culture or even that the existence of these cells was simply tissue culture artefact (Kao *et al*, 2009). The first of these possibilities may be partly true – the Hs578t cell line for example was derived from a metaplastic carcinoma, a special histological sub-type that accounts for just 1% of breast cancers (Hackett *et al*, 1977; Harris *et al*, 2006).

Others have observed that these cell lines are reminiscent of the recently described claudin-low sub-type (Prat *et al*, 2010). Prat and colleagues identified nine cell lines (including the Hs578ts, MDA-MB-231s and SUM159s) with a claudin-low profile: low expression of genes important in cellular adhesion (*CDH1, CLDNs* (Claudins) *3, 4* and *7*), luminal differentiation and an mRNA expression signature characteristic of tumour initiating cells (CD24 low/CD44 high)(Prat *et al*, 2010). Interestingly, the authors went on to propose that the intrinsic molecular sub-types mirror the developmental stages in of mammary epithelium, in which the claudin-low cells/tumours occupy the least differentiated end of the spectrum, followed by the BL tumours and ending with both luminal sub-types (Prat *et al*, 2010).

5.4.4 Conclusion

The results from this validation study, together with those of previous studies, suggest that the MDA-MB-468 and HCC1937 BCLs are the most relevant cell lines for modelling BL breast cancer. Since they both express c-Met, they are ideal for analysing the functional significance of HGF/c-Met signalling in an *in-vitro* setting. Furthermore, as E-Cadherin is present in these cells, the possible role of this protein in c-Met signalling can be addressed.

6.0 Materials and Methods

6.1 Tissue culture

The MDA-MB-468s were cultured as described in section 3.2.4. The HCC1937s were cultured as described in section 5.2.1. Both cell lines were propagated, sub-cultured and preserved as set out in section 3.2.4.

6.2 Tissue samples

6.2.1 UK Nottingham series

Pre-constructed TMAs were made available to us by Professor Ian O Ellis and Dr Andrew Green at Nottingham University NHS Trust. These cases make up the Nottingham-Tenovus Primary Breast Carcinoma Series that includes samples from women presenting with invasive breast carcinoma between 1986 and 1998. In total, samples from 1896 patients were placed onto these TMAs, with a single 0.6 mm representative core taken from each tumour. Sections were cut at a thickness of 4µm and placed onto a glass slide. The samples were accompanied by clinical data including age at presentation, tumour size, tumour grade, histological sub-type, lymph node status, and presence of vascular invasion. Overall survival time was taken as the time (in months) between diagnosis and date of death/last known follow-up. The patients had been treated according to local guidelines (Rakha *et al*, 2009). Biomarker data were also available and included ER, PR, Her2, CK5/6, CK 14, E-Cadherin, p53, Ki67 and EGFR expression. These tissues had been acquired with ethical approval from the Nottingham Research Ethics Committee 2 (title: "Development of a Molecular Genetic Classification of Breast Cancer").

6.2.2 Homerton series

Cases of invasive breast cancer (181 in total) diagnosed between 1994 and 2009 at the Homerton hospital comprised the 'in-house' cohort. These tumours were in the form of FFPE blocks available for assembly into TMAs. The samples were accompanied by the same clinical and biomarker data as the UK Nottingham series, with the exception of E-Cadherin and p53. Self-reported ethnicity data were also available. These tissues were acquired with ethical approval from the Queen Mary's Research Ethics Committee (06/Q0403/162).

TMAs were constructed from these samples, as set out in section 4.2.3.

6.3 Antibodies

See Table 6.1 for details of the primary antibodies used in this study.

Antibody	Target	Supplier	Species	Dil. (IF/IHC)	Dil. (PLA)	Dil. (WB)
CVD13	c-Met	Invitrogen	Rabbit	1:100	1:500	1:500
D26	Phospho-c-Met	Cell Signalling	Rabbit	N/A	N/A	1:1000
4G10	Phospho-tyrosine	Millipore	Mouse	1:100	1:500	N/A
NCH-38	E-Cadherin	Dako	Mouse	1:100	N/A	N/A
36/E-Cadherin	E-Cadherin	BD Trans Labs	Mouse	N/A	N/A	1:1000
14/β-catenin	β-catenin	BD Trans Labs	Mouse	N/A	N/A	1:1000
Vimentin (R28)	Vimentin	Cell Signalling	Rabbit	N/A	N/A	1:1000
B6	HSC70	Santa Cruz	Mouse	N/A	N/A	1:10000

Table 6.1: Antibodies used in this breast cancer study. Abbreviations: Dil. = dilution, IF = immunofluorescence, IHC = immunohistochemistry, PLA = proximity ligation assay, WB = western blot, N/A = not applicable.

6.4 Immunohistochemistry

IHC was performed for c-Met on both tissue sample cohorts (UK Nottingham series and Homerton series) as set out in section 3.2.3. IHC for E-Cadherin was also performed on the Homerton series.

6.4.1 Scoring system

All IHC was scored using the semi-quantitative approach outlined in section 3.2.3. In addition, for E-Cadherin staining, tumour reactivity was recorded as less than or equal to/greater than 10% for the purposes of cut-point selection (see Table 6.2). All cores were scored twice by me on separate occasions to ensure reproducibility. A proportion of TMA cores were also scored independently by a second observer (Louise Jones).

6.4.2 Cut-point selection

The cut-off values to determine tumour positivity for each biomarker (except c-Met) are displayed in Table 6.2. The cut-points selected were as previously described (Rakha *et al*, 2005; Rakha *et al*, 2009). Scores for p53 and Ki67 were kept as continuous variables (% of positive nuclei).

Biomarker	Cut-point indicating tumour positivity
ER	Any tumour reactivity
PR	Any tumour reactivity
Her2	>10%*
CK 5/6	≥10%
CK 14	≥10%
EGFR	≥10%
E-Cadherin	≥10%

Table 6.2: Biomarker cut-points. Cut-points for each of the immunohistochemical biomarkers used for molecular sub-typing (*Strong complete membrane positivity or positive findings at fluorescent in-situ hybridisation (FISH) in cases showing only weak/moderate complete membrane staining).

For the purpose of survival analysis, c-Met scores were dichotomised into c-Met 'high' (total score ≥7) and c-Met 'low' (total score <7) using the X-Tile bioinformatics software package for optimal cut-point selection (Camp *et al*, 2004). The software works by randomly dividing the study population into 'training' and 'validation' cohorts. X-Tile then finds the optimal cut-point in the 'training' set and applies this to the 'validation' set and vice-versa. The population is then randomly cut 1000 times and the process repeated to generate an average cut-point. Finally, X-Tile performs survival analysis using Monte Carlo simulations to arrive at a corrected p-value for this cut-point. X-Tile has been validated in the literature, where the software arrived at cut-points for known prognostic factors in breast cancer (number of involved lymph nodes and tumour size) that were similar to those used in established staging protocols (Camp *et al*, 2004).

6.4.3 Immunoprofile for molecular sub-types

The algorithm used to define the different molecular sub-types of breast cancer on IHC is displayed in Table 6.3. This algorithm is similar to those used in previous studies (Cheang *et al*, 2008; Blows *et al*, 2010; Carey *et al*, 2006).

Molecular sub-type	ER	PR	Her2	CK 5/6	CK 14	EGFR
Luminal A	+/-*	+/-*	-	N/A	N/A	N/A
Luminal B	+/-*	+/-*	+	N/A	N/A	N/A
Her2 positive	-	-	+	N/A	N/A	N/A
Basal-like (BL)	-	-	-	+/-^	+/-^	+/-^
Unclassified	-	-	-	-	-	-

Table 6.3: Molecular sub-type immunoprofile. Immunoprofile used to classify invasive breast cancers into one of five main molecular sub-types (* = positive for at least one of these markers in luminal tumours, ^ = positive for at least one of these markers in BL tumours). Abbreviations: N/A = not applicable.

6.5 Immunofluorescence

IF was performed for c-Met and E-Cadherin on MDA-MB-468s and HCC1937s as outlined in section 3.2.6.

6.5.1 Image capture and quantification

Images were captured using a Zeiss Confocal Fluorescent LSM 710 microscope. E-Cadherin staining was quantified by counting the number of cells with membranous reactivity and expressing this as the percentage of total cells, as identified by DAPI-stained nuclei. Co-localisation analysis for E-Cadherin and c-Met was performed using the Zen 2009 software. For each antibody, the appropriate filter for that fluorophore was selected and the detection threshold adjusted so that only specific staining (membranous for both antibodies in un-stimulated cells) appeared as white

pixels. The co-localised pixels were then expressed as a percentage of the total number of c-Met pixels. At least 50 cells were analysed for each treatment condition.

6.6 Western blot

Western blotting was performed on MDA-MB-468 and HCC1937 cells as outlined in section 3.2.5. Protein expression (band intensity at western blot) was quantified by performing densitometry analysis in ImageJ. For each antibody the untreated cells were regarded as the control and the density of this band was assigned a value of '1'. The densities of the bands from treated cell lysates were then given a value relative to the control band (sample relative density). The same process was repeated for the loading controls. Finally, the adjusted relative density (ARD) was computed by dividing the sample relative density by the loading control relative density.

6.7 Proximity ligation assay

The PLA was applied to the Homerton cohort using the CVD13/4G10 primary antibody combination and method outlined in section 4.2.9.

6.7.1 Image capture and quantification

Images were captured using a Zeiss Epifluorescent Axioplan microscope with a x63 objective. For each TMA core, 2 images were captured. The PLA product was then quantified as set out in section 4.2.9.

6.7.2 Cut-point selection

For the purpose of survival analysis, tumours were dichotomised into PLA 'high' (>3.19 PLA signals per nucleus) and PLA 'low' (0-3.19 signals per nucleus) using the X-Tile bioinformatics package, as set out in section 6.4.2.

6.8 Cell Viability Assay (MTS assay)

The MTS assay utilises the bioreduction of tetrazolium to formazan by nicotinamide adenine dinucleotide phosphate (NADPH) or nicotinamide adenine dinucleotide (NADH) in metabolically active cells to detect and quantify viable cells.

Cells were serum-starved in 1% FCS/growth media (DMEM or RPMI depending on the cell type) for 24 hours, trypsinised and re-suspended in 1% FCS/growth media before counting. A standard curve was set up by seeding a range of cell densities into a 24-well plate (starting with 160000 cells, diluting 1:1 and ending with cell-free media) containing 400µl of media per well. MTS reagent (80µl; Promega, Madison, USA) was added to each well and the plate was incubated at 37^{o}C. After 1 hour of incubation, 120µl aliquots from each well were dispensed in duplicate into a 96-well plate. Absorbance at 492nm was calculated for each cell density using a Tecan F50 plate reader (Tecan UK, Reading, UK) and a standard curve was constructed using Microsoft Excel.

A dose response was set up by seeding 40000 cells per well in a 24-well plate containing 500µl of 1% FCS/growth media and a range of HGF concentrations from 0ng/ml to 100ng/ml. After 8 hours incubation at 37^{o}C, the media was removed and replaced with 400µl of fresh 1% FCS/growth media and 80µl of MTS reagent. The plate was incubated for a further 1 hour at 37^{o}C before aliquoting into a 96-well plate

and reading as outlined above. Finally, viable cell numbers at different HGF concentrations were calculated using the standard curve.

6.9 Transwell migration assay

The cells were serum-starved for 24 hours in 1% FCS/growth media. In order to provide a chemotactic stimulus, the transwell inserts (Appleton Woods, Birmingham, UK) were placed onto the lid of the 24 well-plate and the undersides coated with 100µl of fibronectin (10µg/ml; Sigma) diluted in sterile PBS and left to incubate for 1 hour at room temperature. The excess fibronectin was removed and the undersides of the transwells were rinsed in 100µl of sterile PBS. To each of the lower chambers in the 24 well-plate, 600µl of 1% FCS/growth media was added, along with HGF (100 ng/ml) where appropriate. The transwells were then transferred back into the 24 well-plate.

The serum-starved cells were trypsinised, counted and re-suspended in 1% FCS/growth media so that there were 100000 cells/ml. At this point, SU11274 (2µM) was added where appropriate and the cells were incubated for 10 minutes at 37^{o}C. The cell suspension was added to the upper chamber of the transwells in volumes of 200µl/well (containing 20000 cells) and left to incubate for 8 hours at 37^{o}C.

The media was removed from both the upper and lower chambers and replaced with trypsin (200µl in the upper chamber, 500µl in the lower chamber) and left to incubate for a further hour at 37^{o}C. For each chamber, the trypsin was removed and passed back over membrane twice, before being transferred to a counting tube containing sufficient filtered isoton for an end volume of 10mls per counting tube. Both the upper and lower chambers were counted using the Casy Cell Counter

(Schärfe system GmbH, Reutlingen, Germany) so that the percentage of migrated cells could be calculated.

6.10 Statistical analysis

Since the c-Met IHC/PLA scores did not show a normal distribution, the correlation between c-Met scores and continuous variables were analysed using the non-parametric Spearman's correlation co-efficient. Comparisons between c-Met scores and categorical variables were carried out using the Mann-Whitney test. Multivariate tests of association were carried out using binomial logistic regression with forward step-wise entry.

Univariate survival analysis was carried out using Kaplan-Meier curves and the log-rank test. For multivariate analysis, a Cox regression model was created, with forward step-wise entry.

For *in-vitro* analyses, differences between multiple groups were assessed using the Kruskal-Wallis test, followed by a post-hoc Mann-Whitney test for comparisons between 2 groups. To correct for multiple group testing the significance level was reduced by dividing an α of 0.05 by the number of comparisons (for example, where 6 comparisons are made, a p-value less than 8.3×10^{-3} (0.05/6) would be considered significant).

7.0 Results

7.1 C-Met expression in invasive breast cancer

7.1.1 Patient characteristics

Of the 2077 cases of invasive breast cancer incorporated onto TMAs (1896 from the Nottingham cohort and 181 from the Homerton cohort), c-Met expression could be evaluated on 1455 cases (1274 from the Nottingham cohort and all of the Homerton cases, Figure 7.1). The most common reasons for not scoring c-Met expression on a tumour (missing case) were complete lack of a tissue core for that case or the presence of minimal tumour cells in the core.

The key clinical/pathological characteristics of the entire cohort ('All cases') are compared with those of the patients on which c-Met scores were available ('Cases with c-Met scores') in Table 7.1. Compared with the entire cohort, the patients whose tumours could be scored for c-Met showed a similar mean age at presentation (both around 54 years old), mean tumour size (2.1 cm versus 2.2 cm respectively), degree of tumour differentiation (49% grade 3 versus 52% grade 3 respectively) and frequency of lymph node metastasis (40% versus 41% respectively; Table 7.1).

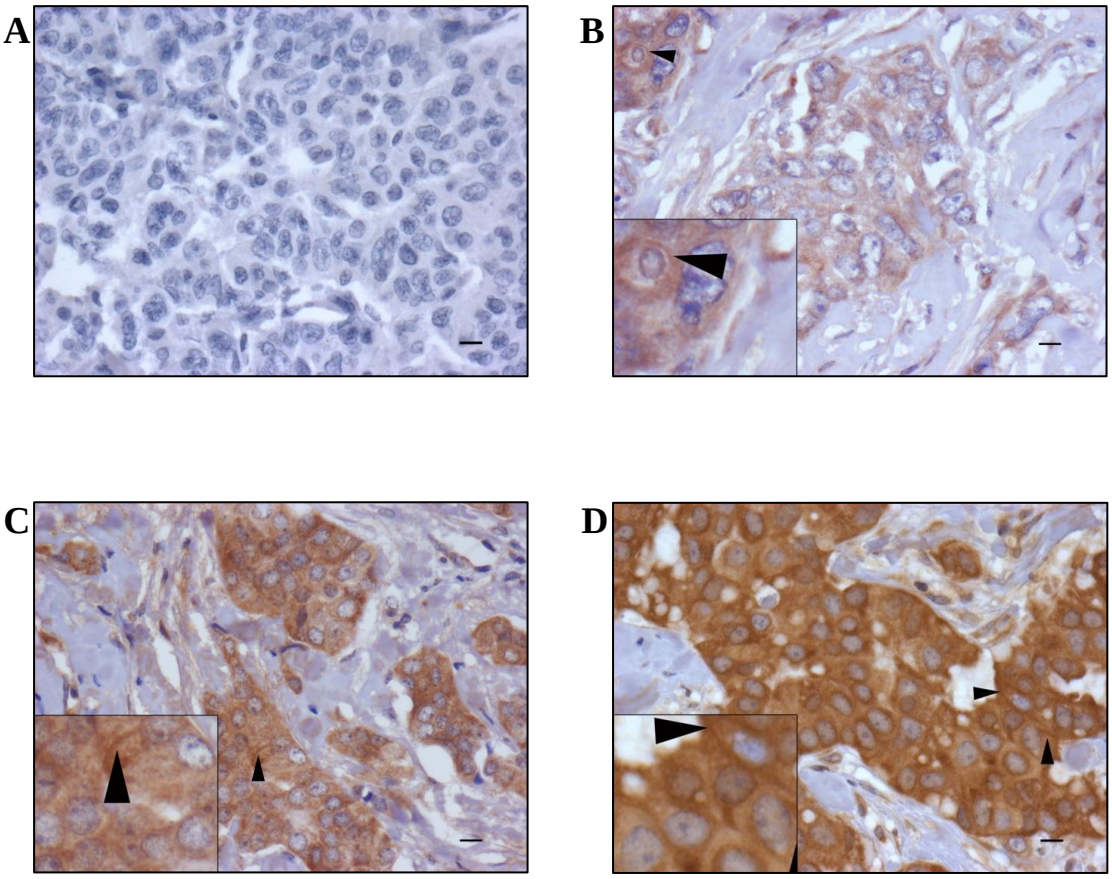

Figure 7.1: Immunohistochemistry for c-Met. **A** is the negative control (primary antibody omitted), **B** shows weak intensity cytoplasmic staining in most tumour cells with focal membrane staining (arrows), **C** shows moderate staining in most tumour cells with focal membrane positivity (arrows) and **D** shows strong cytoplasmic and membranous (arrows) staining (IHC; x40 objective, scale bars represent 10µm, all inset images are at 200% magnification). This figure is modified from Ho-Yen et al, 2014.

Parameter	Cases with c-Met scores	All Cases
Age (mean, 95% CI)	54.4 (37-69) years	54.5 (37-69) years
Tumour size (mean, 95% CI)	2.2 (0.9-4.0) cm	2.1 (0.9-4.0) cm
Tumour grade (% of cases)		
1	15	17
2	33	34
3	52	49
Lymph node involvement (% of cases)		
Yes	41	40
No	59	60

Table 7.1: Characteristics of the study cohort, including missing cases. The table shows some of the key parameters of the entire cohort (n = 2077) compared with the patients whose tumours could be scored for c-Met expression (n = 1455). Abbreviations: CI = confidence interval.

The clinical, pathological and molecular characteristics of the study cohort (minus the missing cases) are shown in greater detail in Table 7.2. The Nottingham and Homerton series, which together make up the study cohort, differed in several respects (Table 7.2). Compared to patients in the Nottingham series, Homerton patients presented at a later age (56.9 versus 54.1 years old) with larger tumours (2.6 versus 2.1 cm) and with a higher frequency of lymph node metastasis (54% versus 39%). The histological category of IDC-NST was more common in the Homerton series (82% of cases versus 59% in the Nottingham series) and a 'Mixed' diagnosis was less common (7% versus 27% in the Nottingham collection). Tumour recurrence was much less common in the Homerton patients (14% compared to 43% in the Nottingham series) although the follow-up time was considerably shorter (61.6 months compared with 121.1 months follow-up for the Nottingham patients).

Parameter	WC (n=1455)	Nottingham (n=1274)	Homerton (n=181)
Age (mean, 95% CI)	54.4 (37-69) years	54.1 (37-69) years	56.9 (37-82) years
Tumour size (mean, 95% CI)	2.2 (0.9-4.0) cm	2.1 (0.9-4.0) cm	2.6 (1.0-5.1) cm
Tumour grade (% of cases)			
1	15	16	8
2	33	33	37
3	52	51	55
LN involvement (% of cases)			
Yes	41	39	54
No	59	61	46
Histological sub-type (% of cases)			
IDC-NST	62	59	82
ILC	7	7	5
Tubular carcinoma	3	3	1
Mucinous carcinoma	1	1	3
Medullary/atypical medullary	2	2	2
Mixed	24	27	7
Other	1	1	0
Molecular sub-type (% of cases)			
Luminal A	67	68	65
Luminal B	7	7	8
Her2 positive	7	7	6
Basal-like	14	13	17
Unclassified	5	5	4
Survival status (% of cases)			
Alive	61	60	63
Dead	39	40	37
Recurrence (% of cases)			
Yes	40	43	14
No	60	57	86
Follow-up (months (mean, 95% CI))	114.1 (19.0-199.0)	121.1 (23-201)	61.6 (7.5-125.8)

Table 7.2: Clinical, pathological and molecular characteristics of the study cohort. The table shows the features of the whole cohort (WC, n = 1455), together with a breakdown of the Nottingham and Homerton components. Abbreviations: CI = confidence interval, LN = lymph node, IDC-NST = invasive ductal carcinoma, no special type, ILC = invasive lobular carcinoma.

7.1.2 Correlation between c-Met expression and prognostic factors

7.1.2.1 Whole cohort

The correlation between c-Met scores and continuous variables is shown in Table 7.3 and the correlation with categorical variables is shown in Table 7.4.

There was a significant inverse correlation between c-Met expression and increasing tumour size (r = -0.113, p <0.001). There were no significant correlations between c-Met scores and age, p53 score or Ki67 score (Table 7.3).

Parameter	Correlation Coefficient	P-Value
Age	0.039	0.138
Tumour size	*-0.113*	*<0.001*
p53 score	0.018	0.538
Ki67 score	-0.046	0.114

Table 7.3: Correlation between c-Met scores and prognostic factors in the whole cohort (continuous variables). Significant correlations are given in italics (Spearman's correlation coefficient, n = 1455).

C-Met expression was significantly higher in lymph node negative tumours (mean score = 7.4) compared with node positive tumours (mean score = 7.2, p = 0.045; Table 7.4). Invasive lobular carcinomas (ILCs) showed significantly lower c-Met scores compared with non-ILCs (mean score = 6.6 versus 7.5 respectively, p <0.001), whereas tubular carcinomas (TC) showed significantly higher c-Met expression (mean score = 8.7 versus 7.4 for non-TC tumours, p = 0.002; Table 7.4).

Tumours classified as luminal A showed significantly lower c-Met scores (mean score = 7.4 versus 7.7 for non-luminal A tumours, p = 0.004) and BL tumours had higher levels of c-Met (mean score = 8.0 compared with 7.4 for all other molecular sub-types, p = 0.004; Table 7.4). Both EGFR and E-Cadherin positive tumours had

significantly higher c-Met scores. The mean c-Met score for EGFR positive tumours was 7.9 versus 7.4 for EGFR negative tumours, $p = 0.003$ and the mean score for E-Cadherin positive tumours was 7.5 versus 7.0 for E-Cadherin negative tumours, $p = 0.003$ (Table 7.4).

There were no significant differences in c-Met expression between high and low grade tumours, tumours with and without vascular invasion, tumours from patients of different ethnicity (black versus white) or between Her2 positive and Her2 negative tumours (Table 7.4).

Parameter	Mean c-Met score (95% CI)	P-Value
Tumour Grade		
1 or 2	7.5 (7.3-7.7)	
3	7.4 (7.3-7.6)	0.878
Lymph node involvement		
Yes	*7.2 (7.0-7.4)*	
No	*7.4 (7.2-7.6)*	*0.045*
Vascular invasion		
Yes	7.6 (7.3-7.4)	
No	7.5 (7.2-7.8)	0.305
Histological sub-type		
IDC-NST vs Non-IDC-NST	7.5 (7.3-7.6) vs 7.5 (7.3-7.7)	0.884
ILC vs Non-ILC	*6.6 (6.0-7.2) vs 7.5 (7.4-7.7)*	*<0.001*
Tubular carcinoma (TC) vs Non-TC	*8.7 (8.0-9.3) vs 7.4 (7.3-7.6)*	*0.002*
Mucinous carcinoma (MC) vs Non-MC	6.6 (5.0-8.1) vs 7.5 (7.4-7.6)	0.269
Medullary/atypical vs Non-medullary/atypical	8.1 (7.0-9.1) vs 7.5 (7.3-7.6)	0.28
Molecular sub-type		
Luminal A vs Non-Luminal A	*7.4 (7.2-7.5) vs 7.7 (7.5-7.9)*	*0.004*
Luminal B vs Non-Luminal B	7.3 (6.8-7.8) vs 7.5 (7.3-7.6)	0.586
Her2 positive vs Non-Her2	7.6 (7.2-8.0) vs 7.5 (7.3-7.6)	0.336
Basal-like (BL) vs Non-BL	*8.0 (7.6-8.4) vs 7.4 (7.2-7.5)*	*0.004*
Unclassified vs Non-Unclassified	7.6 (6.9-8.3) vs 7.5 (7.3-7.6)	0.212
Ethnicity		
Black	7.0 (6.4-7.5)	
White	7.1 (6.7-7.5)	0.898
Her2 status		
Positive	7.5 (7.1-7.8)	
Negative	7.5 (7.3-7.6)	0.733
EGFR status		
Positive	*7.9 (7.6-8.2)*	
Negative	*7.4 (7.3-7.6)*	*0.003*
E-Cadherin status		
Positive	*7.5 (7.4-7.7)*	
Negative	*7.0 (6.7-7.4)*	*0.003*

Table 7.4: Correlation between c-Met scores and prognostic factors in the whole cohort (categorical variables). Significant findings are given in italics (Mann-Whitney test, n = 1455). Abbreviations: CI = confidence interval, IDC-NST = invasive ductal carcinoma, no special type, ILC = invasive lobular carcinoma, TC = tubular carcinoma, MC = mucinous carcinoma.

7.1.2.2 Nottingham cohort

In the Nottingham cohort of patients, there was a significant negative correlation between c-Met expression and tumour size ($p < 0.001$) and a borderline significant negative correlation between c-Met and Ki67 score ($p = 0.050$, Table 7.5). There was no significant correlation between c-Met scores and patient age and p53 score (Table 7.5).

Parameter	Correlation Coefficient	P-Value
Age	0.018	0.531
Tumour size	*-0.104*	*<0.001*
p53 score	0.018	0.538
Ki67 score	-0.061	0.050

Table 7.5: Correlation between c-Met scores and prognostic factors within the Nottingham cohort (continuous variables). Significant correlations are given in italics (Spearman's correlation coefficient, n = 1274).

Patients without lymph node involvement showed significantly higher tumour c-Met expression compared to those with involvement (mean c-Met score = 7.5 versus 7.2 respectively, $p = 0.033$; Table 7.6). Tumours classified histologically as ILC had lower c-Met scores (mean score = 6.7 versus 7.6 for non-ILC tumours, $p = 0.001$) and those categorised as tubular carcinomas had higher c-Met scores (mean score = 8.8 versus 7.5 for non-tubular carcinomas, $p = 0.003$; Table 7.6). BL tumours showed higher c-Met expression (mean c-Met score = 8.0 compared with 7.4 for non-BL tumours, $p = 0.037$) and luminal A tumours showed significantly lower expression of c-Met (mean score = 7.4 versus 7.7 for non-luminal A tumours, $p = 0.014$; Table 7.6). There were no other significant differences in c-Met scores in the other parameters displayed in Table 7.6.

Parameter	Mean c-Met score (95% CI)	P-Value
Tumour Grade		
1 or 2	7.6 (7.3-7.8)	
3	7.5 (7.3-7.7)	0.942
Lymph node involvement		
Yes	*7.2 (7.0-7.5)*	
No	*7.5 (7.3-7.7)*	*0.033*
Vascular invasion		
Yes	7.5 (7.2-7.8)	
No	7.6 (7.4-7.7)	0.305
Histological sub-type		
IDC vs Non-IDC	7.5 (7.3-7.7) vs 7.6 (7.3-7.8)	0.873
ILC vs Non-ILC	*6.7 (6.1-7.3) vs 7.6 (7.5-7.8)*	*0.001*
Tubular carcinoma (TC) vs Non-TC	*8.8 (8.1-9.4) vs 7.5 (7.4-7.7)*	*0.003*
Mucinous carcinoma (MC) vs Non-MC	7.0 (4.9-9.2) vs 7.5 (7.4-7.7)	0.847
Medullary/atypical vs Non-medullary/atypical	8.0 (6.9-9.1) vs 7.5 (7.4-7.7)	0.451
Molecular sub-type		
Luminal A vs Non-Luminal A	*7.4 (7.2-7.6) vs 7.7 (7.5-8.0)*	*0.014*
Luminal B vs Non-Luminal B	7.4 (6.9-7.9) vs 7.5 (7.4-7.7)	0.839
Her2 positive vs Non-Her2	7.6 (7.1-8.1) vs 7.5 (7.4-7.7)	0.447
Basal-like (BL) vs Non-BL	*8.0 (7.6-8.5) vs 7.4 (7.3-7.6)*	*0.037*
Unclassified vs Non-Unclassified	7.7 (6.9-8.5) vs 7.5 (7.4-7.7)	0.140
Her2 status		
Positive	7.6 (7.2-7.9)	
Negative	7.6 (7.4-7.7)	0.675
EGFR status		
Positive	7.9 (7.5-8.2)	
Negative	7.5 (7.3-7.7)	0.065
E-Cadherin status		
Positive	7.6 (7.4-7.7)	
Negative	7.2 (6.7-7.6)	0.104

Table 7.6: Correlation between c-Met scores and prognostic factors within the Nottingham cohort (categorical variables). Significant findings are given in italics (Mann-Whitney test, n = 1274). Abbreviations: CI = confidence interval, IDC-NST = invasive ductal carcinoma, no special type, ILC = invasive lobular carcinoma, TC = tubular carcinoma, MC = mucinous carcinoma.

7.1.2.3 Homerton cohort

In the Homerton group of patients, there was a significant positive correlation between c-Met expression and patient age (p = 0.009, Table 7.7). There were no significant correlations between c-Met and tumour size, p53 or Ki67 scores (Table 7.7).

Parameter	Correlation Coefficient	P-Value
Age	*0.193*	*0.009*
Tumour size	-0.105	0.163
p53 score	-0.028	0.717
Ki67 score	0.022	0.781

Table 7.7: Correlation between c-Met scores and prognostic factors within the Homerton cohort (continuous variables). Significant correlations are given in italics (Spearman's correlation coefficient, n = 181).

Tumours in the IDC-NST histological category showed a significantly higher c-Met score (mean score = 7.2 versus 6.1 for non-IDC-NST tumours, p = 0.003; Table 7.8). Of the molecular sub-types, only BL tumours showed significantly higher c-Met expression (mean score = 8.0 compared with 6.8 for non-BL tumours, p = 0.003; Table 7.8). Both EGFR positive (mean c-Met score = 8.0 versus 6.7 for EGFR negative tumours, p = 0.001) and E-Cadherin positive (mean c-Met score = 7.3 versus 6.7 for E-Cadherin negative tumours, p = 0.039; Table 7.8) tumours showed higher c-Met levels. There were no significant differences in c-Met expression in the other parameters displayed in Table 7.8.

Parameter	Mean c-Met score (95% CI)	P-Value
Tumour Grade		
1 or 2	7.0 (6.5-7.4)	
3	7.1 (6.7-7.5)	0.431
Lymph node involvement		
Yes	7.1 (6.7-7.5)	
No	6.9 (6.4-7.4)	0.369
Histological sub-type		
IDC vs Non-IDC	*7.2 (6.9-7.6) vs 6.1 (5.4-6.7)*	*0.003*
ILC vs Non-ILC	5.9 (5.0-6.8) vs 7.1 (6.8-7.4)	0.065
Mucinous carcinoma (MC) vs Non-MC	5.6 (3.3-7.9) vs 7.1 (6.8-7.4)	0.126
Medullary/atypical vs Non-medullary/atypical	8.3 (3.9-12.7) vs 7.0 (6.7-7.3)	0.319
Molecular sub-type		
Luminal A vs Non-Luminal A	6.9 (6.5-7.2) vs 7.4 (6.9-8.0)	0.077
Luminal B vs Non-Luminal B	6.4 (5.2-7.6) vs 7.1 (6.8-7.4)	0.356
Her2 positive vs Non-Her2	7.3 (6.6-8.1) vs 7.0 (6.7-7.4)	0.632
Basal-like (BL) vs Non-BL	*8.0 (7.2-8.9) vs 6.8 (6.5-7.2)*	*0.003*
Unclassified vs Non-Unclassified	6.6 (4.4-8.8) vs 7.1 (6.8-7.4)	0.444
Ethnicity		
Black	7.0 (6.4-7.5)	
White	7.1 (6.7-7.5)	0.898
Her2 status		
Positive	6.8 (6.1-7.6)	
Negative	7.1 (6.7-7.4)	0.746
EGFR status		
Positive	*8.0 (7.3-8.7)*	
Negative	*6.7 (6.4-7.1)*	*0.001*
E-Cadherin status		
Positive	*7.3 (6.9-7.7)*	
Negative	*6.7 (6.2-7.2)*	*0.039*

Table 7.8: Correlation between c-Met scores and prognostic factors within the Homerton cohort (categorical variables). Significant findings are given in italics (Mann-Whitney test, n = 181). Abbreviations: CI = confidence interval, IDC-NST = invasive ductal carcinoma, no special type, ILC = invasive lobular carcinoma, MC = mucinous carcinoma.

7.1.2.4 Molecular sub-type analysis – whole cohort

7.1.2.4.1 Luminal A tumours

Within the luminal A tumours, there was a significant positive correlation between c-Met expression and age at presentation (p = 0.012, Table 7.9). There was a significant negative correlation between c-Met scores and tumour size (p <0.001) and Ki67 score (p = 0.004, Table 7.9). There was no correlation between c-Met and p53 scores.

Parameter	Correlation Coefficient	P-Value
Age	*0.082*	*0.012*
Tumour size	*-0.142*	*<0.001*
p53 score	0.011	0.763
Ki67 score	*-0.105*	*0.004*

Table 7.9: Correlation between c-Met scores and prognostic factors within the luminal A sub-group (continuous variables). Significant correlations are given in italics (Spearman's correlation coefficient, n = 928).

Lymph node positive tumours showed lower c-Met levels (mean score = 6.9 compared with 7.4 for node positive tumours, p = 0.011; Table 7.10). As with the whole cohort, luminal A ILCs had significantly lower c-Met scores (mean score = 6.6 versus 7.5 for non-ILCs, p = 0.001; Table 7.10) and luminal A tubular carcinomas had higher c-Met expression (mean score = 8.6 versus 7.3 for all other histological sub-types, p = 0.003; Table 7.10). Medullary and atypical medullary carcinomas also had higher c-Met levels (mean score = 9.7 versus 7.4 for the other histological sub-types, p=0.034; Table 7.10). Luminal A tumours that were E-Cadherin positive or EGFR positive showed significantly higher c-Met levels (p < 0.001 and p = 0.002 respectively; Table 7.10). There were no significant differences in c-Met scores between high and low grade tumours, tumours with and without

vascular invasion and between tumours arising in black versus white women (Table 7.10).

Parameter	Mean c-Met score (95% CI)	P-Value
Tumour Grade		
1 or 2	7.4 (7.2-7.6)	
3	7.3 (7.0-7.5)	0.522
Lymph node involvement		
Yes	*6.9 (6.7-7.2)*	
No	*7.4 (7.2-7.6)*	*0.011*
Vascular invasion		
Yes	7.3 (7.0-7.7)	
No	7.5 (7.3-7.7)	0.400
Histological sub-type		
IDC-NST vs Non-IDC-NST	7.3 (7.0-7.5) vs 7.5 (7.2-7.7)	0.300
ILC vs Non-ILC	*6.6 (6.0-7.2) vs 7.5 (7.3-7.6)*	*0.001*
Tubular carcinoma (TC) vs Non-TC	*8.6 (7.9-9.2) vs 7.3 (7.1-7.5)*	*0.003*
Mucinous carcinoma (MC) vs Non-MC	6.8 (5.0-8.7) vs 7.4 (7.2-7.5)	0.742
Medullary/atypical vs Non-medullary/atypical	9.7 (7.4-11.9) vs 7.4 (7.2-7.5)	0.034
Ethnicity		
Black	6.9 (6.2-7.7)	
White	6.8 (6.4-7.3)	0.523
EGFR status		
Positive	*8.1 (7.6-8.5)*	
Negative	*7.3 (7.1-7.5)*	*0.002*
E-Cadherin status		
Positive	*7.5 (7.3-7.7)*	
Negative	*6.7 (6.3-7.2)*	*<0.001*

Table 7.10: Correlation between c-Met scores and prognostic factors within the luminal A sub-group (categorical variables). Significant findings are given in italics (Mann-Whitney test, n = 928). Abbreviations: CI = confidence interval, IDC-NST = invasive ductal carcinoma, no special type, ILC = invasive lobular carcinoma, TC = tubular carcinoma, MC = mucinous carcinoma.

7.1.2.4.2 Luminal B tumours

There was a significant positive correlation between c-Met expression and p53 scores in the luminal B sub-group (p = 0.016, Table 7.11). There were no significant correlations between c-Met scores and age, tumour size or Ki67 index (Table 7.11).

Parameter	Correlation Coefficient	P-Value
Age	-0.089	0.376
Tumour size	0.024	0.815
p53 score	*0.246*	*0.016*
Ki67 score	0.051	0.662

Table 7.11: Correlation between c-Met scores and prognostic factors within the luminal B sub-group (continuous variables). Significant correlations are given in italics (Spearman's correlation coefficient, n = 100).

Within the luminal B sub-group, there were no significant differences in c-Met scores between the categorical variables displayed in Table 7.12.

Parameter	Mean c-Met score (95% CI)	P-Value
Tumour Grade		
1 or 2	7.1 (6.1-8.0)	
3	7.3 (6.8-7.9)	0.514
Lymph node involvement		
Yes	7.0 (6.3-7.7)	
No	7.2 (6.5-8.0)	0.407
Vascular invasion		
Yes	7.3 (6.5-8.1)	
No	7.5 (6.7-8.2)	0.638
Histological sub-type		
IDC-NST vs Non-IDC-NST	7.2 (6.7-7.8) vs 7.5 (6.0-9.0)	0.473
Ethnicity		
Black	5.7 (3.7-7.8)	
White	7.2 (5.4-9.0)	0.116
EGFR status		
Positive	7.7 (6.3-9.0)	
Negative	7.4 (6.8-7.9)	0.536
E-Cadherin status		
Positive	7.4 (6.9-7.9)	
Negative	6.7 (5.0-8.5)	0.543

Table 7.12: Correlation between c-Met scores and prognostic factors within the luminal B sub-group (categorical variables). Only the IDC-NST histological sub-type is shown as the other sub-types contained too few cases (Mann-Whitney test, n = 100). Abbreviations: CI = confidence interval, IDC-NST = invasive ductal carcinoma, no special type.

7.1.2.4.3 Her2 positive tumours

There was a borderline negative correlation between c-Met scores and tumour size in the Her2 positive sub-group (p = 0.063, Table 7.13). There were no significant correlations between c-Met expression and patient age, p53 or Ki67 scores (Table 7.13).

Parameter	Correlation Coefficient	P-Value
Age	0.023	0.825
Tumour size	-0.191	0.063
p53 score	0.139	0.183
Ki67 score	-0.111	0.342

Table 7.13: Correlation between c-Met scores and prognostic factors within the Her2 positive sub-group (continuous variables). Spearman's correlation coefficient (n = 95).

Low grade (grades 1 or 2) tumours in the Her2 positive sub-group showed significantly higher c-Met scores compared to high grade (grade 3) tumours (mean score = 8.9 versus 7.4 respectively, p = 0.012; Table 7.14). There were no significant differences in c-Met scores in the other categorical variables displayed in Table 7.14.

Parameter	Mean c-Met score (95% CI)	P-Value
Tumour Grade		
1 or 2	*8.9 (8.0-9.8)*	
3	*7.4 (7.0-7.9)*	*0.012*
Lymph node involvement		
Yes	7.6 (7.1-8.2)	
No	7.3 (6.5-8.2)	0.917
Vascular invasion		
Yes	7.5 (6.8-8.2)	
No	7.8 (7.1-8.4)	0.148
Histological sub-type		
IDC-NST vs Non-IDC-NST	7.6 (7.2-8.0) vs 8.2 (5.4-10.9)	0.851
Medullary/atypical vs Non-medullary/atypical	9.0 (1.6-14) vs 7.6 (7.2-8.0)	0.454
Ethnicity		
Black	7.0 (5.4-8.6)	
White	7.7 (6.6-8.7)	0.451
EGFR status		
Positive	7.6 (6.7-8.5)	
Negative	7.6 (7.2-8.1)	0.991
E-Cadherin status		
Positive	7.5 (7.0-7.9)	
Negative	8.3 (7.1-9.6)	0.266

Table 7.14: Correlation between c-Met scores and prognostic factors within the Her2 positive sub-group (categorical variables). Significant findings are given in italics (Mann-Whitney test, n = 95). Only the IDC-NST and medullary/atypical medullary histological sub-types are shown as the other sub-types contained too few cases. Abbreviations: CI = confidence interval, IDC-NST = invasive ductal carcinoma, no special type.

7.1.2.4.4 BL tumours

There was a significant inverse correlation between c-Met scores and both p53 and Ki67 scores within the BL sub-group (r = -0.255, p = 0.002; r = -0.255, p = 0.005 respectively; Table 7.15). There were no significant correlations between c-Met scores and patient age or tumour size (Table 7.15).

Parameter	Correlation Coefficient	P-Value
Age	0.057	0.440
Tumour size	-0.005	0.950
p53 score	*-0.255*	*0.002*
Ki67 score	*-0.255*	*0.005*

Table 7.15: Correlation between c-Met scores and prognostic factors within the BL sub-group (continuous variables). Significant correlations are given in italics (Spearman's correlation coefficient, n = 184).

There were no significant differences in c-Met scores in the categorical variables displayed in Table 7.16.

Parameter	Mean c-Met score (95% CI)	P-Value
Tumour Grade		
1 or 2	9.1 (7.4-10.9)	
3	7.9 (7.5-8.3)	0.112
Lymph node involvement		
Yes	7.9 (7.4-8.4)	
No	7.9 (7.3-8.4)	0.679
Vascular invasion		
Yes	8.2 (7.6-8.9)	
No	7.9 (7.3-8.6)	0.992
Histological sub-type		
IDC-NST vs Non-IDC-NST	8.1 (7.7-8.5) vs 8.0 (7.0-9.0)	0.634
Medullary/atypical vs Non-medullary/atypical	7.4 (6.1-8.7) vs 8.1 (7.7-8.6)	0.180
Ethnicity		
Black	8.0 (6.7-9.2)	
White	8.1 (7.1-9.2)	0.951
EGFR status		
Positive	7.8 (7.3-8.3)	
Negative	8.4 (7.6-9.1)	0.360
E-Cadherin status		
Positive	8.0 (7.6-8.5)	
Negative	7.9 (7.0-8.8)	0.897

Table 7.16: Correlation between c-Met scores and prognostic factors within the BL sub-group (categorical variables). Only the IDC-NST and medullary/atypical medullary histological sub-types are shown as the other sub-types contained too few cases (Mann-Whitney test, n = 184). Abbreviations: CI = confidence interval, IDC-NST = invasive ductal carcinoma, no special type.

7.1.2.4.5 Unclassified tumours

There was a significant inverse correlation between c-Met scores and tumour size (r = -0.328, p = 0.005; Table 7.17). There was a borderline significant inverse correlation between c-Met scores and patient age (r = -0.213, p = 0.071; Table 7.17). There were no significant correlations between c-Met scores and p53 or Ki67 scores (Table 7.17).

Parameter	Correlation Coefficient	P-Value
Age	-0.213	0.071
Tumour size	*-0.328*	*0.005*
p53 score	-0.039	0.741
Ki67 score	0.104	0.417

Table 7.17: Correlation between c-Met scores and prognostic factors within the unclassified sub-group (continuous variables). Significant correlations are given in italics (Spearman's correlation coefficient, n = 73).

There were no significant differences in c-Met scores in the categorical variables displayed in Table 7.18.

Parameter	Mean c-Met score (95% CI)	P-Value
Tumour Grade		
1 or 2	7.4 (4.6-10.1)	
3	7.6 (6.8-8.4)	0.936
Lymph node involvement		
Yes	7.8 (6.8-8.5)	
No	7.3 (6.2-8.4)	0.391
Vascular invasion		
Yes	7.7 (6.2-9.2)	
No	7.7 (6.7-8.7)	0.829
Histological sub-type		
IDC-NST vs Non-IDC-NST	7.6 (6.8-8.4) vs 7.4 (5.6-9.3)	0.660
Medullary/atypical vs Non-medullary/atypical	8.9 (6.2-11.5) vs 7.4 (6.6-8.2)	0.678
Ethnicity		
Black	5.5 (0.2-10.9)	
White	7.4 (3.5-11.3)	0.372
E-Cadherin status		
Positive	7.9 (7.1-8.7)	
Negative	6.5 (4.6-8.5)	0.133

Table 7.18: Correlation between c-Met scores and prognostic factors within the unclassified sub-group (categorical variables). Only the IDC-NST and medullary/atypical medullary histological sub-types are shown as the other sub-types contained too few cases (Mann-Whitney test, n = 73). Abbreviations: CI = confidence interval, IDC-NST = invasive ductal carcinoma, no special type.

7.1.3 Correlation between c-Met, other prognostic factors and the BL sub-type in the whole cohort

In the whole cohort analysis, only tumours classified as BL by IHC showed significantly higher c-Met expression. In the next stage of the analysis, I established which other prognostic factors also associated with the BL sub-type.

7.1.3.1 Univariate analysis

Several factors were associated with BL tumours (Table 7.19). These included: increasing tumour size ($p = 0.007$), increasing p53 score ($p < 0.001$), increasing Ki67 score ($p < 0.001$), grade 3 tumours ($p < 0.001$), the histological sub-types IDC-NST and medullary/atypical medullary ($p < 0.001$ for both) and being of black ethnicity

(p = 0.028). Increasing age was associated with a lower chance of having a BL tumour (p < 0.001). Increasing c-Met scores showed an odds ratio of 3.79 for having BL cancer (p = 0.002).

Parameter	LR Chi-Square	OR (95% CI)	P Value
Age	*18.4*	*0.97 (0.95-0.98)*	*<0.001*
Tumour size	*6.5*	*1.16 (1.04-1.30)*	*0.007*
p53 score	*125.5*	*9.80 (6.56-14.64)*	*<0.001*
Ki67 score	*134.0*	*25.78 (14.40-46.17)*	*<0.001*
Tumour grade			
1 or 2		*1*	
3	*154.3*	*12.54 (7.42-21.20)*	*<0.001*
Lymph node involvement			
No		1	
Yes	0.1	1.01 (0.72-1.41)	0.955
Vascular invasion			
No		1	
Yes	3.6	1.41 (0.99-2.0)	0.055
Histological sub-type			
IDC-NST	*55.3*	*4.28 (2.76-6.63)*	*<0.001*
Medullary/atypical medullary	*23.8*	*6.83 (3.31-14.07)*	*<0.001*
Ethnicity			
White		*1*	
Black	*5.0*	*2.45 (1.10-5.44)*	*0.028*
E-Cadherin status			
Negative		1	
Positive	2.2	0.75 (0.51-1.08)	0.127
C-Met score	*9.5*	*3.79 (1.60-8.97)*	*0.002*

Table 7.19: Association between c-Met, other prognostic factors and the BL sub-type. Significant findings are given in italics (univariate logistic regression, n = 1455). Abbreviations: CI = confidence interval, IDC-NST = invasive ductal carcinoma, no special type, LR = likelihood ratio, OR = odds ratio.

7.1.3.2 Multivariate analysis

To establish if c-Met was independently associated with the BL sub-group, I entered c-Met score together with the six other factors associated with BL tumours at univariate analysis (age at presentation, tumour size, p53 score, Ki67 score, tumour

grade and histological sub-type (IDC-NST and medullary/atypical medullary); ethnicity was excluded as an insufficient numbers of cases had this data) into the multivariate model.

After forward stepwise entry (Table 7.20), the five factors that remained in the multivariate model were Ki67 score ($p < 0.001$), p53 score ($p < 0.001$), tumour grade ($p < 0.001$), c-Met score ($p = 0.005$) and age at presentation ($p = 0.006$).

Parameter	Stepwise entry order	LR Chi-Square	OR (95% CI)	P Value
Ki67 score	1	123.7	7.30 (3.24-16.44)	<0.001
p53 score	2	46.2	4.47 (2.72-7.36)	<0.001
Tumour grade	3	18.3	4.98 (2.23-11.13)	<0.001
C-Met score	4	9.5	6.44 (1.74-23.78)	0.005
Age	5	7.6	0.97 (0.95-0.99)	0.006

Table 7.20: Independent association between c-Met, other prognostic factors and the BL sub-type (multivariate logistic regression with forward stepwise entry, n = 945). Abbreviations: CI = confidence interval, LR = likelihood ratio, OR = odds ratio.

7.1.4 C-Met expression and survival

C-Met scores were dichotomised into 'high' (≥ 7) or 'low' (< 7) to create Kaplan Meier curves for survival analysis, as described in section 6.4.2.

7.1.4.1 Whole cohort

Within the whole cohort, overall mean survival time was significantly shorter for patients with c-Met high tumours (159.6 months, 95% confidence interval (CI) = 153.8 – 165.5 versus 181.3 months, 95% CI = 170.1 – 192.5 for c-Met low tumours, $p = 0.009$, log-rank test, n = 1319, Figure 7.2A). After taking into account four other factors associated with poor prognosis in breast cancer (tumour grade, lymph node metastasis, tumour size and patient age), c-Met remained an independent poor

prognostic factor in the whole cohort (hazard ratio = 1.81, 95% confidence interval (CI) = 1.07 – 3.06, p = 0.026, Cox regression, n = 1153, Table 7.21).

Parameter	Stepwise entry order	LR Chi-Square	HR (95% CI)	P-Value
Tumour grade				
1 or 2			1	
3	1	67.9	2.22 (1.81-2.72)	<0.001
Lymph node status				
No			1	
Yes	2	39.1	1.84 (1.52-2.24)	<0.001
Age	3	36.7	1.03 (1.02-1.04)	<0.001
Tumour size	4	14.6	1.20 (1.11-1.30)	<0.001
C-Met score	5	5.1	1.81 (1.07-3.06)	0.026

Table 7.21: Multivariate model for overall survival in the whole cohort. The table contains those parameters that are independently predictive of reduced survival (Cox regression with forward stepwise entry, n = 1153). Abbreviations: LR = likelihood ratio, HR = hazard ratio, CI = confidence interval.

A

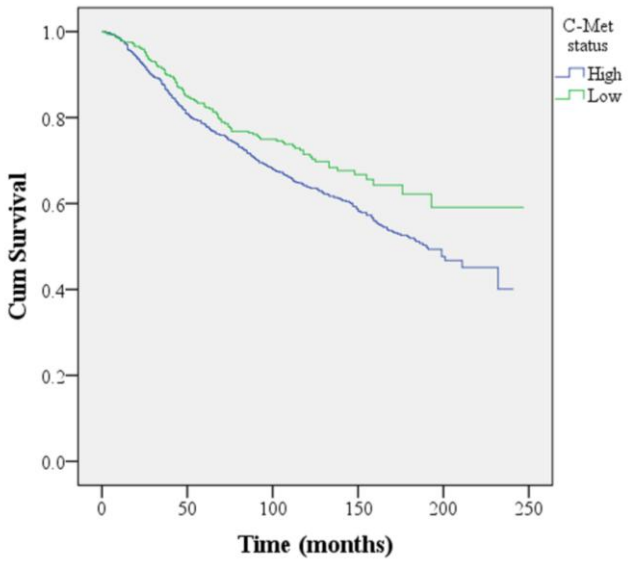

B

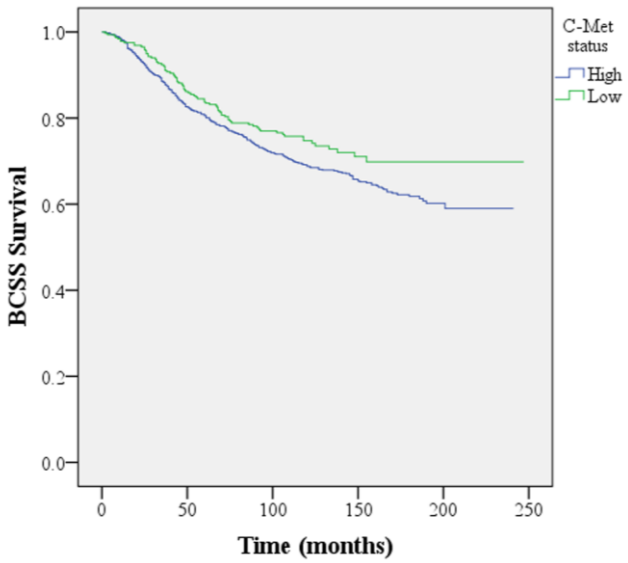

Figure 7.2: Kaplan-Meier survival curves for the whole cohort. **A** shows overall survival and **B** shows breast cancer specific survival (BCSS). For overall survival (**A**), patients with c-Met high tumours showed a worse outcome (p = 0.009, log-rank test, n = 1319; hazard ratio (HR) = 1.81, 95% confidence interval (CI) = 1.07 – 3.06, p = 0.026, Cox regression, n = 1153). For BCSS (**B**), patients with c-Met high tumours also showed reduced survival (p = 0.047, log-rank test, n = 1319; HR = 1.96, 95% CI = 1.07 – 3.56, p = 0.028, Cox regression, n = 1153).

Similarly, patients with c-Met high tumours showed shorter breast cancer specific survival (BCSS) compared to those with c-Met low tumours (mean survival time = 174.7 months, 95% CI = 168.8 – 180.5 versus 192.6 months, 95% CI = 182.2 – 202.9 respectively, p = 0.047, log-rank test, n = 1319, Figure 7.2B). C-Met remained a poor prognostic marker for BCSS after taking into account established prognostic factors (HR = 1.96, 95% CI = 1.07 – 3.56, p = 0.028, Cox regression, n = 1153, Table 7.22).

Parameter	Stepwise entry order	LR Chi-Square	HR (95% CI)	P-Value
Tumour grade				
1 or 2			1	
3	1	90.9	2.77 (2.17-3.53)	<0.001
Lymph node status				
No			1	
Yes	2	63.5	2.34 (1.87-2.93)	<0.001
Tumour size	3	14.8	1.22 (1.13-1.33)	<0.001
Age	4	10.8	1.02 (1.01-1.03)	0.001
C-Met score	5	4.9	1.96 (1.07-3.56)	0.028

Table 7.22: Multivariate model for BCSS in the whole cohort. The table contains those parameters that are independently predictive of reduced survival (Cox regression with forward stepwise entry, n = 1153). Abbreviations: LR = likelihood ratio, HR = hazard ratio, CI = confidence interval.

7.1.4.2 Nottingham cohort

Patients with c-Met high tumours showed shorter overall survival time compared with those who had c-Met low tumours (mean survival time = 162.2 months, 95% CI = 156.5 – 168.6 versus 186.2 months, 95% CI = 174.4 – 197.9 respectively, p = 0.005, log-rank test, n = 1154, Figure 7.3A). C-Met expression remained a poor prognostic factor at multivariate analysis (HR = 1.85, 95% CI = 1.07 – 3.19, p = 0.027, Cox regression, n = 1002).

Similar results were seen with BCSS, where c-Met high tumours were associated with reduced patient survival (mean survival time = 177.5 months, 95% CI = 171.5 – 183.4 versus 198.6 months, 95% CI = 187.9 – 209.3 for patients with c-Met low tumours, p = 0.016, log-rank test, n = 1154, Figure 7.3B). C-Met was a poor prognostic factor for BCSS after taking into account other prognostic factors (HR = 2.09, 95% CI = 1.11 – 3.94, p = 0.022, Cox regression, n = 1002.)

7.1.4.3 Homerton cohort

There were no significant differences in overall survival between patients with c-Met high or c-Met low tumours in the Homerton patients (mean survival time = 102.3, 95% CI = 87.1 – 117.5 versus 103.8 months, 95% CI = 89.9 – 117.7 respectively, p = 0.215, log-rank test, n = 165, Figure 7.4A). C-Met was not an independent predictor of poor outcome (HR = 2.21, 95% CI = 0.29 – 17.10, p = 0.448, Cox regression, n =151).

Regarding BCSS, c-Met expression was not significantly associated with survival at univariate (mean survival time for c-Met high tumours = 109.4 months, 95% CI = 94.1 – 124.7 versus 103.8 months, 95% CI = 89.9 – 117.7 for c-Met low tumours, p = 0.440, log-rank test, n = 165, Figure 7.4B) or multivariate analysis (HR = 1.29, 95% CI = 0.15 – 10.73, p = 0.817, Cox regression, n = 151).

7.1.4.4 Luminal A tumours

Within the luminal A sub-group, patients with c-Met high tumours showed a shorter overall survival compared with c-Met low tumours (mean survival time = 169.5 months, 95% CI = 162.5 – 176.5 versus 188.2 months, 95% CI = 174.6 – 201.8 respectively, p = 0.034, log-rank test, n = 842, Figure 7.5A). C-Met was not an

A

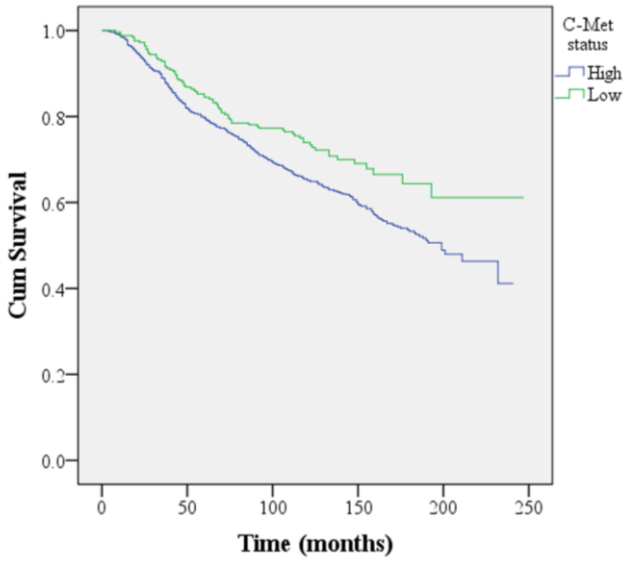

B

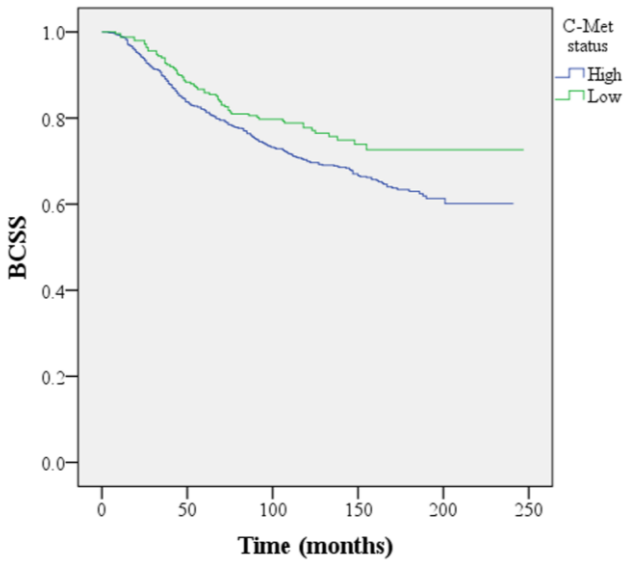

Figure 7.3: Kaplan-Meier survival curves for the Nottingham cohort. **A** shows overall survival and **B** shows breast cancer specific survival (BCSS). For overall survival (**A**), patients with c-Met high tumours showed a worse outcome (p = 0.005, log-rank test, n = 1154; hazard ratio (HR) = 1.85, 95% confidence interval (CI) = 1.07 – 3.19, p = 0.027, Cox regression, n = 1002). For BCSS (**B**), patients with c-Met high tumours also showed reduced survival (p = 0.016, log-rank test, n = 1154; HR = 2.09, 95% CI = 1.11 – 3.94, p = 0.022, Cox regression, n = 1002).

A

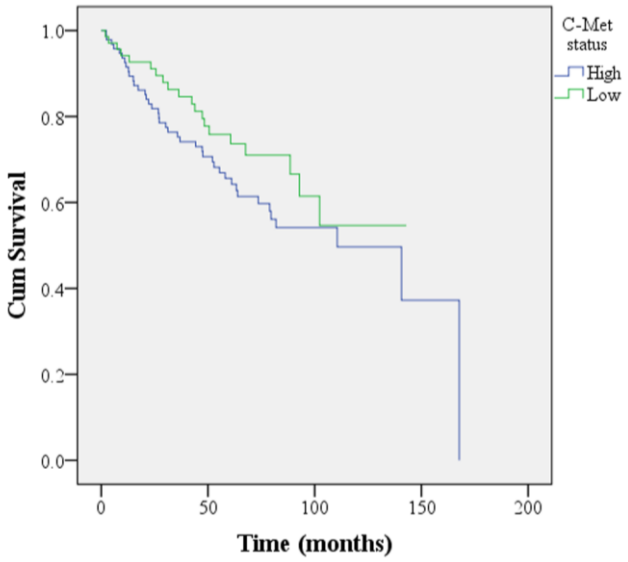

B

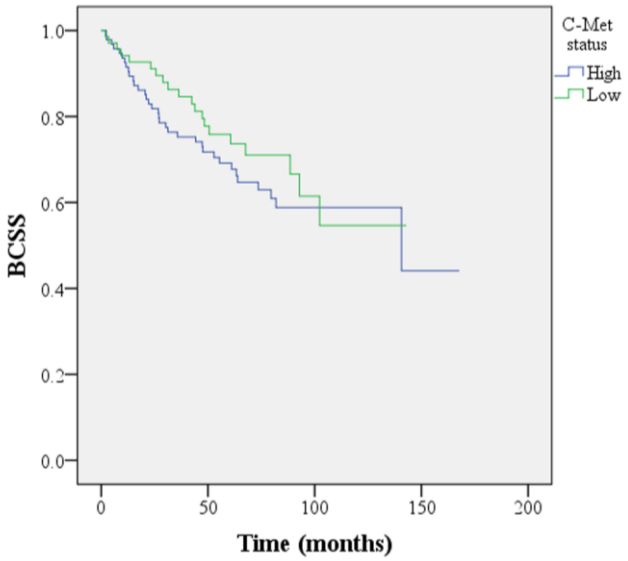

Figure 7.4: Kaplan-Meier survival curves for the Homerton cohort. **A** shows overall survival and **B** shows breast cancer specific survival (BCSS). For both overall survival (**A**) and BCSS (**B**), there was no significant difference between c-Met high and low tumours ($p = 0.215$ and $p = 0.440$ respectively, log-rank test, $n = 165$).

A

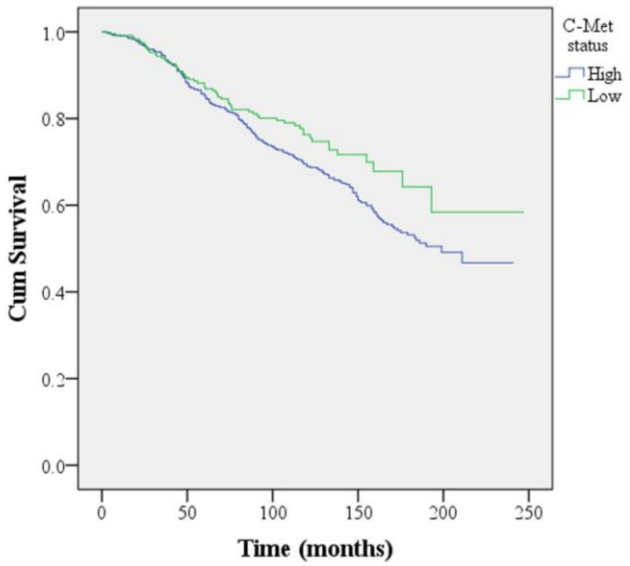

B

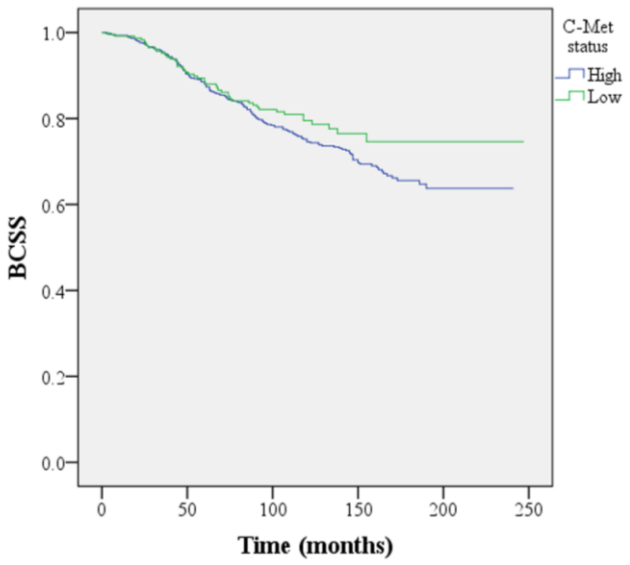

Figure 7.5: Kaplan-Meier survival curves for the luminal A tumours. **A** shows overall survival and **B** shows breast cancer specific survival (BCSS). For overall survival (**A**), patients with c-Met high tumours showed a worse outcome at univariate analysis (p = 0.034, log-rank test, n = 842) but not at multivariate analysis (hazard ratio (HR) = 1.71, 95% confidence interval (CI) = 0.86 – 3.41, p = 0.130, Cox regression, n = 741). For BCSS (**B**), patients with c-Met high tumours also showed a trend towards reduced survival, but this was not significant (p = 0.146, log-rank test, n = 842).

independent poor prognostic factor for overall survival at multivariate analysis (HR = 1.71, 95% CI = 0.86 – 3.41, p = 0.130, Cox regression, n = 741).

Patients with c-Met high tumours showed a trend towards shorter BCSS compared to patients with c-Met low tumours but this was not significant at univariate (mean survival time = 187.3 months, 95% CI = 180.5 – 194.0 versus 203.3 months, 95% CI = 192.1 – 214.5 respectively, p = 0.146, log-rank test, n = 842, Figure 7.5B) or multivariate analysis (HR = 2.05, 95% CI = 0.90 – 4.63, p = 0.087, Cox regression, n = 741).

7.1.4.5 Luminal B tumours

Patients with luminal B, c-Met high tumours showed a trend towards poorer overall survival compared to those with luminal B, c-Met low tumours but this was not significant (mean survival time = 124.2 months, 95% CI = 105.5 – 142.9 versus 154.1 months, 95% CI = 108.4 – 199.7, p = 0.579, log-rank test, n = 93, Figure 7.6A; HR = 1.88, 95% CI = 0.22 – 16.00, p = 0.562, Cox regression, n = 76).

BCSS within the luminal B sub-group showed a similar trend but no significant difference between c-Met high and low tumours (mean survival time = 130 months, 95% CI = 110.8 – 149.1 versus 162.7 months, 95% CI = 116.5 – 208.9 respectively, p = 0.536, log-rank test, n = 93, Figure 7.6B; HR = 2.17, 95% CI = 0.21 – 22.52, p = 0.515, Cox regression, n = 76).

7.1.4.6 Her2 positive tumours

There was no significant difference in overall survival between patients with c-Met high and c-Met low Her2 positive tumours (mean survival time = 130.3 months, 95% CI = 107.3 – 153.3 versus 115.2 months, 95% CI = 64.0 – 166.5 respectively, p =

A

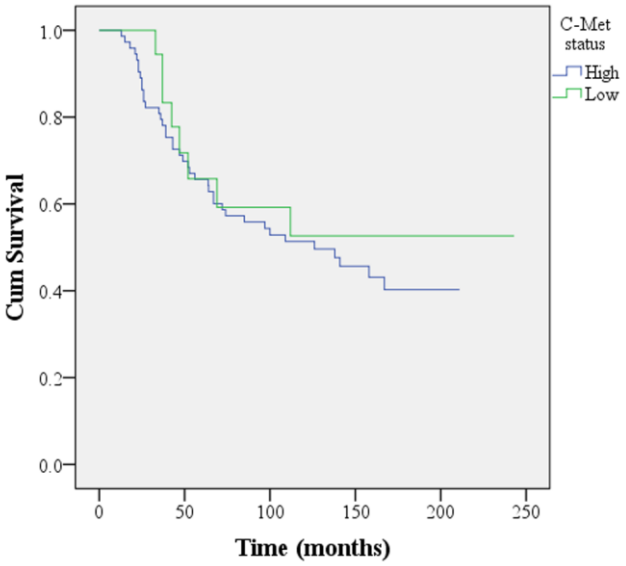

B

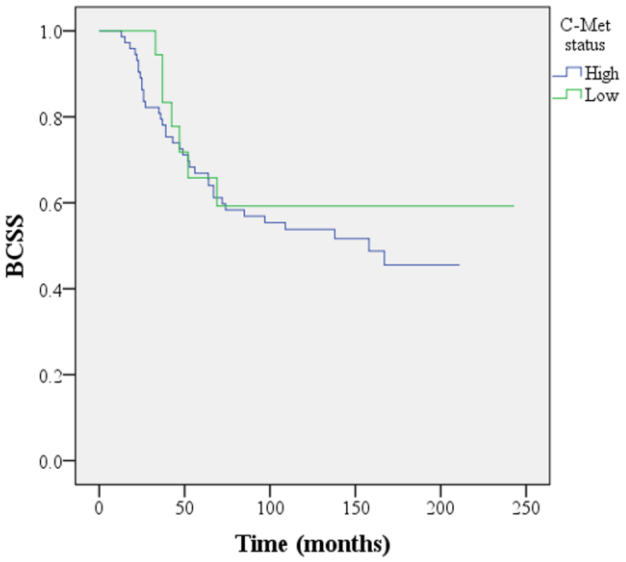

Figure 7.6: Kaplan-Meier survival curves for the luminal B tumours. **A** shows overall survival and **B** shows breast cancer specific survival (BCSS). For both overall survival (**A**) and BCSS (**B**), in patients with c-Met high tumours there was a trend towards worse outcome but this was not significant ($p = 0.579$ and $p = 0.536$ respectively, log-rank test, $n = 93$).

0.968, log-rank test, n = 84, Figure 7.7A). C-Met expression was not a poor prognostic factor at multivariate analysis (HR = 2.66, 95% CI = 0.28 – 25.17, p = 0.395, Cox regression, n = 74).

There was no significant difference in BCSS between those patients with Her2 positive c-Met high tumours and those with c-Met low tumours (mean survival time = 136.8 months, 95% CI = 113.9 – 159.8 versus 115.2 months, 95% CI = 64.0 – 166.5 respectively, p = 0.880, log-rank test, n = 84, Figure 7.7B). C-Met scores were not independently associated with poor BCSS (HR = 2.64, 95% CI = 0.24 – 28.56, p = 0.425, Cox regression, n = 74).

7.1.4.7 BL tumours

Patients with c-Met high BL tumours showed a trend towards shorter overall survival, but this was not significant (mean survival time = 141.7 months, 95% CI = 125.4 – 158 compared with 164.3 months, 95% CI = 129.0 – 199.7 for patients with c-Met low tumours, p = 0.310, log-rank test, n = 167, Figure 7.8A). C-Met expression was not significantly associated with overall survival at regression analysis (HR = 2.26, 95% CI = 0.52 – 9.87, p = 0.280, Cox regression, n = 147).

There were no significant differences in BCSS between the c-Met high and low groups, but again there was a trend towards reduced survival in patients with c-Met high tumours (mean survival time = 148.1 months, 95% CI = 131.6 – 164.5 versus 170.2 months, 95% CI = 134.9 – 205.4 for patients with c-Met low tumours, p = 0.315, log-rank test, n =167, Figure 7.8B). At multivariate analysis c-Met scores were not significantly associated with BCSS (HR = 3.16, 95% CI = 0.64 – 15.51, p = 0.156, Cox regression, n = 147).

A

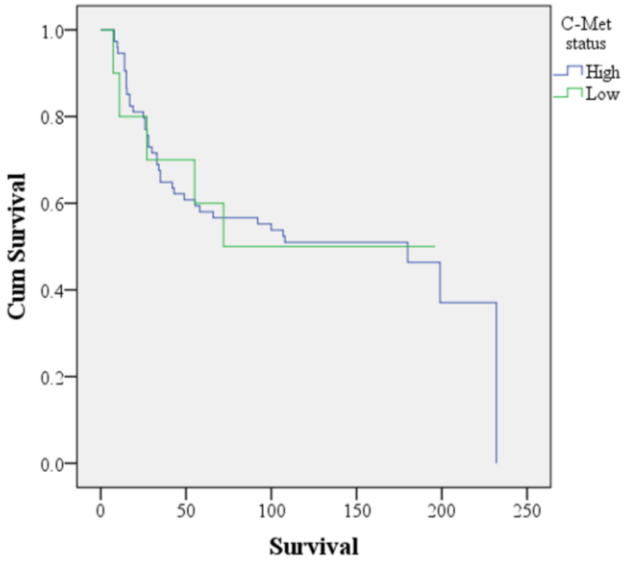

B

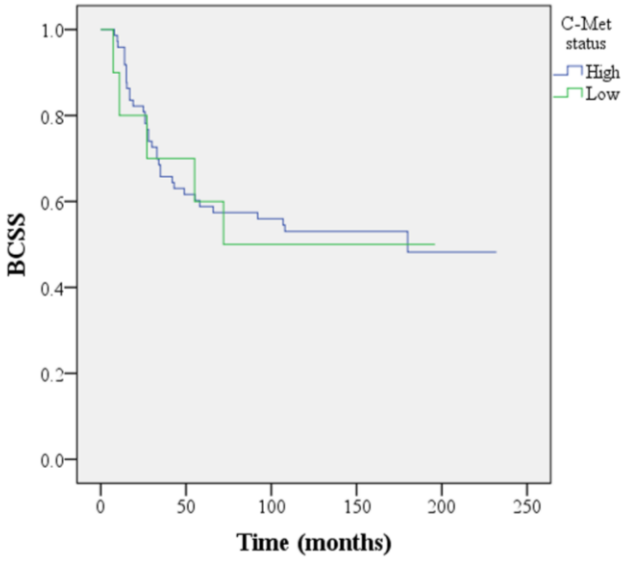

Figure 7.7: Kaplan-Meier survival curves for the Her2 positive tumours. **A** shows overall survival and **B** shows breast cancer specific survival (BCSS). For both overall survival (**A**) and BCSS (**B**), there were no significant differences between c-Met high and c-Met low tumours ($p = 0.968$ and $p = 0.880$ respectively, log-rank test, $n = 84$).

A

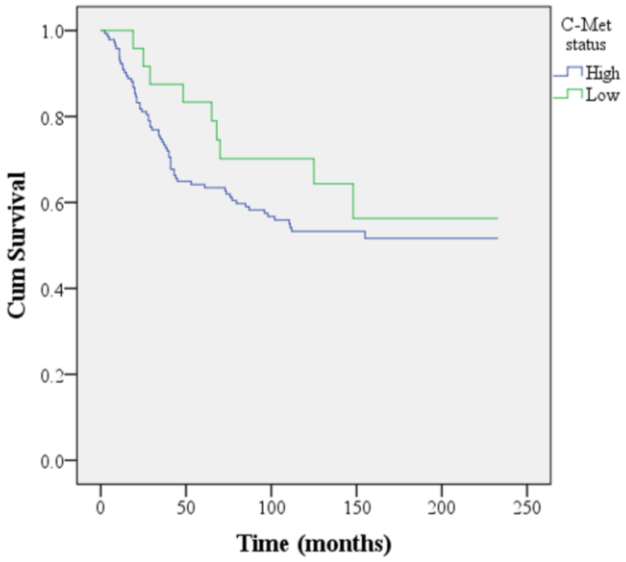

B

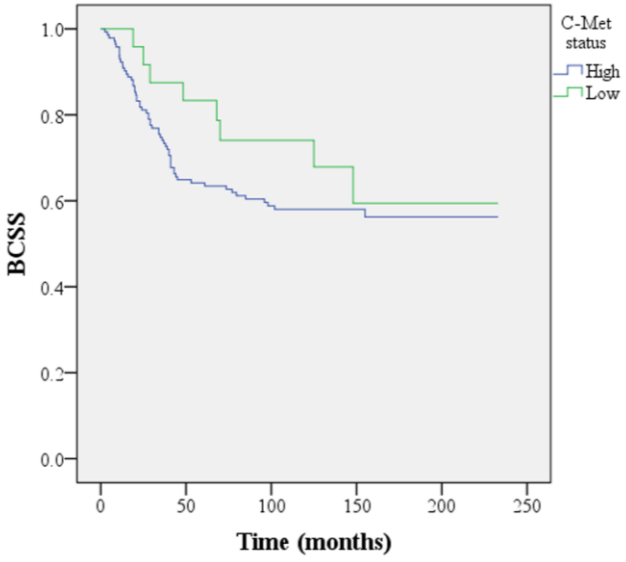

Figure 7.8: Kaplan-Meier survival curves for the BL tumours. **A** shows overall survival and **B** shows breast cancer specific survival (BCSS). For both overall survival (**A**) and BCSS (**B**), there was a trend towards reduced survival in patients with c-Met high tumours but this was not significant ($p = 0.310$ and $p = 0.315$ respectively, log-rank test, $n = 167$).

7.1.4.8 Unclassified tumours

Overall survival for patients with unclassified tumours was longer in those with c-Met high tumours compared to those with c-Met low tumours (mean survival time = 149.5 months, 95% CI = 125.4 – 173.6 versus 86.6 months, 95% CI = 46.6 – 126.7 respectively, p = 0.035, log-rank test, n = 66, Figure 7.9A). This association with survival did not persist at multivariate analysis (HR = 0.73, 95% CI = 0.15 – 3.61, p = 0.698, Cox regression, n = 62).

As with overall survival, patients with c-Met high tumours had a significantly better BCSS than those with c-Met low tumours (mean survival time = 160.0 months, 95% CI = 136 – 184 versus 93.8 months, 95% CI = 51.2 – 136.5 respectively, p = 0.031, log-rank test, n = 66, Figure 7.9B), but this was not significant at multivariate analysis (HR = 0.76, 95% CI = 0.13 – 4.42, p = 0.756, Cox regression, n = 62).

A

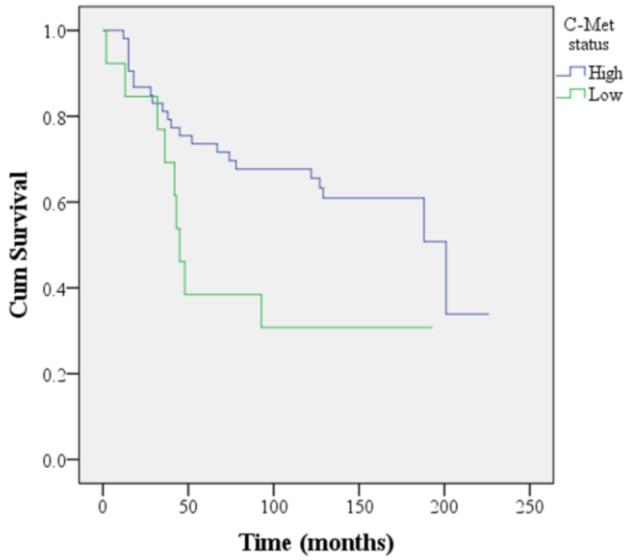

B

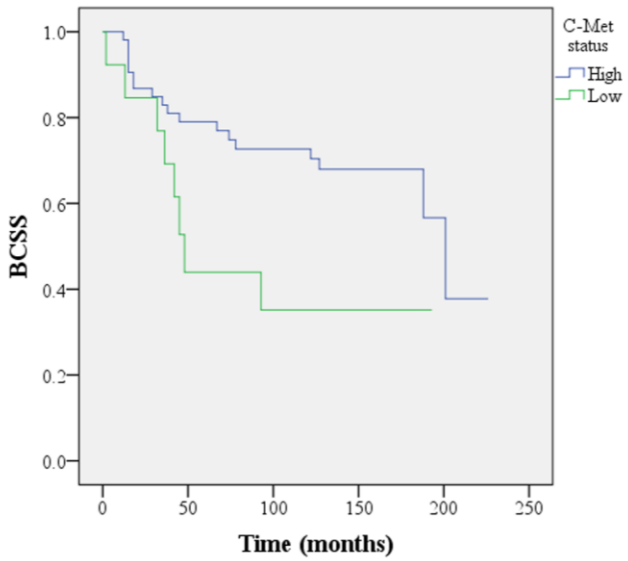

Figure 7.9: Kaplan-Meier survival curves for the unclassified tumours. **A** shows overall survival and **B** shows breast cancer specific survival (BCSS). For both overall survival (**A**) and BCSS (**B**) univariate analysis showed a significantly worse outcome for patients with c-Met low tumours ($p = 0.035$ and $p = 0.031$ respectively, log-rank test, $n = 66$) but this was not significant at multivariate analysis (Hazard ratio (HR) = 0.73, 95% confidence interval (CI) = 0.15 – 3.61, $p = 0.698$ and HR = 0.76, 95% CI = 0.13 – 4.42, $p = 0.756$ respectively, Cox regression, $n = 62$).

7.2 C-Met activity in invasive breast cancer

7.2.1 Patient characteristics

The clinical, pathological and molecular features of the Homerton cohort on which the PLA was performed are outlined in Table 7.2. Of the 181 cases that make up the Homerton cohort, the PLA signal could be evaluated in 155 cases. As with the IHC analysis, the most common reasons for not quantifying the PLA signal on a tumour (missing case) were complete lack of tissue cores or insufficient tumour within a core.

The key clinical and pathological features of the entire Homerton cohort ('All Cases') are shown alongside the features of those cases on which the PLA could be evaluated ('Cases with PLA scores') in Table 7.23. Compared with the entire Homerton cohort, the cases on which the PLA could be evaluated had a similar mean age at presentation (both 56 years old), tumour size (2.6cm versus 2.7cm respectively), percentage of grade 3 tumours (55% versus 56% respectively) and frequency of lymph node involvement (54% compared with 56% respectively).

Parameter	Cases with PLA scores	All Cases
Age (mean, 95% CI)	56.7 (37-82) years	56.9 (37-82) years
Tumour size (mean, 95% CI)	2.7 (1.0-5.4) cm	2.6 (1.0-5.1) cm
Tumour grade (% of cases)		
1	9	8
2	35	37
3	56	55
Lymph node involvement (% of cases)		
Yes	56	54
No	44	46

Table 7.23: Characteristics of the Homerton cohort, including missing cases. The table shows some of the key parameters of the entire Homerton cohort (n = 181) compared with those patients whose tumours could be evaluated for the PLA signal (n = 155). Abbreviations: CI = confidence interval.

7.2.2 Reproducibility of the PLA signals

To establish whether the PLA signal was reproducible, two separate comparisons were made. Firstly, since the Homerton TMAs were constructed in triplicate, correlation analysis between the PLA signals in each replicate was performed. Secondly, after performing the PLA on 2 adjacent serial sections from the same TMA on different days, the average PLA signal for each tumour was correlated with the corresponding signal on the other serial section.

Each core showed a strong positive correlation with each of the replicates ($p < 0.001$ for all comparisons, Table 7.24). There was also a strong positive correlation between the average PLA signal on 1 serial section and the signal on the adjacent serial section ($p < 0.001$, Table 7.24).

Comparison	Correlation Coefficient	P-Value
Core 1 vs Core 2	0.742	<0.001
Core 1 vs Core 3	0.687	<0.001
Core 2 vs Core 3	0.825	<0.001
TMA 1a vs TMA 1b	0.863	<0.001

Table 7.24: Reproducibility of the PLA signals. Correlation between PLA signals on replicates on the same TMA section (for example, Core 1 vs Core 2) and between adjacent serial sections (TMA 1a vs TMA 1b) (Spearman's correlation coefficient).

7.2.3 Correlation between PLA signals and prognostic factors

The PLA signals (Figure 7.10) showed a moderately strong and significant positive correlation with c-Met IHC scores (r = 0.419, p < 0.001, Figure 7.11) and a significant negative correlation with Ki67 scores (p = 0.033, Table 7.25). There were no significant correlations between PLA signals and patient age or tumour size (Table 7.25).

Parameter	Correlation Coefficient	P-Value
Age	0.076	0.350
Tumour size	-0.121	0.140
Ki67 score	*-0.178*	*0.033*

Table 7.25: Correlation between PLA signals and prognostic factors (continuous variables). Significant correlations are given in italics (Spearman's correlation coefficient, n = 155).

PLA signals were significantly higher in low grade tumours compared to high grade tumours (mean PLA signals/nucleus = 3.8 versus 3.0 respectively, p = 0.022, Table 7.26). There were no significant differences in PLA signals with any of the other parameters displayed in Table 7.26).

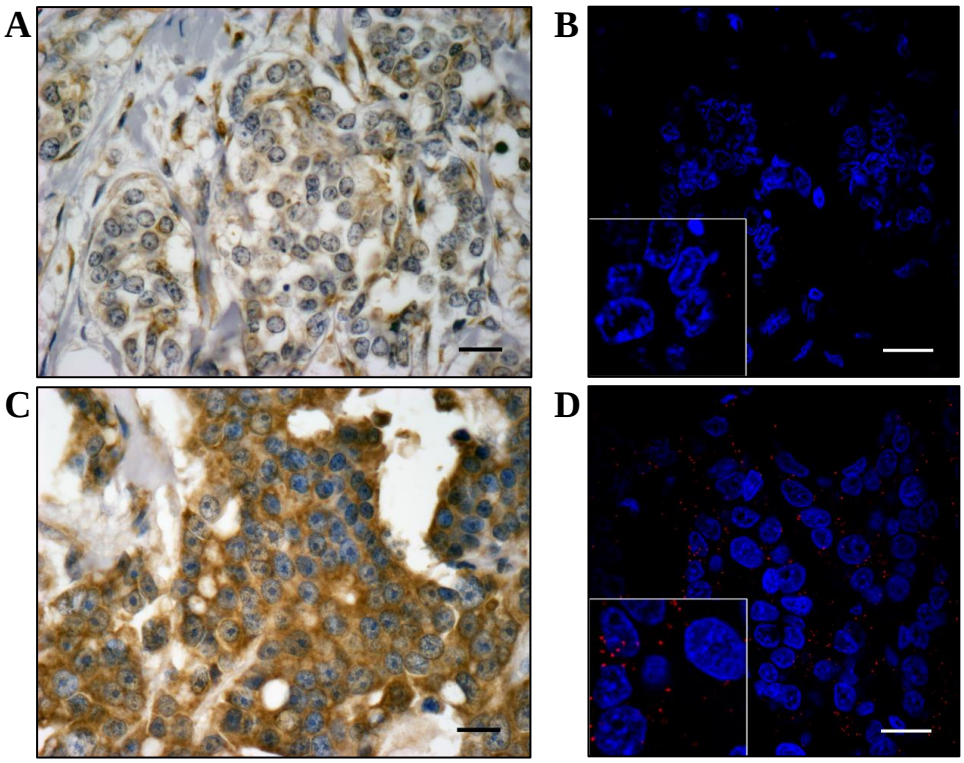

Figure 7.10: Images of the PLA signals in tissue samples, with corresponding IHC images. **A (**IHC) and **B (**PLA) are from the same tumour showing low PLA signal in a tumour with weak c-Met immunopositivity. **C** (IHC) and **D** (PLA) are from another tumour, showing high PLA signal in a tumour that was strongly immunoreactive for c-Met. **A** and **C** are brightfield images (IHC; x40 objective), **B** and **D** are confocal immunofluorescent images (nuclei are in blue (DAPI), the PLA product is in red, x63 objective under oil immersion). All scale bars represent 20µm, inset images are at 200% magnification.

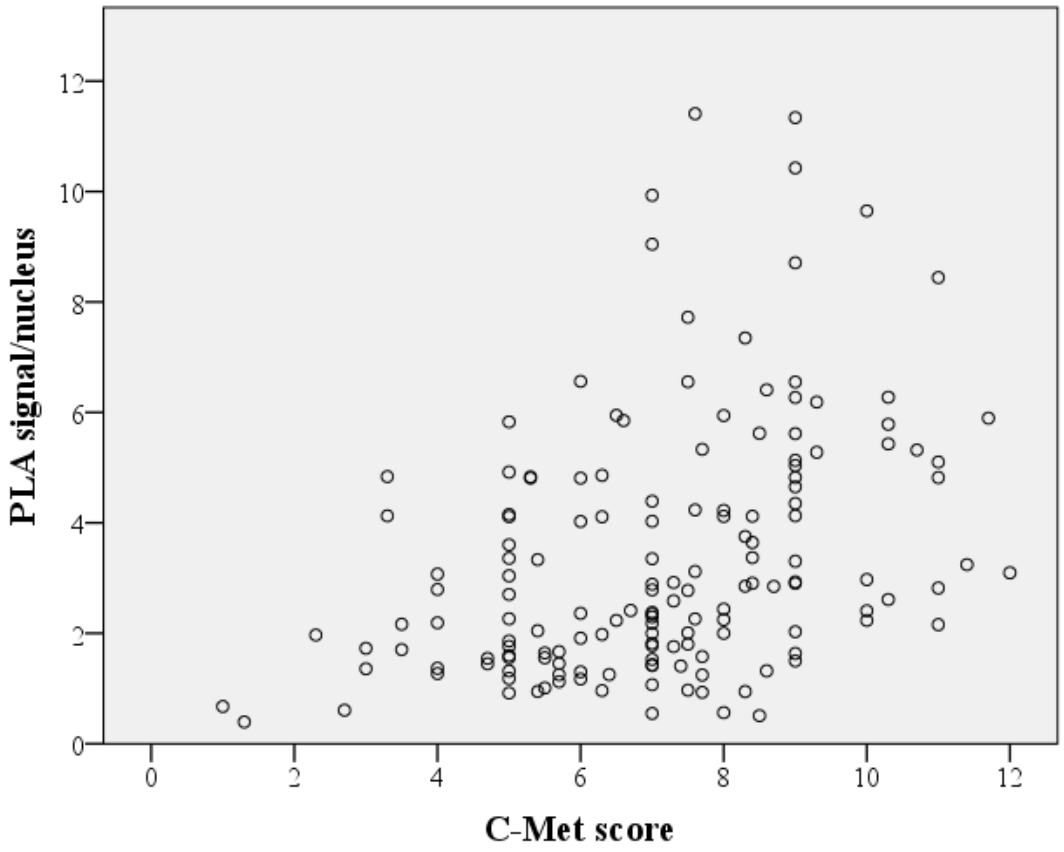

Figure 7.11: Scatter plot showing the correlation between PLA signals/nucleus and c-Met scores at IHC. There is a positive correlation between the 2 variables (r = 0.419, p <0.001, Spearman's correlation co-efficient).

Parameter	Mean PLA score (95% CI)	P-Value
Tumour Grade		
1 or 2	*3.8 (3.2-4.4)*	
3	*3.0 (2.6-3.5)*	*0.022*
Lymph node involvement		
Yes	3.5 (3.0-4.0)	
No	3.2 (2.6-3.8)	0.269
Histological sub-type		
IDC vs Non-IDC	3.4 (3.0-3.8) vs 3.2 (2.1-4.3)	0.308
ILC vs Non-ILC	2.9 (1.3-4.4) vs 3.4 (3.0-3.8)	0.675
Mucinous carcinoma (MC) vs Non-MC	4.4 (0-11.9) vs 3.4 (3.0-3.7)	0.855
Medullary/atypical vs Non-medullary/atypical	2.0 (0.5-3.5) vs 3.4 (3.0-3.8)	0.275
Molecular sub-type		
Luminal A vs Non-Luminal A	3.4 (2.9-3.9) vs 3.3 (2.7-4.0)	0.937
Luminal B vs Non-Luminal B	4.5 (1.8-7.2) vs 3.3 (2.9-3.6)	0.514
Her2 positive vs Non-Her2	4.0 (2.4-5.7) vs 3.3 (2.9-3.7)	0.198
Basal-like (BL) vs Non-BL	3.0 (2.3-3.6) vs 3.5 (3.0-3.9)	0.535
Unclassified vs Non-Unclassified	2.5 (1.4-3.6) vs 3.4 (3.0-3.8)	0.430
Ethnicity		
Black	3.3 (2.8-3.9)	
White	3.4 (2.9-3.9)	0.918
Her2 status		
Positive	4.3 (2.8-5.8)	
Negative	3.3 (2.9-3.6)	0.175
EGFR status		
Positive	3.5 (2.8-4.2)	
Negative	3.5 (3.0-4.0)	0.740
E-Cadherin status		
Positive	3.5 (2.9-4.0)	
Negative	3.2 (2.7-3.8)	0.560

Table 7.26: Correlation between PLA signals and prognostic factors (categorical variables). Significant findings are shown in italics (Mann-Whitney test, n = 155). Abbreviations: CI = confidence interval, IDC-NST = invasive ductal carcinoma, no special type, ILC = invasive lobular carcinoma, MC = mucinous carcinoma.

7.2.4 PLA signals and survival

Cases were dichotomised into 'PLA high' (mean signals/nucleus >3.19) or 'PLA low' (mean signals/nucleus ≤3.19) to create Kaplan-Meier curves for survival analysis, as described in section 6.7.2.

There was a trend towards increased survival time in patients with PLA high tumours compared to those with PLA low tumours, although this was not significant (mean survival time = 122.8 months, 95% CI = 105.2 – 140.3 versus 89.4 months, 95% CI = 76.2 – 102.6 respectively, p = 0.098, log-rank test, n = 139, Figure 7.12A). Tumour PLA signals were not significantly associated with outcome at multivariate analysis (HR = 0.98, 95% CI = 0.85 – 1.14, p = 0.807, Cox regression, n = 129).

A similar trend was seen for BCSS, with longer survival time in PLA high tumours (mean survival time = 129.2 months, 95% CI = 112.6 – 145.9 versus 93.0 months, 95% CI = 79.8 – 106.2 for PLA low tumours, p = 0.064, log-rank test, n = 139, Figure 7.12B), although this was of borderline significance. At multivariate analysis, tumour PLA signals were not an independent predictor of outcome (HR = 0.93, 95% CI = 0.78 – 1.10, p = 0.390, Cox regression, n = 129).

A

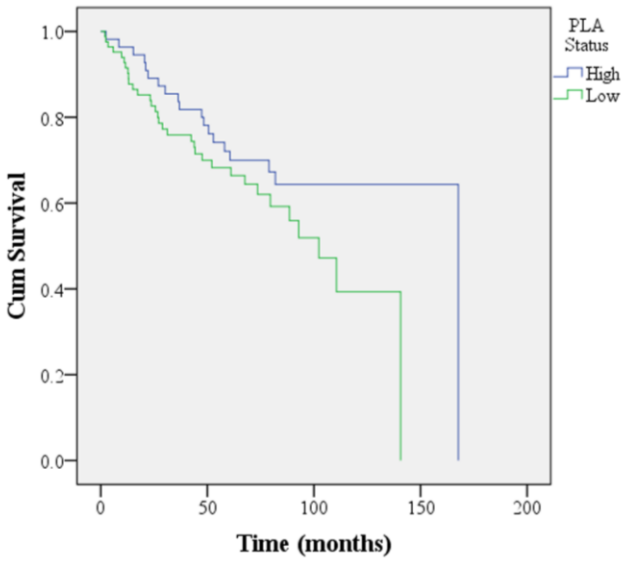

B

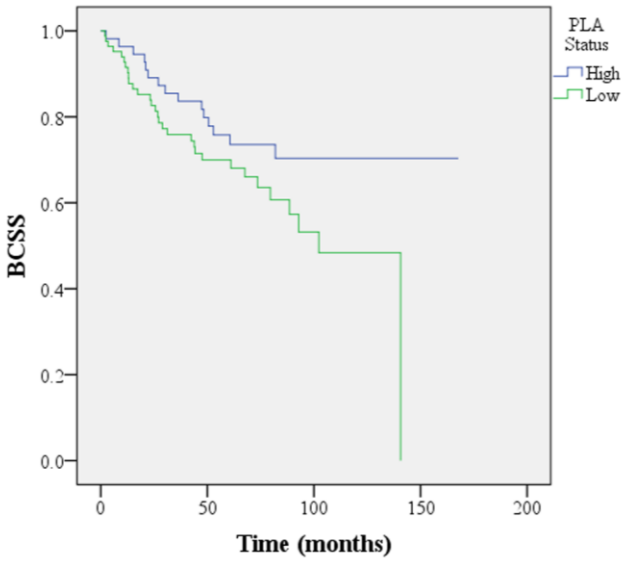

Figure 7.12: Kaplan-Meier survival curves for PLA high and PLA low tumours. **A** shows overall survival and **B** shows breast cancer specific survival (BCSS). For both overall survival (**A**) and BCSS (**B**), univariate analysis showed a trend towards longer survival in PLA high tumours that was of borderline significance in BCSS (p = 0.098 and p = 0.064 respectively, log-rank test, n = 139) but PLA signals were not significant at multivariate analysis (HR = 0.98, 95% CI = 0.85 – 1.14, p = 0.807 and HR = 0.93, 95% CI = 0.78 – 1.10, p = 0.390 respectively, Cox regression, n = 129).

7.3 The effect of HGF in *in-vitro* models of BL cancer

7.3.1 The effect of HGF on migration

To establish whether HGF-mediated c-Met phosphorylation may contribute to the migratory phenotype in BL breast cancer, transwell migration assays (n = 4) were performed on the MDA-MB-468 and HCC1937 breast cancer cell lines.

After 8 hours, there was a significant difference in cell migration in the MDA-MB-468s under the 4 treatment conditions (un-stimulated, HGF stimulation, SU inhibition and combined SU/HGF treatment) ($p = 0.003$, Figure 7.13A). Between group comparisons showed a significantly higher percentage of cells migrated after HGF stimulation (mean migration = 46.9%) compared to un-stimulated cells (36.4%, $p = 0.004$), SU treated cells (38.8%, $p = 0.004$) and SU/HGF treated cells (38.7%, $p = 0.006$). There were no significant differences between the other conditions.

Similarly, the HCC1937 cells showed significant differences in migration under the different conditions ($p = 0.001$, Figure 7.13B). Again, the HGF stimulated cells showed a higher mean percentage migration (60%) compared to un-stimulated cells (46.4%, $p = 0.006$) and SU treated cells (49.6%, $p = 0.004$). The SU/HGF treated cells also showed lower mean migration, but this was of borderline significance after correcting for multiple group testing (52.2%, $p = 0.011$). There were no significant differences between the other conditions.

7.3.2 The effect of HGF on cell viability

To assess whether the increased migration in HGF stimulated cells was due to increased proliferation, MTS cell viability assays (n = 3) were performed, comparing un-stimulated cells with cells exposed to increasing doses of HGF (up to 100ng/ml).

A

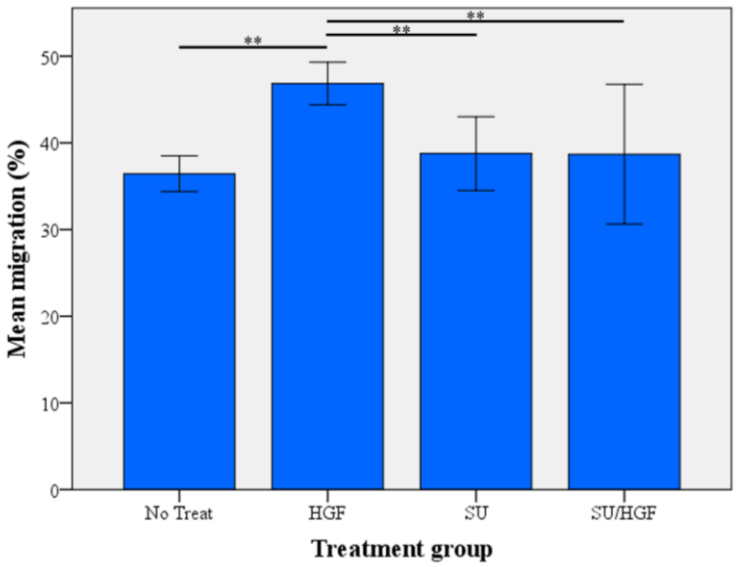

B

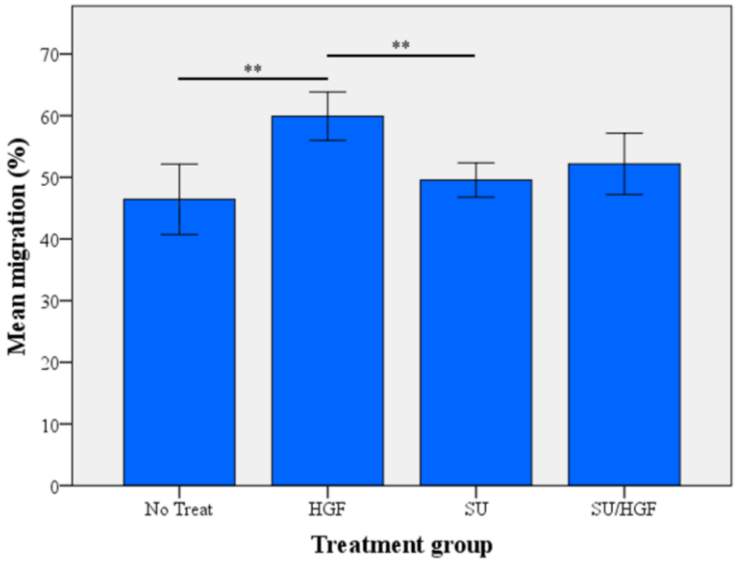

Figure 7.13: Transwell migration assays. The bar charts show the mean migration (expressed as a percentage of total cells seeded) over an 8 hour time period in the **A** MDA-MB-468s and **B** HCC1937s with and without treatment with HGF and SU. There was a significant increase in migration after HGF stimulation in both cell lines but this was abrogated when the cells were treated with SU. The results are derived from pooled data from 4 experiments (** = $p<0.01$).

A standard curve was used to estimate the number of viable cells (Figure 7.14). After 8 hours, there was no significant difference in the mean number of viable cells (both the MDA-MB-468 cells and HCC1937 cells, p = 0.502 and 0.812 respectively, Figure 7.15A and B). There were no significant differences noted in between group comparisons.

7.3.3 The effect of HGF on protein expression

To address whether the effect of HGF on migration may be due to the acquisition of an EMT phenotype and an alteration in the E-Cadherin/β-Catenin complex, western blot analysis were performed on lysates from MDA-MB-468 and HCC1937 cells exposed to different treatment conditions and probed for E-Cadherin, β-Catenin and vimentin, as well as phospho-c-Met and c-Met.

7.3.3.1 MDA-MB-468 breast cancer cells

There was no significant difference in E-Cadherin expression at 20 minutes of HGF stimulation (mean adjusted relative density (mARD) = 0.87) or 120 minutes (mARD = 0.98), relative to un-stimulated cells (mARD = 1, p = 0.191, Figure 7.16A and B).

There was no significant change in β-Catenin expression under these treatment conditions (mARD after 20 minutes HGF = 1.06, mARD after 120 minutes = 0.98) relative to un-stimulated cells (mARD = 1, p = 0.832, Figure 7.16A and C). There was no expression of vimentin (Figure 7.16A).

A

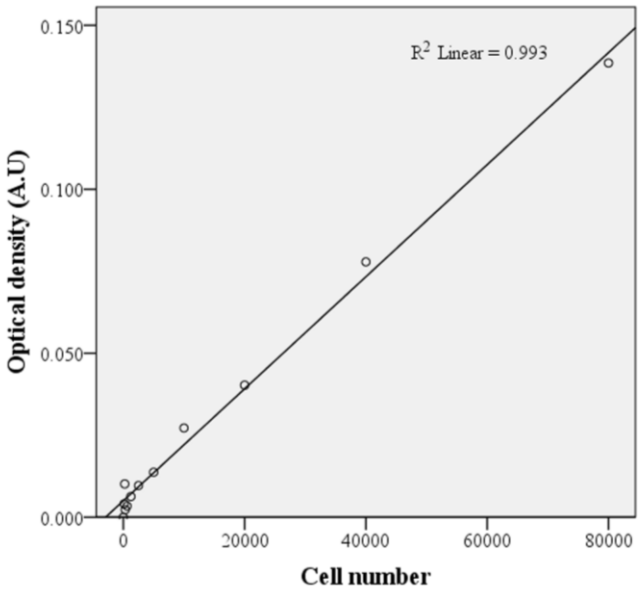

B

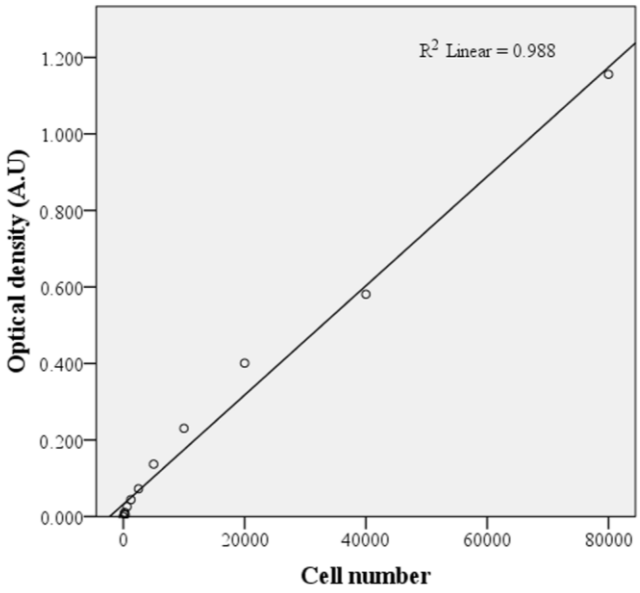

Figure 7.14: Representative standard curves used to calculate cell viability in the MTS assay. The graph in **A** shows the MDA-MB-468s, the graph in **B** shows the HCC1937s. Both graphs show increasing optical densities correlating with increasing cell numbers. The R^2 Linear figure represents the Pearson coefficient of determination. Abbreviations: A.U = arbitrary units.

A

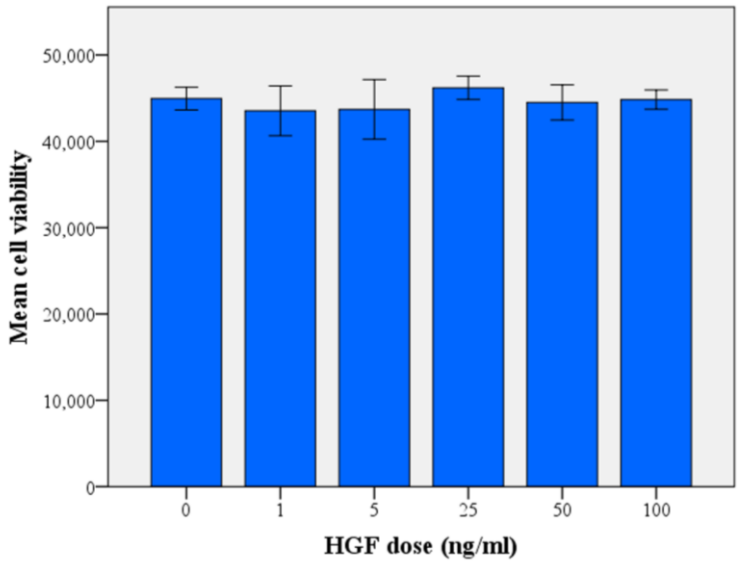

B

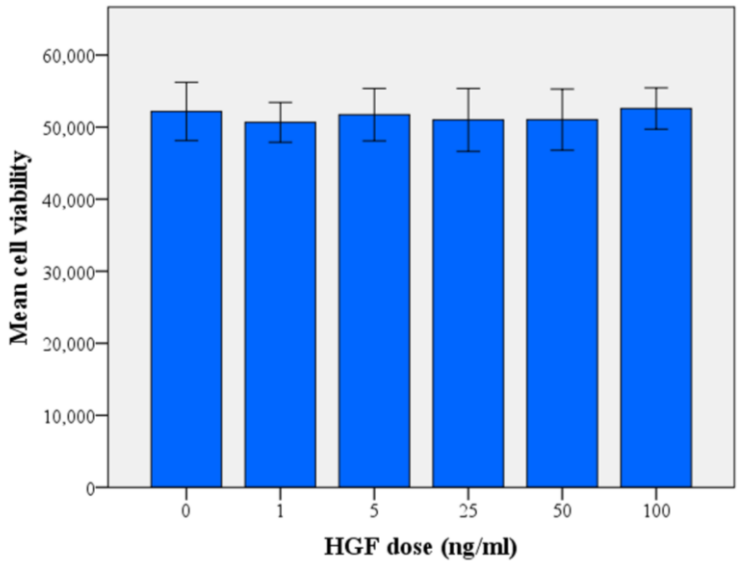

Figure 7.15: MTS cell viability assays. The bar charts show the number of viable cells (MDA-MB-468s in **A** and HCC1937s in **B**) after an 8 hour time point. There is no statistically significant change in the number of viable cells in either cell line after stimulation with 1-100 ng/ml of HGF. The results represent the pooled data from 3 experiments.

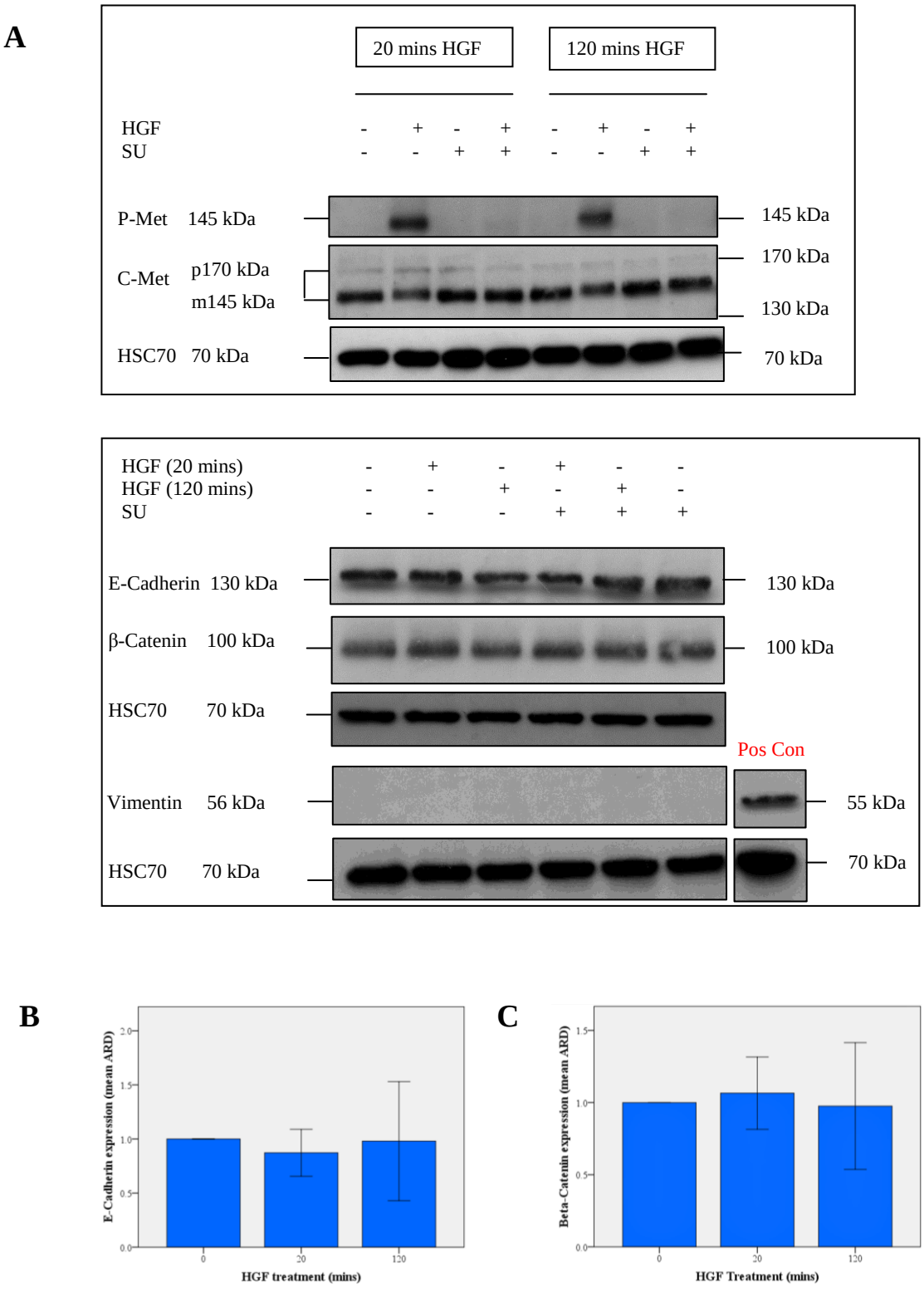

Figure 7.16: Protein expression in MDA-MB-468s by western blot. In **A** only the unopposed HGF lanes show c-Met phosphorylation. There is no change in E-Cadherin or β-Catenin expression with HGF treatment, which is quantified in **B** and **C**. There is no expression of vimentin in any treatment condition; the positive control is a lysate from the MDA-MB-231 cell line. Abbreviations: ARD = adjusted relative density.

7.3.3.2 HCC1937 breast cancer cells

As with the MDA-MB-468s, there were no significant differences in E-Cadherin expression at 20 or 120 minutes relative to un-stimulated cells (mARD = 1.04, 1.19 and 1 respectively, $p = 0.550$, Figure 7.17A and B) or in β-Catenin expression at 20 and 120 minutes (mARD = 1.03 and 0.97 respectively, relative to 1 for un-treated cells, $p = 0.832$, Figure 7.17A and C). There was no expression of vimentin (Figure 7.17A).

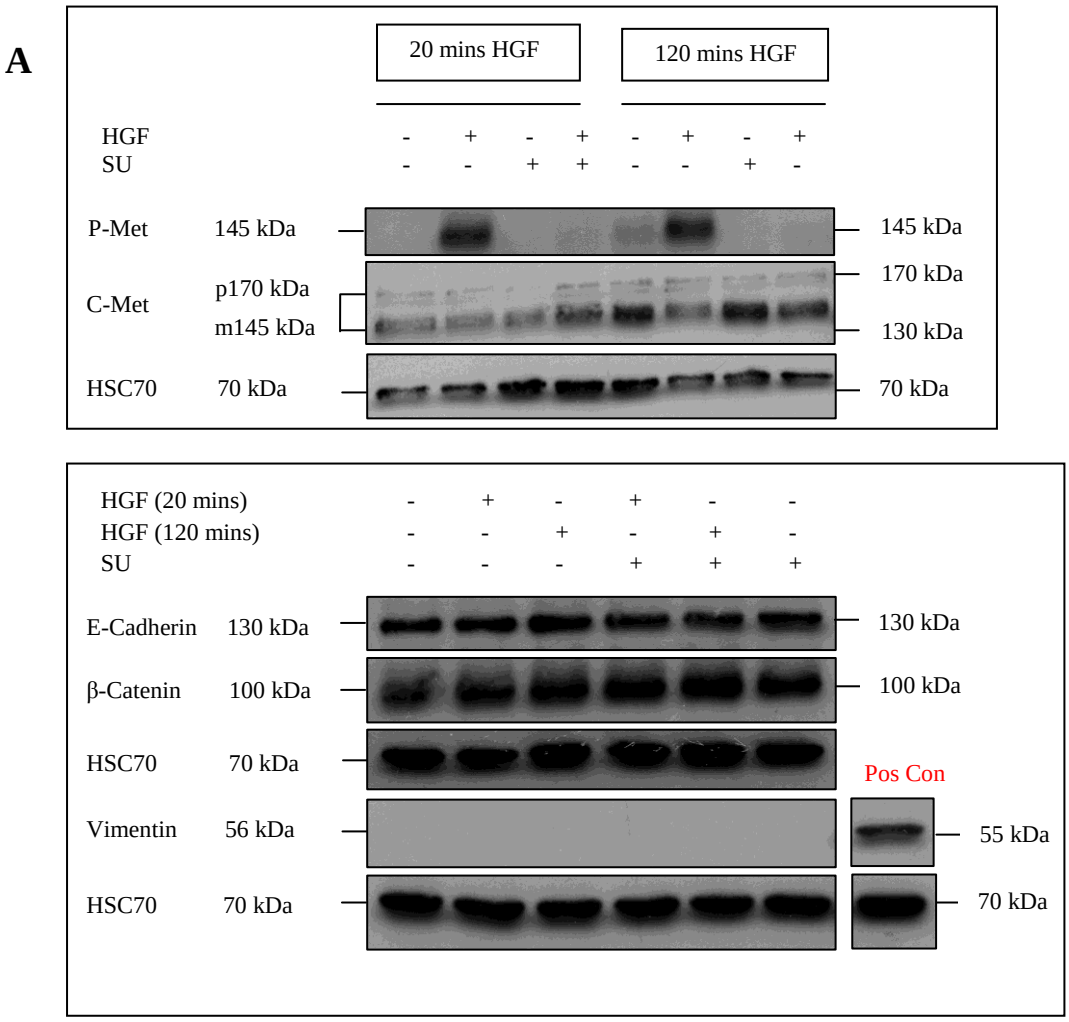

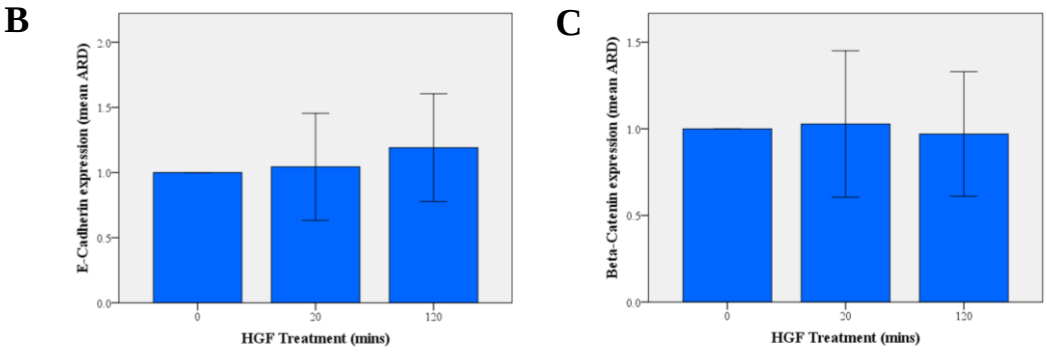

Figure 7.17: Protein expression in HCC1937s by western blot. In **A** only the unopposed HGF lanes show c-Met phosphorylation. There is no change in E-Cadherin or β-Catenin expression with HGF treatment, which is quantified in **B** and **C**. There is no expression of vimentin in any treatment condition; the positive control is a lysate from the MDA-MB-231 cell line. Abbreviations: ARD = adjusted relative density.

7.3.4 The effect of HGF on E-Cadherin localisation and co-localisation

After finding no effect on the amount of protein expression, I sought to establish if HGF could be having an effect on migration by altering the location of E-Cadherin within the cell and whether the protein trafficked to the cytosol in a similar way to c-Met following ligand binding. Therefore, immunofluorescence for E-Cadherin and c-Met was performed on the MDA-MB-468 and HCC1937 cells after 20, 60 and 120 minutes of HGF treatment.

7.3.4.1 MDA-MB-468 breast cancer cells

In untreated MDA-MB-468 cells, the majority of cells showed membranous E-Cadherin expression (84.4%, Figure 7.18 and 7.19A). There was a reduction in membrane expression at 20 minutes (76.6%) followed by an increase to 83.4% at 60 minutes and 93% at 120 minutes, resulting in a borderline significant difference across the four groups ($p = 0.062$). However, there were no significant differences in the between group comparisons, after correcting for multiple group testing.

Co-localisation analysis showed a reduction in E-Cadherin/c-Met co-localisation with increasing duration of HGF stimulation (Figure 7.18 and 7.19B) and this was significant across the four groups ($p = 0.001$). Between group analysis showed significant differences between a) un-stimulated cells (mean co-localisation = 41.8%) and cells stimulated for 60 min (mean co-localisation = 13.6%, $p = 0.009$), b) un-stimulated cells and cells exposed to 120 minutes of HGF (mean co-localisation = 11%, $p = 0.009$), c) cells stimulated with 20 minutes of HGF (29.6%) and the 60 minute group ($p = 0.009$) and d) the 20 minute group versus cells exposed to 120 minutes of the ligand ($p = 0.009$). There were no significant differences between the other groups.

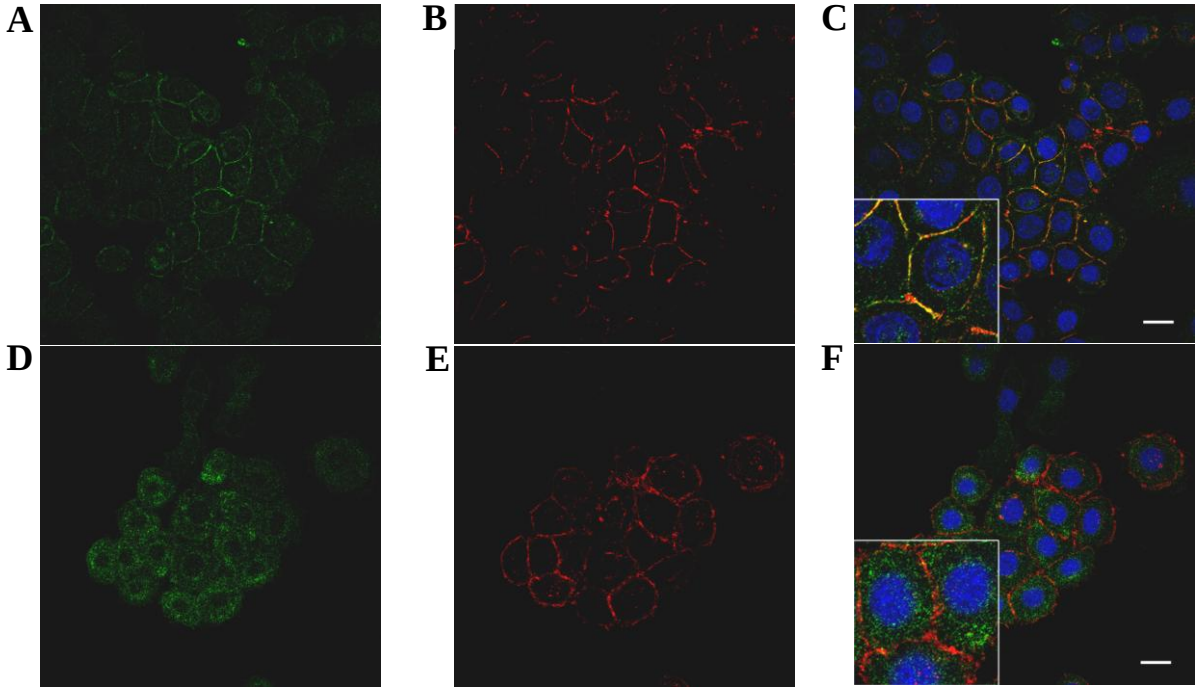

Figure 7.18: Immunofluorescence for c-Met and E-Cadherin in MDA-MB-468s. Images **A** – **C** are untreated cells and **D – F** are of cells stimulated for 20 minutes with HGF; C-Met (**A** and **D**) is in green, E-Cadherin (**B** and **E**) is in red; **C** and **F** are the merged images, where yellow represents c-Met/E-Cadherin co-localisation. There is trafficking of c-Met from the membrane to the perinuclear compartment after HGF stimulation but E-Cadherin remains at the membrane. Consequently, co-localisation is reduced in the treated cells (confocal immunofluorescent microscopy, x63 objective under oil immersion, nuclei are in blue (DAPI stain); scale bars represent 20µm).

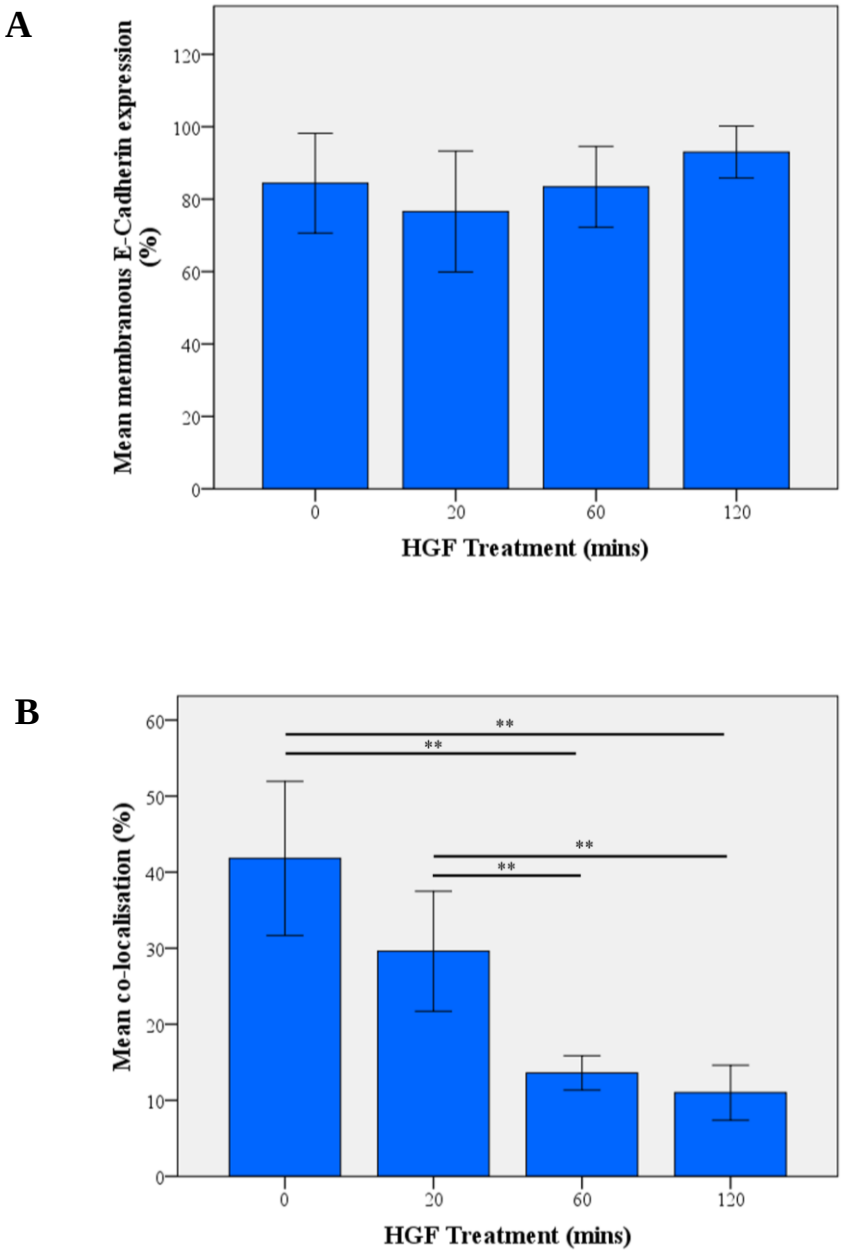

Figure 7.19: Membranous expression of E-Cadherin and c-Met/E-Cadherin co-localisation in MDA-MB-468 cells. **A** shows the percentage of cells that express E-Cadherin at the membrane in unstimulated cells and at different time points of HGF treatment. There were no statistically significant differences. **B** shows the percentage of total E-Cadherin pixels that co-localised with c-Met. Overall, co-localisation decreased with HGF treatment ($p = 0.001$, Kruskal-Wallis test) and this was significant at pair-wise analysis after 60 and 120 minutes compared to untreated cells and cells treated for 20 minutes ($p = 0.009$ for all, Mann-Whitney test). Error bars represent the 95% CI, ** = $p<0.01$.

7.3.4.2 HCC1937 breast cancer cells

HCC1937 cells in the different treatment conditions showed similar amounts of mean membranous E-Cadherin: 94.4% in un-stimulated cells, 94% after 20 minutes HGF, 96.2% after 60 minutes and 93.2% after 120 minutes (Figure 7.20 and 7.21A). Correspondingly, there was no statistically significant difference across the groups ($p = 0.768$) and no significant between group differences.

As with the MDA-MB-468s, mean co-localisation showed a downward trend with increasing duration of HGF treatment, albeit with a small increase between 60 and 120 minutes (Figure 7.20 and 7.21B). The mean co-localisation at baseline was 21.8%, falling to 10.8% after 20 minutes of HGF treatment, 6.8% after 60 minutes and 7.8% after 2 hours. Statistically, there was a significant difference across the groups ($p = 0.016$) but between group analysis showed only a borderline difference between baseline and 60 minutes treatment and baseline and 120 minutes of HGF ($p = 0.014$ for both). The other groups showed no significant differences after correcting for multiple group testing.

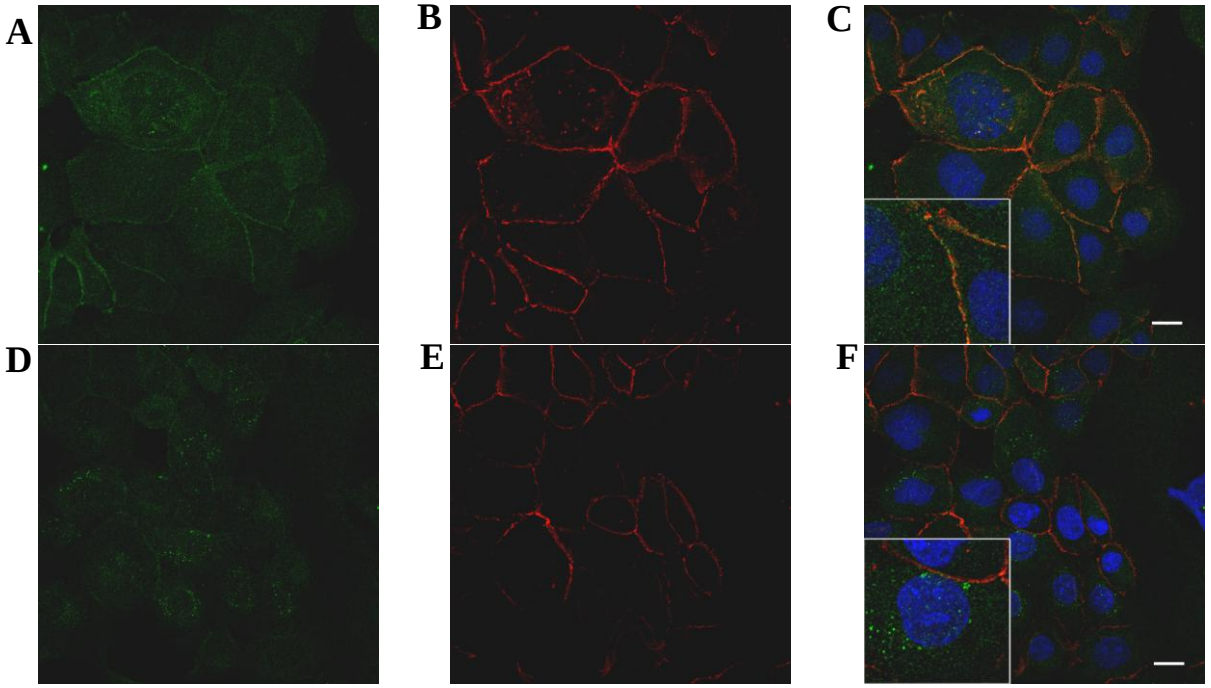

Figure 7.20: Immunofluorescence for c-Met and E-Cadherin in HCC1937s. Images **A** – **C** are untreated cells and **D – F** are of cells stimulated for 20 minutes with HGF; C-Met (**A** and **D**) is in green, E-Cadherin (**B** and **E**) is in red; **C** and **F** are the merged images, where yellow represents c-Met/E-Cadherin co-localisation. There is trafficking of c-Met from the membrane to the perinuclear compartment after HGF stimulation but E-Cadherin remains at the membrane. Consequently, co-localisation is reduced in the treated cells (confocal immunofluorescent microscopy, x63 objective under oil immersion, nuclei are in blue (DAPI stain); scale bars represent 20µm).

A

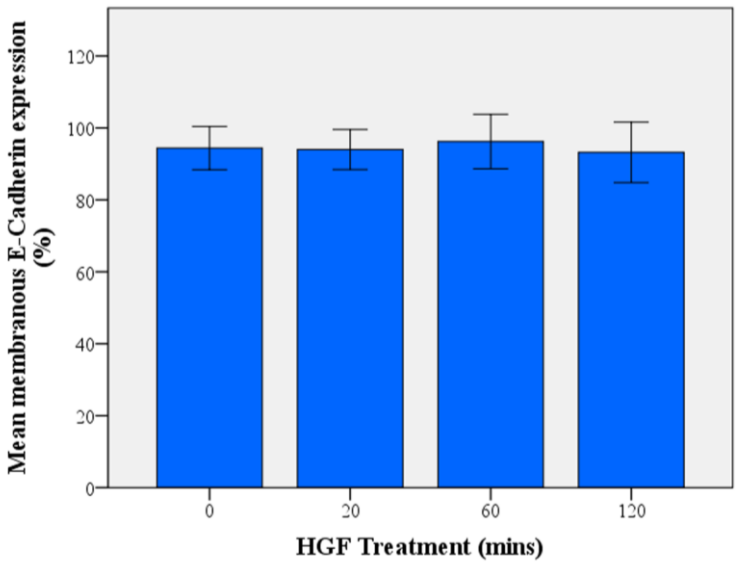

B

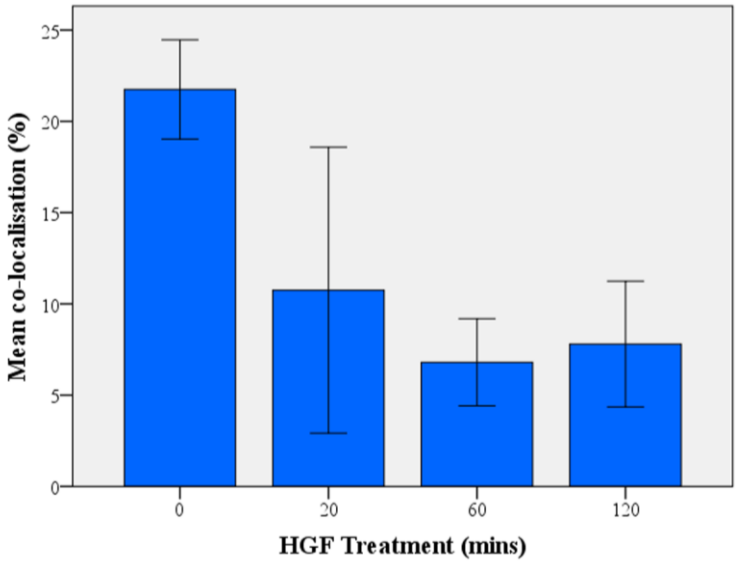

Figure 7.21: Membranous expression of E-Cadherin and c-Met/E-Cadherin co-localisation in HCC1937 cells. **A** shows the percentage of cells that express E-Cadherin at the membrane in unstimulated cells and at different time points of HGF treatment. There were no statistically significant differences. **B** shows the percentage of total E-Cadherin pixels that co-localised with c-Met. Overall, co-localisation was reduced with HGF treatment ($p = 0.016$, Kruskal-Wallis test) and this was of borderline significance at pair-wise analysis at the 60 and 120 minutes versus untreated cells ($p = 0.014$ for both). Error bars represent the 95% CI.

8.0 Discussion

8.1 C-Met expression in invasive breast cancer

8.1.1 C-Met expression and molecular sub-type

The results from this study of over 1450 samples show that significantly higher levels of c-Met are present in the BL sub-type compared to other molecular sub-types of breast cancer. In contrast, the luminal A tumours showed significantly lower c-Met expression. Those triple negative (TN) tumours that lacked basal cytokeratin/EGFR expression – the unclassified tumours – did not show higher levels of c-Met. (Ho-Yen *et al*, 2013; Ho-Yen *et al*, 2014). This finding reinforces the argument for distinguishing BL tumours from the wider TN group and raises the possibility that c-Met may contribute to the poorer outlook associated with BL TN tumours compared to non-BL TN cancers (Cheang *et al*, 2008). Importantly, this is the first study to demonstrate an association between c-Met and BL tumours that is independent of other relevant clinical, pathological and immunohistochemical parameters (Ho-Yen *et al*, 2014).

Previously, smaller studies have described higher levels of c-Met in human BL tumours (Charafe-Jauffret *et al*, 2006; Garcia *et al*, 2007a; Graveel *et al*, 2009). Charafe-Jauffret and co-workers used a set of 388 genes (including *MET*) to perform hierarchical clustering on 122 breast tissue samples (comprising 115 cancers and 7 non-malignant samples)(Charafe-Jauffret *et al*, 2006). It was shown that this gene set correctly separated the luminal A tumours from the BL tumours, with *MET* over-expression forming part of the BL cluster (Charafe-Jauffret *et al*, 2006). In an immunohistochemical analysis of 137 invasive breast carcinomas, Graveel et al

identified significantly higher levels of c-Met in BL tumours at univariate analysis (Graveel *et al*, 2009). Another IHC-based study used TMAs (constructed from over 900 samples) to look at the relationship between c-Met, a variety of other BL markers (including CK5/6, p63 and c-Kit) and outcome (Garcia *et al*, 2007a). The authors noted a worse outcome for c-Met high tumours, but no direct relationship between c-Met and the BL phenotype was presented (Garcia *et al*, 2007a).

My findings are further supported by the fact that the association between c-Met and BL status was present in both the Nottingham and Homerton cohorts, two quite different and independent collections of invasive breast cancers. Furthermore, the characteristics of the BL tumours in the current study are similar to those previously described in the literature. These include: younger age at presentation (Cheang *et al*, 2008), larger tumour size (Kuroda *et al*, 2008), predominance of the histological category of IDC-NST (Carey *et al*, 2006), high proliferation rate and high nuclear grade (Fulford *et al*, 2006) and high levels of p53 expression (Manié *et al*, 2009). Thus, the current cohort would appear to be an accurate representation of the BL category and as such, my findings (with respect to c-Met expression) could be extrapolated to the wider population.

The current findings are supported further by *in-vivo* work using different mouse models of mutated *MET* (Ponzo *et al*, 2009; Graveel *et al*, 2009). A knock-in mouse model with mutationally activated *MET* developed mammary carcinomas with varying histological appearances, but showed a high frequency (65% of tumours) of squamous metaplasia, a feature more commonly seen in human BL tumours (Graveel *et al*, 2009; Fulford *et al*, 2006). Moreover, the basal cytokeratin CK5 was detected in the majority of tumours arising in these mice (Graveel *et al*, 2009). Similarly, Ponzo and colleagues generated a transgenic mouse model in which c-Met was

expressed in the mammary epithelium (Ponzo *et al*, 2009). The tumours that subsequently developed could be placed into one of two morphological categories: 1) tumours with a solid nodular architecture or, 2) those with papillary, scirrhous, adenosquamous or spindle-cell appearances (referred to as 'mixed pathology' tumours)(Ponzo *et al*, 2009). As well as squamous and spindle-cell differentiation, the 'mixed pathology' tumours showed other BL characteristics such as high nuclear grade, necrosis and lymphocytic infiltration (Ponzo *et al*, 2009; Livasy *et al*, 2006). In addition, these tumours clustered with human BL cancers at gene expression profiling and expressed cytokeratins 5, 6 and 14 on IHC (Ponzo *et al*, 2009).

Of note, the 'solid' tumours more closely resembled luminal tumours on gene expression and IHC analysis, prompting the authors to speculate that multi-potent stem cells with the potential to differentiate into either luminal or basal cells may be a key target of c-Met (Ponzo *et al*, 2009). The fact that neither of these mouse models develops BL mammary tumours exclusively is consistent with the current analysis, where c-Met was expressed in each of the five molecular sub-types. Clearly, c-Met should not be regarded as a specific marker of the BL sub-type. Rather, the main message from this sub-type analysis is that patients with BL tumours should be included in future clinical trials of c-Met inhibitors, given the high level of c-Met expression in this sub-type and the lack of alternative targeted therapy.

It is also emerging that anti-c-Met therapy may have a role in the treatment of patients who have already received systemic molecular treatment (Minuti *et al*, 2012). In an analysis of 130 patients with Her2 positive metastatic breast cancer, Minuti and colleagues found that tumours with high gene copy numbers of *HGF* or *MET* (as assessed by FISH) were associated with a higher risk of trastuzumab-based

treatment failure (Minuti *et al*, 2012). This study is supported by other work showing that HGF-mediated c-Met activation abolished the growth inhibitory response of Her2 expressing SKBR3 breast cancer cells to trastuzumab (Shattuck *et al*, 2008). Both the SKBR3 cell line and another Her2 positive cell line – BT474 – significantly up-regulated c-Met expression after less than 2 days of trastuzumab treatment (Shattuck *et al*, 2008). These workers also observed that trastuzumab-dependent p27 (a cyclin-dependent kinase inhibitor) expression was reduced when either cell line was treated with HGF, suggesting a possible mechanism for HGF/c-Met mediated protection from the inhibitory effect of trastuzumab (Shattuck *et al*, 2008).

Although c-Met expression in the current study was not significantly increased in the Her2 positive sub-type (or associated with positivity for the Her2 receptor), one should bear in mind that many of the samples in the Homerton cohort and all of the Nottingham cohort pre-date the widespread use of trastuzumab in the UK.

8.1.2 C-Met expression and other prognostic factors

8.1.2.1 Tumour size

This study demonstrated an inverse correlation between c-Met expression and tumour size. This relationship was significant in the cohort as a whole, the Nottingham cohort and within the luminal A and unclassified sub-types. This finding was unexpected given the fact that BL tumours have a larger mean size at presentation (Kuroda *et al*, 2008). This is true also in the current analysis, where increasing tumour size was significantly associated with BL status at univariate analysis.

Others have found no association between c-Met expression and tumour size (Jin *et al*, 1997; Camp *et al*, 1999; Nakopoulou *et al*, 2000; Lengyel *et al*, 2005; Lindemann *et al*, 2007; Zagouri *et al*, 2013). Previously, it has been shown that tumour size is not a good predictor of outcome in BL cancer, possibly due to the relatively early occurrence of blood-borne metastasis in this molecular sub-type (Foulkes *et al*, 2009). Hence, one could speculate that c-Met plays an important part in the aggressive behaviour of some smaller tumours. Interestingly, in a previous analysis of the Homerton cohort, black women with smaller breast cancers (≤ 2 cm) had a poorer prognosis than white women matched for tumour size (Bowen *et al*, 2008). It is possible that c-Met contributed to the poorer outlook for these black patients.

8.1.2.2 Lymph node involvement

The propensity for BL cancers to metastasize via the haematogenous route rather than through the lymphatics to the lymph nodes (Rakha *et al*, 2009), also explains the finding of higher c-Met scores in lymph node negative tumours in the current analysis.

8.1.2.3 Patient age

As is the case with previous studies, this study found no significant association between c-Met and patient age at presentation in the whole cohort analysis (Camp *et al*, 1999; Nakopoulou *et al*, 2000; Lengyel *et al*, 2005; Lindemann *et al*, 2007; Zagouri *et al*, 2013). Interestingly, there was a significant positive association between these variables when only the Homerton cohort was considered. It could be argued that this reflects the differences in demographics between the two collections of patient samples (the mean age at presentation was nearly three years older in the Homerton series compared to the Nottingham collection). However, the finding that

the luminal A tumours alone (most of which come from the Nottingham set) show the same correlation suggests that this is not the case.

8.1.2.4 Tumour grade

Regarding tumour grade, there was no association with c-Met in the wider cohort, or in the sub-type analysis, with the exception of the Her2 positive sub-type, where c-Met scores were significantly lower in high grade tumours. Other groups have made conflicting observations when considering c-Met and tumour differentiation (Jin *et al*, 1997; Camp *et al*, 1999; Nakopoulou *et al*, 2000; Zagouri *et al*, 2013). Some found no association between tumour grade and c-Met (Jin *et al*, 1997; Lengyel *et al*, 2005; Chen *et al*, 2007), while others noted higher expression of the receptor in high grade tumours, although the study by Zagouri *et al* focused only on TN tumours (Camp *et al*, 1999; Zagouri *et al*, 2013). In contrast, Nakopoulou and colleagues identified more frequent c-Met staining in grade 1 carcinomas, where 75% of tumours were positive compared to 43.8% of grade 3 tumours (Nakopoulou *et al*, 2000). The study by Nakopoulou *et al* emerged before the widespread acceptance of the molecular classification proposed by Perou *et al* (Perou *et al*, 2000) and therefore no sub-type analysis is presented, but since only 10% of tumours were immuno-reactive for Her2 it is unlikely that the Her2 positive sub-type was over-represented in their study (Nakopoulou *et al*, 2000).

8.1.2.5 Histological sub-type

Tubular carcinomas had the highest c-Met scores in the whole and Nottingham cohorts, but only one case of tubular carcinoma was present in the Homerton series (precluding further statistical analysis). Unlike the Nottingham cohort, the Homerton tumours classified as IDC showed significantly higher c-Met expression compared to

non-IDC tumours. In all probability, these differences are due to the different reporting practices employed at the two centres. The striking difference in the percentage of tumours classified as IDC (82% in the Homerton cohort versus 59% in the Nottingham cohort) strongly suggests a higher threshold for diagnosing tubular (and mixed histology) carcinomas in our 'in-house' series. It is not possible to say whether there were too many IDCs classified as tubular carcinomas in the Nottingham cohort or too few in the Homerton cohort, although data from the Surveillance, Epidemiology and End Results (SEER) registry does quote a tubular carcinoma frequency of 0.7% (Berg and Hutter, 1995). Either way, if the proportions of each of the histological sub-types were more similar then it would seem plausible that the statistical trends of both cohorts, with regard to c-Met, would match up more closely.

C-Met expression in ILC was more consistent across the cohorts, with lower levels in the cohort as a whole and both the Nottingham and Homerton components (although the association was only of borderline significance in the Homerton series). Few clinical studies have specifically addressed the relationship between c-Met and histological sub-type. Tubular carcinomas are a well differentiated form of breast cancer, characterised by angulated tubules that frequently demonstrate 'apical snouting' (Harris *et al*, 2006). It seems paradoxical that these tumours that are generally associated with a favourable outcome compared to controls (Harris *et al*, 2006) should express higher levels of c-Met. However, some have stated that the role of HGF (and c-Met) may vary depending on the degree of tumour differentiation, such that HGF/c-Met contributes to the invasive profile of poorly differentiated tumours whilst driving gland formation in those tumours with functioning adhesion complexes (Rosen *et al*, 1994). With reference to c-Met expression in ILC, other

studies have shown mixed results (Nakopoulou *et al*, 2000; Chen *et al*, 2007; Carracedo *et al*, 2009; Zagouri *et al*, 2013). Carracedo *et al* found a significantly higher number of c-Met positive cases in IDCs compared to ILCs (Carracedo *et al*, 2009) whereas Nakopoulou and co-workers noted the opposite: 22.2% of ILCs showed strong staining in more than 50% of tumour cells compared to 3.9% of tumours classified as IDC (Nakopoulou *et al*, 2000). Two other studies found no statistical difference in c-Met expression when comparing histological sub-types (Chen *et al*, 2007; Zagouri *et al*, 2013).

Classical ILCs have a distinct histological appearance in which relatively bland discohesive tumour cells infiltrate the breast stroma, accompanied by absent or reduced expression of E-Cadherin on IHC (Harris *et al*, 2006).

8.1.2.6 E-Cadherin status

My findings regarding c-Met and ILC are mirrored and supported by the analysis of the correlation between c-Met score and E-Cadherin status, where c-Met was consistently over-expressed in E-Cadherin positive tumours (significantly so in the whole cohort and the Homerton component). Given the relative scarcity of ILCs (this sub-type accounted for only 7% of the whole cohort), it should be appreciated that the analysis of E-Cadherin status in this study is mostly based on non-ILCs.

Other workers have considered the relationship between c-Met and E-Cadherin in non-ILCs, but a clear consensus has not yet been established. Götte and colleagues looked at IHC expression of these proteins in pure DCIS and where DCIS co-existed with invasive carcinoma (though only the DCIS component was analysed in the latter)(Götte *et al*, 2007). They found a significant positive correlation between c-Met and E-Cadherin in the pure DCIS cases, but noted a significant reduction in c-

Met levels in co-existent DCIS samples (Götte *et al*, 2007), suggesting that co-expression is lost with disease progression. Another study looked at 55 IDCs and 95 cases of DCIS, performing IHC for a variety of markers associated with EMT (Logullo *et al*, 2010). There was no significant correlation between c-Met and E-Cadherin in either the invasive or *in-situ* carcinomas (Logullo *et al*, 2010). In an analysis of 41 cases of inflammatory breast carcinomas (IBCs) – an uncommon form of breast cancer linked with an aggressive clinical course – Garcia *et al* found that all of the IBCs showed immunopositivity for E-Cadherin and c-Met (Garcia *et al*, 2007b).

These studies illustrate how the E-Cadherin/c-Met relationship varies across different groups and in different types of samples. Yet it is tempting to find the results of the current study puzzling since HGF/c-Met signalling is thought to drive epithelial dissociation by negatively regulating cadherins (Rosen *et al*, 1994). Some have suggested that c-Met may influence adhesion and migration despite the presence of E-Cadherin (Garcia *et al*, 2007b). It is possible that in such cases E-Cadherin is ineffective or that an intact cell-cell adhesion apparatus is actually necessary for the formation and dissemination of compact tumour emboli consisting of several tumour cells (Garcia *et al*, 2007b).

8.1.2.7 EGFR status

Another biomarker that demonstrated a relatively consistent positive association with c-Met expression was EGFR. This is not surprising, since EGFR was one of the basal markers used to identify BL tumours in this study and it has already been shown that c-Met is independently predictive of this sub-type. In lung cancer cells, EGFR activation due to EGF stimulation or an activating mutation has been shown

to increase both the gene and protein levels of c-Met, via the hypoxia-inducible factor (HIF)-1α pathway (Xu *et al*, 2010). Also in non-small cell lung carcinoma cells (NSCLCs), amplification of the *MET* gene has been linked with resistance to the EGFR inhibitor gefitinib by stimulating ErbB3 (Her3) signalling and PI3K activation (Engelman *et al*, 2007). A similar compensatory relationship has been described in SUM229 breast cancer cells (Mueller *et al*, 2008). These cells were able to maintain EGFR phosphorylation in the presence of gefitinib, when c-Met and c-Src were also phosphorylated (Mueller *et al*, 2008). The authors went on to demonstrate that inhibition of c-Met reduced c-Src phosphorylation, EGFR phosphorylation and cell growth during treatment with EGFR inhibitors (Mueller *et al*, 2008). Taken together with the results of the current study, these findings re-iterate the point that co-expression of EGFR and c-Met may have implications in the treatment of BL breast cancer.

8.1.2.8 Ki67 scores

The HGF/c-Met signalling axis is thought to drive cellular proliferation through several down-stream signalling cascades (Trusolino *et al*, 2010). Therefore, a significant inverse correlation between c-Met and Ki67 scores in the sub-type analysis in luminal A and BL tumours was unexpected. It is very likely that this inverse correlation partly explains why c-Met expression was included in the multivariate model predictive of BL status. If c-Met had positively correlated with Ki67 (a strong predictor of BL status), c-Met scores may not have provided any additional predictive power to the model, potentially leading to its exclusion.

Other immunohistochemical studies have correlated c-Met expression with Ki67 scores in *in-situ* and invasive breast carcinoma (Edakuni *et al*, 2001; Tolgay Ocal *et*

al, 2003; Lindemann *et al*, 2007). Tolgay Ocal *et al* found a positive correlation between c-Met and Ki67 (Tolgay Ocal *et al*, 2003) and Edakuni and colleagues showed a higher Ki67 index in those cases where HGF and c-Met were co-expressed (c-Met in the tumour cells and HGF in the tumour cells and/or stromal cells) (Edakuni *et al*, 2001). In their analysis of DCIS samples, Lindemann *et al* found no association between c-Met and Ki67 expression, but they did see a significant correlation between HGF and Ki67 (Lindemann *et al*, 2007). These last two studies suggest that HGF-mediated c-Met activation rather than c-Met expression *per se* may be a more accurate marker of tumour proliferation.

8.1.2.9 p53 scores

Expression of p53, like Ki67, showed no significant correlation with c-Met in the whole cohort, but did show a significant inverse correlation in the BL tumours. A couple of recent studies have sought to examine the role of c-Met and p53 in pre-clinical models of mammary tumourigenesis (Smolen *et al*, 2006; Knight *et al*, 2013). Mammary tumours generated by combining a heterogeneous *TP53* mutation with a *BRCA1* deletion were analysed by oligonucleotide arrays (Smolen *et al*, 2006). Out of the 15 mice included in the study, 11 (73%) showed amplification of the *MET* gene (Smolen *et al*, 2006). In contrast, these workers found no high level amplification of *MET* when they analysed 100 sporadic human breast cancers, prompting the authors to suggest that *MET* amplification may not be a crucial event in human breast tumours (Smolen *et al*, 2006).

To further investigate the events leading to TN breast cancer, another study combined a transgenic mouse model expressing oncogenic *MET* with a conditional deletion of *TP53* (Knight *et al*, 2013). The vast majority (80%) of tumours from

these mice showed a spindle-cell morphological appearance and this contrasted with the varied histology observed in mice harbouring only the oncogenic *MET* (Knight *et al* 2013; Ponzo *et al*, 2009). Moreover, these spindle-cell tumours showed weak or sporadic expression of the cytokeratins, but strong vimentin and c-Met immunoreactivity (Knight *et al*, 2013). Gene expression profiling showed that these spindle-cell tumours clustered with the claudin-low sub-group of human breast cancers. The authors concluded that *MET* and *TP53* synergise to promote the formation of claudin-low tumours (Knight *et al*, 2013).

Claudin-low tumours are usually TN and show similar gene expression profiles to BL cancers (Perou, 2011). As there is currently no established immunohistochemical marker for claudin-low tumours, one would expect these tumours to fall into the BL or non-BL TN (unclassified in my cohort) groups of tumours (Knight *et al*, 2013). Perhaps the inverse correlation between c-Met and p53 in the BL tumours in the current analysis reflects a paucity of claudin-low tumours.

8.1.3 C-Met expression and survival

This study confirmed that overall, patients with c-Met high tumours had a poorer prognosis than those whose tumours had lower levels of c-Met expression: this was true even after accounting for other prognostic factors. This observation is consistent with previous studies identifying c-Met as a poor prognostic factor in lymph node negative and positive breast carcinoma (Ghoussoub *et al*, 1998; Camp *et al*, 1999; Tolgay Ocal *et al*, 2003; Kang *et al*, 2003; Lengyel *et al*, 2005; Chen *et al*, 2007; Zagouri *et al*, 2013). Only one study has found c-Met expression to be a favourable prognostic factor in breast cancer (Nakopoulou *et al*, 2000). Unlike the above studies, which used arbitrary cut-points to divide the study population into ‘positive’

or ‘negative’ for c-Met, or selected the cut-point based on the distribution of c-Met scores, I used the X-Tile bioinformatics tool to select an appropriate c-Met score to divide the cohort. Cut-point selection can have a profound effect on the outcome of a study and when different cut-points are used between studies, valid comparisons may be impossible (Altman *et al*, 1994). Using the S-phase fraction (SPF) in breast cancer by way of example, Altman *et al* showed that 19 studies published between 1988 and 1993 used cut-points for SPF between 2.6 and 15 (Altman *et al*, 1994). These workers questioned whether any of these cut-points could be regarded as ‘optimal’ and added that the use of multiple cut-points may lead to a false positive rate in excess of 40% (Altman *et al*, 1994).

X-Tile offers several advantages in biomarker statistical analysis (Camp *et al*, 2004). Firstly, by basing the cut-point on survival, the population is divided in a clinically relevant way. Secondly, by randomly separating the study population into training and validation cohorts and applying the optimal cut-point in the training set to the validation set and vice versa, the software insures that each time the analysis is performed, the same p-value and cut-point is obtained. Thirdly, the software performs cross-validation to give a corrected p-value, thus making allowance for multiple cut-point selection (Camp *et al*, 2004).

Survival analysis in the Homerton cohort alone showed no statistical differences between c-Met high and low cases. It is possible that this is due to the relatively small number of patients. The characteristics of the cohort may also have a bearing on the analysis: these patients presented with larger tumours and more frequent lymph node metastasis than their Nottingham counterparts. Whether c-Met expression has more prognostic power in early or late stage disease has not been established.

In my analysis of the different molecular sub-types, the lack of statistically significant findings may again be related to the fact that smaller groups of patients are being assessed. The trend of the survival curve for the c-Met high BL tumours is reminiscent of the BL group in general, where the first five years are associated with a particularly poor survival, followed by a plateau in the curve (Cheang *et al*, 2008). It would be of particular interest to extend the survival analysis to a larger group of BL cancer patients. Notably, the unclassified tumours with high c-Met expression did better than those with low c-Met expression and this was significant (albeit at univariate analysis only) in a group of just 66 patients. This finding further emphasizes the importance of sub-dividing the wider TN group in biomarker analysis and for stratifying patients for novel therapy. In a study of 170 TN breast cancer patients, Zagouri *et al* found that patients with c-Met high tumours had a significantly increased risk of tumour recurrence and death (HR = 3.43 and 3.74 respectively) than those with c-Met low tumours (Zagouri *et al*, 2013). These workers did not stain for basal markers, but my findings would suggest that the bulk of their c-Met high tumours had a BL phenotype.

8.1.4 Conclusion

In summary, the results from this large retrospective study confirm that immunohistochemical expression of c-Met is an independant poor prognostic factor in invasive breast cancer. My analysis of the relationship between c-Met expression and several established prognostic factors and biomarkers generated mixed results, some of which were predictable, others were unexpected. This perhaps reflects the numerous cellular processes influenced by c-Met and the complexity of the HGF/c-Met pathway. Importantly, this study has demonstrated that c-Met expression is

independently predictive of the BL sub-type. This novel finding indicates that patients with these tumours should be included in future studies looking at the therapeutic benefit of c-Met inhibition in breast cancer.

Such clinical studies would be more informative if they stratify patients based not only on tumour c-Met expression, but also on the level of activation of the receptor. The PLA is one assay that offers the potential to quantify levels of c-Met activation on FFPE samples with more sensitivity and specificity than conventional IHC with anti-phospho-c-Met antibodies.

8.2 The PLA and invasive breast carcinoma

8.2.1 The PLA signal and clinical, pathological and molecular parameters

In this study, I have shown for the first time that the PLA can be used to generate a quantifiable signal in FFPE breast cancer samples, using a pan-c-Met antibody and a pan-phospho-tyrosine antibody. The results showed a significant positive correlation between the PLA signal and c-Met expression, as detected by conventional IHC. However, there were key differences between the two variables when they were correlated with relevant prognostic factors and outcome.

Unlike the c-Met scores from the Homerton cohort, the PLA signal (also based on the Homerton cohort) showed no relationship with molecular sub-type of breast cancer. Further, the PLA signals inversely correlated with Ki67 score and worsening tumour grade, two associations not seen in the Homerton c-Met scores. Finally, patients with PLA 'high' tumours showed a trend towards better survival, a trend that reached borderline significance (at univariate analysis only) for BCSS.

To date, there have been no studies specifically designed to look at c-Met phosphorylation/activation in FFPE breast cancer samples so it is difficult to make direct comparisons with the literature. Several other groups have used IHC to phospho-c-Met in other types of cancer with inconsistent results (Nakamura *et al*, 2007; Miyata *et al*, 2009; Lahat *et al*, 2011; Arriola *et al*, 2011; Tsuta *et al*, 2012), perhaps reflecting the lack of robustness of conventional techniques in detecting phospho-proteins in archival material (Dua *et al*, 2011). In bladder cancer, phosphorylation of the Y1349 (pY1349) residue was associated with reduced survival at univariate and multivariate analysis (Miyata *et al*, 2009) and

phosphorylation of the Y1234/5 residue has been linked with a poor outcome at univariate analysis in unclassified pleomorphic sarcoma/malignant fibrous histiocytoma (Lahat *et al*, 2011). In lung cancer, Arriola *et al* found phospho-c-Met (pY1349) expression to be associated with advanced tumour stage and poor survival (Arriola *et al*, 2011). On the other hand, Tsuta and colleagues found higher pY1234/5 expression in smaller lung carcinomas and no correlation with survival (Tsuta *et al*, 2012). In an analysis of 130 primary lung adenocarcinomas, Nakamura et al observed that pY1234/5 expression associated with the absence of vascular invasion and well-differentiated tumours (Nakamura *et al*, 2007). This last finding has some similarities to the findings in this study and it prompted the authors to postulate whether abnormalities other than c-Met activation drive progression in poorly-differentiated carcinomas (Nakamura *et al*, 2007).

With reference to breast cancer, a study by Hochgräfe and co-workers failed to identify phospho-c-Met (pY1234/5) on IHC in their cohort of FFPE breast cancer samples, but they could identify the protein using reverse phase protein analysis (RPPA), noting higher pY1234/5 expression in TN breast cancers (Hochgräfe *et al*, 2010). A more recent study analysed 257 snap-frozen breast cancers, quantifying the c-Met and phospho-c-Met (pY1235), again using RPPA (Raghav *et al*, 2012). The authors found no relationship with molecular sub-type, but both c-Met and pY1235 expression were found to be poor prognostic factors at multivariate analysis (Raghav *et al*, 2012). While the study by Raghav *et al* supports the findings in the current study regarding molecular sub-type, the survival analysis contrasts with my own results. Clearly, these workers used a different technique to assess phospho-c-Met expression, but the use of frozen tissue is also an important distinction. Indeed, how

tissue is prepared and processed are relevant factors that may have influenced the PLA result and merit further discussion.

8.2.2 Confounding factors that may have impacted upon the PLA result

During the validation study of the PLA (section 4.0), a reduction in the number of PLA signals in FFPE samples compared with frozen section from the same tumour was demonstrated. This was not unexpected, given estimates about the efficiency of the PLA in FFPE tissue (approximately 9%, Söderberg *et al*, 2008), but it is apparent that only a small proportion of the signal is being analysed in these samples. It also suggests that the PLA may give more reliable results if its use was restricted to frozen material.

The time that it takes to fix or freeze tissue once it is removed from the body influences the phosphorylation of proteins (Baker *et al*, 2005; Jones *et al*, 2008). After realising that phospho-Akt (p-Akt) was detectable only in biopsy samples from patients with gastro-oesophageal junction adenocarcinomas and not surgical resections, Baker and colleagues investigated the stability of this protein in xenograft samples generated from HT-29 human colon cancer cells (Baker *et al*, 2005). They established that p-Akt was present in those tumour samples that were fixed immediately following resection, but no p-Akt staining was detected in samples that had been left at room temperature for 30-60 minutes prior to fixation. They went on to show that, at western blotting p-Akt had a half-life of just 20 minutes compared to 180 minutes for total Akt (Baker *et al*, 2005). Morphological evidence of a prolonged delay before fixation (as manifest by tumour autolysis) was not a common feature in the Homerton samples. Clearly though, there would have been a degree of

variation in the time to fixation across the cohort and this may have impacted upon the quantity of PLA signals.

Another valid consideration is the identity of phosphotyrosine being detected, since the PLA in the current study used a pan-phosphotyrosine antibody (4G10) as opposed to a more specific phospho-c-Met antibody. Previously, two studies compared the expression of different phospho-c-Met residues (pY1003, pY1230/1234/1235 and pY1349) in frozen and FFPE samples from a variety of tumours (Ma *et al*, 2005; Dua *et al*, 2011). In FFPE non-small cell lung carcinomas (NSCLCs) pY1003 was detected more often than pY1230/1234/1235 and in squamous carcinomas and carcinoid tumours in particular, the difference was marked with 71% and 40% expressing pY1003 respectively versus no expression of pY1230/1234/1235 (Ma *et al*, 2005). Dua *et al* performed western blots on lysates from frozen NSCLCs and gastric tumours (Dua *et al*, 2011). They identified pY1003 in 9/15 NSCLCs and 2/6 gastric tumours, but could not detect either pY1234/1235 or pY1349, prompting the authors to suggest that the pY1003 site may be more stable than pY1234/1235/1349 (Dua *et al*, 2011).

This suggestion may have important implications for the current study because pY1003 has been shown to interact with the tyrosine kinase binding domain of c-Cbl (Peschard *et al*, 2001). C-Cbl is regarded as a negative regulator of many RTKs due to its role in the polyubiquitination of these proteins. The negative regulatory role of c-Cbl also extends to c-Met, where c-Cbl recruitment and subsequent ubiquitination of c-Met is dependent on the juxtamembrane tyrosine Y1003. In cells where Y1003 is substituted for a phenylalanine residue, the mutated receptor (Met Y1003F) becomes oncogenic, promoting morphological changes and cell scattering in the absence of HGF (Peschard *et al*, 2001). Moreover, breast cancer cells (T47Ds)

expressing Met Y1003F demonstrated sustained Ras-MAPK pathway activation compared to cells with wild-type c-Met (Abella *et al*, 2005). These *in-vitro* findings are supported by *in-vivo* models, where subcutaneous injections of NIH3T3 cells expressing Met Y1003F into nude mice resulted in the formation of larger tumours in a shorter time period than those in mice injected with cells containing the wild-type receptor (Abella *et al*, 2005). Thus, it is possible that the PLA signal in the current study reflects the binding of 4G10 to pY1003, an arguably more stable epitope than other phosphorylation sites, which has an important role in the negative regulation of c-Met. This would perhaps explain why patients with 'PLA high' tumours showed a more favourable outcome than those with 'PLA low' tumours at univariate survival analysis.

8.2.3 Conclusion

In summary, I have shown that the PLA can be used to quantify c-Met activation in FFPE breast cancer samples. Correlating the PLA signal with prognostic factors and survival yielded unexpected results, not least a borderline association between high signal and improved survival. However, it is apparent that issues relating to the detection of phospho-proteins in archival material limit the conclusions that can be drawn from these PLA findings. Despite efforts to validate the PLA in cells and tissues, it is clear that 1) the time taken to fix the tissue samples, 2) formaldehyde cross-linking of epitopes and 3) variations in the stability of functionally distinct phospho-epitopes may have had a profound effect on the PLA signal. While these factors do not preclude the use of the PLA in quantifying c-Met activation, they do suggest that the PLA may be better suited to a more controlled setting, such as on rapidly frozen tissue, perhaps utilising different antibodies.

An alternative approach to evaluating the significance of c-Met activation in breast cancer is through *in-vitro* studies. The use of appropriate cell lines permits both functional and mechanistic analysis of the HGF/c-Met pathway in an environment lacking some of the confounding factors present in tissue samples.

8.3 HGF/c-Met in *in-vitro* models of BL cancer

8.3.1 The effect of HGF on BL cancer cell migration

The results from the *in-vitro* experiments show that the presence of HGF in the lower chamber of a transwell leads to a significant increase in migration over an eight hour time period in both BL cancer cell lines. This increase is abrogated by pre-incubating the cells with the c-Met specific kinase inhibitor SU11274 (significantly so in the case of the MDA-MB-468s). Given the well described mitogenic properties of HGF (Gastaldi *et al*, 2010; Nakamura *et al*, 2011) it was necessary to demonstrate that this result was not simply due to increased proliferation of the cells on the underside of the transwell in the HGF-treated chambers. My MTS cell viability assay findings suggest this is not the case, as there were no significant changes in viable cells over eight hours across a range of HGF concentrations, including the concentration used for the migration assay (100ng/ml).

The current findings are supported by previous studies that have investigated HGF-induced cell migration in non-BL and mesenchymal-like (section 5.0) BCLs (Castro and Lange, 2010; Hung *et al*, 2011; Ayoub *et al*, 2013). Castro and Lange showed significantly increased migration by the luminal T47Ds and the mesenchymal-like MDA-MB-231s over a six hour time period when 50ng/ml of HGF was used as a chemo-attractant (Castro and Lange, 2010). Using a wound healing assay to evaluate cell migration by luminal MCF7s, Hung and colleagues demonstrated a significant increase in wound closure over 24 hours when cells were incubated with HGF (Hung *et al*, 2011). Interestingly, these workers also noted that osthole, a fatty acid synthase inhibitor reduced HGF-induced migration and c-Met levels, perhaps by disrupting the lipid rafts utilised by receptors such as c-Met for optimal signalling (Hung *et al*,

2011). Also using a wound healing assay, Ayoub *et al* quantified wound closure after a 24 hour period in MDA-MB-231s and +SA cells (a highly malignant murine mammary cancer cell line) treated with SU11274, with HGF present as a chemo-attractant (Ayoub *et al*, 2013). In both cell lines, cells treated with SU11274 showed a significant reduction in wound closure compared to vehicle treated controls (Ayoub *et al*, 2013). Taken together with the results from the current study, these observations suggest that the HGF/c-Met pathway contributes to the migratory phenotype of different models of breast cancer, including BL breast cancer.

8.3.2 The effect of HGF on BL cancer cell protein expression

To investigate whether the migratory effects of HGF on BL cell lines are accompanied by the acquisition of an EMT-like phenotype, protein expression was quantified using western blotting and protein localisation was assessed using IF-based studies.

After 20 and 120 minutes of HGF treatment, no detectable change in total expression of the EMT markers E-Cadherin, β-Catenin or vimentin was found, as assessed by western blotting. This result was not entirely surprising, since 120 minutes is perhaps not long enough for a change in protein expression to develop. A similar study also found no change in E-Cadherin and β-Catenin levels in MCF10 and MCF7 cells after 30 and 60 minutes of HGF stimulation (Matteucci *et al*, 2006). Elsewhere, others have been able to demonstrate changes in EMT marker levels using lysates from cells exposed to HGF for a longer time period (Hung *et al*, 2011; Ayoub *et al*, 2013). After 18 hours of HGF stimulation, Hung *et al* noted a reduction in E-Cadherin expression, along with increased vimentin levels in MCF7 cells (Hung *et al*, 2011). When the mammary +SA tumour cells were treated with HGF and SU11274 over

three days, levels of E-Cadherin and β-Catenin were elevated and vimentin levels were lower, compared to those cells exposed to HGF alone (Ayoub *et al*, 2013). This finding suggests that c-Met inhibition reverses HGF-induced EMT features.

The results from these cell line based studies are supported by work utilising cell lines from upper aero-digestive cancers (Anderson *et al*, 2006; Kim *et al*, 2007; Xie *et al*, 2010). Using varying HGF concentrations (10 – 100 ng/ml), hypopharyngeal cancer FaDu cells, oesophageal adenocarcinoma OE33 cells and nasopharyngeal carcinoma CNE-1/2 cells all showed a reduction in total E-Cadherin at western blotting after 24-48 hours of treatment (Anderson *et al*, 2006; Kim *et al*, 2007; Xie *et al*, 2010). Hence, it seems that 18-24 hours of HGF stimulation may be necessary before total levels of E-Cadherin expression show a detectable decrease.

Nevertheless, it could be reasoned that a shorter period of HGF stimulation may still be sufficient to observe a change in E-Cadherin localisation. This reasoning is based on growing evidence of co-localisation and a direct interaction between E-Cadherin and c-Met and the fact that I (and others) have already demonstrated intracellular trafficking of c-Met after just 20 minutes of HGF treatment (section 4.0; Kermorgant *et al*, 2003; Kermorgant *et al*, 2004; Reshetnikova, 2007; Reshetnikova *et al*, 2007; Hiscox and Jiang, 1999).

Using IF, it was shown that while c-Met trafficked from the membrane to a perinuclear compartment, E-Cadherin staining remained at the membrane even after 120 minutes. This resulted in a marked reduction in c-Met/E-Cadherin co-localisation (although this only reached statistical significance in the MDA-MB-468s). This finding contrasts with a previous study looking at E-Cadherin localisation in MCF7 cells (Matteucci *et al*, 2006). These workers noted that E-

Cadherin and c-Met accumulated asymmetrically following 30 minutes of HGF treatment, culminating in complete internalisation (and co-localisation) of the proteins by 120 minutes (Matteucci *et al*, 2006). Of course, one cannot compare directly the luminal MCF7 cells with the BL cells used in the current study and, as with my western blot findings it may be that 120 minutes is simply too early to see reproducible alterations in E-Cadherin localisation. Indeed, work on Madin-Darby canine kidney (MDCK) cells demonstrated membrane co-localisation of c-Met and E-Cadherin in resting cells but both c-Met and E-cadherin were shown to partially disappear from the membrane at four hours and accumulate in the perinuclear region at 18 hours post-HGF stimulation (Kamei *et* al, 1999).

Much of the current literature focuses on the tumour suppressor role of E-Cadherin in cancer (Rodriguez *et al*, 2012). E-Cadherin is regarded as a key component of adherens junctions (specialised intraepithelial cell-cell junctions) and an important regulator of β-Catenin activity along with other transcriptional factors implicated in the acquisition of a mesenchymal phenotype (Thiery, 2002; Logullo *et al*, 2010). As such, E-Cadherin has been referred to as one of the 'caretakers of the epithelial phenotype' and its loss may be pivotal to the EMT process in cancer (Thiery, 2002).

However, recent studies have also demonstrated a potential tumour promoter role for E-Cadherin (Rodriguez *et al*, 2012). For example, in oral squamous cell carcinoma (SCC) cell lines, E-Cadherin and EGFR have been found to be co-localised at points of cell-cell adhesion (Shen and Kramer, 2004). This co-localisation leads to ligand independent phosphorylation of EGFR and subsequent activation of the downstream Erk/MAPK pathway resulting in an accumulation of the anti-apoptotic protein Bcl-2 (Shen and Kramer, 2004).

In addition to promoting tumour cell survival, intact E-Cadherin may also contribute to cellular migration (Rodriguez *et al*, 2012). Knockdown of p120-catenin in a vulval SCC cell line (A431) results in the loss of E-Cadherin expression and a reduction in tumour cell invasion (as assessed by an *in-vitro* invasion assay) (Macpherson *et al*, 2007). The authors of this study suggested that p120 contributed to A431 cell invasion by maintaining the E-Cadherin associated junctions that are necessary for the characteristic invasion pattern of groups of cells as opposed to single cells (Macpherson *et al*, 2007). This concept of 'collective cell migration' (the movement of groups of cells that maintain cell-cell junctions throughout their migration) is thought to be particularly important in wound repair and cancer (Friedl *et al*, 2004). In this model, the front edge of the invasive group of cancer cells generate traction with the substrate via the actin cytoskeleton and the rest of the group is effectively pulled along behind due to the presence of intact cell-cell junctions (to which the Cadherin family are central)(Friedl *et al*, 2004). The invasion/migration of groups of cells rather than individual cells may favour tumour progression by not only increasing the quantity of invasive cells, but also facilitating the movement of a heterogeneous group composed of cells with different characteristics. A diverse cluster of cells that are able to interact with each other may be more successful at embolising into the bloodstream and surviving at sites of metastasis (Friedl *et al*, 2004). It is possible that the BL cell lines used in the current study utilise collective cell migration, however more sophisticated models such as those incorporating 3D collagen lattices or *in-vivo* models (Friedl *et al*, 2004) would perhaps be required to test this hypothesis.

8.3.3 Conclusion

In summary, the results of this *in-vitro* study show that the HGF/c-Met pathway contributes to the migration of two different BL cancer cell lines, suggesting that HGF-mediated c-Met phosphorylation may contribute to the progression of BL cancer. After stimulating these cell lines with HGF, there was no significant change in the expression of EMT-associated markers or change in E-Cadherin localisation. These results do not in themselves question whether EMT and/or E-Cadherin trafficking contribute to the migration of these cell lines, but they do indicate that if such processes are occurring, they may only be detectable at a later time point. It is also possible the HGF can contribute to migration despite a functional E-Cadherin network, perhaps by collective cell migration.

9.0 General Discussion

The main goals of this study were: 1) to establish the clinical significance of c-Met expression in a large, well-characterised cohort of breast cancers (in particular the correlation with molecular sub-type), 2) to quantify c-Met activity in a selection of these tumours and 3) to address the functional and phenotypic effects of HGF/c-Met signalling in BL cancer cells.

The first part of this study was dedicated to validating the techniques and materials that would subsequently be used on the breast cancer samples and selecting appropriate cell lines for the *in-vitro* analysis. During the initial evaluation of various c-Met antibodies, a recognised problem in quantifying protein expression of the receptor was encountered – poor reproducibility between commercially available antibodies on FFPE tissue (Pozner-Moulis *et al*, 2007; Cecchi *et al*, 2010). Fortunately, the polyclonal rabbit antibody CVD13 demonstrated specificity for c-Met and a reproducible staining pattern on breast cancer cells and a variety of FFPE tissues. The ability of CVD13 to recognise the active form of c-Met made it a suitable candidate for quantifying phospho-c-Met using the PLA. The PLA probes also appeared specific, with the number of detectable signals being related to the proximity of the target proteins. Characterisation of several 'BL' cell lines identified two (the MDA-MB-468s and HCC1937s) which had a protein expression profile similar to human BL cancers, suggesting they would be plausible models for investigating c-Met signalling in BL cancer in an *in-vitro* environment.

The IHC analysis of c-Met expression confirmed that a high level of the receptor in breast cancer is a poor prognostic factor and perhaps, more importantly, demonstrated an independent association with BL cancer. Crucially, c-Met appeared

to distinguish BL cancer from other TN cancers in terms of absolute levels and survival outcomes, stressing the need to distinguish these two over-lapping sub-groups. Although expression of c-Met is often cited as a cause of c-Met activation (Nakamura *et al*, 2007; Sierra and Tsao, 2011), IHC for total c-Met expression is not a direct measure of activity.

For a more specific measure of c-Met phosphorylation, the PLA was applied to a proportion of the invasive breast cancer cohort. Although the PLA offered clear advantages over conventional IHC in the assessment of protein phosphorylation (Blokzijl *et al*, 2010), when the PLA results were correlated with clinico-pathological factors and survival, it was evident that the PLA was of limited prognostic value. In section 8.2 the limitations, not just of the PLA, but of detecting phospho-proteins in general were discussed and these suggested caution should be applied when interpreting the PLA results. The key questions that remain therefore include 1) is c-Met activation important in breast cancer progression? 2) Does c-Met activity vary amongst the molecular sub-types (as expression does)? 3) Finally, is c-Met activity more relevant than c-Met expression?

The only other study to specifically address these questions did identify phospho-c-Met as a poor prognostic factor (using an anti-phospho-c-Met antibody), but phospho-c-Met levels did not offer more prognostic information (in terms of overall and relapse-free survival) than total c-Met levels (Raghav *et al*, 2012). Moreover, phospho-c-Met expression did not vary significantly between the molecular sub-types (Raghav *et al*, 2012). The findings on cell lines in this study, together with those of previous studies, suggest that HGF/c-Met signalling may contribute to the migratory phenotype of different sub-types of breast cancer, including BL breast cancer (Castro and Lange, 2010; Hung *et al*, 2011; Ayoub *et al*, 2013).

Comparing the relative merits of expression versus phosphorylation of c-Met is not straightforward, due in part to the issues outlined in section 8.2 and also the fact that protein/RTK phosphorylation may be a transient event, triggered by dynamic changes in the microenvironment such as hypoxia (Baker *et al*, 2005; Wang and Schneider, 2010; Halle *et al*, 2011). These changes may not be consistently represented in archival material, where one gets a 'snap-shot' of a tumour at a particular time. As such, it could be argued that expression of the receptor is a more reliable measure than activation. In addition, another RTK (EGFR) has been shown to exhibit oncogenic effects that are independent of its kinase activity (Weihua *et al*, 2008).

Another study, looking at recurrent glioblastomas, also questioned the benefits of measuring receptor phosphorylation over expression. Paulsson *et al* assessed PDGFRα expression and activity (using the PLA) finding that both parameters correlated with each other and higher levels of each were associated with reduced survival (Paulsson *et al*, 2011). However, the authors concluded that measuring PDGFRα phosphorylation offered no additional prognostic information (Paulsson *et al*, 2011). Notably, this study also considered the predictive role of PDGFRα expression/activation by correlating these markers with the response to treatment (hydroxyurea monotherapy versus combined treatment with hydroxyurea and imatinib, the RTK inhibitor). They observed that neither PDGFRα expression nor activation levels identified patients likely to respond to the combined treatment (Paulsson *et al*, 2011).

This study highlights another potential application for c-Met IHC/phospho-c-Met PLA – predicting the response to anti-c-Met therapy. The predictive role of these

assays is beyond the scope of this thesis, but represents an area of intended future work and would complement well the prognostic data contained herein.

The relationship between c-Met and E-Cadherin is one explored in some depth in the IHC analysis (section 8.1) and the *in-vitro* part of this study (section 8.3). The decision to investigate these proteins was largely based on the increasing body of literature suggesting a relationship between c-Met and E-Cadherin, in particular their possible involvement in EMT (Hiscox and Jiang, 1999; Reshetnikova, 2007; Reshetnikova *et al*, 2007). In the tissue-based analysis, co-expression of c-Met and E-Cadherin was seen across the whole cohort and *in-vitro* IF studies demonstrated co-localisation of these proteins in resting (un-stimulated) BL cell lines. These findings support the notion that E-Cadherin may occupy a facilitatory role, maintaining c-Met at the membrane to optimise ligand/receptor binding (Reshetnikova *et al*, 2007). The methodology used in the current study may explain why no trafficking of E-Cadherin was observed and why there was no reduction in total protein levels following HGF-stimulation, given the results of similar studies (Matteucci *et al*, 2006; Hung *et al*, 2011; Ayoub *et al*, 2013).

Evidently, the role of E-Cadherin in cancer progression is complex: on the one hand loss of the protein favours EMT, on the other hand over-expression favours collective cell migration and tumour emboli formation (as in inflammatory breast cancer)(Rodriguez *et al*, 2012). Investigating the significance of EMT is further complicated by the knowledge that this event is frequently incomplete and sensitive to culture conditions *in-vitro* and difficult to identify in human tumours (Thiery, 2002). Further work is necessary to elucidate the relationship between E-Cadherin and c-Met, and the nature of this relationship in BL breast cancer.

In conclusion, c-Met expression is a poor prognostic factor in breast cancer, independently associated with the aggressive BL sub-type (TN tumours with expression of one or more basal markers). The PLA can be used to detect c-Met phosphorylation in cells and tissues, but more work is needed to refine the technique and establish its prognostic utility in breast cancer. HGF stimulation results in increased migration in BL cell lines, but EMT-like phenotypic changes were not seen in the relatively short time period studied. The results from this study advocate the continued investigation of anti-c-Met therapy as a novel treatment for BL breast cancer.

References

1) Abella JV, Peschard P, Naujokas MA, Lin T, Saucier C, Urbé S, Park M. Met/Hepatocyte growth factor receptor ubiquitination suppresses transformation and is required for Hrs phosphorylation. *Mol Cell Biol.* 2005 Nov;25(21):9632-45.

2) Ademuyiwa FO, Edge SB, Erwin DO, Orom H, Ambrosone CB, Underwood W 3rd. Breast cancer racial disparities: unanswered questions. *Cancer Res.* 2011 Feb 1;71(3):640-4. doi: 10.1158/0008-5472.CAN-10-3021. Epub 2010 Dec 6.

3) Adesunkanmi AR, Lawal OO, Adelusola KA, Durosimi MA. The severity, outcome and challenges of breast cancer in Nigeria. *Breast.* 2006 Jun;15(3):399-409. Epub 2005 Aug 8.

4) Al-Hajj M, Wicha MS, Benito-Hernandez A, Morrison SJ, Clarke MF. Prospective identification of tumorigenic breast cancer cells. *Proc Natl Acad Sci U S A.* 2003 Apr 1;100(7):3983-8. Epub 2003 Mar 10.

5) Allred DC, Clark GM, Elledge R, Fuqua SA, Brown RW, Chamness GC, Osborne CK, McGuire WL. Association of p53 protein expression with tumor cell proliferation rate and clinical outcome in node-negative breast cancer. *J Natl Cancer Inst.* 1993 Feb 3;85(3):200-6.

6) Altman DG, Lausen B, Sauerbrei W, Schumacher M. Dangers of using "optimal" cutpoints in the evaluation of prognostic factors. *J Natl Cancer Inst.* 1994 Jun 1;86(11):829-35.

7) Amir E, Freedman OC, Seruga B, Evans DG. Assessing women at high risk of breast cancer: a review of risk assessment models. *J Natl Cancer Inst.* 2010 May 19;102(10):680-91. doi: 10.1093/jnci/djq088. Epub 2010 Apr 28.

8) Anderson MR, Harrison R, Atherfold PA, Campbell MJ, Darnton SJ, Obszynska J, Jankowski JA. Met receptor signaling: a key effector in esophageal adenocarcinoma. *Clin Cancer Res.* 2006 Oct 15;12(20 Pt 1):5936-43.

9) Arnes JB, Bégin LR, Stefansson I, Brunet JS, Nielsen TO, Foulkes WD, Akslen LA. Expression of epidermal growth factor receptor in relation to BRCA1 status, basal-like markers and prognosis in breast cancer. *J Clin Pathol.* 2009 Feb;62(2):139-46. doi: 10.1136/jcp.2008.056291. Epub 2008 Aug 4.

10) Arriola E, Cañadas I, Arumí-Uría M, Dómine M, Lopez-Vilariño JA, Arpí O, Salido M, Menéndez S, Grande E, Hirsch FR, Serrano S, Bellosillo B, Rojo F, Rovira A, Albanell J. MET phosphorylation predicts poor outcome in small cell lung carcinoma and its inhibition blocks HGF-induced effects in MET mutant cell lines. *Br J Cancer.* 2011 Sep 6;105(6):814-23. doi: 10.1038/bjc.2011.298. Epub 2011 Aug 16.

11) Ayoub NM, Akl MR, Sylvester PW. Combined γ-tocotrienol and Met inhibitor treatment suppresses mammary cancer cell proliferation, epithelial-to-mesenchymal transition and migration. *Cell Prolif.* 2013 Oct;46(5):538-53. doi: 10.1111/cpr.12059. Epub 2013 Aug 23.

12) Badve S, Dabbs DJ, Schnitt SJ, Baehner FL, Decker T, Eusebi V, Fox SB, Ichihara S, Jacquemier J, Lakhani SR, Palacios J, Rakha EA, Richardson AL, Schmitt FC, Tan PH, Tse GM, Weigelt B, Ellis IO, Reis-Filho JS. Basal-like and triple-negative breast cancers: a critical review with an emphasis on the implications for pathologists and oncologists. *Mod Pathol.* 2011 Feb;24(2):157-67. doi: 10.1038/modpathol.2010.200. Epub 2010 Nov 12.

13) Baker AF, Dragovich T, Ihle NT, Williams R, Fenoglio-Preiser C, Powis G. Stability of phosphoprotein as a biological marker of tumor signaling. *Clin Cancer Res.* 2005 Jun 15;11(12):4338-40.

14) Banerjee S, Reis-Filho JS, Ashley S, Steele D, Ashworth A, Lakhani SR, Smith IE. Basal-like breast carcinomas: clinical outcome and response to chemotherapy. *J Clin Pathol.* 2006 Jul;59(7):729-35. Epub 2006 Mar 23.

15) Bean J, Brennan C, Shih JY, Riely G, Viale A, Wang L, Chitale D, Motoi N, Szoke J, Broderick S, Balak M, Chang WC, Yu CJ, Gazdar A, Pass H, Rusch V, Gerald W, Huang SF, Yang PC, Miller V, Ladanyi M, Yang CH, Pao W. MET amplification occurs with or without T790M mutations in EGFR mutant lung tumors with acquired resistance to gefitinib or erlotinib. *Proc Natl Acad Sci U S A.* 2007 Dec 26;104(52):20932-7. Epub 2007 Dec 18.

16) Berg JW and Hutter RV. Breast cancer. *Cancer.* 1995 Jan 1;75(1 Suppl):257-69.

17) Bertotti A, Comoglio PM, Trusolino L. Beta4 integrin activates a Shp2-Src signaling pathway that sustains HGF-induced anchorage-independent growth. *J Cell Biol.* 2006 Dec 18;175(6):993-1003. Epub 2006 Dec 11.

18) Bertucci F, Finetti P, Cervera N, Esterni B, Hermitte F, Viens P, Birnbaum D. How basal are triple-negative breast cancers? *Int J Cancer.* 2008 Jul 1;123(1):236-40. doi: 10.1002/ijc.23518.

19) Bex A, Blank C, Meinhardt W, van Tinteren H, Horenblas S, Haanen J. A phase II study of presurgical sunitinib in patients with metastatic clear-cell renal carcinoma and the primary tumor in situ. *Urology.* 2011 Oct;78(4):832-7. doi: 10.1016/j.urology.2011.05.034. Epub 2011 Jul 29.

20) Biganzoli E, Coradini D, Ambrogi F, Garibaldi JM, Lisboa P, Soria D, Green AR, Pedriali M, Piantelli M, Querzoli P, Demicheli R, Boracchi P, Nenci I, Ellis IO, Alberti S. p53 status identifies two subgroups of triple-negative breast cancers with distinct biological features. *Jpn J Clin Oncol.* 2011 Feb;41(2):172-9. doi: 10.1093/jjco/hyq227. Epub 2011 Jan 2.

21) Blokzijl A, Friedman M, Pontén F, Landegren U. Profiling protein expression and interactions: proximity ligation as a tool for personalized medicine. *J Intern Med.* 2010 Sep;268(3):232-45. doi: 10.1111/j.1365-2796.2010.02256.x.

22) Blows FM, Driver KE, Schmidt MK, Broeks A, van Leeuwen FE, Wesseling J, Cheang MC, Gelmon K, Nielsen TO, Blomqvist C, Heikkilä P, Heikkinen T, Nevanlinna H, Akslen LA, Bégin LR, Foulkes WD, Couch FJ, Wang X, Cafourek V, Olson JE, Baglietto L, Giles GG, Severi G, McLean CA, Southey MC, Rakha E, Green AR, Ellis IO, Sherman ME, Lissowska J, Anderson WF, Cox A, Cross SS, Reed MW, Provenzano E, Dawson SJ, Dunning AM, Humphreys M, Easton DF, García-Closas M, Caldas C, Pharoah PD, Huntsman D. Subtyping of breast cancer by immunohistochemistry to investigate a relationship between subtype and short and long term survival: a collaborative analysis of data for 10,159 cases from 12 studies. *PLoS Med.* 2010 May 25;7(5):e1000279. doi: 10.1371/journal.pmed.1000279.

23) Boecker W and Buerger H. Evidence of progenitor cells of glandular and myoepithelial cell lineages in the human adult female breast epithelium: a new progenitor (adult stem) cell concept. *Cell Prolif.* 2003 Oct;36 Suppl 1:73-84.

24) Boleti E, Sarwar N, Jones R, Chowdhury S, Crabb SJ, Shamash J, Peters J, Oades G, O'Brien TS, Berney D, Rockall A, Powles T. The safety and efficacy of pazopanib prior to planned nephrectomy in metastatic clear cell renal cancer. *J Clin Oncol*, 2012 (suppl 5; abstr 427).

25) Bottaro DP, Rubin JS, Faletto DL, Chan AM, Kmiecik TE, Vande Woude GF, Aaronson SA. Identification of the hepatocyte growth factor receptor as the c-met proto-oncogene product. *Science.* 1991 Feb 15;251(4995):802-4.

26) Bowen RL, Duffy SW, Ryan DA, Hart IR, Jones JL. Early onset of breast cancer in a group of British black women. *Br J Cancer*. 2008 Jan 29;98(2):277-81. doi: 10.1038/sj.bjc.6604174. Epub 2008 Jan 8.

27) Boyd NF, Guo H, Martin LJ, Sun L, Stone J, Fishell E, Jong RA, Hislop G, Chiarelli A, Minkin S, Yaffe MJ. Mammographic density and the risk and detection of breast cancer. *N Engl J Med.* 2007 Jan 18;356(3):227-36.

28) Brennan DJ, Kelly C, Rexhepaj E, Dervan PA, Duffy MJ, Gallagher WM. Contribution of DNA and tissue microarray technology to the identification and validation of biomarkers and personalised medicine in breast cancer. *Cancer Genomics Proteomics.* 2007 May-Jun;4(3):121-34.

29) Buchwalow IB and Böcker W. *Immunohistochemistry: Basics and Methods.*Heidleberg: Springer, 2010: v-51.

30) Burness ML, Grushko TA, Olopade OI. Epidermal growth factor receptor in triple-negative and basal-like breast cancer: promising clinical target or only a marker? *Cancer J.* 2010 Jan-Feb;16(1):23-32. doi: 10.1097/PPO.0b013e3181d24fc1.

31) Camp RL, Dolled-Filhart M, Rimm DL. X-tile: a new bio-informatics tool for biomarker assessment and outcome-based cut-point optimization. *Clin Cancer Res.* 2004 Nov 1;10(21):7252-9.

32) Camp RL, Rimm EB, Rimm DL. Met expression is associated with poor outcome in patients with axillary lymph node negative breast carcinoma. *Cancer.* 1999 Dec 1;86(11):2259-65.

33) Cancer Research UK. Cancer Stats: Cancer Statistics for the UK – Breast cancer. http://info.cancerresearchuk.org/cancerstats. March 2014.

34) Carey LA, Perou CM, Livasy CA, Dressler LG, Cowan D, Conway K, Karaca G, Troester MA, Tse CK, Edmiston S, Deming SL, Geradts J, Cheang MC, Nielsen TO, Moorman PG, Earp HS, Millikan RC. Race, breast cancer subtypes, and survival in the Carolina Breast Cancer Study. *JAMA.* 2006 Jun 7;295(21):2492-502.

35) Carracedo A, Egervari K, Salido M, Rojo F, Corominas JM, Arumi M, Corzo C, Tusquets I, Espinet B, Rovira A, Albanell J, Szollosi Z, Serrano S, Solé F. FISH and immunohistochemical status of the hepatocyte growth factor receptor (c-Met) in 184 invasive breast tumors. *Breast Cancer Res.* 2009;11(2):402. doi: 10.1186/bcr2239. Epub 2009 Apr 21.

36) Carter BA, Page DL, O'Malley FP. Usual epithelial hyperplasia and atypical ductal hyperplasia. In O'Malley FP and Pinder SE, editors. *Breast Pathology*. Philadelphia: Elsevier, 2006: 159-168.

37) Carter CL, Allen C, Henson DE. Relation of tumor size, lymph node status, and survival in 24,740 breast cancer cases. *Cancer.* 1989 Jan 1;63(1):181-7.

38) Castro NE and Lange CA. Breast tumor kinase and extracellular signal-regulated kinase 5 mediate Met receptor signaling to cell migration in breast cancer cells. *Breast Cancer Res.* 2010;12(4):R60. doi: 10.1186/bcr2622. Epub 2010 Aug 5.

39) Cecchi F, Rabe DC, Bottaro DP. Targeting the HGF/Met signalling pathway in cancer. *Eur J Cancer.* 2010 May;46(7):1260-70. doi: 10.1016/j.ejca.2010.02.028. Epub 2010 Mar 19.

40) Charafe-Jauffret E, Ginestier C, Monville F, Finetti P, Adélaïde J, Cervera N, Fekairi S, Xerri L, Jacquemier J, Birnbaum D, Bertucci F. Gene expression profiling of breast cell lines identifies potential new basal markers. *Oncogene.* 2006 Apr 6;25(15):2273-84.

41) Cheang MC, Chia SK, Voduc D, Gao D, Leung S, Snider J, Watson M, Davies S, Bernard PS, Parker JS, Perou CM, Ellis MJ, Nielsen TO. Ki67 index, HER2 status, and prognosis of patients with luminal B breast cancer. *J Natl Cancer Inst.* 2009 May 20;101(10):736-50. doi: 10.1093/jnci/djp082. Epub 2009 May 12.

42) Cheang MC, Voduc D, Bajdik C, Leung S, McKinney S, Chia SK, Perou CM, Nielsen TO. Basal-like breast cancer defined by five biomarkers has superior prognostic value than triple-negative phenotype. *Clin Cancer Res.* 2008 Mar 1;14(5):1368-76. doi: 10.1158/1078-0432.CCR-07-1658.

43) Chekhun S, Bezdenezhnykh N, Shvets J, Lukianova N. Expression of biomarkers related to cell adhesion, metastasis and invasion of breast cancer cell lines of different molecular subtype. *Exp Oncol.* 2013 Sep;35(3):174-9.

44) Chen HH, Su WC, Lin PW, Guo HR, Lee WY. Hypoxia-inducible factor-1alpha correlates with MET and metastasis in node-negative breast cancer. *Breast Cancer Res Treat.* 2007 Jun;103(2):167-75. Epub 2006 Sep 21.

45) Cheuk W and Chan JK. Subcellular localization of immunohistochemical signals: knowledge of the ultrastructural or biologic features of the antigens helps predict the signal localization and proper interpretation of immunostains. *Int J Surg Pathol.* 2004 Jul;12(3):185-206.

46) Clark SE, Warwick J, Carpenter R, Bowen RL, Duffy SW, Jones JL. Molecular subtyping of DCIS: heterogeneity of breast cancer reflected in pre-invasive disease. *Br J Cancer.* 2011 Jan 4;104(1):120-7. doi: 10.1038/sj.bjc.6606021. Epub 2010 Dec 7.

47) ClinicalTrials.gov. http://www.clinicaltrials.gov. March 2014.

48) Collaborative Group on Hormonal Factors in Breast Cancer. Breast cancer and hormone replacement therapy: collaborative reanalysis of data from 51 epidemiological studies of 52,705 women with breast cancer and 108,411 women without breast cancer. *Lancet.* 1997 Oct 11;350(9084):1047-59.

49) Collett K, Stefansson IM, Eide J, Braaten A, Wang H, Eide GE, Thoresen SØ, Foulkes WD, Akslen LA. A basal epithelial phenotype is more frequent in interval breast cancers compared with screen detected tumors. *Cancer Epidemiol Biomarkers Prev.* 2005 May;14(5):1108-12.

50) Collins LC, Tamimi RM, Baer HJ, Connolly JL, Colditz GA, Schnitt SJ. Outcome of patients with ductal carcinoma in situ untreated after diagnostic biopsy: results from the Nurses' Health Study. *Cancer.* 2005 May 1;103(9):1778-84.

51) Cooke VG, LeBleu VS, Keskin D, Khan Z, O'Connell JT, Teng Y, Duncan MB, Xie L, Maeda G, Vong S, Sugimoto H, Rocha RM, Damascena A, Brentani RR, Kalluri R. Pericyte depletion results in hypoxia-associated epithelial-to-mesenchymal transition and metastasis mediated by met signaling pathway. *Cancer Cell.* 2012 Jan 17;21(1):66-81. doi: 10.1016/j.ccr.2011.11.024.

52) Cooper CS, Park M, Blair DG, Tainsky MA, Huebner K, Croce CM, Vande Woude GF. Molecular cloning of a new transforming gene from a chemically transformed human cell line. *Nature.* 1984 Sep 6-11;311(5981):29-33.

53) Curtis C, Shah SP, Chin SF, Turashvili G, Rueda OM, Dunning MJ, Speed D, Lynch AG, Samarajiwa S, Yuan Y, Gräf S, Ha G, Haffari G, Bashashati A, Russell R, McKinney S; METABRIC Group, Langerød A, Green A, Provenzano E, Wishart G, Pinder S, Watson P, Markowetz F, Murphy L, Ellis I, Purushotham A, Børresen-Dale AL, Brenton JD, Tavaré S, Caldas C, Aparicio S. The genomic and transcriptomic architecture of 2,000 breast tumours reveals novel subgroups. *Nature.* 2012 Apr 18;486(7403):346-52. doi: 10.1038/nature10983.

54) Da Silva L and Lakhani SR. Pathology of hereditary breast cancer. *Mod Pathol.* 2010 May;23 Suppl 2:S46-51. doi: 10.1038/modpathol.2010.37.

55) Dabbs DJ, Chivukula M, Carter G, Bhargava R. Basal phenotype of ductal carcinoma in situ: recognition and immunohistologic profile. *Mod Pathol.* 2006 Nov;19(11):1506-11. Epub 2006 Aug 25.

56) de Azambuja E, Cardoso F, de Castro G Jr, Colozza M, Mano MS, Durbecq V, Sotiriou C, Larsimont D, Piccart-Gebhart MJ, Paesmans M. Ki-67 as prognostic marker in early breast cancer: a meta-analysis of published studies involving 12,155 patients. *Br J Cancer.* 2007 May 21;96(10):1504-13. Epub 2007 Apr 24.

57) De Laurentiis M, Cianniello D, Caputo R, Stanzione B, Arpino G, Cinieri S, Lorusso V, De Placido S. Treatment of triple negative breast cancer (TNBC): current options and future perspectives. *Cancer Treat Rev.* 2010 Nov;36 Suppl 3:S80-6. doi: 10.1016/S0305-7372(10)70025-6.

58) Dietz MS, Haße D, Ferraris DM, Göhler A, Niemann HH, Heilemann M. Single-molecule photobleaching reveals increased MET receptor dimerization upon ligand binding in intact cells. *BMC Biophys.* 2013 Jun 3;6(1):6. doi: 10.1186/2046-1682-6-6.

59) Dua R, Zhang J, Parry G, Penuel E. Detection of hepatocyte growth factor (HGF) ligand-c-MET receptor activation in formalin-fixed paraffin embedded specimens by a novel proximity assay. *PLoS One.* 2011 Jan 21;6(1):e15932. doi: 10.1371/journal.pone.0015932.

60) Dupont WD, Parl FF, Hartmann WH, Brinton LA, Winfield AC, Worrell JA, Schuyler PA, Plummer WD. Breast cancer risk associated with proliferative breast disease and atypical hyperplasia. *Cancer.* 1993 Feb 15;71(4):1258-65.

61) Edakuni G, Sasatomi E, Satoh T, Tokunaga O, Miyazaki K. Expression of the hepatocyte growth factor/c-Met pathway is increased at the cancer front in breast carcinoma. *Pathol Int.* 2001 Mar;51(3):172-8.

62) Elston CW and Ellis IO. Pathological prognostic factors in breast cancer. I. The value of histological grade in breast cancer: experience from a large study with long-term follow-up. *Histopathology.* 1991 Nov;19(5):403-10.

63) Engelman JA, Zejnullahu K, Mitsudomi T, Song Y, Hyland C, Park JO, Lindeman N, Gale CM, Zhao X, Christensen J, Kosaka T, Holmes AJ, Rogers AM, Cappuzzo F, Mok T, Lee C, Johnson BE, Cantley LC, Jänne PA. MET amplification leads to gefitinib resistance in lung cancer by activating ERBB3 signaling. *Science.* 2007 May 18;316(5827):1039-43. Epub 2007 Apr 26

64) Farmer H, McCabe N, Lord CJ, Tutt AN, Johnson DA, Richardson TB, Santarosa M, Dillon KJ, Hickson I, Knights C, Martin NM, Jackson SP, Smith GC, Ashworth A. Targeting the DNA repair defect in BRCA mutant cells as a therapeutic strategy. *Nature.* 2005 Apr 14;434(7035):917-21.

65) Fedele CG, Ooms LM, Ho M, Vieusseux J, O'Toole SA, Millar EK, Lopez-Knowles E, Sriratana A, Gurung R, Baglietto L, Giles GG, Bailey CG, Rasko JE, Shields BJ, Price JT, Majerus PW, Sutherland RL, Tiganis T, McLean CA, Mitchell CA. Inositol polyphosphate 4-phosphatase II regulates PI3K/Akt signaling and is lost in human basal-like breast cancers. *Proc Natl Acad Sci U S A.* 2010 Dec 21;107(51):22231-6. doi: 10.1073/pnas.1015245107. Epub 2010 Dec 2.

66) Foulkes WD, Brunet JS, Stefansson IM, Straume O, Chappuis PO, Bégin LR, Hamel N, Goffin JR, Wong N, Trudel M, Kapusta L, Porter P, Akslen LA. The prognostic implication of the basal-like (cyclin E high/p27 low/p53+/glomeruloid-microvascular-proliferation+) phenotype of BRCA1-related breast cancer. *Cancer Res.* 2004 Feb 1;64(3):830-5.

67) Foulkes WD, Grainge MJ, Rakha EA, Green AR, Ellis IO. Tumor size is an unreliable predictor of prognosis in basal-like breast cancers and does not correlate closely with lymph node status. *Breast Cancer Res Treat.* 2009 Sep;117(1):199-204. doi: 10.1007/s10549-008-0102-6. Epub 2008 Jul 4.

68) Foulkes WD, Smith IE, Reis-Filho JS. Triple-negative breast cancer. *N Engl J Med.* 2010 Nov 11;363(20):1938-48. doi: 10.1056/NEJMra1001389.

69) Foulkes WD, Stefansson IM, Chappuis PO, Bégin LR, Goffin JR, Wong N, Trudel M, Akslen LA. Germline BRCA1 mutations and a basal epithelial phenotype in breast cancer. *J Natl Cancer Inst.* 2003 Oct 1;95(19):1482-5.

70) Fregene A and Newman LA. Breast cancer in sub-Saharan Africa: how does it relate to breast cancer in African-American women? *Cancer.* 2005 Apr 15;103(8):1540-50.

71) Friedl P, Hegerfeldt Y, Tusch M. Collective cell migration in morphogenesis and cancer. *Int J Dev Biol.* 2004;48(5-6):441-9.

72) Fulford LG, Easton DF, Reis-Filho JS, Sofronis A, Gillett CE, Lakhani SR, Hanby A. Specific morphological features predictive for the basal phenotype in grade 3 invasive ductal carcinoma of breast. *Histopathology.* 2006 Jul;49(1):22-34.

73) Galea MH, Blamey RW, Elston CE, Ellis IO.The Nottingham Prognostic Index in primary breast cancer. *Breast Cancer Res Treat.* 1992;22(3):207-19.

74) Garcia S, Dalès JP, Charafe-Jauffret E, Carpentier-Meunier S, Andrac-Meyer L, Jacquemier J, Andonian C, Lavaut MN, Allasia C, Bonnier P, Charpin C. Poor prognosis in breast carcinomas correlates with increased expression of targetable CD146 and c-Met and with proteomic basal-like phenotype. *Hum Pathol.* 2007a Jun;38(6):830-41. Epub 2007 Feb 20.

75) Garcia S, Dalès JP, Jacquemier J, Charafe-Jauffret E, Birnbaum D, Andrac-Meyer L, Lavaut MN, Allasia C, Carpentier-Meunier S, Bonnier P, Charpin-Taranger C. c-Met overexpression in inflammatory breast carcinomas: automated quantification on tissue microarrays. *Br J Cancer*. 2007b Jan 29;96(2):329-35.

76) Gastaldi S, Comoglio PM, Trusolino L. The Met oncogene and basal-like breast cancer: another culprit to watch out for? *Breast Cancer Res.* 2010;12(4):208. doi: 10.1186/bcr2617. Epub 2010 Aug 23.

77) Gentile A, Trusolino L, Comoglio PM. The Met tyrosine kinase receptor in development and cancer. *Cancer Metastasis Rev.* 2008 Mar;27(1):85-94. doi: 10.1007/s10555-007-9107-6.

78) Gherardi E, Birchmeier W, Birchmeier C, Vande Woude G. Targeting MET in cancer: rationale and progress. *Nat Rev Cancer.* 2012 Jan 24;12(2):89-103. doi: 10.1038/nrc3205.

79) Ghoussoub RA, Dillon DA, D'Aquila T, Rimm EB, Fearon ER, Rimm DL. Expression of c-met is a strong independent prognostic factor in breast carcinoma. *Cancer.* 1998 Apr 15;82(8):1513-20.

80) Giordano S, Ponzetto C, Di Renzo MF, Cooper CS, Comoglio PM. Tyrosine kinase receptor indistinguishable from the c-met protein. *Nature.* 1989 May 11;339(6220):155-6.

81) Going, J. Normal breast. In O'Malley FP and Pinder SE, editors. *Breast Pathology*. Philadelphia: Elsevier, 2006: 55-65.

82) Goldhirsch A, Ingle JN, Gelber RD, Coates AS, Thürlimann B, Senn HJ; Panel members. Thresholds for therapies: highlights of the St Gallen International Expert Consensus on the primary therapy of early breast cancer 2009. *Ann Oncol.* 2009 Aug;20(8):1319-29. doi: 10.1093/annonc/mdp322. Epub 2009 Jun 17.

83) Goldoni S, Humphries A, Nyström A, Sattar S, Owens RT, McQuillan DJ, Ireton K, Iozzo RV. Decorin is a novel antagonistic ligand of the Met receptor. *J Cell Biol.* 2009 May 18;185(4):743-54. doi: 10.1083/jcb.200901129. Epub 2009 May 11.

84) Gordon MS, Sweeney CS, Mendelson DS, Eckhardt SG, Anderson A, Beaupre DM, Branstetter D, Burgess TL, Coxon A, Deng H, Kaplan-Lefko P, Leitch IM, Oliner KS, Yan L, Zhu M, Gore L. Safety, pharmacokinetics, and pharmacodynamics of AMG 102, a fully human hepatocyte growth factor-neutralizing monoclonal antibody, in a first-in-human study of patients with advanced solid tumors. *Clin Cancer Res.* 2010 Jan 15;16(2):699-710. doi: 10.1158/1078-0432.CCR-09-1365. Epub 2010 Jan 12.

85) Gorski JJ, James CR, Quinn JE, Stewart GE, Staunton KC, Buckley NE, McDyer FA, Kennedy RD, Wilson RH, Mullan PB, Harkin DP. BRCA1 transcriptionally regulates genes associated with the basal-like phenotype in breast cancer. *Breast Cancer Res Treat.* 2010 Aug;122(3):721-31. doi: 10.1007/s10549-009-0565-0. Epub 2009 Oct 31.

86) Götte M, Kersting C, Radke I, Kiesel L, Wülfing P. An expression signature of syndecan-1 (CD138), E-cadherin and c-met is associated with factors of angiogenesis and lymphangiogenesis in ductal breast carcinoma in situ. *Breast Cancer Res.* 2007;9(1):R8.

87) Graveel CR, DeGroot JD, Su Y, Koeman J, Dykema K, Leung S, Snider J, Davies SR, Swiatek PJ, Cottingham S, Watson MA, Ellis MJ, Sigler RE, Furge KA, Vande Woude GF. Met induces diverse mammary carcinomas in mice and is associated with human basal breast cancer. *Proc Natl Acad Sci U S A.* 2009 Aug 4;106(31):12909-14. doi: 10.1073/pnas.0810403106. Epub 2009 Jun 30.

88) Grigoriadis A, Mackay A, Noel E, Wu PJ, Natrajan R, Frankum J, Reis-Filho JS, Tutt A. Molecular characterisation of cell line models for triple-negative breast cancers. *BMC Genomics.* 2012 Nov 14;13:619. doi: 10.1186/1471-2164-13-619.

89) Gusterson B. Do 'basal-like' breast cancers really exist? *Nat Rev Cancer.* 2009 Feb;9(2):128-34. doi: 10.1038/nrc2571. Epub 2008 Dec 29.

90) Hackett AJ, Smith HS, Springer EL, Owens RB, Nelson-Rees WA, Riggs JL, Gardner MB. Two syngeneic cell lines from human breast tissue: the aneuploid mammary epithelial (Hs578T) and the diploid myoepithelial (Hs578Bst) cell lines. *J Natl Cancer Inst.* 1977 Jun;58(6):1795-806.

91) Halle C, Lando M, Sundfør K, Kristensen GB, Holm R, Lyng H. Phosphorylation of EGFR measured with in situ proximity ligation assay: relationship to EGFR protein level and gene dosage in cervical cancer. *Radiother Oncol.* 2011 Oct;101(1):152-7. doi: 10.1016/j.radonc.2011.05.052. Epub 2011 Jun 15.

92) Hammond ME, Hayes DF, Dowsett M, Allred DC, Hagerty KL, Badve S, Fitzgibbons PL, Francis G, Goldstein NS, Hayes M, Hicks DG, Lester S, Love R, Mangu PB, McShane L, Miller K, Osborne CK, Paik S, Perlmutter J, Rhodes A, Sasano H, Schwartz JN, Sweep FC, Taube S, Torlakovic EE, Valenstein P, Viale G, Visscher D, Wheeler T, Williams RB, Wittliff JL, Wolff AC. American Society of Clinical Oncology/College of American Pathologists guideline recommendations for immunohistochemical testing of estrogen and progesterone receptors in breast cancer. *Arch Pathol Lab Med.* 2010 Jun;134(6):907-22. doi: 10.1043/1543-2165-134.6.907.

93) Hanna JA, Bordeaux J, Rimm DL, Agarwal S. The function, proteolytic processing, and histopathology of Met in cancer. *Adv Cancer Res.* 2009;103:1-23. doi: 10.1016/S0065-230X(09)03001-2.

94) Harris G, Pinder SE, O'Malley FP. Invasive carcinoma: special types. In O'Malley FP and Pinder SE, editors. *Breast Pathology*. Philadelphia: Elsevier, 2006: 201-223.

95) Haupt B, Ro JY, Schwartz MR. Basal-like breast carcinoma: a phenotypically distinct entity. *Arch Pathol Lab Med.* 2010 Jan;134(1):130-3. doi: 10.1043/1543-2165-134.1.130.

96) Hayes DF, Ethier S, Lippman ME. New guidelines for reporting of tumor marker studies in breast cancer research and treatment: REMARK. *Breast Cancer Res Treat.* 2006 Nov;100(2):237-8. Epub 2006 Jun 14.

97) Hiscox S and Jiang WG. Association of the HGF/SF receptor, c-met, with the cell-surface adhesion molecule, E-cadherin, and catenins in human tumor cells. *Biochem Biophys Res Commun.* 1999 Aug 2;261(2):406-11.

98) Hochgräfe F, Zhang L, O'Toole SA, Browne BC, Pinese M, Porta Cubas A, Lehrbach GM, Croucher DR, Rickwood D, Boulghourjian A, Shearer R, Nair R, Swarbrick A, Faratian D, Mullen P, Harrison DJ, Biankin AV, Sutherland RL, Raftery MJ, Daly RJ. Tyrosine phosphorylation profiling reveals the signaling network characteristics of Basal breast cancer cells. *Cancer Res.* 2010 Nov 15;70(22):9391-401. doi: 10.1158/0008-5472.CAN-10-0911. Epub 2010 Sep 21.

99) Hoeflich KP, O'Brien C, Boyd Z, Cavet G, Guerrero S, Jung K, Januario T, Savage H, Punnoose E, Truong T, Zhou W, Berry L, Murray L, Amler L, Belvin M, Friedman LS, Lackner MR. In vivo antitumor activity of MEK and phosphatidylinositol 3-kinase inhibitors in basal-like breast cancer models. *Clin Cancer Res.* 2009 Jul 15;15(14):4649-64. doi: 10.1158/1078-0432.CCR-09-0317. Epub 2009 Jun 30.

100) Holstege H, Horlings HM, Velds A, Langerød A, Børresen-Dale AL, van de Vijver MJ, Nederlof PM, Jonkers J. BRCA1-mutated and basal-like breast cancers have similar aCGH profiles and a high incidence of protein truncating TP53 mutations. *BMC Cancer*. 2010 Nov 30;10:654. doi: 10.1186/1471-2407-10-654.

101) Honeth G, Bendahl PO, Ringnér M, Saal LH, Gruvberger-Saal SK, Lövgren K, Grabau D, Fernö M, Borg A, Hegardt C. The CD44+/CD24- phenotype is enriched in basal-like breast tumors. *Breast Cancer Res*. 2008;10(3):R53. doi: 10.1186/bcr2108. Epub 2008 Jun 17.

102) Ho-Yen C, Bowen RL, Jones JL. Characterization of basal-like breast cancer: an update. *Diagnostic Histopathology*. March 2012.18(3):104-111.

103) Ho-Yen C, Bowen RL, Kermorgant S, Jones JL. Comment on 'High MET expression is an adverse prognostic factor in patients with triple-negative breast cancer'. *Br J Cancer*. 2013 May 28;108(10):2195-6. doi: 10.1038/bjc.2013.249. Epub 2013 May 14.

104) Ho-Yen CM, Green AR, Rakha EA, Brentnall AR, Ellis IO, Kermorgant S, Jones JL. C-Met in invasive breast cancer: is there a relationship with the basal-like subtype? *Cancer*. 2014 Jan 15;120(2):163-71. doi: 10.1002/cncr.28386. Epub 2013 Oct 21.

105) Hu Z, Fan C, Livasy C, He X, Oh DS, Ewend MG, Carey LA, Subramanian S, West R, Ikpatt F, Olopade OI, van de Rijn M, Perou CM. A compact VEGF signature associated with distant metastases and poor outcomes. *BMC Med*. 2009 Mar 16;7:9. doi: 10.1186/1741-7015-7-9.

106) Hu Z, Fan C, Oh DS, Marron JS, He X, Qaqish BF, Livasy C, Carey LA, Reynolds E, Dressler L, Nobel A, Parker J, Ewend MG, Sawyer LR, Wu J, Liu Y, Nanda R, Tretiakova M, Ruiz Orrico A, Dreher D, Palazzo JP, Perreard L, Nelson E, Mone M, Hansen H, Mullins M, Quackenbush JF, Ellis MJ, Olopade OI, Bernard PS, Perou CM. The molecular portraits of breast tumors are conserved across microarray platforms. *BMC Genomics.* 2006 Apr 27;7:96.

107) Hung CM, Kuo DH, Chou CH, Su YC, Ho CT, Way TD. Osthole suppresses hepatocyte growth factor (HGF)-induced epithelial-mesenchymal transition via repression of the c-Met/Akt/mTOR pathway in human breast cancer cells. *J Agric Food Chem.* 2011 Sep 14;59(17):9683-90. doi: 10.1021/jf2021489. Epub 2011 Aug 8.

108) Hunter T. Tyrosine phosphorylation: thirty years and counting. *Curr Opin Cell Biol.* 2009 Apr;21(2):140-6. doi: 10.1016/j.ceb.2009.01.028. Epub 2009 Mar 9.

109) Huo D, Ikpatt F, Khramtsov A, Dangou JM, Nanda R, Dignam J, Zhang B, Grushko T, Zhang C, Oluwasola O, Malaka D, Malami S, Odetunde A, Adeoye AO, Iyare F, Falusi A, Perou CM, Olopade OI. Population differences in breast cancer: survey in indigenous African women reveals over-representation of triple-negative breast cancer. *J Clin Oncol.* 2009 Sep 20;27(27):4515-21. doi: 10.1200/JCO.2008.19.6873. Epub 2009 Aug 24.

110) Ihemelandu CU, Leffall LD Jr, Dewitty RL, Naab TJ, Mezghebe HM, Makambi KH, Adams-Campbell L, Frederick WA. Molecular breast cancer subtypes in premenopausal African-American women, tumor biologic factors and clinical outcome. *Ann Surg Oncol.* 2007 Oct;14(10):2994-3003. Epub 2007 Jul 24.

111) Inoue K, Kurabayashi A, Shuin T, Ohtsuki Y, Furihata M. Overexpression of p53 protein in human tumors. *Med Mol Morphol.* 2012 Jun;45(3):115-23. Epub 2012 Sep 22.

112) Jarvius M, Paulsson J, Weibrecht I, Leuchowius KJ, Andersson AC, Wählby C, Gullberg M, Botling J, Sjöblom T, Markova B, Ostman A, Landegren U, Söderberg O. In situ detection of phosphorylated platelet-derived growth factor receptor beta using a generalized proximity ligation method. *Mol Cell Proteomics.* 2007 Sep;6(9):1500-9. Epub 2007 Jun 12.

113) Jin L, Fuchs A, Schnitt SJ, Yao Y, Joseph A, Lamszus K, Park M, Goldberg ID, Rosen EM. Expression of scatter factor and c-met receptor in benign and malignant breast tissue. *Cancer.* 1997 Feb 15;79(4):749-60.

114) Joffre C, Barrow R, Ménard L, Calleja V, Hart IR, Kermorgant S. A direct role for Met endocytosis in tumorigenesis. *Nat Cell Biol.* 2011 Jun 5;13(7):827-37. doi: 10.1038/ncb2257.

115) Jones JL. Overdiagnosis and overtreatment of breast cancer: progression of ductal carcinoma in situ: the pathological perspective. *Breast Cancer Res.* 2006;8(2):204. Epub 2006 Apr 21.

116) Jones RJ, Boyce T, Fennell M, Jacobs V, Pinto F, Duffield E, Clack G, Green T, Kelly J, Robertson J. The impact of delay in cryo-fixation on biomarkers of Src tyrosine kinase activity in human breast and bladder cancers. *Cancer Chemother Pharmacol.* 2008 Jan;61(1):23-32. Epub 2007 Mar 20.

117) Kamei T, Matozaki T, Sakisaka T, Kodama A, Yokoyama S, Peng YF, Nakano K, Takaishi K, Takai Y. Coendocytosis of cadherin and c-Met coupled to disruption of cell-cell adhesion in MDCK cells--regulation by Rho, Rac and Rab small G proteins. *Oncogene.* 1999 Nov 18;18(48):6776-84.

118) Kang JY, Dolled-Filhart M, Ocal IT, Singh B, Lin CY, Dickson RB, Rimm DL, Camp RL. Tissue microarray analysis of hepatocyte growth factor/Met pathway components reveals a role for Met, matriptase, and hepatocyte growth factor activator inhibitor 1 in the progression of node-negative breast cancer. *Cancer Res.* 2003 Mar 1;63(5):1101-5.

119) Kao J, Salari K, Bocanegra M, Choi YL, Girard L, Gandhi J, Kwei KA, Hernandez-Boussard T, Wang P, Gazdar AF, Minna JD, Pollack JR. Molecular profiling of breast cancer cell lines defines relevant tumor models and provides a resource for cancer gene discovery. *PLoS One.* 2009 Jul 3;4(7):e6146. doi: 10.1371/journal.pone.0006146.

120) Kermorgant S, Parker PJ. Receptor trafficking controls weak signal delivery: a strategy used by c-Met for STAT3 nuclear accumulation. *J Cell Biol.* 2008 Sep 8;182(5):855-63. doi: 10.1083/jcb.200806076.

121) Kermorgant S, Zicha D, Parker PJ. PKC controls HGF-dependent c-Met traffic, signalling and cell migration. *EMBO J.* 2004 Oct 1;23(19):3721-34. Epub 2004 Sep 23.

122) Kermorgant S, Zicha D, Parker PJ. Protein kinase C controls microtubule-based traffic but not proteasomal degradation of c-Met. *J Biol Chem.* 2003 Aug 1;278(31):28921-9. Epub 2003 Apr 24.

123) Kim CH, Kim J, Kahng H, Choi EC. Change of E-cadherin by hepatocyte growth factor and effects on the prognosis of hypopharyngeal carcinoma. *Ann Surg Oncol.* 2007 May;14(5):1565-74. Epub 2007 Feb 10.

124) Knight JF, Lesurf R, Zhao H, Pinnaduwage D, Davis RR, Saleh SM, Zuo D, Naujokas MA, Chughtai N, Herschkowitz JI, Prat A, Mulligan AM, Muller WJ, Cardiff RD, Gregg JP, Andrulis IL, Hallett MT, Park M. Met synergizes with p53 loss to induce mammary tumors that possess features of claudin-low breast cancer. *Proc Natl Acad Sci U S A.* 2013 Apr 2;110(14):E1301-10. doi: 10.1073/pnas.1210353110. Epub 2013 Mar 18.

125) Koos B, Paulsson J, Jarvius M, Sanchez BC, Wrede B, Mertsch S, Jeibmann A, Kruse A, Peters O, Wolff JE, Galla HJ, Söderberg O, Paulus W, Ostman A, Hasselblatt M. Platelet-derived growth factor receptor expression and activation in choroid plexus tumors. *Am J Pathol.* 2009 Oct;175(4):1631-7. doi: 10.2353/ajpath.2009.081022. Epub 2009 Aug 28.

126) Kordon EC, Smith GH. An entire functional mammary gland may comprise the progeny from a single cell. *Development.* 1998 May;125(10):1921-30.

127) Kuroda H, Ishida F, Nakai M, Ohnisi K, Itoyama S. Basal cytokeratin expression in relation to biological factors in breast cancer. *Hum Pathol.* 2008 Dec;39(12):1744-50. doi: 10.1016/j.humpath.2008.06.007. Epub 2008 Aug 28.

128) Lahat G, Zhang P, Zhu QS, Torres K, Ghadimi M, Smith KD, Wang WL, Lazar AJ, Lev D. The expression of c-Met pathway components in unclassified pleomorphic sarcoma/malignant fibrous histiocytoma (UPS/MFH): a tissue microarray study. *Histopathology.* 2011 Sep;59(3):556-61. doi: 10.1111/j.1365-2559.2011.03946.x.

129) Lai AZ, Abella JV, Park M. Crosstalk in Met receptor oncogenesis. *Trends Cell Biol.* 2009 Oct;19(10):542-51. doi: 10.1016/j.tcb.2009.07.002. Epub 2009 Sep 14.

130) Lehmann BD, Bauer JA, Chen X, Sanders ME, Chakravarthy AB, Shyr Y, Pietenpol JA. Identification of human triple-negative breast cancer subtypes and preclinical models for selection of targeted therapies. *J Clin Invest.* 2011 Jul;121(7):2750-67. doi: 10.1172/JCI45014.

131) Lengyel E, Prechtel D, Resau JH, Gauger K, Welk A, Lindemann K, Salanti G, Richter T, Knudsen B, Vande Woude GF, Harbeck N. C-Met overexpression in node-positive breast cancer identifies patients with poor clinical outcome independent of Her2/neu. *Int J Cancer.* 2005 Feb 10;113(4):678-82.

132) Lester SC. The Breast. In Kumar V, Abbas AK, Fausto N editors. *Robbins and Cotran Pathologic Basis of Disease*. Philadelphia: Elsevier, 2005: 1119-54.

133) Leuchowius KJ, Weibrecht I, Söderberg O. In situ proximity ligation assay for microscopy and flow cytometry. *Curr Protoc Cytom.* 2011 Apr;Chapter 9:Unit 9.36. doi: 10.1002/0471142956.cy0936s56.

134) Li Y, Chen CQ, He YL, Cai SR, Yang DJ, He WL, Xu JB, Zan WH. Abnormal expression of E-cadherin in tumor cells is associated with poor prognosis of gastric carcinoma. *J Surg Oncol.* 2012 Sep 1;106(3):304-10. doi: 10.1002/jso.23008. Epub 2012 Jan 9.

135) Lindemann K, Resau J, Nährig J, Kort E, Leeser B, Annecke K, Welk A, Schäfer J, Vande Woude GF, Lengyel E, Harbeck N. Differential expression of c-Met, its ligand HGF/SF and HER2/neu in DCIS and adjacent normal breast tissue. *Histopathology.* 2007 Jul;51(1):54-62.

136) Linderholm BK, Lindahl T, Holmberg L, Klaar S, Lennerstrand J, Henriksson R, Bergh J. The expression of vascular endothelial growth factor correlates with mutant p53 and poor prognosis in human breast cancer. *Cancer Res.* 2001 Mar 1;61(5):2256-60.

137) Lipworth L, Bailey LR, Trichopoulos D. History of breast-feeding in relation to breast cancer risk: a review of the epidemiologic literature. *J Natl Cancer Inst.* 2000 Feb 16;92(4):302-12.

138) Livasy CA, Karaca G, Nanda R, Tretiakova MS, Olopade OI, Moore DT, Perou CM. Phenotypic evaluation of the basal-like subtype of invasive breast carcinoma. *Mod Pathol.* 2006 Feb;19(2):264-71.

139) Logullo AF, Nonogaki S, Pasini FS, Osório CA, Soares FA, Brentani MM. Concomitant expression of epithelial-mesenchymal transition biomarkers in breast ductal carcinoma: association with progression. *Oncol Rep.* 2010 Feb;23(2):313-20.

140) López-Knowles E, O'Toole SA, McNeil CM, Millar EK, Qiu MR, Crea P, Daly RJ, Musgrove EA, Sutherland RL. PI3K pathway activation in breast cancer is associated with the basal-like phenotype and cancer-specific mortality. *Int J Cancer.* 2010 Mar 1;126(5):1121-31. doi: 10.1002/ijc.24831.

141) Ma PC, Jagadeeswaran R, Jagadeesh S, Tretiakova MS, Nallasura V, Fox EA, Hansen M, Schaefer E, Naoki K, Lader A, Richards W, Sugarbaker D, Husain AN, Christensen JG, Salgia R. Functional expression and mutations of c-Met and its therapeutic inhibition with SU11274 and small interfering RNA in non-small cell lung cancer. *Cancer Res.* 2005 Feb 15;65(4):1479-88.

142) Macpherson IR, Hooper S, Serrels A, McGarry L, Ozanne BW, Harrington K, Frame MC, Sahai E, Brunton VG. p120-catenin is required for the collective invasion of squamous cell carcinoma cells via a phosphorylation-independent mechanism. *Oncogene.* 2007 Aug 9;26(36):5214-28. Epub 2007 Mar 5.

143) Mahler-Araujo B, Savage K, Parry S, Reis-Filho JS. Reduction of E-cadherin expression is associated with non-lobular breast carcinomas of basal-like and triple negative phenotype. *J Clin Pathol.* 2008 May;61(5):615-20. Epub 2007 Dec 21.

144) Mangia A, Malfettone A, Simone G, Darvishian F. Old and new concepts in histopathological characterization of familial breast cancer. *Ann Oncol.* 2011 Jan;22 Suppl 1:i24-30. doi: 10.1093/annonc/mdq662.

145) Manié E, Vincent-Salomon A, Lehmann-Che J, Pierron G, Turpin E, Warcoin M, Gruel N, Lebigot I, Sastre-Garau X, Lidereau R, Remenieras A, Feunteun J, Delattre O, de Thé H, Stoppa-Lyonnet D, Stern MH. High frequency of TP53 mutation in BRCA1 and sporadic basal-like carcinomas but not in BRCA1 luminal breast tumors. *Cancer Res.* 2009 Jan 15;69(2):663-71. doi: 10.1158/0008-5472.CAN-08-1560.

146) Marchbanks PA, McDonald JA, Wilson HG, Folger SG, Mandel MG, Daling JR, Bernstein L, Malone KE, Ursin G, Strom BL, Norman SA, Wingo PA, Burkman RT, Berlin JA, Simon MS, Spirtas R, Weiss LK. Oral contraceptives and the risk of breast cancer. *N Engl J Med.* 2002 Jun 27;346(26):2025-32.

147) Marginean F, Rakha EA, Ho BC, Ellis IO, Lee AH. Histological features of medullary carcinoma and prognosis in triple-negative basal-like carcinomas of the breast. *Mod Pathol.* 2010 Oct;23(10):1357-63. doi: 10.1038/modpathol.2010.123. Epub 2010 Jun 25.

148) Massarelli E, Varella-Garcia M, Tang X, Xavier AC, Ozburn NC, Liu DD, Bekele BN, Herbst RS, Wistuba II. KRAS mutation is an important predictor of resistance to therapy with epidermal growth factor receptor tyrosine kinase inhibitors in non-small-cell lung cancer. *Clin Cancer Res.* 2007 May 15;13(10):2890-6.

149) Matros E, Wang ZC, Lodeiro G, Miron A, Iglehart JD, Richardson AL. BRCA1 promoter methylation in sporadic breast tumors: relationship to gene expression profiles. *Breast Cancer Res Treat.* 2005 May;91(2):179-86.

150) Matteucci E, Ridolfi E, Desiderio MA. Hepatocyte growth factor differently influences Met-E-cadherin phosphorylation and downstream signaling pathway in two models of breast cells. *Cell Mol Life Sci.* 2006 Sep;63(17):2016-26.

151) McShane LM, Altman DG, Sauerbrei W, Taube SE, Gion M, Clark GM; Statistics Subcommittee of the NCI-EORTC Working Group on Cancer Diagnostics. REporting recommendations for tumour MARKer prognostic studies (REMARK). *Br J Cancer.* 2005 Aug 22;93(4):387-91.

152) Millikan RC, Newman B, Tse CK, Moorman PG, Conway K, Dressler LG, Smith LV, Labbok MH, Geradts J, Bensen JT, Jackson S, Nyante S, Livasy C, Carey L, Earp HS, Perou CM. Epidemiology of basal-like breast cancer. *Breast Cancer Res Treat.* 2008 May;109(1):123-39. Epub 2007 Jun 20.

153) Minuti G, Cappuzzo F, Duchnowska R, Jassem J, Fabi A, O'Brien T, Mendoza AD, Landi L, Biernat W, Czartoryska-Arłukowicz B, Jankowski T, Zuziak D, Zok J, Szostakiewicz B, Foszczyńska-Kłoda M, Tempińska-Szałach A, Rossi E, Varella-Garcia M. Increased MET and HGF gene copy numbers are associated with trastuzumab failure in HER2-positive metastatic breast cancer. *Br J Cancer.* 2012 Aug 21;107(5):793-9. doi: 10.1038/bjc.2012.335. Epub 2012 Jul 31.

154) Miyata Y, Sagara Y, Kanda S, Hayashi T, Kanetake H. Phosphorylated hepatocyte growth factor receptor/c-Met is associated with tumor growth and prognosis in patients with bladder cancer: correlation with matrix metalloproteinase-2 and -7 and E-cadherin. *Hum Pathol.* 2009 Apr;40(4):496-504. doi: 10.1016/j.humpath.2008.09.011. Epub 2009 Jan 3.

155) Mohammed ZM, McMillan DC, Edwards J, Mallon E, Doughty JC, Orange C, Going JJ. The relationship between lymphovascular invasion and angiogenesis, hormone receptors, cell proliferation and survival in patients with primary operable invasive ductal breast cancer. *BMC Clin Pathol.* 2013 Nov 25;13(1):31. doi: 10.1186/1472-6890-13-31.

156) Montero C. The antigen-antibody reaction in immunohistochemistry. *J Histochem Cytochem.* 2003 Jan;51(1):1-4.

157) Mueller KL, Hunter LA, Ethier SP, Boerner JL. Met and c-Src cooperate to compensate for loss of epidermal growth factor receptor kinase activity in breast cancer cells. *Cancer Res.* 2008 May 1;68(9):3314-22. doi: 10.1158/0008-5472.CAN-08-0132.

158) Nagle RB, Böcker W, Davis JR, Heid HW, Kaufmann M, Lucas DO, Jarasch ED. Characterization of breast carcinomas by two monoclonal antibodies distinguishing myoepithelial from luminal epithelial cells. *J Histochem Cytochem.* 1986 Jul;34(7):869-81.

159) Nakamura T, Nawa K, Ichihara A. Partial purification and characterization of hepatocyte growth factor from serum of hepatectomized rats. *Biochem Biophys Res Commun.* 1984 Aug 16;122(3):1450-9.

160) Nakamura T, Sakai K, Nakamura T, Matsumoto K. Hepatocyte growth factor twenty years on: Much more than a growth factor. *J Gastroenterol Hepatol.* 2011 Jan;26 Suppl 1:188-202. doi: 10.1111/j.1440-1746.2010.06549.x.

161) Nakamura Y, Niki T, Goto A, Morikawa T, Miyazawa K, Nakajima J, Fukayama M. c-Met activation in lung adenocarcinoma tissues: an immunohistochemical analysis. *Cancer Sci.* 2007 Jul;98(7):1006-13. Epub 2007 Apr 24.

162) Nakopoulou L, Gakiopoulou H, Keramopoulos A, Giannopoulou I, Athanassiadou P, Mavrommatis J, Davaris PS. c-met tyrosine kinase receptor expression is associated with abnormal beta-catenin expression and favourable prognostic factors in invasive breast carcinoma. *Histopathology.* 2000 Apr;36(4):313-25.

163) Nath D, Williamson NJ, Jarvis R, Murphy G. Shedding of c-Met is regulated by crosstalk between a G-protein coupled receptor and the EGF receptor and is mediated by a TIMP-3 sensitive metalloproteinase. *J Cell Sci.* 2001 Mar;114(Pt 6):1213-20.

164) National Institute for Health and Care Excellence (NICE). Trastuzumab for the adjuvant treatment of early-stage HER2-positive breast cancer. *NICE technology appraisal guidance 107*. London: National Institute for Health and Care Excellence. 2006.

165) National Institute for Health and Care Excellence (NICE). Early and locally advanced breast cancer. *NICE Clinical Guideline 80*. London: National Institute for Health and Care Excellence. 2009.

166) Neve RM, Chin K, Fridlyand J, Yeh J, Baehner FL, Fevr T, Clark L, Bayani N, Coppe JP, Tong F, Speed T, Spellman PT, DeVries S, Lapuk A, Wang NJ, Kuo WL, Stilwell JL, Pinkel D, Albertson DG, Waldman FM, McCormick F, Dickson RB, Johnson MD, Lippman M, Ethier S, Gazdar A, Gray JW. A collection of breast cancer cell lines for the study of functionally distinct cancer subtypes. *Cancer Cell.* 2006 Dec;10(6):515-27.

167) Nielsen TO, Hsu FD, Jensen K, Cheang M, Karaca G, Hu Z, Hernandez-Boussard T, Livasy C, Cowan D, Dressler L, Akslen LA, Ragaz J, Gown AM, Gilks CB, van de Rijn M, Perou CM. Immunohistochemical and clinical characterization of the basal-like subtype of invasive breast carcinoma. *Clin Cancer Res.* 2004 Aug 15;10(16):5367-74.

168) Novocastra Laboratories. Datasheet: C-Met (Hepatocyte Growth Factor Receptor). http://www.nonocastra.co.uk. May 2010.

169) Orian-Rousseau V, Morrison H, Matzke A, Kastilan T, Pace G, Herrlich P, Ponta H. Hepatocyte growth factor-induced Ras activation requires ERM proteins linked to both CD44v6 and F-actin. *Mol Biol Cell.* 2007 Jan;18(1):76-83. Epub 2006 Oct 25.

170) Ou SH, Kwak EL, Siwak-Tapp C, Dy J, Bergethon K, Clark JW, Camidge DR, Solomon BJ, Maki RG, Bang YJ, Kim DW, Christensen J, Tan W, Wilner KD, Salgia R, Iafrate AJ. Activity of crizotinib (PF02341066), a dual mesenchymal-epithelial transition (MET) and anaplastic lymphoma kinase (ALK) inhibitor, in a non-small cell lung cancer patient with de novo MET amplification. *J Thorac Oncol.* 2011 May;6(5):942-6. doi: 10.1097/JTO.0b013e31821528d3.

171) Paulsson J, Lindh MB, Jarvius M, Puputti M, Nistér M, Nupponen NN, Paulus W, Söderberg O, Dresemann G, von Deimling A, Joensuu H, Ostman A, Hasselblatt M. Prognostic but not predictive role of platelet-derived growth factor receptors in patients with recurrent glioblastoma. *Int J Cancer.* 2011 Apr 15;128(8):1981-8. doi: 10.1002/ijc.25528.

172) Payne SJ, Bowen RL, Jones JL, Wells CA. Predictive markers in breast cancer--the present. *Histopathology.* 2008 Jan;52(1):82-90. doi: 10.1111/j.1365-2559.2007.02897.x.

173) Pereira H, Pinder SE, Sibbering DM, Galea MH, Elston CW, Blamey RW, Robertson JF, Ellis IO. Pathological prognostic factors in breast cancer. IV: Should you be a typer or a grader? A comparative study of two histological prognostic features in operable breast carcinoma. *Histopathology.* 1995 Sep;27(3):219-26.

174) Perou CM, Sørlie T, Eisen MB, van de Rijn M, Jeffrey SS, Rees CA, Pollack JR, Ross DT, Johnsen H, Akslen LA, Fluge O, Pergamenschikov A, Williams C, Zhu SX, Lønning PE, Børresen-Dale AL, Brown PO, Botstein D. Molecular portraits of human breast tumours. *Nature.* 2000 Aug 17;406(6797):747-52.

175) Perou CM. Molecular stratification of triple-negative breast cancers. *Oncologist.* 2011;16 Suppl 1:61-70. doi: 10.1634/theoncologist.2011-S1-61.

176) Peschard P, Fournier TM, Lamorte L, Naujokas MA, Band H, Langdon WY, Park M. Mutation of the c-Cbl TKB domain binding site on the Met receptor tyrosine kinase converts it into a transforming protein. *Mol Cell.* 2001 Nov;8(5):995-1004.

177) Peschard P and Park M. From Tpr-Met to Met, tumorigenesis and tubes. *Oncogene.* 2007 Feb 26;26(9):1276-85.

178) Pinder SE, Brown JP, Gillett C, Purdie CA, Speirs V, Thompson AM, Shaaban AM; Translational Subgroup of the NCRI Breast Clinical Studies Group. The manufacture and assessment of tissue microarrays: suggestions and criteria for analysis, with breast cancer as an example. *J Clin Pathol.* 2013 Mar;66(3):169-77. doi: 10.1136/jclinpath-2012-201091. Epub 2012 Oct 19.

179) Pinder SE, Ellis IO, Galea M, O'Rouke S, Blamey RW, Elston CW. Pathological prognostic factors in breast cancer. III. Vascular invasion: relationship with recurrence and survival in a large study with long-term follow-up. *Histopathology.* 1994 Jan;24(1):41-7.

180) Ponzo MG, Lesurf R, Petkiewicz S, O'Malley FP, Pinnaduwage D, Andrulis IL, Bull SB, Chughtai N, Zuo D, Souleimanova M, Germain D, Omeroglu A, Cardiff RD, Hallett M, Park M. Met induces mammary tumors with diverse histologies and is associated with poor outcome and human basal breast cancer. *Proc Natl Acad Sci U S A.* 2009 Aug 4;106(31):12903-8. doi: 10.1073/pnas.0810402106. Epub 2009 Jul 17.

181) Powles T, Blank C, Chowdhury S, Horenblas S, Peters J, Shamash J, Sarwar N, Boleti E, Sahdev A, O'Brien T, Berney D, Beltran L, Nathan P, Haanen J, Bex A. The outcome of patients treated with sunitinib prior to planned nephrectomy in metastatic clear cell renal cancer. *Eur Urol.* 2011 Sep;60(3):448-54. doi: 10.1016/j.eururo.2011.05.028. Epub 2011 May 17.

182) Pozner-Moulis S, Cregger M, Camp RL, Rimm DL. Antibody validation by quantitative analysis of protein expression using expression of Met in breast cancer as a model. *Lab Invest.* 2007 Mar;87(3):251-60. Epub 2007 Jan 29.

183) Prat A, Parker JS, Karginova O, Fan C, Livasy C, Herschkowitz JI, He X, Perou CM. Phenotypic and molecular characterization of the claudin-low intrinsic subtype of breast cancer. *Breast Cancer Res.* 2010;12(5):R68. doi: 10.1186/bcr2635. Epub 2010 Sep 2.

184) Raghav KP, Wang W, Liu S, Chavez-MacGregor M, Meng X, Hortobagyi GN, Mills GB, Meric-Bernstam F, Blumenschein GR Jr, Gonzalez-Angulo AM. cMET and phospho-cMET protein levels in breast cancers and survival outcomes. *Clin Cancer Res.* 2012 Apr 15;18(8):2269-77. doi: 10.1158/1078-0432.CCR-11-2830. Epub 2012 Feb 28.

185) Rakha EA, Abd El Rehim D, Pinder SE, Lewis SA, Ellis IO. E-cadherin expression in invasive non-lobular carcinoma of the breast and its prognostic significance. *Histopathology.* 2005 Jun;46(6):685-93.

186) Rakha EA, El-Sayed ME, Green AR, Paish EC, Lee AH, Ellis IO. Breast carcinoma with basal differentiation: a proposal for pathology definition based on basal cytokeratin expression. *Histopathology.* 2007 Mar;50(4):434-8.

187) Rakha EA, Elsheikh SE, Aleskandarany MA, Habashi HO, Green AR, Powe DG, El-Sayed ME, Benhasouna A, Brunet JS, Akslen LA, Evans AJ, Blamey R, Reis-Filho JS, Foulkes WD, Ellis IO. Triple-negative breast cancer: distinguishing between basal and nonbasal subtypes. *Clin Cancer Res.* 2009 Apr 1;15(7):2302-10. doi: 10.1158/1078-0432.CCR-08-2132. Epub 2009 Mar 24.

188) Rakha EA, Putti TC, Abd El-Rehim DM, Paish C, Green AR, Powe DG, Lee AH, Robertson JF, Ellis IO. Morphological and immunophenotypic analysis of breast carcinomas with basal and myoepithelial differentiation. *J Pathol.* 2006 Mar;208(4):495-506.

189) Ray PS, Wang J, Qu Y, Sim MS, Shamonki J, Bagaria SP, Ye X, Liu B, Elashoff D, Hoon DS, Walter MA, Martens JW, Richardson AL, Giuliano AE, Cui X. FOXC1 is a potential prognostic biomarker with functional significance in basal-like breast cancer. *Cancer Res.* 2010 May 15;70(10):3870-6. doi: 10.1158/0008-5472.CAN-09-4120. Epub 2010 Apr 20.

190) Rehman FL, Lord CJ, Ashworth A. Synthetic lethal approaches to breast cancer therapy. *Nat Rev Clin Oncol.* 2010 Dec;7(12):718-24. doi: 10.1038/nrclinonc.2010.172. Epub 2010 Oct 19.

191) Reis-Filho JS, Milanezi F, Steele D, Savage K, Simpson PT, Nesland JM, Pereira EM, Lakhani SR, Schmitt FC. Metaplastic breast carcinomas are basal-like tumours. *Histopathology.* 2006 Jul;49(1):10-21.

192) Reshetnikova G, Troyanovsky S, Rimm DL. Definition of a direct extracellular interaction between Met and E-cadherin. *Cell Biol Int.* 2007 Apr;31(4):366-73. Epub 2007 Jan 21.

193) Reshetnikova G. Met receptor subcellular localization depends on E-cadherin function. *ScientificWorldJournal.* 2007 Dec 18;7:2009-11. doi: 10.1100/tsw.2007.312.

194) Richardson AL, Wang ZC, De Nicolo A, Lu X, Brown M, Miron A, Liao X, Iglehart JD, Livingston DM, Ganesan S. X chromosomal abnormalities in basal-like human breast cancer. *Cancer Cell.* 2006 Feb;9(2):121-32.

195) Rodriguez FJ, Lewis-Tuffin LJ, Anastasiadis PZ. E-cadherin's dark side: possible role in tumor progression. *Biochim Biophys Acta.* 2012 Aug;1826(1):23-31. doi: 10.1016/j.bbcan.2012.03.002. Epub 2012 Mar 13.

196) Rosai J. *Rosai and Ackerman's Surgical Pathology*. Philadelphia: Elsevier, 2004: 1763-1876.

197) Rosen EM, Nigam SK, Goldberg ID. Scatter factor and the c-met receptor: a paradigm for mesenchymal/epithelial interaction. *J Cell Biol.* 1994 Dec;127(6 Pt 2):1783-7.

198) Rouzier R, Perou CM, Symmans WF, Ibrahim N, Cristofanilli M, Anderson K, Hess KR, Stec J, Ayers M, Wagner P, Morandi P, Fan C, Rabiul I, Ross JS, Hortobagyi GN, Pusztai L. Breast cancer molecular subtypes respond differently to preoperative chemotherapy. *Clin Cancer Res.* 2005 Aug 15;11(16):5678-85.

199) Sanders ME, Schuyler PA, Dupont WD, Page DL. The natural history of low-grade ductal carcinoma in situ of the breast in women treated by biopsy only revealed over 30 years of long-term follow-up. *Cancer*. 2005 Jun 15;103(12):2481-4.

200) Sarrió D, Rodriguez-Pinilla SM, Hardisson D, Cano A, Moreno-Bueno G, Palacios J. Epithelial-mesenchymal transition in breast cancer relates to the basal-like phenotype. *Cancer Res.* 2008 Feb 15;68(4):989-97. doi: 10.1158/0008-5472.CAN-07-2017.

201) Sattler M, Pride YB, Ma P, Gramlich JL, Chu SC, Quinnan LA, Shirazian S, Liang C, Podar K, Christensen JG, Salgia R. A novel small molecule met inhibitor induces apoptosis in cells transformed by the oncogenic TPR-MET tyrosine kinase. *Cancer Res.* 2003 Sep 1;63(17):5462-9.

202) Savage KI, Matchett KB, Barros EM, Cooper KM, Irwin G, Gorski JJ, Orr KS, Vohhodina J, Kavanagh JN, Madden AF, Powell A, Manti L, McDade SS, Park BH, Prise KM, McIntosh S, Salto-Tellez M, Richard DJ, Elliot CT, Harkin DP. BRCA1 deficiency exacerbates estrogen induced DNA damage and genomic instability. *Cancer Res.* 2014 Mar 17. [Epub ahead of print].

203) Schmidt C, Bladt F, Goedecke S, Brinkmann V, Zschiesche W, Sharpe M, Gherardi E, Birchmeier C. Scatter factor/hepatocyte growth factor is essential for liver development. *Nature.* 1995 Feb 23;373(6516):699-702.

204) Schmidt L, Duh FM, Chen F, Kishida T, Glenn G, Choyke P, Scherer SW, Zhuang Z, Lubensky I, Dean M, Allikmets R, Chidambaram A, Bergerheim UR, Feltis JT, Casadevall C, Zamarron A, Bernues M, Richard S, Lips CJ, Walther MM, Tsui LC, Geil L, Orcutt ML, Stackhouse T, Lipan J, Slife L, Brauch H, Decker J, Niehans G, Hughson MD, Moch H, Storkel S, Lerman MI, Linehan WM, Zbar B. Germline and somatic mutations in the tyrosine kinase domain of the MET proto-oncogene in papillary renal carcinomas. *Nat Genet.* 1997 May;16(1):68-73.

205) Sennino B, Ishiguro-Oonuma T, Schriver BJ, Christensen JG, McDonald DM. Inhibition of c-Met reduces lymphatic metastasis in RIP-Tag2 transgenic mice. *Cancer Res.* 2013 Jun 15;73(12):3692-703. doi: 10.1158/0008-5472.CAN-12-2160. Epub 2013 Apr 10.

206) Sennino B, Ishiguro-Oonuma T, Wei Y, Naylor RM, Williamson CW, Bhagwandin V, Tabruyn SP, You WK, Chapman HA, Christensen JG, Aftab DT, McDonald DM. Suppression of tumor invasion and metastasis by concurrent inhibition of c-Met and VEGF signaling in pancreatic neuroendocrine tumors. *Cancer Discov.* 2012 Mar;2(3):270-87. doi: 10.1158/2159-8290.CD-11-0240. Epub 2012 Feb 24.

207) Sequist LV, von Pawel J, Garmey EG, Akerley WL, Brugger W, Ferrari D, Chen Y, Costa DB, Gerber DE, Orlov S, Ramlau R, Arthur S, Gorbachevsky I, Schwartz B, Schiller JH. Randomized phase II study of erlotinib plus tivantinib versus erlotinib plus placebo in previously treated non-small-cell lung cancer. *J Clin Oncol.* 2011 Aug 20;29(24):3307-15. doi: 10.1200/JCO.2010.34.0570. Epub 2011 Jul 18.

208) Shah SP, Roth A, Goya R, Oloumi A, Ha G, Zhao Y, Turashvili G, Ding J, Tse K, Haffari G, Bashashati A, Prentice LM, Khattra J, Burleigh A, Yap D, Bernard V, McPherson A, Shumansky K, Crisan A, Giuliany R, Heravi-Moussavi A, Rosner J, Lai D, Birol I, Varhol R, Tam A, Dhalla N, Zeng T, Ma K, Chan SK, Griffith M, Moradian A, Cheng SW, Morin GB, Watson P, Gelmon K, Chia S, Chin SF, Curtis C, Rueda OM, Pharoah PD, Damaraju S, Mackey J, Hoon K, Harkins T, Tadigotla V, Sigaroudinia M, Gascard P, Tlsty T, Costello JF, Meyer IM, Eaves CJ, Wasserman WW, Jones S, Huntsman D, Hirst M, Caldas C, Marra MA, Aparicio S. The clonal and mutational evolution spectrum of primary triple-negative breast cancers. *Nature.* 2012 Apr 4;486(7403):395-9. doi: 10.1038/nature10933.

209) Sharpe K, Stewart GD, Mackay A, Van Neste C, Rofe C, Berney D, Kayani I, Bex A, Wan E, O'Mahony FC, O'Donnell M, Chowdhury S, Doshi R, Ho-Yen C, Gerlinger M, Baker D, Smith N, Davies B, Sahdev A, Boleti E, De Meyer T, Van Criekinge W, Beltran L, Lu YJ, Harrison DJ, Reynolds AR, Powles T. The effect of VEGF-targeted therapy on biomarker expression in sequential tissue from patients with metastatic clear cell renal cancer. *Clin Cancer Res.* 2013 Dec 15;19(24):6924-34. doi: 10.1158/1078-0432.CCR-13-1631. Epub 2013 Oct 15.

210) Shattuck DL, Miller JK, Carraway KL 3rd, Sweeney C. Met receptor contributes to trastuzumab resistance of Her2-overexpressing breast cancer cells. *Cancer Res.* 2008 Mar 1;68(5):1471-7. doi: 10.1158/0008-5472.CAN-07-5962.

211) Shen X and Kramer RH. Adhesion-mediated squamous cell carcinoma survival through ligand-independent activation of epidermal growth factor receptor. *Am J Pathol.* 2004 Oct;165(4):1315-29.

212) Sierra JR and Tsao MS. c-MET as a potential therapeutic target and biomarker in cancer. *Ther Adv Med Oncol.* 2011 Nov;3(1 Suppl):S21-35. doi: 10.1177/1758834011422557.

213) Smolen GA, Muir B, Mohapatra G, Barmettler A, Kim WJ, Rivera MN, Haserlat SM, Okimoto RA, Kwak E, Dahiya S, Garber JE, Bell DW, Sgroi DC, Chin L, Deng CX, Haber DA. Frequent met oncogene amplification in a Brca1/Trp53 mouse model of mammary tumorigenesis. *Cancer Res.* 2006 Apr 1;66(7):3452-5.

214) Söderberg O, Leuchowius KJ, Gullberg M, Jarvius M, Weibrecht I, Larsson LG, Landegren U. Characterizing proteins and their interactions in cells and tissues using the in situ proximity ligation assay. *Methods.* 2008 Jul;45(3):227-32. doi: 10.1016/j.ymeth.2008.06.014. Epub 2008 Jul 11.

215) Sørlie T, Perou CM, Tibshirani R, Aas T, Geisler S, Johnsen H, Hastie T, Eisen MB, van de Rijn M, Jeffrey SS, Thorsen T, Quist H, Matese JC, Brown PO, Botstein D, Lønning PE, Børresen-Dale AL. Gene expression patterns of breast carcinomas distinguish tumor subclasses with clinical implications. *Proc Natl Acad Sci U S A.* 2001 Sep 11;98(19):10869-74.

216) Sørlie T, Tibshirani R, Parker J, Hastie T, Marron JS, Nobel A, Deng S, Johnsen H, Pesich R, Geisler S, Demeter J, Perou CM, Lønning PE, Brown PO, Børresen-Dale AL, Botstein D. Repeated observation of breast tumor subtypes in independent gene expression data sets. *Proc Natl Acad Sci U S A.* 2003 Jul 8;100(14):8418-23. Epub 2003 Jun 26.

217) Sotiriou C, Neo SY, McShane LM, Korn EL, Long PM, Jazaeri A, Martiat P, Fox SB, Harris AL, Liu ET. Breast cancer classification and prognosis based on gene expression profiles from a population-based study. *Proc Natl Acad Sci U S A.* 2003 Sep 2;100(18):10393-8. Epub 2003 Aug 13.

218) Stella GM, Benvenuti S, Gramaglia D, Scarpa A, Tomezzoli A, Cassoni P, Senetta R, Venesio T, Pozzi E, Bardelli A, Comoglio PM. MET mutations in cancers of unknown primary origin (CUPs). *Hum Mutat.* 2011 Jan;32(1):44-50. doi: 10.1002/humu.21374. Epub 2010 Nov 9.

219) Storci G, Sansone P, Trere D, Tavolari S, Taffurelli M, Ceccarelli C, Guarnieri T, Paterini P, Pariali M, Montanaro L, Santini D, Chieco P, Bonafé M. The basal-like breast carcinoma phenotype is regulated by SLUG gene expression. *J Pathol.* 2008 Jan;214(1):25-37.

220) Stuart-Harris R, Caldas C, Pinder SE, Pharoah P. Proliferation markers and survival in early breast cancer: a systematic review and meta-analysis of 85 studies in 32,825 patients. *Breast.* 2008 Aug;17(4):323-34. doi: 10.1016/j.breast.2008.02.002. Epub 2008 May 2.

221) Surveillance, Epidemiology, and End Results Program (SEER). Cancer Statistics Factsheets: Breast Cancer. National Cancer Institute. Bethesda, MD, http://seer.cancer.gov/statfacts/html/breast.html. April 2014.

222) Thiery JP. Epithelial-mesenchymal transitions in tumour progression. *Nat Rev Cancer.* 2002 Jun;2(6):442-54.

223) Toft DJ and Cryns VL. Minireview: Basal-like breast cancer: from molecular profiles to targeted therapies. *Mol Endocrinol.* 2011 Feb;25(2):199-211. doi: 10.1210/me.2010-0164. Epub 2010 Sep 22.

224) Tolgay Ocal I, Dolled-Filhart M, D'Aquila TG, Camp RL, Rimm DL. Tissue microarray-based studies of patients with lymph node negative breast carcinoma show that met expression is associated with worse outcome but is not correlated with epidermal growth factor family receptors. *Cancer.* 2003 Apr 15;97(8):1841-8.

225) Trusolino L, Bertotti A, Comoglio PM. MET signalling: principles and functions in development, organ regeneration and cancer. *Nat Rev Mol Cell Biol.* 2010 Dec;11(12):834-48. doi: 10.1038/nrm3012.

226) Tsuta K, Kozu Y, Mimae T, Yoshida A, Kohno T, Sekine I, Tamura T, Asamura H, Furuta K, Tsuda H. c-MET/phospho-MET protein expression and MET gene copy number in non-small cell lung carcinomas. *J Thorac Oncol.* 2012 Feb;7(2):331-9. doi: 10.1097/JTO.0b013e318241655f.

227) Turner N, Moretti E, Siclari O, Migliaccio I, Santarpia L, D'Incalci M, Piccolo S, Veronesi A, Zambelli A, Del Sal G, Di Leo A. Targeting triple negative breast cancer: is p53 the answer? *Cancer Treat Rev.* 2013 Aug;39(5):541-50. doi: 10.1016/j.ctrv.2012.12.001. Epub 2013 Jan 12.

228) Turner N, Tutt A, Ashworth A. Hallmarks of 'BRCAness' in sporadic cancers. *Nat Rev Cancer.* 2004 Oct;4(10):814-9.

229) Turner NC, Reis-Filho JS, Russell AM, Springall RJ, Ryder K, Steele D, Savage K, Gillett CE, Schmitt FC, Ashworth A, Tutt AN. BRCA1 dysfunction in sporadic basal-like breast cancer. *Oncogene.* 2007 Mar 29;26(14):2126-32. Epub 2006 Oct 2.

230) Uehara Y, Minowa O, Mori C, Shiota K, Kuno J, Noda T, Kitamura N. Placental defect and embryonic lethality in mice lacking hepatocyte growth factor/scatter factor. *Nature.* 1995 Feb 23;373(6516):702-5.

231) Voduc KD, Cheang MC, Tyldesley S, Gelmon K, Nielsen TO, Kennecke H. Breast cancer subtypes and the risk of local and regional relapse. *J Clin Oncol.* 2010 Apr 1;28(10):1684-91. doi: 10.1200/JCO.2009.24.9284. Epub 2010 Mar 1.

232) Wang X, Le P, Liang C, Chan J, Kiewlich D, Miller T, Harris D, Sun L, Rice A, Vasile S, Blake RA, Howlett AR, Patel N, McMahon G, Lipson KE. Potent and selective inhibitors of the Met [hepatocyte growth factor/scatter factor (HGF/SF) receptor] tyrosine kinase block HGF/SF-induced tumor cell growth and invasion. *Mol Cancer Ther.* 2003 Nov;2(11):1085-92.

233) Wang X and Schneider A. HIF-2alpha-mediated activation of the epidermal growth factor receptor potentiates head and neck cancer cell migration in response to hypoxia. *Carcinogenesis.* 2010 Jul;31(7):1202-10. doi: 10.1093/carcin/bgq078. Epub 2010 Apr 15.

234) Weibrecht I, Leuchowius KJ, Clausson CM, Conze T, Jarvius M, Howell WM, Kamali-Moghaddam M, Söderberg O. Proximity ligation assays: a recent addition to the proteomics toolbox. *Expert Rev Proteomics.* 2010 Jun;7(3):401-9. doi: 10.1586/epr.10.10.

235) Weigelt B, Baehner FL, Reis-Filho JS. The contribution of gene expression profiling to breast cancer classification, prognostication and prediction: a retrospective of the last decade. *J Pathol.* 2010 Jan;220(2):263-80. doi: 10.1002/path.2648.

236) Weihua Z, Tsan R, Huang WC, Wu Q, Chiu CH, Fidler IJ, Hung MC. Survival of cancer cells is maintained by EGFR independent of its kinase activity. *Cancer Cell.* 2008 May;13(5):385-93. doi: 10.1016/j.ccr.2008.03.015.

237) Wolters R, Regierer AC, Schwentner L, Geyer V, Possinger K, Kreienberg R, Wischnewsky MB, Wöckel A. A comparison of international breast cancer guidelines - do the national guidelines differ in treatment recommendations? *Eur J Cancer.* 2012 Jan;48(1):1-11. doi: 10.1016/j.ejca.2011.06.020. Epub 2011 Jul 7.

238) Xie LQ, Bian LJ, Li Z, Li Y, Li ZX, Li B. Altered expression of E-cadherin by hepatocyte growth factor and effect on the prognosis of nasopharyngeal carcinoma. *Ann Surg Oncol.* 2010 Jul;17(7):1927-36. doi: 10.1245/s10434-010-0922-6. Epub 2010 Feb 4.

239) Xu L, Nilsson MB, Saintigny P, Cascone T, Herynk MH, Du Z, Nikolinakos PG, Yang Y, Prudkin L, Liu D, Lee JJ, Johnson FM, Wong KK, Girard L, Gazdar AF, Minna JD, Kurie JM, Wistuba II, Heymach JV. Epidermal growth factor receptor regulates MET levels and invasiveness through hypoxia-inducible factor-1alpha in non-small cell lung cancer cells. *Oncogene.* 2010 May 6;29(18):2616-27. doi: 10.1038/onc.2010.16. Epub 2010 Feb 15.

240) Yano S and Nakagawa T. The current state of molecularly targeted drugs targeting HGF/Met. *Jpn J Clin Oncol.* 2014 Jan;44(1):9-12. doi: 10.1093/jjco/hyt188. Epub 2013 Dec 25.

241) Yap TA and de Bono JS. Targeting the HGF/c-Met axis: state of play. *Mol Cancer Ther.* 2010 May;9(5):1077-9. doi: 10.1158/1535-7163.MCT-10-0122. Epub 2010 May 4.

242) Yap TA, Olmos D, Brunetto AT, Tunariu N, Barriuso J, Riisnaes R, Pope L, Clark J, Futreal A, Germuska M, Collins D, deSouza NM, Leach MO, Savage RE, Waghorne C, Chai F, Garmey E, Schwartz B, Kaye SB, de Bono JS. Phase I trial of a selective c-MET inhibitor ARQ 197 incorporating proof of mechanism pharmacodynamic studies. *J Clin Oncol.* 2011 Apr 1;29(10):1271-9. doi: 10.1200/JCO.2010.31.0367. Epub 2011 Mar 7.

243) Yerushalmi R, Woods R, Ravdin PM, Hayes MM, Gelmon KA. Ki67 in breast cancer: prognostic and predictive potential. *Lancet Oncol.* 2010 Feb;11(2):174-83. doi: 10.1016/S1470-2045(09)70262-1.

244) Youlden DR, Cramb SM, Dunn NA, Muller JM, Pyke CM, Baade PD.The descriptive epidemiology of female breast cancer: an international comparison of screening, incidence, survival and mortality. *Cancer Epidemiol*. 2012. **36**(3): p. 237-48.

245) Zagouri F, Bago-Horvath Z, Rössler F, Brandstetter A, Bartsch R, Papadimitriou CA, Dimitrakakis C, Tsigginou A, Papaspyrou I, Giannos A, Dimopoulos MA, Filipits M. High MET expression is an adverse prognostic factor in patients with triple-negative breast cancer. *Br J Cancer.* 2013 Mar 19;108(5):1100-5. doi: 10.1038/bjc.2013.31. Epub 2013 Feb 19.